Porphyrin-based [3]- and [4]rotaxanes : towards an adaptable molecular receptor

Cécile Roche

UNIVERSITÉ DE STRASBOURG

EDSC
Ecole Doctorale des Sciences Chimiques

et

THE UNIVERSITY OF SYDNEY

ÉCOLE DOCTORALE DES SCIENCES CHIMIQUES

Institut de Chimie

THÈSE présentée par :

Cécile ROCHE

soutenue le: **20 avril 2012**

pour obtenir le grade de : **Docteur de l'Université de Strasbourg**

Discipline: Chimie

Porphyrin-based [3]- and [4]Rotaxanes

Towards an Adaptable Molecular Receptor

THÈSE en COTUTELLE dirigée par :

Prof. Jean-Pierre SAUVAGE	Université de Strasbourg
Dr. Angélique SOUR	Université de Strasbourg
Prof. Maxwell J. CROSSLEY	The University of Sydney

RAPPORTEURS :

Prof. David AMABILINO	Consejo Superior de Investigaciones Científicas, Barcelona
Prof. Jay SIEGEL	Universität Zürich

AUTRES MEMBRES DU JURY :

Prof. Véronique BULACH	Université de Strasbourg

“Learn from yesterday, live for today, hope for tomorrow.
The important thing is not to stop questioning.”

Albert EINSTEIN

Remerciements

First, I would like to thank my examiners, Prof. David Amabilino, Prof. Jay Siegel and Prof. Véronique Bulach for their interest in my research work.

Je voudrais également remercier mes directeurs de thèse, français et australien. Un grand merci à Jean-Pierre Sauvage et Angélique Sour pour m'avoir accueillie à Strasbourg. Après un passage à Paris, j'ai été très heureuse de retrouver l'Alsace et d'intégrer une équipe aussi sympathique et dynamique. Vous avez encadré ma thèse avec énormément d'enthousiasme et de disponibilité, et vous avez su me soutenir dans les bons comme dans les moins bons moments. J'ai beaucoup appris en travaillant avec vous pendant ces quelques années et je vous en suis très reconnaissante. I am very grateful to Max Crossley for his warm welcome in his group and for giving me the opportunity to have a very fulfilling research experience in Australia.

My thanks also go to all the people who have participated in parts of this research project. These are David Amabilino, who initiated the synthesis of the porphyrin tetra-macrocycle as a postdoc a long time ago; Nathan Strutt, who started the work on the [6]rotaxane project here in Strasbourg and who is now taking over this part of the project as a PhD student with Prof. Fraser Stoddart at Northwestern University; Frédéric Niess, who spared me the tedious synthesis and purification of the mesityldipyrrylmethane; Bernhard Schäfer, who helped with the synthesis of the rod; and Derrick Roberts, who kindly gave me a sample of a porphyrin tetraone precursor.

Je remercie aussi les membres des laboratoires dans lesquels j'ai pu travailler pendant cette thèse. Merci à Jean-Paul Collin, toujours disponible et de bon conseil, et à Valérie Heitz pour son soutien et son hospitalité dans son nouveau laboratoire. Merci Yann, ton rail et tes conseils ont été très utiles! My thanks also go to Sasha Martynov for very helpful discussions about synthetic issues. Je remercie vivement tous les membres, anciens et actuels, du LCOM et du LSAMM à Strasbourg, grâce auxquels l'ambiance était toujours excellente. Merci Julien et Anh-Thu, compagnons de rédaction! Au cours de ces trois (et quelques) années de thèse vous êtes devenus de vrais amis et j'ai été très contente de partager les joies et les épreuves de la thèse avec vous, surtout la rédaction… Merci Julien pour toutes ces (magnifiques) chansons que tu nous as si gentiment fredonnées… encore… encore… et encore…… Le labo aurait été bien triste sans toi! Merci Steph, toujours partante pour un pot ou une petite séance de grimpe :-) Merci

Felipe pour avoir enrichi mon vocabulaire en espagnol (mais ouiiiii!!!). Je tiens particulièrement à remercier Geneviève Stoll pour son amitié et son aide précieuse concernant toutes les tracasseries administratives. Merci beaucoup Gene, sans toi je ne m'en serais jamais sortie… Et bien sûr merci à tous ceux que je n'ai pas encore cités: Maryline, Antoine J., Julie, Jacques, Fabien, Julien F. Christian, Jon, Michel K., Pauline, Srba, Jean-François, Massimo, Michelle, Yoko ("yes, yes, yes!!!"), René, Tung, Michel T., Maya, Laurent, et tous les autres…

I am very grateful to the members of the Crossley group, in particular Fargol, Derrick and Dianne, who gave me a very warm welcome in Sydney. Fargol, you are one of the kindest people I have ever met, thank you so much for your help and friendliness. Derrick, you became an excellent colleague and friend, the Ritchie lab was so much more lively when you were there! Thanks for teaching me how to speak "Aussie" ;-) Dianne, I was so sad when you left the lab, thank you for everything! My thanks also go to Jimmy, Ben, James, Kafi, Dwi and all other members of the group.

Je remercie les différents organismes qui m'ont apporté un soutien financier au cours de ma thèse: l'Ecole Normale Supérieure de Paris et l'Université de Strasbourg pour une allocation de thèse; la Région Alsace, le Collège Doctoral Européen de l'Université de Strasbourg et le "Postgraduate Research Support Scheme" de l'Université de Sydney pour des bourses de voyages; et le prix Agnes Campbell de l'Université de Sydney (2010 et 2011).

Je tiens aussi à remercier les autres chimistes strasbourgeois que j'ai rencontrés au cours de ma thèse: Charles (je t'attribue la palme du plus beau T-shirt!), Hélène, Philippe, Yannis, Caroline, Clarisse, Gilles, Catherine, nos voisins de l'équipe de Dermatochimie, …

Many thanks to all the friends I made at the School of Chemistry in Sydney and to my Australian housemates: Alex, Lara, Claudia, Sandra, Gajan, Nat, Jenny, Xiao, Vinnie, Annie, Joe, Vince, Nico, Mark, Nick, Sven, Greg, and Damien!

Merci aux personnels des services communs de RMN, de spectrométrie de masse, de radiocristallographie et d'analyses, de mesures physiques et de spectroscopie optique.

Je remercie également ma famille, en particulier mes parents, ma sœur Aurélie et mon frère Julien, qui m'ont beaucoup encouragée tout au long de cette thèse. Un grand merci à Aurélie pour m'avoir supportée pendant la rédaction!

Merci Endymion, même quand tu es loin je sais que tu es de tout cœur avec moi.

Collège Doctoral Européen

M^elle^ Cécile Roche a été membre de la promotion Jane Goodall du Collège doctoral européen de l'Université de Strasbourg pendant la préparation de sa thèse de 2008 à 2012. Elle a bénéficié des aides spécifiques du CDE et a suivi un enseignement hebdomadaire sur les affaires européennes dispensé par des spécialistes internationaux. Ses travaux de recherche ont été effectués dans le cadre d'une convention de cotutelle avec l'Université de Sydney (Australie) et l'Université de Strasbourg.

Ms Cécile Roche was a member of the European Doctoral College of the University of Strasbourg during the preparation of her PhD, from 2008 to 2012, class name Jane Goodall. She has benefited from specific financial supports offered by the College and, along with her mainstream research, has followed a special course on topics of general European interests presented by international experts. This PhD research project has been led with the collaboration of two universities: The University of Sydney, Australia and the University of Strasbourg, France.

Abstract

Rotaxanes and porphyrins are two particularly active fields of research in chemistry. However, molecules that *combine* the interesting properties of these types of structures are not so common. In this thesis we describe new porphyrin-based multi-rotaxanes, whose syntheses constitute interesting challenges.

Porphyrins linked to two or four coordinating macrocycles were synthesised. The "gathering-and-threading" effect of copper(I) was used to thread molecular rods through the rings; the subsequent introduction of stoppers led to the formation of rotaxanes. In the case of the porphyrinic bis-macrocycle a [4]rotaxane was obtained. Host/guest complexation studies with rigid nitrogen ligands showed that the rotaxane behaves as a distensible molecular receptor that can adopt an "inflated" or "deflated" conformation and adjust its shape to the size of the guest. In the case of the porphyrinic tetra-macrocycle the formation of a [3]rotaxane of novel architecture was observed.

The synthesis of a new, more rigid bis-macrocycle is in progress. This compound will be used for the construction of a [4]rotaxane that could act as a molecular press able to change the conformation of a guest substrate by compression.

Keywords: rotaxane, porphyrin, macrocycle, phenanthroline, bipyridine, copper(I), zinc(II), organic synthesis, coordination chemistry, template effect, host-guest chemistry, molecular receptor.

Abstract in French

La synthèse et l'étude de rotaxanes et de porphyrines sont deux domaines particulièrement actifs de la recherche en chimie. Cependant, les composés *combinant* les propriétés intéressantes de ces deux types de structures sont plus rares. De nouveaux multi-rotaxanes à base de porphyrines, dont la préparation représente un défi synthétique, sont décrits dans cette thèse.

Des porphyrines liées à deux ou quatre anneaux coordinants ont été synthétisées. Des rails moléculaires à deux chélates ont été enfilés dans les anneaux grâce à l'effet template du cuivre(I); l'introduction de bouchons a mené à la formation de rotaxanes. Dans le cas du bis-macrocycle porphyrinique, un [4]rotaxane a été obtenu. Des études de complexation hôte/invité avec des ligands azotés rigides ont montré que ce rotaxane est un récepteur moléculaire qui peut s'adapter à la taille du substrat invité en se "gonflant" ou en se "dégonflant". Dans le cas du tétra-macrocycle porphyrinique, la formation d'un [3]rotaxane d'architecture originale a été observée.

La synthèse d'un nouveau bis-macrocycle plus rigide est en cours. Ce composé sera utilisé pour la construction d'un [4]rotaxane, qui pourrait présenter un caractère de presse moléculaire capable de modifier la conformation d'un substrat invité en le comprimant.

Mots-clés: rotaxane, porphyrine, macrocycle, phénanthroline, bipyridine, cuivre(I), zinc(II), synthèse organique, chimie de coordination, effet template, système hôte/invité, récepteur moléculaire.

Table of Contents

Remerciements ..... **iii**

Abstract ..... **vii**

Abstract in French ..... **viii**

Table of Contents ..... **ix**

List of Figures ..... **xiii**

List of Abbreviations ..... **xxiii**

Publications and Communications ..... **xxvii**

Summary in French ..... **xxix**

Chapter I. General Introduction **1**

I. 1. Rotaxanes: Topology, Synthetic Strategies and Applications **1**

I. 1. a) Interlocked Structures: Catenanes, Rotaxanes and Knots 1

I. 1. b) Strategies for the Synthesis of Rotaxanes 6

I. 1. c) [2]Rotaxanes and Multi-Rotaxanes 8

I. 1. d) Applications of Rotaxanes 9

I. 2. Molecular Machines: From Natural Systems to Synthetic Devices **10**

I. 2. a) Natural Molecular Machines 10

I. 2. b) Artificial Molecular Machines 13

I. 2. c) Rotaxane-based Machines 16

I. 3. Porphyrins: Bright and Versatile Tools in Chemistry **18**

I. 3. a) Axial ligation on metalloporphyrins 19
I. 3. b) Host-guest chemistry with porphyrins 23
I. 3. c) Porphyrins and Molecular Machines 26
I. 4. Porphyrin-containing Rotaxanes 28
I. 4. a) Examples of Porphyrin-containing Rotaxanes 28
I. 4. b) Previous Work Related to this Project: Molecular Receptors Based on Rigid Bis-Porphyrinic [3]- and [4]Rotaxanes 31
I. 4. c) Present Research Project: Design and Synthesis of Porphyrin-Based Multi-Rotaxanes as Adaptable Molecular Receptors 34

Chapter II. Rotaxane Building Blocks: 37
A New Zinc Porphyrin Substituted with Two Coordinating Macrocycles, a Molecular Rod and a Stopper
II. 1. Design of the System 37
II. 1. a) Chemical Structures of the Target Building Blocks 37
II. 1. b) Comparison of the Present Porphyrinic Bis-Macrocycle with the Previous System 38
II. 2. A dpp-Containing Macrocyclic Precursor 40
II. 2. a) Target Structure and Retrosynthesis 40
II. 2. b) Synthesis of the dpp-Containing m-31 Macrocycle 40
II. 2. c) Characterisation of the Macrocycle: X-Ray Crystal Structure 41
II. 3. A Zn-Porphyrin Substituted with Two Lateral m-31 Rings 43
II. 3. a) [2+2] MacDonald Condensation for the Formation of *trans*-A_2B_2 Porphyrins 43
II. 3. b) Synthesis of the Porphyrinic Bis-Macrocycle 44
II. 4. Threading Tests with dap: Formation and Characterisation of a [3]Pseudorotaxane 46
II. 4. a) Threading Reaction 46
II. 4. b) NMR Characterisation of Bis-Macrocycle 8 and [3]Pseudorotaxane 9^{2+} 47
II. 4. c) UV-visible Characterisation of Bis-Macrocycle 8 and [3]Pseudorotaxane 9^{2+} 48
II. 5. A Molecular Rod with Two Binding Sites and a Stopper 50
II. 5. a) Design of the Axle and Stopper 50
II. 5. b) Synthesis of a Two-Station Axle terminated with Acetylenic Functions 51
II. 5. c) Synthesis of an Azide-Functionalised Stopper 54

Chapter III. A Cyclic [4]Rotaxane Composed of Two Dumbbells and Two Bis-Macrocycles: 55

A Distensible Molecular Receptor

III. 1. Synthetic Approach for the Formation of a [4]rotaxane 55

III. 1. a) General Strategies for the Synthesis of Rotaxanes 55

III. 1. b) Design of the System and [4]Rotaxane Formation Strategy 57

III. 2. Synthesis and Characterisation of the Copper(I)-Complexed [4]Rotaxane 60

III. 2. a) Threading and Stoppering Reactions: [4]Rotaxane Synthesis 60

III. 2. b) HRES-MS Characterisation of the [4]Rotaxane 62

III. 2. c) NMR Characterisation of the [4]Rotaxane 63

III. 2. d) UV-visible Absorption Characterisation of the [4]rotaxane 68

III. 2. e) Demetalation of the Copper(I)-Complexed [4]Rotaxane 70

III. 3. The [4]Rotaxane used as a Host for Guest Molecules of Different Lengths 71

III. 3. a) Presentation and Synthesis of the Guest Molecules 71

III. 3. b) Titration with the DABCO Guest G1 73

III. 3. c) Titration with the 4,4'-Bipy Guest G2 75

III. 3. d) Titrations with Guests G3 and G4 77

III. 3. e) Titration Results Analysis: A Distensible Molecular Host 79

Chapter IV. Towards A New Porphyrinic Bis-Macrocycle: 83

Two Coordinating Rings Linked to a Central Porphyrin via an Extended Aromatic System

IV. 1. Design of the New Porphyrinic Bis-Macrocycle and Retrosynthetic Strategies 83

IV. 1. a) Design of the System 83

IV. 1. b) The Crossley Method for β,β'-Functionalisation of Porphyrins 85

IV. 1. c) Retrosynthetic Strategies 86

IV. 1. d) Synthesis of a Linear Porphyrin Tetraone 88

IV. 2. Synthetic Strategy A: Double Macrocyclisation on a Bis(dihydroxyquinoxalino)-Porphyrin 90

IV. 2. a) Retrosynthetic Routes to the Bis(dihydroxyquinoxalino)-Porphyrin 90

IV. 2. b) Route A.1: Attempted Deprotection of a Linear Bis(dimethoxyquinoxalino)-Porphyrin 91

IV. 2. c) Route A.2: Formation of a Bis-Catechol Extended Porphyrin and Attempted Bis-Macrocyclisation 92

IV. 3. Synthetic Strategy B: Condensation of a Porphyrin-Tetraone with a Diamino-Substituted Macrocycle 94

IV. 3. a) Route B.1: Attempted Synthesis of a Dinitro-Substituted Macrocycle 94

IV. 3. b) Route B.2: Attempted Synthesis of a Boc-Protected Diamino-Macrocycle 95

IV. 3. c) Route B.3: Protection of the Amine Groups using Anisaldehyde 96

IV. 3. d) Route B.4: Post-Macrocyclisation Introduction of Amine Groups 100

Chapter V. A [3]Rotaxane of Novel Architecture and its Precursor: 103

A New Zinc Porphyrin Substituted with Four Coordinating Macrocycles

V. 1. A Zinc Porphyrin Substituted with Four Coordinating Macrocycles 103

V. 1. a) Design of the system 103

V. 1. b) Synthetic Approaches for the Formation of Porphyrins 105

V. 1. c) Synthesis of the New Porphyrinic Tetra-Macrocycle 106

V. 2. A [3]Rotaxane Composed of a Porphyrinic Tetra-Macrocycle and Two Dumbbells 110

V. 2. a) Threading and Stoppering Reactions: Formation of a [3]Rotaxane 110

V. 2. b) HRES-MS Characterisation of the [3]Rotaxane 113

V. 2. c) NMR Characterisation of the [3]Rotaxane 114

V. 2. d) UV-visible Characterisation of the [3]Rotaxane 116

V. 3. Towards a [6]Rotaxane: Design of a New Axle 117

V. 3. a) Strategy for the Formation of a [6]Rotaxane 117

V. 3. b) Design of the Axle and First Results 118

Conclusion 123

Experimental Part 127

List of Molecules 155

References 159

List of Figures

Summary in French

Figure 1. Principe du récepteur moléculaire modulable. xxx

Figure 2. Structures chimiques du précurseur macrocyclique et du [3]pseudorotaxane obtenu par complexation du nouveau bis-macrocycle porphyrinique et du ligand dap avec le cuivre(I). xxxi

Figure 3. Structures chimiques du rail et du bouchon. xxxii

Figure 4. Structure chimique du [4]rotaxane. xxxiii

Figure 5. Molécules invitées testées avec le [4]rotaxane. xxxiv

Figure 6. Titration UV-visible (bande de Soret) pour la complexation entre la 4,4'-bipyridine **G2** et le [4]rotaxane. xxxiv

Figure 7. Projet de nouveau bis-macrocycle porphyrinique rigide. xxxvi

Figure 8. Schéma rétrosynthétique pour l'obtention du nouveau bis-macrocycle porphyrinique. xxxvii

Figure 9. Structure chimique du nouveau tétra-macrocycle porphyrinique. xxxviii

Figure 10. Représentation d'un [6]rotaxane composé de deux tétra-macrocycles porphyriniques et de quatre rails. xxxviii

Figure 11. Structure chimique du [3]rotaxane obtenu. xxxix

Chapter I. General Introduction

Figure I.1. Schematic views of a) a molecular trefoil knot, b) a molecular figure-of-eight and c) a molecular ring. A knot is topologically non-trivial, whereas the figure-of-eight and ring are trivial structures. 2

Figure I.2. First synthetic trefoil knot reported by C. O. Dietrich-Buchecker and J.-P. Sauvage. The strategy involves the formation of a double helical complex of bis-phenanthroline ligands around two copper(I) centres, followed by ring closure and demetalation. The knotted structure of the Cu(I) complex was confirmed by X-ray crystallography.[10,14,16,17] 2

Figure I.3. a) Schematic view of a [2]catenane. b) First copper(I)-templated catenane synthesised by C. O. Dietrich-Buchecker and J.-P. Sauvage.[25] 3

Figure I.4. A non-covalent catenane assembled *via* labile metal-ligand coordination bonds. The [2]catenane is in equilibrium with the corresponding non-interlocked macrocycles. The catenated form is largely predominant at high concentration.[29] 4

Figure I.5. Schematic views of a) a [2]rotaxane composed of a ring threaded on an axle ending with bulky stoppers (to prevent unthreading); and b) a pseudorotaxane. 4

Figure I.6. Strategy used by G. Schill in the first directed rotaxane synthesis, involving the use of covalent bonds as templates.[35] 5

Figure I.7. Examples of other interlocked structures. a) A molecular Solomon link (doubly interlocking [2]catenane);[36] b) Molecular Borromean rings (three interlocking, but non-catenated macrocycles);[37] c) A [3]rotacatenane (combination of [2]catenane and [2]rotaxane structures).[39] 6

Figure I.8. Three examples of rotaxanes assembled *via* directed strategies. a) Use of the gathering effect of the copper(I) template;[40] b) Preorganisation of the system *via* hydrogen bonding between the ring component and the dumbbell component;[41] c) Interlocking favoured by π-donor/π-acceptor interactions between the axle and the macrocycle.[42] 6

Figure I.9. The first [2]rotaxane exclusively made of double-stranded DNA, assembled *via* base-pairing between the axle and the ring.[50] 7

Figure I.10. Different possible geometries for a [3]rotaxane. Instances of these geometries have been described in the literature: a) Two rings threaded on one axle;[51-54] b) Two axles passing through the same ring;[55-57] c) and d) Two axles passing through the rings formed by a bis-macrocyclic component.[58,59] 8

Figure I.11. An original rotaxane architecture: a hetero-[7]rotaxane incorporating two different macrocycles.[65] 9

Figure I.12. A thermally activated, near infrared chemiluminescent squaraine rotaxane for optical imaging.[75] 9

Figure I.13. The ATP synthase, a natural molecular machine.[80,81] ATP synthases are rotary motors: a flow of protons through the membrane causes rotation of the rotor component (γ, ε and c) in relation to the stator component ($\alpha_3\beta_3$). This motion triggers sequential conformational changes in the β subunits, which are responsible for the consecutive steps of the formation of ATP: binding of the substrates ADP and P_i, chemical transformation and release of the newly formed ATP. 11

Figure I.14. a) Structure of the GroEL chaperonin and the GroEL/GroES complex (side view). b) Section of the internal cavities of the GroEL/GroES complex. c) Mechanism of action of the GroEL chaperonin: (i) an unfolded protein (red) is trapped at the entrance of the cavity (green/blue); (ii) fixation of ATP (T) triggers conformational changes and binding of the GroES lid (grey) and allows folding of the guest protein; (iii) hydrolysis of ATP to ADP (D) weakens the GroEL/GroES complex and induces release of the lid and folded protein.[83,84] 12

Figure I.15. Macroscopic bending motion of a cocrystal of a dithienylethene derivative and perfluoronaphthalene. The motion is due to the shape change of the dithienylethene units by photocyclisation upon irradiation with UV light.[86] 13

Figure I.16. A molecular crystal cantilever at work: a 0.17 mg photochromic crystal lifts a 47 mg lead ball upon irradiation with UV light.[86] 14

Figure I.17. A unidirectional molecular motor based on a [3]catenane structure (left). The sequential rotary motion of the two small rings around the larger ring is illustrated (right). Successive *E* to *Z* photoisomerisation of site A, followed by *E* to *Z* photoisomerisation of site B and then thermal reconversion of sites A and B to the *E* isomers promotes successive rotary motions of the small rings. The rotation direction is restricted by the presence of the second small ring. Conditions: (1) 350 nm, 5 min; (2) 254 nm, 20 min; (3) heat, 100 °C, 24h or catalytic Br_2, 400-670 nm, -78 °C, 10 min.[108] 15

Figure I.18. A fast-moving copper-complexed [2]rotaxane shuttle. The translational motion is controlled electrochemically: copper(I) binds preferentially to the sterically hindered bidentate chelate of the axle

while copper(II) binds to the less hindered bidentate site that allows coordination of an additional ligand.[118] 16

Figure I.19. A molecular elevator based on a triply interlocked [2]rotaxane structure. The interactions of the rings on the axles depend on the pH: the rings bind on the ammonium units when these are protonated and switch to the bipyridinium sites upon deprotonation of the ammonium groups. The shuttling motion of the rings along the axles lifts the central platform up and down.[119] 17

Figure I.20. Chemical structures of the porphyrin core and of two related heterocycles: the chlorin family and the bacteriochlorin family. One or two C=C double bonds are reduced in the chlorins and bacteriochlorins, respectively, compared to the porphyrin structure. 18

Figure I.21. Structure of metalloporphyrins and coordination of axial ligands. 19

Figure I.22. [2]catenanes obtained by axial coordination of bifunctional pyridyl ligands on Zn-porphyrins.[141,142] 20

Figure I.23. A novel approach for the templated synthesis of large multi-porphyrin rings. A linear porphyrin tetramer and a cyclic six-site template with mismatched numbers of binding sites were assembled by axial porphyrin coordination to give Vernier complexes. Covalent coupling of the porphyrin oligomers followed by template removal afforded a 12-porphyrin nano-ring.[143] 21

Figure I.24. Discrimination between the *syn* and *anti* isomers of a bis-porphyrin using axial coordination with a "molecular ruler". The bifunctional ruler ligand forms a strong complex with the *syn* isomer but is too short to bind both Zn-porphryin sites on the *anti* isomer.[148,149] 22

Figure I.25. Host-guest complexes of covalently linked Zn-porphyrin dimers and ditopic nitrogen ligands (DABCO or 4,4'-bipyridine) synthesised and studied in the group of J. K. M. Sanders.[153,154] 23

Figure I.26. Chemical structure (left) and molecular model (right) of a self-assembled capsule formed by axial coordination of a tetramine guest on the zinc(II) sites of two bis-porphyrin receptors.[159] 24

Figure I.27. Determination of the absolute configuration of α-chiral carboxylic acids with a bis-porphyrin host. Binding of the chiral guest induces a conformational change of the host with a preferred helicity, which is measured by circular dichroism.[160] 24

Figure I.28. a) A porphyrin-faced cubic host for C_{70} fullerene.[162] b) A supramolecular polymer formed through head-to-tail host-guest self-recognition of a hermaphroditic monomer. The host part of the monomer is an electron-rich bis-porphyrin unit, which is linked to an electron-deficient trinitrofluorenone guest moiety.[163] 25

Figure I.29. A tris-porphyrin prism host that can encapsulate and fold short peptides in hybrid α-helix/β-turn conformations.[171] 26

Figure I.30. A photoresponsive, porphyrin-containing molecular machine whose motion is reminiscent of a molecular pedal. Photoisomerisation of the azobenzene unit results in a rotary motion of the ferrocene pivot and of a pedal-like conformational change of the zinc porphyrin dimer. This motion is transferred to the biisoquinoline guest, which undergoes twisting around its central C-C bond.[174] 27

Figure I.31. A molecular gate composed of a Sn(IV)-porphyrin rotor linked to a handle stator by axial coordination. The gate is closed by coordination of silver(I) on the pyridyl sites of the handle and of the porphyrin.[176,177] 28

Figure I.32. Pirouetting motion of a [2]rotaxane that contains three porphyrin units. A gold(III) porphyrin is incorporated in the macrocyclic component, and the axle bears two zinc(II) porphyrins as stoppers.[190] 29

Figure I.33. A porphyrin-incorporating [6]pseudorotaxane structure reminiscent of the special pair of the photosynthetic reaction centre. Two central copper(II) porphyrins are held in a slipped cofacial arrangement by the surrounding interlocked scaffold. Parallel spin electron coupling between the Cu(II) centres results from the close proximity of the metalloporphyrins.[192] 30

Figure I.34. A tetra-interlocked [2]rotaxane with face-to-face Cu(II)-porphyrin and Cu(II)-phthalocyanine units. The distance between the copper(II) centres is monitored by protonation/deprotonation of amine groups on the axles. Switchable spin-spin communication is achieved: the spins are isolated in the protonated state of the rotaxane whereas antiferromagnetic coupling is observed upon deprotonation.[193] 31

Figure I.35. Schematic views of the copper(I)-complexed (top) and copper-free (bottom) forms of a [3]rotaxane. The rotaxane is a good molecular receptor for ditopic pyridyl guests of various lengths. The copper(I)-complexed rotaxane forms stronger complexes with short guests, while the copper-free rotaxane has better affinity for long guests.[194,195] 32

Figure I.36. A [4]rotaxane with two face-to-face porphyrins. The copper(I)-complexed rotaxane forms guest inclusion complexes with short substrates. However, the rotaxane collapses upon demetalation of the copper(I) centres and does not show any host-guest properties after demetalation.[196,197] 33

Figure I.37. Schematic view of the target [4]rotaxane. Zn-porphyrins are depicted as diamond-shaped symbols; phenanthroline and bipyridine binding sites are blue and green U-shaped symbols, respectively; copper(I) centres are pink dots and stoppers are large grey spheres. 35

Figure I.38. Proposed mechanism of action of a molecular press based on a [4]rotaxane. A flexible guest molecule bound in the central cavity of the rotaxane by axial coordination on the Zn-porphyrins is depicted in red. In the absence of copper(I) the guest can adopt an elongated conformation. In the presence of copper(I) the porphyrins are expected to be in closer proximity and induce conformational changes on the guest. 35

Figure I.39. Design of a [6]rotaxane composed of two porphyrinic tetra-macrocycles and of four dumbbells. 36

Chapter II. Rotaxane Building Blocks: *A New Zinc Porphyrin Substituted with Two Coordinating Macrocycles, a Molecular Rod and a Stopper*

Figure II.1. Retrosynthetic scheme displaying the chemical structures of the target building blocks needed for the formation of a [4]rotaxane with two cofacial Zn-porphyrins. The pink spheres represent copper(I), the "gathering-and-threading" centre. 37

Figure II.2. Schematic view of the structural difference between two porphyrinic bis-macrocycles: (a) previously made in our group[196] and (b) described in this chapter. The main differences reside in *(i)* the nature of the bridge (highlighted in blue) between the central porphyrin (purple) and the macrocycles (rigid pyrazine-benzene-pyrazine motif *vs*. single C-C bond); *(ii)* the position of the bridge on the porphyrin (β-pyrrolic *vs*. *meso* substitution); *(iii)* the orientation of the coordinating dpp unit (yellow) (*exo vs*. *endo* coordination mode with respect to the porphyrin); and *(iv)* the electronic coupling between the dpp chelate and the porphyrin (electronically coupled *vs*. decoupled). 38

Figure II.3. Chemical structure of the macrocyclic precursor and retrosynthetic route.....40

Figure II.4. Synthesis of the dpp-incorporating aldehyde-appended macrocycle **5**.....41

Figure II.5. X-Ray structure of the 31-membered ring **5**. A dichloromethane molecule resides in the structure (Carbon atoms are represented in grey, nitrogen atoms in blue, oxygen atoms in red, chlorine atoms in green; hydrogen atoms are omitted for clarity). (i) Top view; (ii) side view. 42

Figure II.6. [2+2] MacDonald condensation of a dipyrrylmethane and an aldehyde for the formation of *trans*-A_2B_2 porphyrins.....43

Figure II.7. Synthesis of compound **8**, a Zn-porphyrin substituted with two dpp-containing macrocycles at antipodal *meso* positions.....44

Figure II.8. Threading reaction of bis-macrocycle **8** with dap chelate **1** *via* copper(I) templating to afford the [3]pseudorotaxane $\mathbf{9^{2+}}$. 46

Figure II.9. ^{1}H NMR of the porphyrinic bis-macrocycle **8** and [3]pseudorotaxane $\mathbf{9^{2+}}$ (signals in the aromatic region are displayed). The chemical shifts observed for $\mathbf{9^{2+}}$ are typical of this type of threaded species. In particular, protons 3, 8 and m undergo strong upfield shifts upon threading of dap (blue arrows). 47

Figure II.10. UV-visible absorption and normalised emission spectra of porphyrinic bis-macrocycle **8** and [3]pseudorotaxane $\mathbf{9^{2+}}$ in CH_2Cl_2. Both compounds have a Soret band at 421 nm and Q bands at 548 and 585 nm. Emission spectra were recorded upon excitation at 548 nm. In both cases emission maxima are observed at 595 and 646 nm. 48

Figure II.11. The Huisgen Copper(I)-catalysed Azide-Alkyne Cycloaddition (CuAAC) reaction. With Cu(I) as a catalyst the reaction usually proceeds in high yields and the *anti* 1,2,3-triazole is formed selectively. 51

Figure II.12. Target chemical structures of the dumbbell building blocks. The molecular rod, or axle, is functionalised with two terminal alkyne groups and contains two coplanar 2,2'-bipyridine chelates facing towards the same side of the axle (left). The stopper comprises a hindering group at one end and an azide group at the other end (right). 51

Figure II.13. Synthesis of the dibromo bis-bidentate fragment **14**.....52

Figure II.14. Synthesis of the two-station axle **16** functionalised with acetylenic groups.....53

Figure II.15. Synthesis of the azide-functionalised stopper **18**. 54

Chapter III. A Cyclic [4]Rotaxane Composed of Two Dumbbells and Two Bis-Macrocycles: *A Distensible Molecular Receptor*

Figure III.1. Different strategies used in the assembly of rotaxanes.....56

Figure III.2. Chemical structure of the target copper(I)-complexed [4]rotaxane. 58

Figure III.3. Preparation of a [4]rotaxane composed of two axles and two bis-macrocycles. Each bis-macrocycle consists of two flexible rings attached to a central Zn porphyrin. The synthetic strategy is based on the ''gathering-and-threading'' approach using a copper(I) template, followed by stoppering. The porphyrin is represented as a square or a diamond, the bidentate chelates are indicated by green or

blue U-shaped symbols and the gathering metal centre (copper(I)) is a pink dot. The stoppers are depicted as large grey spheres. 59

Figure III.4. Two-step, one-pot synthesis of [4]rotaxane **19^{4+}** in 50% yield by (1) threading of bis-macrocycle **8** and axle **16** into a [4]pseudorotaxane and (2) quadruple CuAAC stoppering reaction with azide stopper **18**. 61

Figure III.5. High resolution electrospray mass spectrum of rotaxane **19^{4+}**. The main signal is magnified to show the isotope profile (top right); this profile fits well with the calculated spectrum (bottom). 62

Figure III.6. Hypothetical threading and stoppering scheme leading to a [2]rotaxane. Mass spectrometry results indicated that this threading scheme is not favoured. The isotope profile is consistent with a [4]rotaxane containing four copper(I) centres 63

Figure III.7. Variable temperature ^{1}H NMR spectra of [4]rotaxane **19^{4+}** in CD_3NO_2. Signals in the aromatic region are displayed. 63

Figure III.8. ^{1}H NMR spectrum of rotaxane **19^{4+}** in CD_2Cl_2 at room temperature. Signals in the aromatic region are displayed (top), as well as proton assignments on the bis-macrocycle and dumbbell components of the rotaxane (bottom). Split signals are annotated with “a” and “b” subscripts. Signals were assigned using COSY, NOESY, HSQC and HMBC data. 64

Figure III.9. Part of the NOESY spectrum of rotaxane **19^{4+}** displaying NOE interactions between the central part of the dumbbell (protons 1' - 4') and the ethyleneglycol chains of the macrocycles. 65

Figure III.10. Schematic view of the proposed geometry of rotaxane **19^{4+}** in solution deduced from the NMR data....66

Figure III.11. DOSY spectrum of rotaxane **19^{4+}** in CD_2Cl_2, displaying signals in the aromatic region. The DOSY data show the presence of a single chemical species in solution; arrows point at minor signals that belong to a second, minor conformer of the [4]rotaxane in very slow exchange with the major conformer. This minor conformer diffuses at the same rate as the major conformer. A good fit is obtained for the estimated size of the rotaxane using CPK models and the diffusion coefficient measured by DOSY NMR. The rotaxane approximates to a 48 Å sphere....67

Figure III.12. UV-visible absorption spectra (Soret band) of [4]rotaxane **19^{4+}** and its precursor, porphyrinic bis-macrocycle **8** in CH_2Cl_2 with [porphyrin] = $1.9*10^{-6}$ M. The blue shift and broadening of the Soret band of the rotaxane is attributed to exciton coupling between the two central porphyrins. 68

Figure III.13. Scheme highlighting the similarities and differences between the present [4]rotaxane **19^{4+}** and the [3]rotaxane that will be described in Chapter V. Both rotaxanes comprise exactly the *same dumbbell* resulting from the click reaction of two stoppers **18** on the axle **16**, and are complexed to four Cu(I) centres. However, only *one* porphyrin is incorporated in the [3]rotaxane while the [4]rotaxane contains *two* cofacial porphyrins. 69

Figure III.14. Chemical structures of guests **G1** - **G4**....71

Figure III.15. Synthesis of guests **G3** and **G4**.[261] 72

Figure III.16. Possible coordination modes of guests **G1** - **G4** with rotaxane host **19^{4+}**. a) 1:1 host-guest stoichiometry, internal complex (guest inclusion); b) 1:1 stoichiometry, external complex; c) 1:2 host-guest stoichiometry, internal complexes; d) 1:2 stoichiometry, external complexes, e) 1:2 stoichiometry with one internal and one external guest. 73

Figure III.17. UV-visible titration spectra in toluene (Soret band) of rotaxane **19^{4+}** (0.92 x 10^{-6} M) with DABCO guest **G1** (2.8 x 10^{-5} M) from 0.0 to 2.0 equiv. Arrows show changes in the host spectrum with increasing guest concentration; a 6 nm red shift from 423 to 429 nm is observed. 74

Figure III.18. UV-visible titration spectra in toluene (Soret band) of rotaxane **19^{4+}** (0.92 x 10^{-6} M) with 4,4'-bipyridine guest **G2** (2.8 x 10^{-5} M) from 0.0 to 2.0 equiv. Arrows show changes in the host spectrum with increasing guest concentration; a 5 nm red shift from 423 to 428 nm is observed. 76

Figure III.19. UV-visible titration of rotaxane **19^{4+}** with guests **G1** and **G2** in toluene. Absorbance plotted against the added guest equivalents at λ_{max} = 423 nm. 77

Figure III.20. UV-visible titration spectra in toluene (Soret band) of rotaxane **19^{4+}** (0.92 x 10^{-6} M) with guest **G3** (2.8 x 10^{-5} M) from 0.0 to 2.0 equiv. Arrows show changes in the host spectrum with increasing guest concentration; a 2 nm red shift from 423 to 425 nm is observed. 78

Figure III.21. UV-visible titration spectra in toluene (Soret band) of rotaxane **19^{4+}** (0.92 x 10^{-6} M) with guest **G4** (2.8 x 10^{-5} M) from 0.0 to 2.0 equiv. Arrows show changes in the host spectrum with increasing guest concentration; a 1 nm red shift from 423 to 424 nm is observed. 78

Figure III.22. a) "inflated" and b) "deflated" conformations of the host **19^{4+}**. The rotaxane can adjust its geometry to accommodate either extended guests (*e.g.* **G4**) or very short guests (*e.g.* DABCO). 80

Chapter IV. Towards A New Porphyrinic Bis-Macrocycle: *Two Coordinating Rings Linked to a Central Porphyrin via an Extended Aromatic System*

Figure IV.1. Schematic view of the structural differences between three porphyrinic bis-macrocycles: (a) compound **8** described in Chapters II and III of this thesis; (b) new target compound; (c) compound used in previous studies.[196,197,217] The rigidity of the new system will be intermediate between the very flexible bis-macrocycle **8** and the very rigid bis-macrocycle studied by former members of the Sauvage group. ..84

Figure IV.2. The Crossley synthetic approach for the functionalisation of porphyrins at the β positions. The method involves the formation of porphyrin-dione (a) or tetraone (b) derivatives, followed by condensation with a (substituted) 1,2-phenylenediamine unit. It allows the formation of linear or "corner" planar multifunctional systems, whose functional groups are covalently linked to the porphyrin via an extended aromatic system (Ar = aryl group).[265] 85

Figure IV.3. Chemical structure of the target extended porphyrin substituted with two coordinating macrocycles. 86

Figure IV.4. Two retrosynthetic strategies for the synthesis of the target porphyrinic bis-macrocycle. **Strategy A**: double macrocyclisation on a bis(dihydroxyquinoxalino)-porphyrin. **Strategy B**: condensation of a porphyrin-tetraone with a diamino-substituted macrocycle. 87

Figure IV.5. Six-step synthesis of linear porphyrin-tetraone **25** *via* a literature procedure.[265] 88

Figure IV.6. Two retrosynthetic routes for the formation of a linear bis(dihydroxyquinoxalino)-porphyrin derivative. 90

Figure IV.7. Attempted deprotection of the methoxyl groups of a bis(dimethoxyquinoxalino)-porphyrin. 91

Figure IV.8. Synthesis of 4,5-diaminocatechol hydrobromide **29**.[275] 92

Figure IV.9. Synthesis of the linear bis(dihydroxyquinoxalino)-porphyrin **30**. 92

Figure IV.10. Tautomerisation of the dihydroxyquinoxaline moieties of compound **30**. 93

Figure IV.11. Attempted synthesis of the target porphyrinic bis-macrocycle....93

Figure IV.12. Route B.1: Attempted synthesis of a dinitro-substituted macrocycle. 94

Figure IV.13. Route B.2: Attempted synthesis of a Boc-protected diamino-macrocycle. 95

Figure IV.14. Condensation reaction of 4,5-diaminocatechol **29** with anisaldehyde. The 1-benzyl-2-phenylbenzimidazole derivative **33** was obtained instead of the expected bis(N-anisylidenamine) species. 96

Figure IV.15. Proton NMR spectrum of the 1-benzyl-2-phenylbenzimidazole derivative **33** in DMSO-d_6 (500 MHz). Signals were assigned using COSY, ROESY, HSQC and HMBC data. 97

Figure IV.16. Possible mechanism for the formation of **33** in the presence of catalytic acid. 98

Figure IV.17. Synthesis of macrocycle **34** and attempted deprotection of the amine groups. 99

Figure IV.18. Synthesis of the dibromo-substituted macrocycle **36**. 100

Figure IV.19. Synthesis of bis-imine macrocycle **37** by Buchwald-Hartwig reaction with benzophenone imine.[289] 101

Chapter V. A [3]Rotaxane of Novel Architecture and its Precursor: *A New Zinc Porphyrin Substituted with Four Coordinating Macrocycles*

Figure V.1. Schematic view of the target [6]rotaxane constituted of two face-to-face porphyrins, each of them covalently linked to four coordinating macrocycles and mechanically linked to four dumbbells. The retrosynthetic route for the formation of this [6]rotaxane involves the use of a two-station axle, a stopper and a new porphyrinic tetra-macrocycle whose target chemical structure is depicted. 104

Figure V.2. Porphyrin synthesis by condensation of an aldehyde and pyrrole to a porphyrinogen intermediate, followed by oxidation to form the aromatic porphyrin ring. The conditions for the Adler-Rothemund and the Lindsey procedures are given. 105

Figure V.3. Synthesis of tetra-substituted free-base porphyrin **38**. Optimised conditions for the condensation: **5** (1 eq., 200 mM), pyrrole (1 eq., 200 mM), propionic acid/nitrobenzene 7:3, microwaves, 141°C, 10 min (25%). 106

Figure V.4. Synthesis of tetra-substituted zinc(II) porphyrin **39** (quantitative yield). 109

Figure V.5. Preparation of a [3]rotaxane whose central fragment consists of a Zn-complexed porphyrin bearing four coordinating rings. The synthetic strategy is based on the "gathering-and-threading" approach followed by stoppering. The threading scheme that prevails in this case differs from that observed for the formation of the [4]rotaxane in Chapter III. Free rotation of the rings in relation to the porphyrin allows threading of the axles through two adjacent rings of the porphyrin. 111

Figure V.6. Two-step, one-pot synthesis of rotaxane $\mathbf{40^{4+}}$ by (1) formation of a [3]pseudorotaxane and (2) quadruple CuAAC stoppering reaction. 112

Figure V.7. HRES-MS spectrum of [3]rotaxane $\mathbf{40^{4+}}$ and isotope profile evidencing the 1:2 porphyrin/rod stoichiometry. 113

Figure V.8. ^{1}H NMR spectra of rotaxane **40**$^{4+}$, Zn-porphyrin **39** and rod **15;** signals in the aromatic region are displayed (top). NMR assignments of the [3]rotaxane **40**$^{4+}$ (bottom).....114

Figure V.9. Aromatic region of the ^{1}H-^{1}H NOESY (600 MHz) spectrum of rotaxane **40**$^{4+}$. NOE correlations between the rod and the tetra-macrocycle in the aromatic region are highlighted. 115

Figure V.10. UV-visible absorption spectra of free-base porphyrin **38**, Zn-porphyrin **39** and rotaxane **40**$^{4+}$ in CH_2Cl_2.....116

Figure V.11. Introduction of a longer spacer between the bidentate sites of the axle to avoid the formation of a [3]rotaxane and consequently favour the formation of a [6]rotaxane. 118

Figure V.12. Chemical structures of bis-bidentate molecular rods. a) Rod **16** used in the previous studies, with a very short spacer between the coordination sites. b) Design of a rod with two phenylene spacers, abandoned due to synthetic problems. c) New rod with one phenylene spacer. A threading test with a precursor of this rod gave the [3]pseudorotaxane. d) and e) Target structures of rods with very long spacers between the bidentate sites.....119

Figure V.13. Schematic view of a new topologically interesting [2]catenane. This type of structure could be obtained by junction of the axle ends of the [3]pseudorotaxane resulting from threading of rods **16** with tetra-macrocycle **39**. 121

List of Tables

Tableau 1. Constantes d'association des molécules invitées **G1** à **G4** avec le [4]rotaxane.....xxxv

Table III.1. Association constants of guests **G1** - **G4** with rotaxane host **19**$^{4+}$ and lengths of the ligands. 79

Table V.1. Synthesis of free-base porphyrin **38** in classical Lindsey conditions or mild conditions. 107

Table V.2. Synthesis of free-base porphyrin **38** in conditions derived from the Adler-Rothemund method. 108

List of Abbreviations

ADP Adenosine DiPhosphate 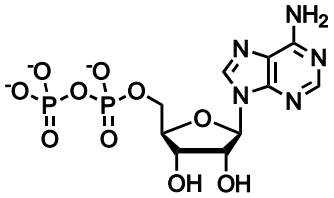

ATP Adenosine TriPhosphate 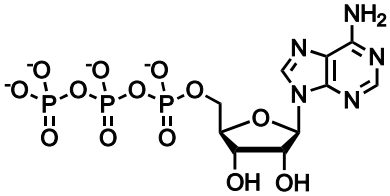

a.u. arbitrary unit

BINAP 2,2'-bis(diphenylphosphino)-1,1'-binaphtyl 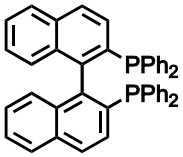

bipy 2,2'-bipyridine 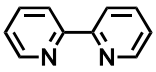 or 4,4'-bipyridine 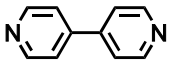

Boc *t*-Butyl carbamate 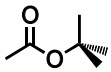

CAN Ceric Ammonium Nitrate $(NH_4)_2Ce(NO_3)_6$

COSY Correlation SpectroscopY

CPK Corey-Pauling-Koltun

CuAAC Copper(I)-catalysed Azide-Alkyne Cycloaddition

δ chemical shift

DABCO 1,4-diazabicyclo[2,2,2]octane 

dap 2,9-dianisyl-1,10-phenanthroline 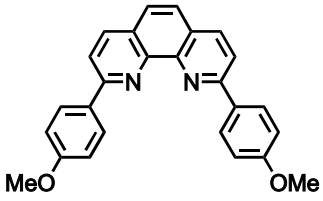

dba dibenzylideneacetone 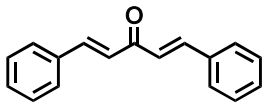

DDQ 2,3-dichloro-5;6-dicyanobenzoquinone 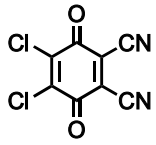

DEPT Distortionless Enhancement by Polarisation Transfer

DMF N,N-dimethylformamide 

DMSO dimethylsulfoxide 

DNA DeoxyriboNucleic Acid

DOSY Diffusion-Ordered SpectrscopY

dpp 2,9-diphenol-1,10-phenanthroline 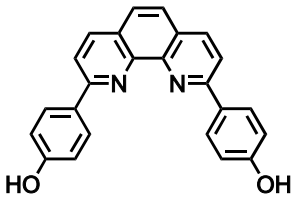

or 2,9-diphenyl-1,10-phenanthroline 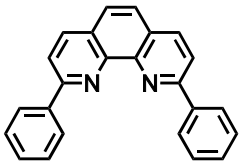

EDTA EthyleneDiamineTetraAcetic acid 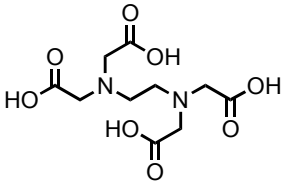

eq. equivalent(s)

ES-MS ElectroSpray Mass Spectrometry

HMBC Heteronuclear Multiple Bond Correlation

HRES-MS High Resolution ElectroSpray Mass Spectrometry

HSQC Heteronuclear Single-Quantum Correlation

J coupling constant

M $mol.L^{-1}$

MLCT Metal-to-Ligand Charge Transfer

NMR Nuclear Magnetic Resonance

NOE	Nuclear Overhauser Effect
NOESY	Nuclear Overhauser Effect SpectroscopY
P_i	inorganic phosphate 
ppm	part per million
rac	racemic
ROESY	Rotating frame Overhauser Effect SpectroscopY
RT	Room Temperature
TBAF	TetraButylAmmonium Fluoride 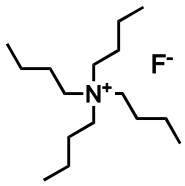
terpy	2,2';6',2"-terpyridine 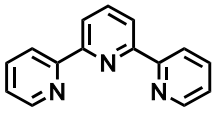
TFA	TriFluoroAcetic acid 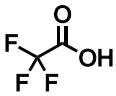
THF	TetraHydroFurane 
TIPS	TriIsoPropylSilyl 
TLC	Thin Layer Chromatography
UV	Ultra-Violet

Publications and Communications

Publications

The work developed in Chapters II, V, and III (respectively) has been described in the following publications:

Cécile Roche, Angélique Sour, Frédéric Niess, Valérie Heitz, Jean-Pierre Sauvage, **A Zinc Porphyrin Bearing Two Lateral dpp-Containing Rings and Its [3]Pseudorotaxane (dpp: 2,9-diphenyl-1,10-phenanthroline)**, *Eur. J. Org. Chem.* **2009**, 2795-2800.

Cécile Roche, Jean-Pierre Sauvage, Angélique Sour, Nathan L. Strutt, **A [3]Rotaxane Composed of a Zinc Porphyrin Tetra-substituted with Coordinating Macrocycles and of Two Rigid Axles**, *New J. Chem.* **2011**, 35, 2820-2825.

Cécile Roche, Angélique Sour, Jean-Pierre Sauvage, **A flexible copper(I)-complexed [4]rotaxane containing two face-to-face porphyrinic plates which behaves as a distensible receptor**, *Chem. Eur. J.* **2012**, *18*, 8366-8376 (*selected as Very Important Paper*).

Communications

Cécile Roche, Angélique Sour, Jean-Pierre Sauvage, **Rotaxanes porphyriniques: vers une presse moléculaire**, *Oral Presentation at the "Journée des Doctorants" (Postgraduate Symposium)*, Université de Strasbourg, November 2009.

Cécile Roche, Angélique Sour, Jean-Pierre Sauvage, **Multirotaxanes porphyriniques: vers une presse moléculaire,** *Poster presentation at GECOM-CONCOORD (International conference in coordination chemistry, organometallic chemistry and catalysis)*, Lyon, France, June 2010 (**2nd Poster Prize**).

Cécile Roche, Nathan L. Strutt, Angélique Sour, Jean-Pierre Sauvage, Maxwell J. Crossley, **Porphyrinic Multirotaxanes: Towards a Molecular Press**, *Oral communication at the "RACI NSW Organic Symposium" of the Royal Australian Chemical Institute*, The University of Wollongong, Australia, December 2010.

Cécile Roche, Nathan L. Strutt, Angélique Sour, Jean-Pierre Sauvage, Maxwell J. Crossley, **Porphyrinic Multirotaxanes: Towards a Molecular Press**, *Flash oral presentation and poster presentation at ISMSC 6 (International Symposium on Macrocyclic and Supramolecular Chemistry)*, Brighton, UK, July 2011 (***Chem. Soc. Rev.* Poster Prize**).

Summary in French

[3]- et [4]Rotaxanes à base de Porphyrines
Vers un Récepteur Moléculaire Adaptable

I. Introduction

Les caténanes et rotaxanes sont très intéressants de par le défi synthétique que représente leur préparation, ainsi que dans le domaine des machines et moteurs moléculaires. Les applications des machines moléculaires sont variées, et les recherches dans ce domaine portent sur le transfert d'électron ou d'énergie, l'élaboration de dispositifs de stockage de l'information, ou encore l'imitation de systèmes naturels. La nature utilise de nombreuses machines moléculaires nanométriques afin d'assurer des fonctions essentielles chez les organismes vivants. Par exemple, l'ATP synthase est un moteur moléculaire dont la rotation permet de promouvoir successivement la fixation des réactifs, la transformation chimique et la libération de l'ATP formé. Un autre exemple de machine moléculaire naturelle est celui des protéines chaperonnes, qui ont pour fonction d'aider le repliement d'autres protéines. Elles possèdent une cavité centrale dans laquelle une protéine "invitée" peut être piégée. La protéine est alors manipulée par le chaperon, ce qui conduit à un changement de conformation important: elle est transformée en sa forme active d'un point de vue enzymatique, puis est éjectée de la cavité. Le développement de nano-machines artificielles reproduisant l'action de ces machines moléculaires naturelles reste un challenge pour le chimiste synthétique.

Notre projet s'inspire du mode de fonctionnement des protéines chaperonnes. L'objectif n'est pas exactement de modeler une protéine mais de créer un système basé sur des mouvements plus simples, qui serait capable de piéger une molécule invitée, et qui pourrait par la suite changer la conformation du substrat piégé par compression. Le projet porte donc sur la synthèse et l'étude de multi-rotaxanes porphyriniques se comportant comme des récepteurs moléculaires

modulables et présentant un caractère de "presse moléculaire". Les porphyrines de zinc ont été choisies comme plaques de la presse pour leur capacité à se lier à divers substrats organiques. Le mouvement des porphyrines l'une par rapport à l'autre est permis grâce à la structure de type rotaxane. Le principe général du projet est schématisé ci-dessous (**Figure 1**).

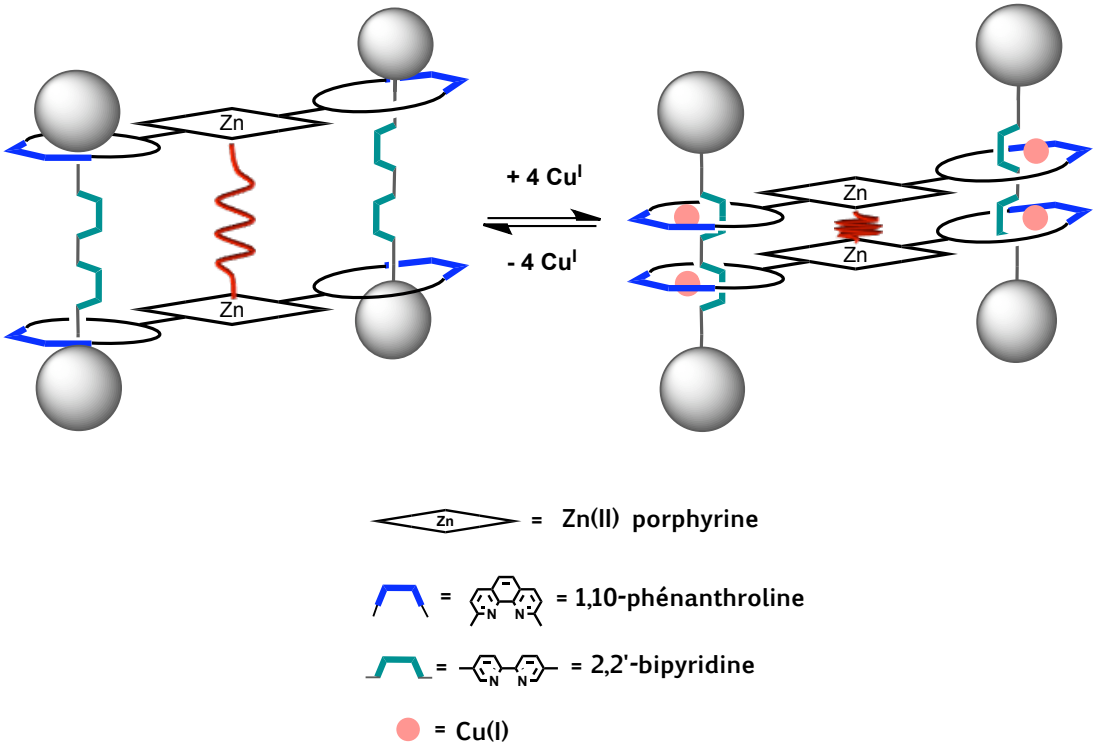

Figure 1. Principe du récepteur moléculaire modulable.

Comme indiqué sur le schéma, le mouvement est déclenché par un signal chimique, plus précisément par la présence ou l'absence de cuivre(I). Lorsque le [4]rotaxane est libre (en l'absence de cuivre(I)), les plaques porphyriniques peuvent se déplacer librement l'une par rapport à l'autre. Comme représenté en rouge sur le schéma, un substrat coordiné aux ions zinc, entre les deux porphyrines, peut alors adopter une conformation étendue, stable du point de vue thermodynamique. En revanche, en présence de cuivre(I), la position des anneaux sur les axes est fixée au niveau des complexes de Cu(I), ce qui devrait provoquer le rapprochement des plaques porphyriniques, et par conséquent la compression du substrat localisé entre ces deux plaques.

La réalisation de ce projet implique la synthèse de nouvelles porphyrines liées à des anneaux chélatants, la synthèse d'un axe (ou rail moléculaire) et d'un "bouchon" encombrant, ainsi que la construction de multi-rotaxanes à partir de ces composants et l'étude des propriétés de récepteur moléculaire des rotaxanes.

II. Synthèse de Précurseurs de Rotaxane: Une Porphyrine de Zinc liée à Deux Anneaux, un Rail Moléculaire et un Bouchon

La première partie de ce travail a porté sur la synthèse de trois composants organiques – un nouveau bis-macrocycle porphyrinique, un rail moléculaire et un bouchon – pouvant par la suite être assemblés en une structure de type rotaxane. Le premier composant, une porphyrine de zinc reliée à deux macrocycles, a été obtenu à partir d'un précurseur macrocyclique incorporant un chélate de la famille de la 1,10-phénanthroline (**Figure 2**). Le précurseur macrocyclique a été synthétisé en cinq étapes à partir de produits commerciaux, la dernière étape consistant en une macrocyclisation dans des conditions de haute dilution. Le macrocycle, obtenu avec un rendement de 67 %, contient un fragment 2,9-diphényl-1,10-phénanthroline (dpp) et est fermé par un cycle benzaldéhyde substitué. La structure a été confirmée par diffraction aux rayons X. Le bis-macrocycle porphyrinique a été obtenu par condensation de MacDonald entre le macrocycle et le mésityldipyrrylméthane. La porphyrine a ensuite été métallée par de l'acétate de zinc, le rendement global pour ces deux dernières étapes étant de 18 %. Afin de tester la capacité de ce nouveau bis-macrocycle à former des structures entrelacées, une complexation par le cuivre(I) et la 2,9-dianisyl-1,10-phénanthroline (dap) a été effectuée. Un [3]pseudorotaxane a été obtenu quantitativement (**Figure 2**), ce qui nous a encouragés à poursuivre la synthèse de rotaxanes plus élaborés.

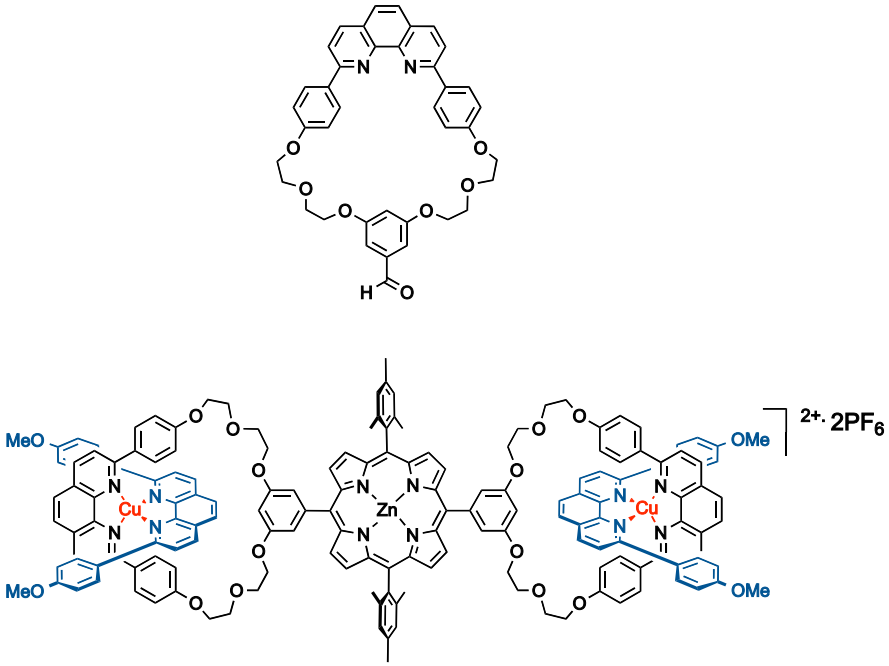

Figure 2. Structures chimiques du précurseur macrocyclique et du [3]pseudorotaxane obtenu par complexation du nouveau bis-macrocycle porphyrinique et du ligand dap avec le cuivre(I).

Afin de pouvoir construire des structures de type rotaxane, nous avons également synthétisé un axe à deux chélates et une molécule de type "bouchon" possédant des groupes terminaux volumineux (**Figure 3**). La synthèse de ces deux molécules a été réalisée selon un mode opératoire récemment développé au laboratoire. L'axe à deux chélates et le bouchon sont fonctionnalisés respectivement par des groupements acétyléniques et azotures, afin de pouvoir par la suite greffer le bouchon sur l'axe par une réaction "click" de type CuAAC (Copper(I)-catalysed Azide-Alkyne Cycloaddition).

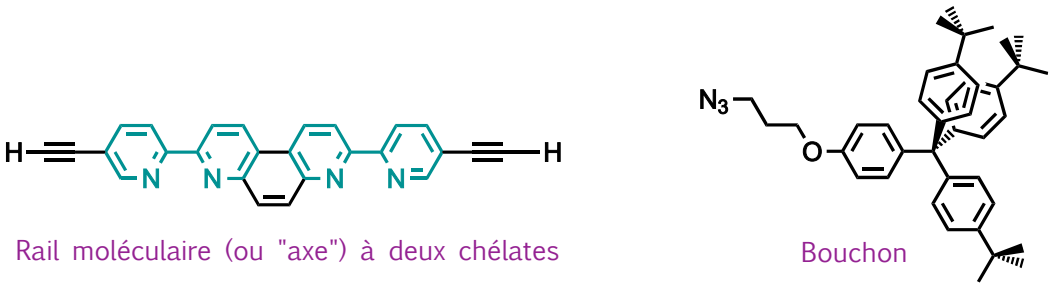

Rail moléculaire (ou "axe") à deux chélates

Bouchon

Figure 3. Structures chimiques du rail et du bouchon.

III. Un [4]Rotaxane cyclique composé de Deux Rails et de Deux Bis-Macrocycles: Un Récepteur Moléculaire "Gonflable"

Cette partie porte sur la synthèse d'un rotaxane à partir des composants décrits en II., ainsi que sur l'étude des propriétés de récepteur moléculaire du rotaxane. L'enfilage du bis-macrocycle porphyrinique par le rail à deux chélates a mené à la formation d'un [4]pseudorotaxane, puis le [4]rotaxane cible a été obtenu par réaction "click" (**Figure 4**). Ce rotaxane a été caractérisé par spectrométrie de masse, par spectroscopie d'absorption UV-visible et par de nombreuses expériences de RMN dans différents solvants (^{1}H, ^{13}C, COSY, NOESY, HSQC, HMBC, DOSY, températures variables). La RMN montre une perte de symétrie dans l'assemblage final par rapport à ses constituants libres. Nous proposons une conformation torsadée pour le rotaxane en solution, avec des rails non parallèles entre eux. Une telle conformation serait favorisée par la flexibilité du bis-macrocycle porphyrinique. En effet, ce composé possède des connecteurs flexibles entre les différents groupements fonctionnels: des chaînes éthylène-glycol sont incorporées dans le macrocycle, et une liaison C-C simple relie la

porphyrine aux macrocycles, permettant une rotation des sites chélatants par rapport au plan du noyau porphyrinique. La RMN du rotaxane montre également que plusieurs conformations différentes sont en équilibre en solution, et cet équilibre est dépendant du solvant. L'une des conformations est largement majoritaire dans le dichlorométhane, cependant les différentes conformations s'échangent à l'échelle de temps de la RMN dans les autres solvants testés, comme l'attestent les signaux larges observés à température ambiante. La caractérisation par absorption UV-visible a mis en évidence un couplage excitonique entre les deux porphyrines du rotaxane, témoignant ainsi de la proximité spatiale des porphyrines.

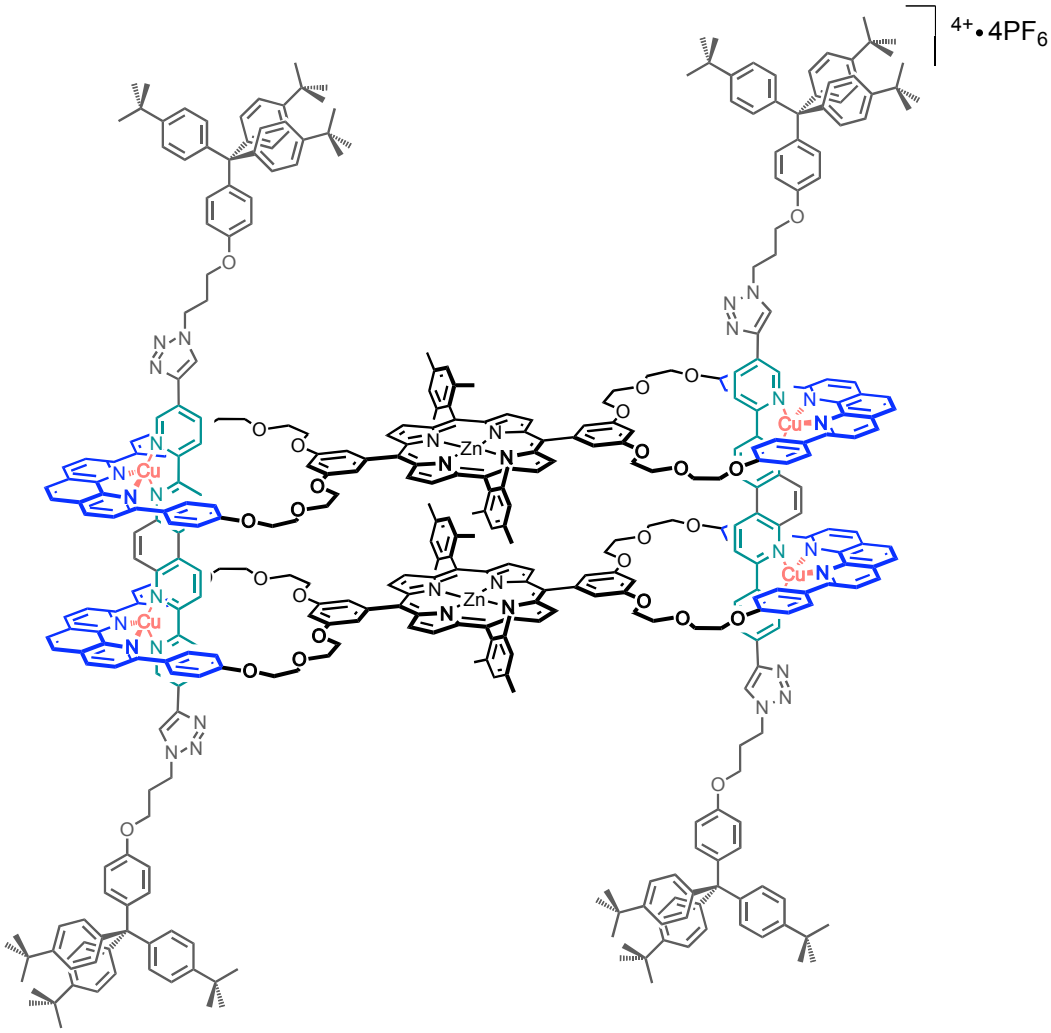

Figure 4. Structure chimique du [4]rotaxane.

Afin de tester ses propriétés de récepteur moléculaire, les constantes d'association du rotaxane avec diverses molécules invitées ont été mesurées. Les substrats choisis sont des ligands azotés ditopiques rigides de longueur croissante (**Figure 5**). La coordination des différentes molécules invitées avec le [4]rotaxane a été étudiée par spectroscopie d'absorption UV-visible.

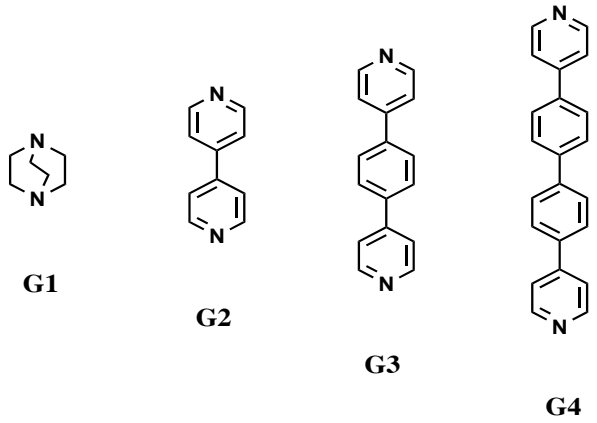

Figure 5. Molécules invitées testées avec le [4]rotaxane.

Dans le cas du DABCO (**G1**), un complexe d'inclusion du DABCO entre les deux porphyrines du rotaxane se forme en présence de quantités sub-stœchiométriques de substrat, et un complexe de stœchiométrie 2:1 (DABCO : rotaxane) se forme en présence d'excès de DABCO. Dans le cas de **G2**, **G3** et **G4**, seul le complexe d'inclusion de stœchiométrie 1:1 est formé, comme l'attestent les points isosbestiques observés et les valeurs des constantes d'association. A titre d'exemple, les spectres de titration obtenus pour le substrat **G2** sont représentés sur la **Figure 6**.

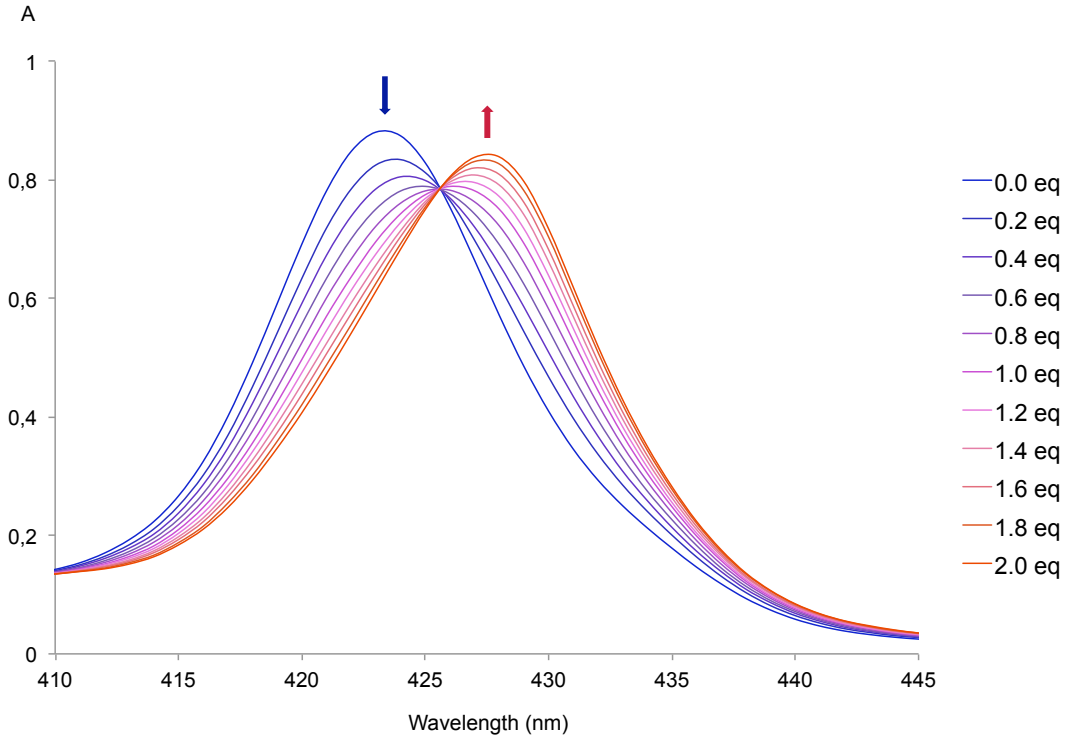

Figure 6. Titration UV-visible (bande de Soret) pour la complexation entre la 4,4'-bipyridine **G2** et le [4]rotaxane.

Les constantes d'association mesurées pour les différentes molécules invitées sont résumées dans le **Tableau 1**. Les valeurs obtenues pour les substrats **G2** et **G3** sont très proches, ce qui atteste de la flexibilité du rotaxane. La molécule **G3**, longue de 11.4 Å, peut se loger entre les deux porphyrines du rotaxane tout aussi bien que **G2** qui mesure 7.1 Å. La molécule invitée **G4** a une constante d'association plus faible avec le rotaxane, probablement du fait de contraintes stériques. Cependant, le fait que cette molécule forme un complexe hôte/invité avec le rotaxane montre que ce dernier peut adopter des formes très variables et se "gonfler" de manière exceptionnelle lors de l'insertion d'une molécule invitée très longue (15.8 Å).

Tableau 1. Constantes d'association des molécules invitées **G1** à **G4** avec le [4]rotaxane. *pour les complexes hôte/invité de stoechiométrie 1:1. Dans le cas du DABCO (**G1**), des complexes 1:2 sont également formés avec une constante d'association de log K_2 = 14.5 ± 0.2.

Molécules invitées	log K*	Distance N-N en Å (d'après des données cristallographiques)
G1	8.1 ± 0.5	2.6
G2	6.2 ± 0.1	7.1
G3	6.1 ± 0.1	11.4
G4	5.6 ± 0.1	15.8

Ainsi, nous avons conçu, synthétisé et entièrement caractérisé un nouveau [4]rotaxane. Les études hôte/invité ont montré que le rotaxane présente des propriétés très intéressantes, puisqu'il s'agit d'un excellent récepteur moléculaire pour des substrats de longueurs variables. La distance entre les plaques porphyriniques du rotaxane peut s'adapter à la taille de la molécule invitée, d'une manière analogue à l'ajustement induit du site actif de certaines enzymes par la complexation du substrat.

IV. Vers un nouveau Bis-Macrocycle Porphyrinique Rigide

Afin d'obtenir un rotaxane pouvant changer la conformation d'une molécule invitée par compression, nous avons conçu une nouvelle porphyrine liée à deux anneaux, plus rigide que la celle décrite en II. et III. La synthèse de ce nouveau bis-macrocycle implique l'utilisation de méthodes développées par le groupe du Professeur Crossley, qui a réalisé de nombreuses études sur des porphyrines possédant un système aromatique étendu. Cette synthèse a donc été entreprise dans le cadre de ma cotutelle de thèse avec l'Université de Sydney.

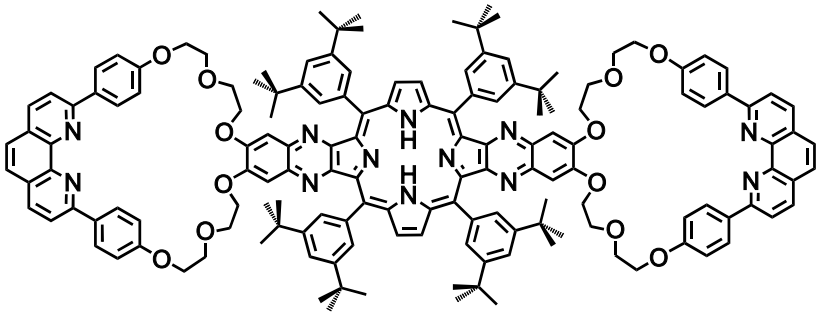

Figure 7. Projet de nouveau bis-macrocycle porphyrinique rigide.

La nouvelle molécule cible est une porphyrine liée à deux macrocycles par un pont rigide, et non plus par une liaison C-C simple comme dans le système décrit précédemment. Les macrocycles contiennent le même site chélatant de type dpp que le macrocycle utilisé dans les parties I et II. Ils sont reliés à la porphyrine par un cycle pyrazine au niveau des positions β, ce qui résulte en un dérivé de type bis(quinoxalino)porphyrine présentant un système aromatique étendu (**Figure 7**). Cependant, de nombreuses difficultés ont été rencontrées lors de la synthèse et la molécule cible n'a pas encore été obtenue. La stratégie de synthèse a dû être modifiée à plusieurs reprises du fait d'étapes posant problème. La méthode finalement retenue consistera à condenser un macrocycle fonctionnalisé par deux amines sur une porphyrine tétra-one (**Figure 8**). A l'heure actuelle, un macrocycle comportant deux amines protégées sous forme d'imines a été obtenu.

Après la synthèse du bis-macrocycle final, un rotaxane pourra être construit à partir du même rail que celui utilisé précédemment. Nous pourrions alors étudier les interactions entre le [4]rotaxane (forme libre et forme complexée avec du cuivre) et des substrats de diverses longueurs susceptibles d'être complexés à l'intérieur de l'espace disponible entre les deux porphyrines, afin de tester la capacité du récepteur à comprimer ces substrats.

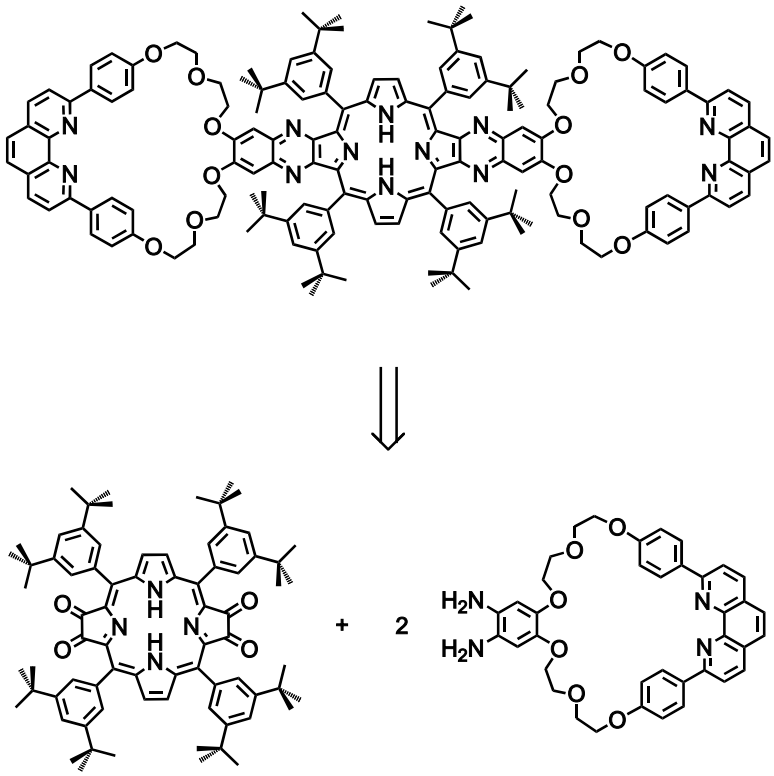

Figure 8. Schéma rétrosynthétique pour l'obtention du nouveau bis-macrocycle porphyrinique.

V. Un [3]Rotaxane présentant une Architecture Nouvelle et son Précurseur: Une Porphyrine de Zinc liée à Quatre Macrocycles

Dans le but d'augmenter les possibilités d'enfilage et d'élaboration de multi-rotaxanes, une étude portant sur une nouvelle porphyrine reliée à quatre macrocycles coordinants a également été entreprise (**Figure 9**). Cette porphyrine a été obtenue par condensation du pyrrole avec le précurseur macrocyclique décrit dans la partie I. La synthèse du tétra-macrocycle porphyrinique a été optimisée, et il est à présent obtenu avec un rendement de 25%. La méthode utilisée est dérivée de la méthode d'Adler-Rothemund pour la synthèse des porphyrines (chauffage à reflux de l'aldéhyde et du pyrrole dans l'acide propionique). L'emploi d'un mélange d'acide propionique et de nitrobenzène comme co-solvant ainsi que l'activation par micro-ondes ont permis d'augmenter le rendement de manière significative. La porphyrine a ensuite été métallée par le zinc(II) de manière quantitative.

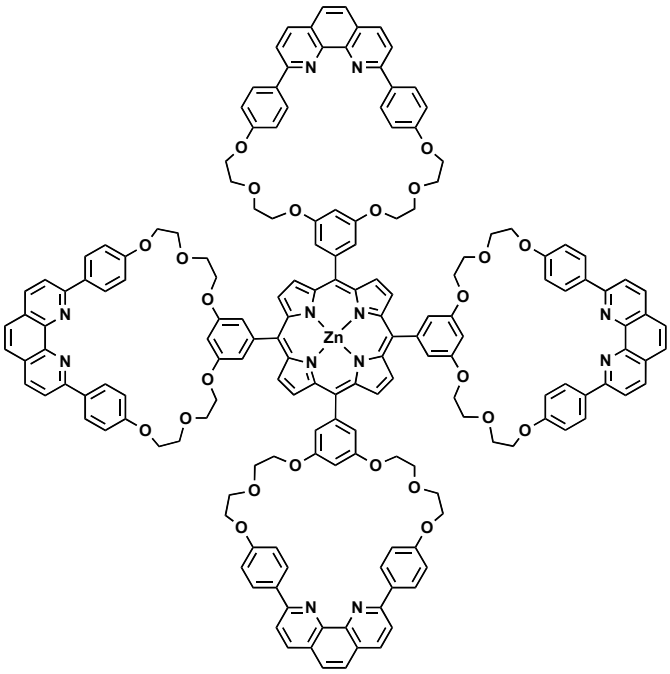

Figure 9. Structure chimique du nouveau tétra-macrocycle porphyrinique.

A partir de ce nouveau tétra-macrocycle porphyrinique, nous envisagions de construire un [6]rotaxane. Ce rotaxane serait constitué de deux porphyrines superposées, dont les anneaux seraient enfilés par quatre rails perpendiculaires au plan des porphyrines (**Figure 10**). Un tel système, comportant des porphyrines à quatre anneaux, pourrait permettre un contrôle géométrique de la presse encore plus strict que celui présenté dans l'introduction, qui était basé sur l'utilisation d'une porphyrine à deux anneaux.

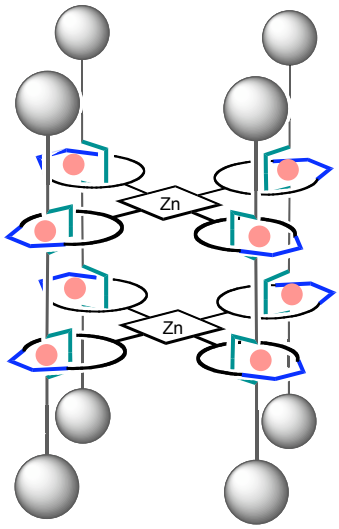

Figure 10. Représentation d'un [6]rotaxane composé de deux tétra-macrocycles porphyriniques et de quatre rails.

L'effet "d'assemblage et d'enfilage" (en anglais: "gathering and threading") du cuivre(I) a été exploité lors de la réaction d'enfilage des axes à deux chélates (présentés en II.) sur le tétra-macrocycle. Après introduction des bouchons aux extrémités des axes, un [3]rotaxane a été obtenu (**Figure 11**).

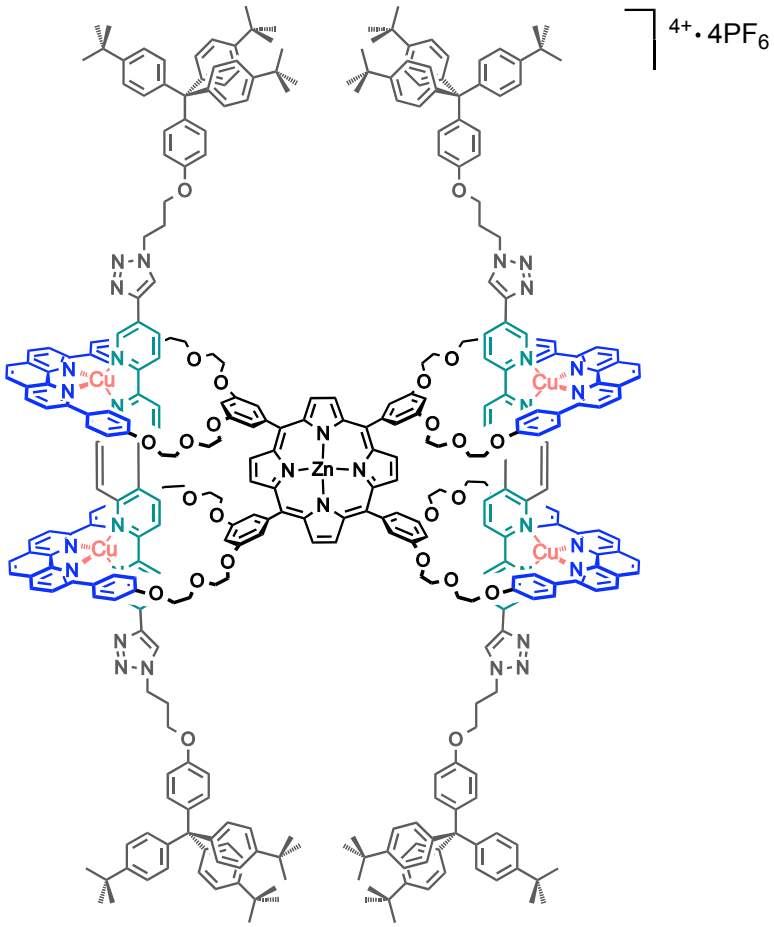

Figure 11. Structure chimique du [3]rotaxane obtenu.

Ce composé n'a pas la géométrie requise pour piéger un substrat, mais il possède une architecture très originale. Le rotaxane comprend un tétra-macrocycle porphyrinique central et deux rails, chaque rail étant enfilé dans deux macrocycles adjacents de la porphyrine.

Dans le cadre d'une collaboration, Nathan Strutt, doctorant dans le groupe du Professeur Stoddart aux Etats-Unis et ancien étudiant en stage dans notre équipe, travaille actuellement sur la synthèse d'un nouveau rail comportant deux sites chélatants plus espacés. L'emploi de ce nouveau rail pour la réaction d'enfilage avec le tétra-macrocycle porphyrinique devrait permettre l'obtention d'un [6]rotaxane. Des études de complexation avec des molécules invitées pourraient alors être menées en l'absence et en présence de cuivre(I), afin de tester les propriétés de presse moléculaire du rotaxane.

Conclusion

Ces travaux de recherche ont été réalisés dans le cadre d'une Cotutelle de thèse entre l'Université de Strasbourg et l'Université de Sydney. Deux nouvelles porphyrines portant deux et quatre macrocycles coordinants (respectivement) ont été synthétisées. Un [4]rotaxane basé sur le bis-macrocycle porphyrinique a été synthétisé et entièrement caractérisé, et les études d'insertion de quatre substrats de longueurs différentes ont montré que le [4]rotaxane se comporte comme un récepteur moléculaire adaptable et gonflable. Un [3]rotaxane possédant une architecture originale a été obtenu à partir du tétra-macrocycle porphyrinique. Nous avons préparé des précurseurs d'un nouveau bis-macrocycle porphyrinique, plus rigide, qui pourra être utilisé dans la construction d'un nouveau [4]rotaxane et pourrait ouvrir la voie vers un modèle de presse moléculaire amélioré.

De futurs travaux pourraient porter sur l'étude de rotaxanes comportant différents métaux au niveau des centres porphyriniques. Par exemple, à l'aide d'un [4]rotaxane comportant une porphyrine de zinc et une porphyrine d'étain, il devrait être possible de piéger des acides aminés ou de courts peptides. La compression d'oligopeptides par la presse moléculaire et l'étude de leur changement de conformation au sein de la presse constituerait un nouveau pas vers un modèle de protéine chaperonne. D'autres recherches futures pourraient porter sur la construction d'espèces intéressantes d'un point de vue topologique à partir du tétra-macrocycle porphyrinique. Par une stratégie de synthèse analogue à celle employée pour la synthèse du [3]rotaxane, nous pourrions former un caténane d'architecture nouvelle, constitué d'un grand anneau enfilé sur les quatre macrocycles de la porphyrine.

Chapter I. General Introduction

The ultimate aim of our research project is to create a chemical system able to trap a guest molecule and to change its conformation by compression. This model is a new type of molecular machine that we named a "Molecular Press". In this thesis we will describe our work and results towards a molecular press. This work was fulfilled as part of a Cotutelle PhD, in a collaboration between the group of Jean-Pierre Sauvage at the University of Strasbourg and the group of Maxwell J. Crossley at The University of Sydney. Chapters II, III and V of this thesis relate to the work performed in Strasbourg. We will discuss the design of new rotaxanes that incorporate porphyrins, and describe their syntheses and properties as molecular receptors. Chapter IV deals with the work accomplished in Sydney. The chemistry of extended porphyrins developed by the group of M. J. Crossley will be exploited in the design of a new porphyrinic building block. As an introduction to this thesis we will give an insight into the fields of rotaxanes, molecular machines, and porphyrins, and explain how we intend to combine the use of rotaxanes and porphyrins in the construction of molecular press prototypes.

I. 1. Rotaxanes: Topology, Synthetic Strategies and Applications

I. 1. a) Interlocked Structures: Catenanes, Rotaxanes and Knots

A topologically interesting branch of chemistry deals with molecules displaying an interlaced structure, like catenanes, rotaxanes and knots.[1-10] In this introduction we do not intend to review this field of research exhaustively; we will give definitions and describe a selection of historical and significant examples of interlocked compounds. A **molecular knot** has a topologically non-trivial structure: it cannot be drawn in two dimensions without any intersection. This feature distinguishes a knot from an eight-shaped molecule for example. A figure-of-eight can be distorted to a simple ring and drawn with no intersection; therefore, it has a trivial topology (**Figure I.1**).

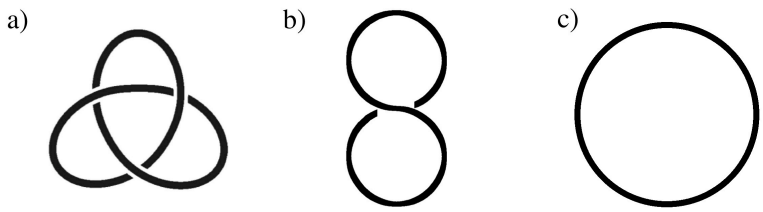

Figure I.1. Schematic views of a) a molecular trefoil knot, b) a molecular figure-of-eight and c) a molecular ring. A knot is topologically non-trivial, whereas the figure-of-eight and ring are trivial structures.

Tying knots on a string is very easy (and often happens involuntarily), and the discovery of complex knotted DNA architectures proved that it is possible even at the nanometric scale.[11-13] However, the construction of synthetic molecular knots turned out to be very challenging. The first successful strategy for the synthesis of a molecular trefoil knot, reported in 1989 by C. O. Dietrich-Buchecker and J.-P. Sauvage, was based on the metal-templated formation of double-stranded helices. After ring closing and demetallation a macrocycle of the desired trefoil-knotted topology was obtained (**Figure I.2**).[14] Careful design of the system allowed for the formation of trefoil knots in high yields using this strategy, as reported in subsequent papers.[15]

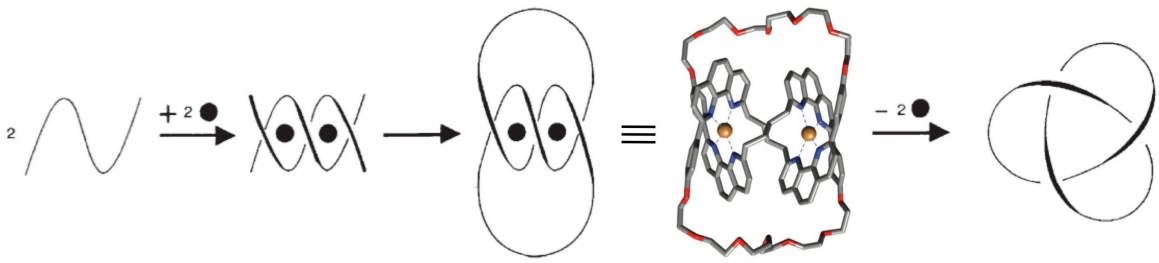

Figure I.2. First synthetic trefoil knot reported by C. O. Dietrich-Buchecker and J.-P. Sauvage. The strategy involves the formation of a double helical complex of bis-phenanthroline ligands around two copper(I) centres, followed by ring closure and demetalation. The knotted structure of the Cu(I) complex was confirmed by X-ray crystallography.[10,14,16,17]

Some alternative strategies for the formation of molecular trefoil knots were reported later. The group of F. Vögtle described the first metal-free synthesis of a trefoil knot. The knot is formed in one step from short linear precursors assembled *via* hydrogen bonds.[18] C. A. Hunter and coworkers synthesised a trefoil knot by complexation of a linear tris-bipyridine ligand with Zn(II),[19] followed by ring-closing metathesis and demetalation.[20] The group of J. S. Siegel prepared a trigonal ligand with six bipyridine chelates arranged around a 1,3,5-trisubstituted benzene core and preorganised by copper(I) coordination.[21] A knotted structure was subsequently obtained by homocoupling between the terminal alkyne groups.[22]

The class of the **catenanes** constitutes another type of topologically non-trivial molecules. A catenane is composed of (at least) two mechanically interlocked macrocycles (**Figure I.3.** a). The mechanical link in a catenated structure makes it impossible to separate the rings without breaking a chemical bound and opening one of the macrocycles. In a similar manner to a molecular knot, a catenane has a topologically non-trivial structure: it cannot be drawn in two dimensions without any intersection. Historically, the formation of the first synthetic catenane was evidenced by E. Wasserman in 1960.[23] However, the statistical method employed gave rise to a very low yield of catenane, which could not be isolated from non-catenated macrocycles. In 1964, G. Schill and A. Lüttringhaus reported the *directed* synthesis of a catenane.[24] The limitations of their elegant approach arise from the numerous synthetic steps required for the formation of the catenane. A significant breakthrough in the synthesis of catenanes was made by C. O. Dietrich-Buchecker and J.-P. Sauvage in 1983 (**Figure I.3.** b).[25] They introduced the use of a metal template to gather and preorganise the building blocks in an interlaced way before cyclisation of the rings and demetallation to yield the metal-free catenane. This method affords catenated compounds in high yields. The groups of J. F. Stoddart, C. A. Hunter and F. Vögtle later made significant contributions to the field of synthetic catenanes. Templated syntheses were used in all cases; the catenane made by J. F. Stoddart and coworkers is based on electron donor-acceptor interactions,[26] while C. A. Hunter and F. Vögtle independently described the syntheses of two very similar catenanes based on hydrogen bonds and π-π interactions.[27,28]

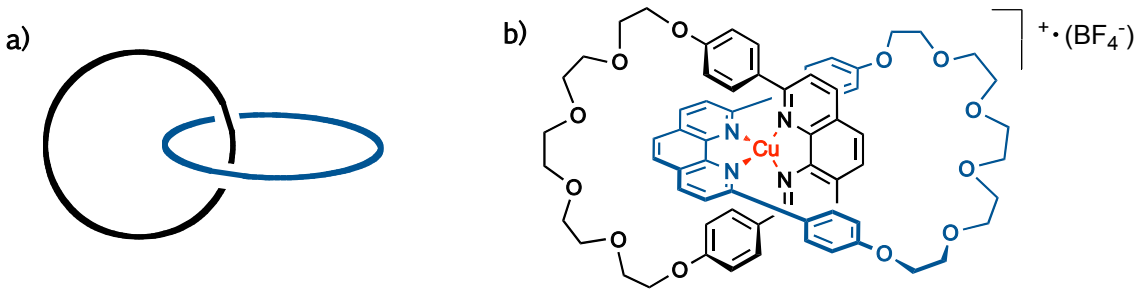

Figure I.3. a) Schematic view of a [2]catenane. b) First copper(I)-templated catenane synthesised by C. O. Dietrich-Buchecker and J.-P. Sauvage.[25]

While the macrocycles of the catenane depicted in **Figure I.3**. b) consist exclusively of strong covalent bonds, it is also possible to synthesise catenanes whose rings are closed by labile metal-ligand coordination bonds. The first instance of a non-covalent catenane was described by M. Fujita in 1994.[29] He observed the self-assembly of a [2]catenane in solution from a preformed macrocycle composed of two bis-pyridyl ligands and two Pd(II) centres (**Figure I.4**). The driving force for the formation of the catenane is attributed to aromatic-aromatic interactions between the phenylene moieties of the bis-pyridyl ligands in the interlocked structure.

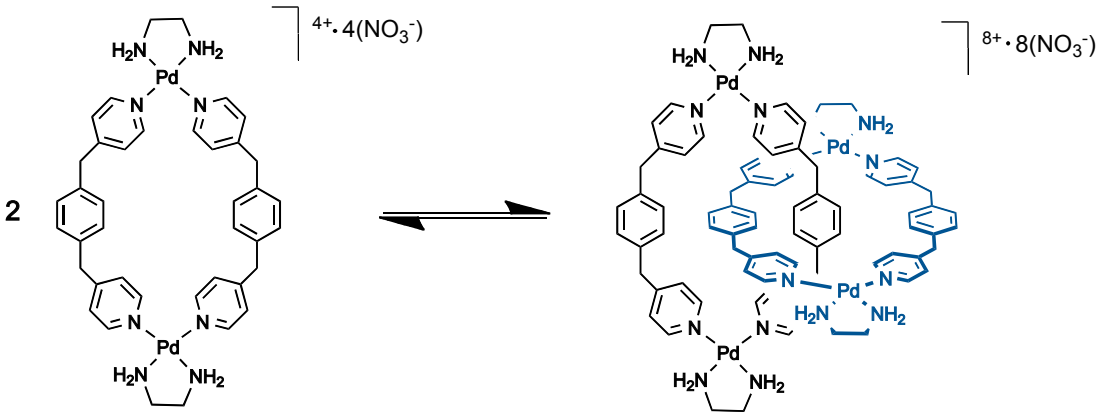

Figure I.4. A non-covalent catenane assembled *via* labile metal-ligand coordination bonds. The [2]catenane is in equilibrium with the corresponding non-interlocked macrocycles. The catenated form is largely predominant at high concentration.[29]

Since these pioneering works on the formation of [2]catenanes, the syntheses of numerous catenated compounds have been reported. Some of them consist of more than two interlocking rings. Notable reports of such molecules include catenanes composed of three to five interlocking rings,[30,31] a cyclic [3]catenane made of three interlocking bis-macrocyclic components,[32] and a [5]catenane resembling the Olympic rings, named olympiadane.[33]

A class of interlocked molecules called **rotaxanes** is derived from an extension of the definition of catenanes. By elongating one of the rings of a [2]catenane infinitely the structure can be seen as equivalent to a ring threaded by an infinite axle. Chemists imagined the substitution of the infinite axle for a finite axle ending with bulky groups called stoppers, that are big enough to prevent unthreading of the ring. The definition of the simplest rotaxane emerged from this idea: a *[2]rotaxane* is a molecular species composed of a ring threaded on a stoppered axle, reminiscent of the shape of a dumbbell (**Figure I.5**. a). According to the mathematical definition a rotaxane is a trivial object. Indeed, it is theoretically possible to dissociate the ring from the axle and consequently to draw the two components without crossing by simply enlarging the ring. In practice, if the stoppering groups are big enough then it is physically impossible to unthread the macrocycle from the axle, so rotaxanes are definitely part of the family of interlocked molecules. A *pseudorotaxane* can be an intermediate in the synthesis of a rotaxane; it is the non-stoppered equivalent of the rotaxane structure (**Figure I.5**. b).

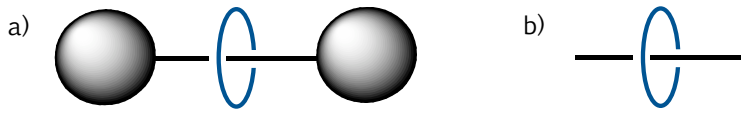

Figure I.5. Schematic views of a) a [2]rotaxane composed of a ring threaded on an axle ending with bulky stoppers (to prevent unthreading); and b) a pseudorotaxane.

After the theoretical mention of the [2]rotaxane structure by H. L. Frisch and E. Wasserman,[1] the first rotaxane was synthesised using a statistical method in 1967.[34] The authors, I. T. Harrison and S. Harrison, proposed the name *hooplane* for this type of structure, but the term *rotaxane* was later adopted, as suggested by G. Schill who described the first *directed* rotaxane synthesis in 1969.[35] His approach involved the use of covalent bonds as templates in the construction of the desired interlocked architecture (**Figure I.6**). He synthesised a bis-macrocycle with two functionalised chains hanging out on either side of the plane of the bis-macrocycle. Introduction of bulky end groups and cleavage of the orienting covalent bonds afforded the free [2]rotaxane.

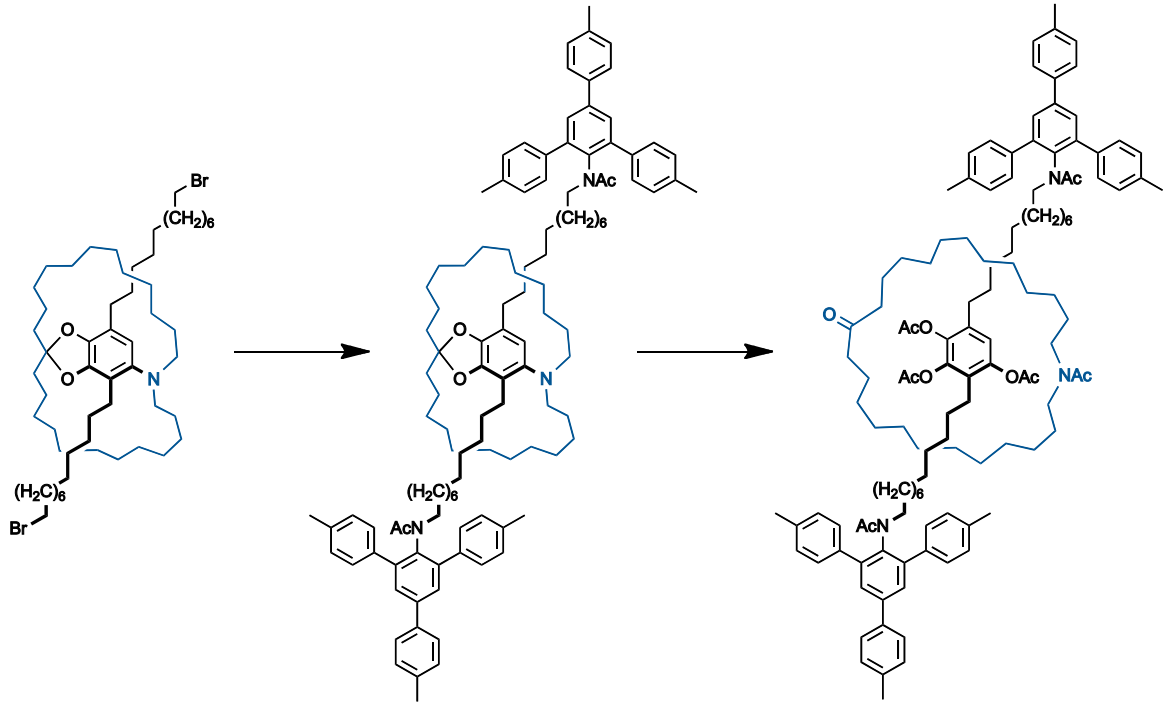

Figure I.6. Strategy used by G. Schill in the first directed rotaxane synthesis, involving the use of covalent bonds as templates.[35]

Besides the catenanes, rotaxanes and knots, a number of other interlocked structures have attracted the attention of chemists over the years. For instance, molecular Solomon links, Borromean rings, and rotacatenanes (combinations of rotaxane and catenane structures) have been described (**Figure I.7**).[10,36-39] The beauty of mechanically interlocked molecules has fascinated topological chemists for decades and their challenging syntheses keep inspiring them. The elaboration of new interlocked architectures, and in particular rotaxane-type structures, forms part of the motivation for this PhD project.

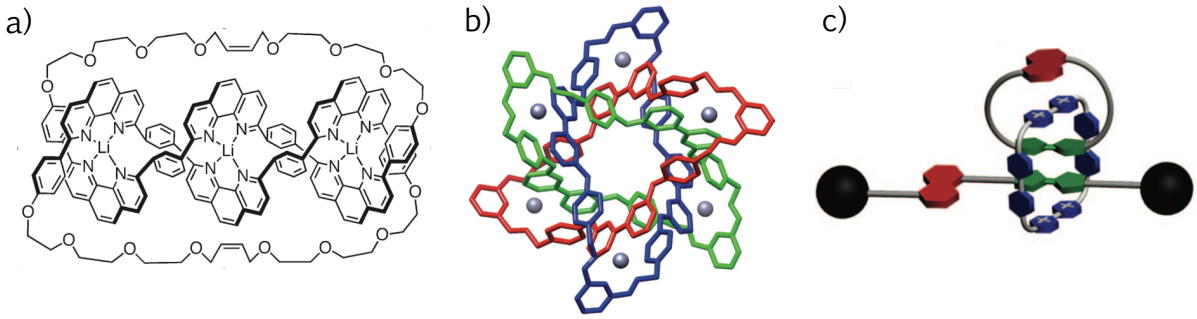

Figure I.7. Examples of other interlocked structures. a) A molecular Solomon link (doubly interlocking [2]catenane);[36] b) Molecular Borromean rings (three interlocking, but non-catenated macrocycles);[37] c) A [3]rotacatenane (combination of [2]catenane and [2]rotaxane structures).[39]

I. 1. b) Strategies for the Synthesis of Rotaxanes

Various synthetic strategies have been developed towards the formation of rotaxane structures. A key point for obtaining rotaxanes in high yields resides in the use of a *templated* synthesis that will drive the system towards the formation of the interlocked species and favour it over the independent components. This can be done either by means of coordination to a metal cation, or *via* interactions between the ring and the axle, or their precursors (*e.g.* hydrogen bonds, aromatic donor-acceptor interactions or hydrophobic interactions). A few examples are depicted in **Figure I.8**.

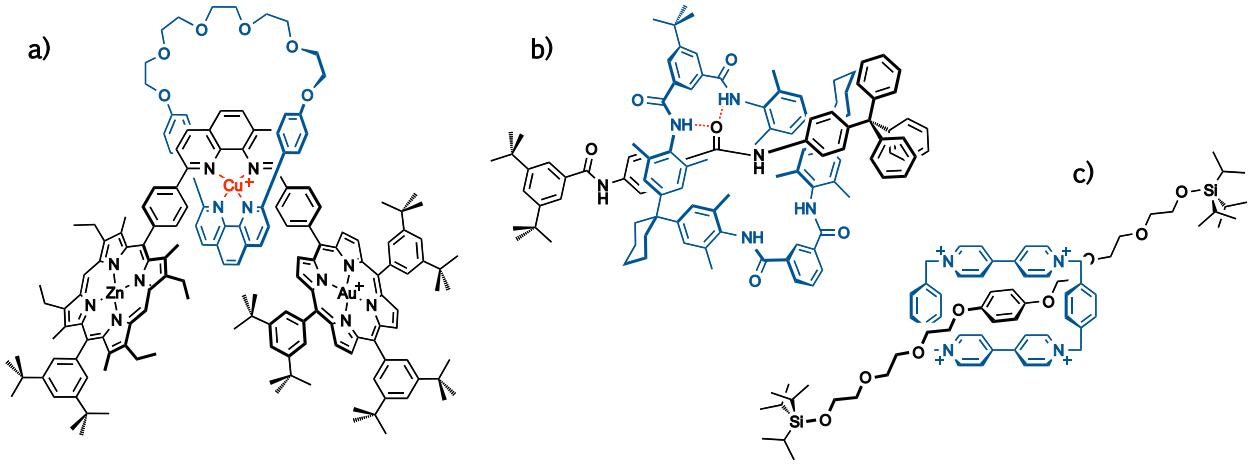

Figure I.8. Three examples of rotaxanes assembled *via* directed strategies. a) Use of the gathering effect of the copper(I) template;[40] b) Preorganisation of the system *via* hydrogen bonding between the ring component and the dumbbell component;[41] c) Interlocking favoured by π-donor/π-acceptor interactions between the axle and the macrocycle.[42]

Copper(I) can be used as a templating agent as described for the synthesis of catenanes in the previous part. Since copper(I) preferentially forms tetrahedral complexes, coordination with two bidentate chelates affords complexes whose ligands are orthogonal to each other and therefore ideally preorganised for the formation of an interlocked species. Metal templating has been used in the synthesis of many rotaxanes (*e.g.* the rotaxane depicted in **Figure I.8**. a)[40,43-45] and was chosen in the design of the rotaxanes described in this thesis.

Other assembling methods involving non-covalent interactions between the ring and dumbbell precursors have been widely exploited. For instance F. Vögtle and coworkers designed an amide-containing macrocycle and axle that interact *via* multiple hydrogen bonds (**Figure I.8**. b).[41] J. F. Stoddart's "blue box" macrocycle is a very versatile tool for the assembly of rotaxanes based on aromatic donor-acceptor interactions (**Figure I.8**. c).[42] Threading of cyclodextrins driven by hydrophobic interactions,[46] and molecular recognition between crown ethers and cationic axles[47] are other efficient methods for the assembly of rotaxanes.

In addition to these "passive" template methods, an "active" metal template strategy was developed and reported independently by the groups of D. A. Leigh and S. Saito in 2006. In this approach, the metal template plays a dual role: *(i)* it gathers the rotaxane precursors and preorganises them in an intertwined geometry; and *(ii)* it serves as a catalyst in the covalent bond formation between the dumbbell precursors that will lock the system into the threaded architecture.[48,49]

An original approach was taken recently by the group of M. Famulok who combined the fields of rotaxane synthesis and DNA nanotechnology. They reported the formation of the first [2]rotaxane whose dumbbell and macrocycle are both exclusively made of double-stranded DNA (**Figure I.9**). In this case the system is assembled by base-pairing interactions.[50]

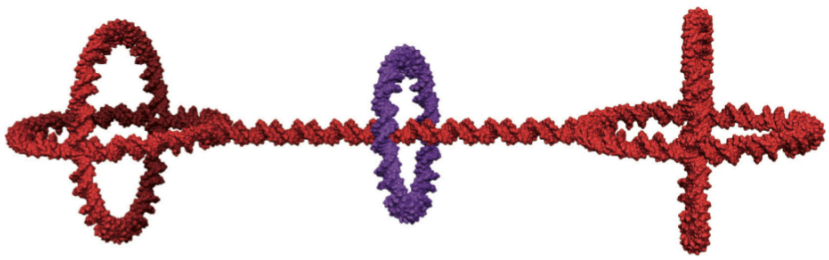

Figure I.9. The first [2]rotaxane exclusively made of double-stranded DNA, assembled *via* base-pairing between the axle and the ring.[50]

I. 1. c) [2]Rotaxanes and Multi-Rotaxanes

The architectures described above belong to the simplest form of rotaxanes: they consist in one ring and one dumbbell, *i.e.* two interlocked organic components that are not covalently linked together. This type of structure is denominated as a [2]rotaxane. More generally, a [*n*]rotaxane is composed of several interlocked rings and threads, the number *n* designating the total number of independent organic components. According to this definition a single denomination can designate several types of rotaxane architectures. For example, two rings threaded on the one dumbbell form a [3]rotaxane (**Figure I.10**. a). Alternatively, a [3]rotaxane can be composed of two axles passing through the same macrocycle (**Figure I.10**. b), or of two axles, each of them passing through one of the rings formed by a bis-macrocycle (**Figure I.10**. c and d). In this last case, the rotaxane possesses two dumbbells threaded through two rings. However, the structure corresponds to a [3]rotaxane, not a [4]rotaxane, because the rings are covalently linked together.

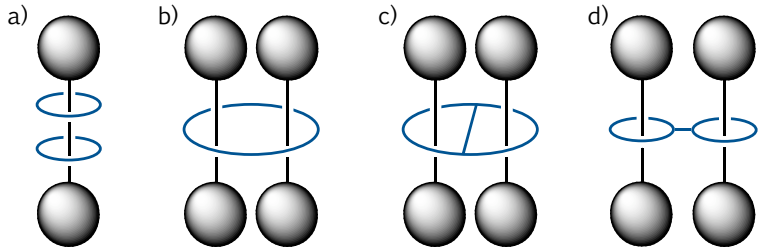

Figure I.10. Different possible geometries for a [3]rotaxane. Instances of these geometries have been described in the literature: a) Two rings threaded on one axle;[51-54] b) Two axles passing through the same ring;[55-57] c) and d) Two axles passing through the rings formed by a bis-macrocyclic component.[58,59]

The geometries depicted above give an insight into the countless potential geometries of rotaxanes. The design of new rotaxane architectures is a fascinating research area that will probably keep chemists busy for many more years. Rotaxane structures can be finite or polymeric.[60,61] Various finite multi-rotaxanes have been described, including [3]-, [4]-, [5]- and [7]rotaxanes.[62-65] At the boundary between oligo- and polyrotaxanes, a linear [11]rotaxane composed of ten rings threaded on one long axle has also been described.[64] A characteristic feature of the [7]rotaxane synthesised by Y. Liu and coworkers is the incorporation of two different macrocycles. The *hetero*-[7]rotaxane is composed of two dumbbells, each of them bearing two rings and connected to each other *via* threading through a fifth, large ring (**Figure I.11**).[65] These multi-rotaxanes pave the way towards the still challenging synthesis of more sophisticated higher-order rotaxanes.

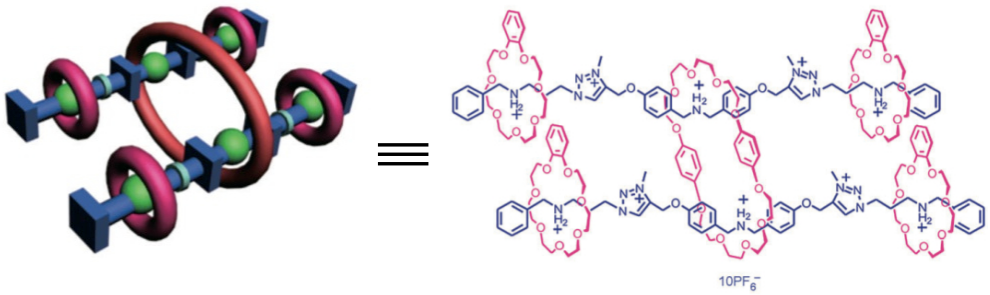

Figure I.11. An original rotaxane architecture: a hetero-[7]rotaxane incorporating two different macrocycles.[65]

I. 1. d) Applications of Rotaxanes

The interest of rotaxanes is not limited to their challenging syntheses; they find applications in various fields.[66,67] For instance, rotaxanes with appended chromophores have been used as light-harvesting antennae in the design of photosynthetic models.[68-70] Other rotaxane systems have been designed and shown properties in catalysis,[71] anion sensing[72,73] and peptide delivery.[74] Another, novel application was developed by B. D. Smith, who described squaraine rotaxane endoperoxides exhibiting remarkable chemiluminescent properties, paving the way towards new optical imaging agents.[75] The system is a [2]rotaxane whose axle contains a central squaraine unit and whose ring incorporates an anthracene endoperoxide group (**Figure I.12**). The endoperoxide is stable at low temperature, but undergoes a cycloreversion reaction upon heating to body temperature. The energy released by the reaction is transferred to the squaraine chromophore, which emits near-infrared light that can pass through a living mouse.

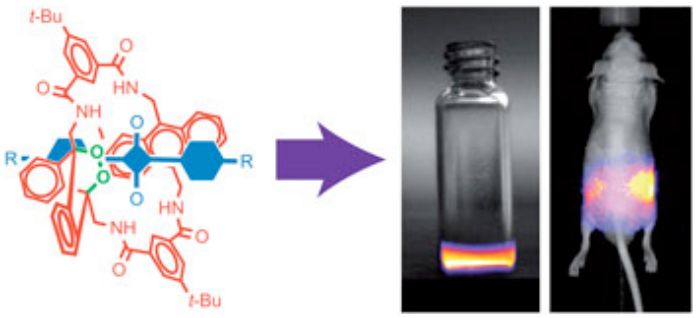

Figure I.12. A thermally activated, near infrared chemiluminescent squaraine rotaxane for optical imaging.[75]

Another major field of applications of rotaxanes is the vast domain of molecular machines. This topic will be covered in the next part of this introduction.

I. 2. Molecular Machines: From Natural Systems to Synthetic Devices

By definition, a **molecular machine** is a molecular system able to perform mechanical work. A molecular machine is generally composed of at least two components that can be set in motion in relation to each other. This motion must be triggered by an external stimulus, and be controlled and of relatively great amplitude, by opposition to the Brownian motion that animates all molecules. Typically, the stimulus can be chemical (variation of pH, exchange of ion or other chemical signal), photochemical or electrochemical. Moreover, the motion of a molecular machine is characterised by its reversibility: the system must be able to go back to its initial state and start over the cycle. Molecular machines were defined by analogy with macroscopic machines. In the macroscopic world, a machine is an apparatus that functions by applying a mechanical power, thereby inducing changes in the relative positions of the components. The relative motion of the constituents of a machine at the molecular level is reminiscent of a macroscopic machine at work.[76-79]

Molecular devices were defined using a similar analogy between the macroscopic and the nanometric worlds. The term "molecular device" refers to molecular systems that have a specific functionality, other than their intrinsic chemical reactivity; it is a broader concept than molecular machines. For example, molecular electronics and molecular sensors fall into the category of molecular devices. It would be impossible in this introduction to provide an exhaustive review on molecular machines and devices; we will describe only a short selection of some remarkable natural and synthetic systems.

I. 2. a) Natural Molecular Machines

Chemists may have defined molecular machines, but Nature invented them. Various nanometric molecular machines are used in nature to carry out essential functions in living organisms. The **ATP synthase** is a beautiful example of a natural machine. ATP synthases are membrane protein complexes present in vegetal, animal and bacterial organisms. The role of the enzyme is to produce ATP (adenosine triphosphate) from ADP (adenosine diphosphate) and inorganic phosphate P_i. It is subdivided in two major components: a central part composed of the

protein subunits γ, ε and c often referred to as *rotor*, capped by a cylindrical headpiece ($\alpha_3\beta_3$) called *stator* (**Figure I.13**).[80,81] The action of the enzyme is triggered by a proton flow through the membrane. This proton flow causes the rotation of the rotor unit, and the motion of the rotor in relation to the stator induces conformational changes in the α and β subunits, which in turn promote the chemical reaction. Each β sub-protein has an active site that passes sequentially through three different states associated to the three steps of the reaction: fixation of the substrates ADP and P_i, chemical transformation into ATP, and release of the product. Switching from one state to the other is promoted by the conformational changes triggered by rotation of the γ subunit. It is noteworthy that the motion of ATP synthase is reversible. The rotor component can rotate in the reverse direction to pump protons into the cell.[81] The complex mechanisms involved in the functioning of ATP synthase make it one of the most fascinating molecular rotors.

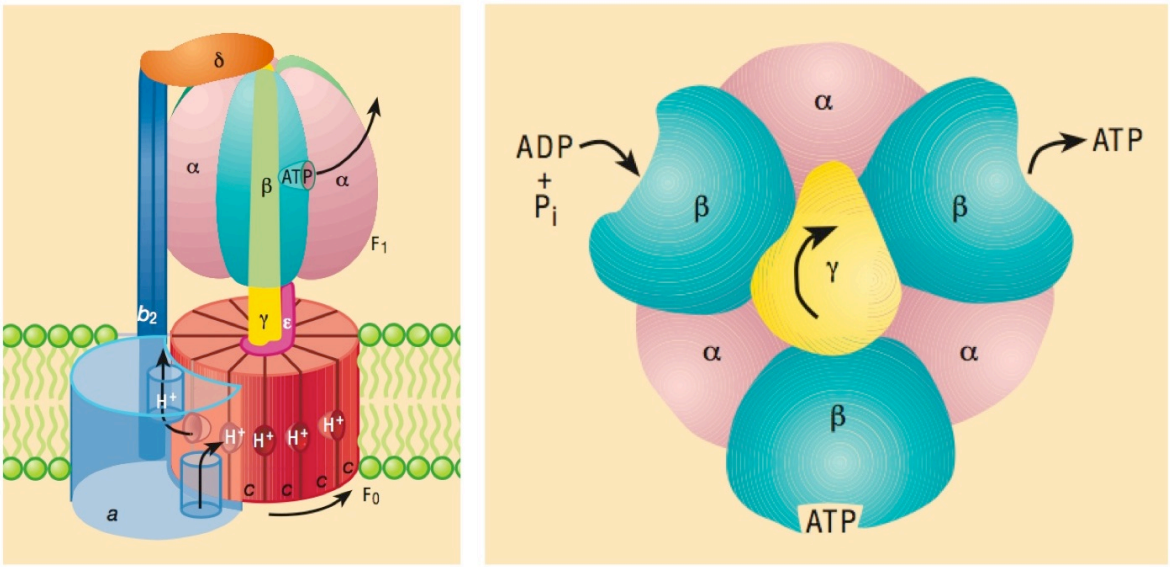

Figure I.13. The ATP synthase, a natural molecular machine.[80,81] ATP synthases are rotary motors: a flow of protons through the membrane causes rotation of the rotor component (γ, ε and c) in relation to the stator component ($\alpha_3\beta_3$). This motion triggers sequential conformational changes in the β subunits, which are responsible for the consecutive steps of the formation of ATP: binding of the substrates ADP and P_i, chemical transformation and release of the newly formed ATP.

The **chaperone proteins**, or chaperonins are other inspiring examples of natural molecular machines. Native proteins have a defined three-dimensional structure that is essential to their function. Most newly formed proteins are not fully folded into their active structure and present hydrophobic sites at their surface that can cause undesired aggregation or misfolding in the cytosol. They need to be isolated from the intracellular medium in an environment that allows correct folding. Chaperonins possess an internal cavity where unfolded proteins can be

trapped. They assist the folding of newly translated proteins in the cavity using the energy derived from binding and hydrolysis of ATP. An extensively studied example of chaperone protein is GroEL, a chaperonin found in bacteria. The GroEL system is an oligomer of fourteen proteins assembled in a double cylindrical cavity. It is associated to the co-chaperonin GroES, a lid-shaped protein heptamer that can interact with GroEL to close its cavity (**Figure I.14**).[82,83]

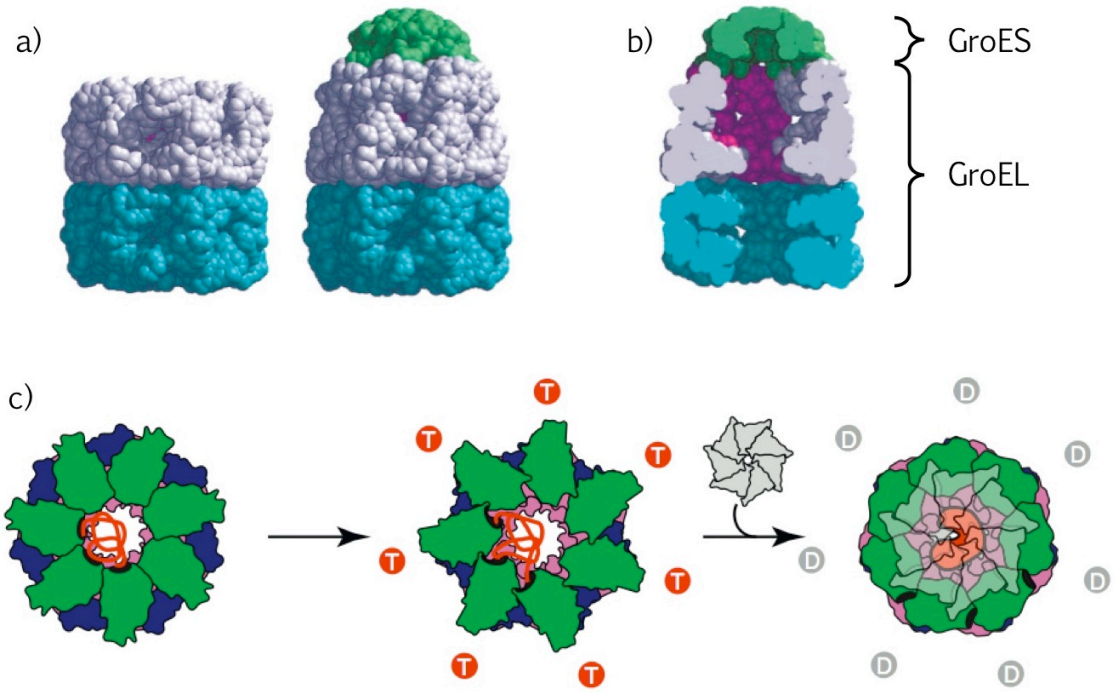

Figure I.14. a) Structure of the GroEL chaperonin and the GroEL/GroES complex (side view). b) Section of the internal cavities of the GroEL/GroES complex. c) Mechanism of action of the GroEL chaperonin: (i) an unfolded protein (red) is trapped at the entrance of the cavity (green/blue); (ii) fixation of ATP (T) triggers conformational changes and binding of the GroES lid (grey) and allows folding of the guest protein; (iii) hydrolysis of ATP to ADP (D) weakens the GroEL/GroES complex and induces release of the lid and folded protein.[83,84]

The mechanism of action of the GroEL chaperonin involves several key steps. First, an unfolded protein binds to the hydrophobic sites at the entrance of the cavity of GroEL. Then, concerted fixation of seven molecules of ATP on GroEL triggers conformational changes that facilitate binding of the GroES lid. This results in an enlargement of the cavity that allows folding of the guest protein. Finally, hydrolysis of the bound ATP to ADP weakens the GroEL/GroES complex and induces release of the lid and folded protein.[77,84] The action of the chaperonin can be summarised in three consecutive steps: capture, folding and release of a guest protein.

I. 2. b) Artificial Molecular Machines

As shown by the above examples, Nature has developed extremely efficient tools to direct motion and perform tasks in living organisms. These natural molecular machines are an endless source of inspiration for synthetic chemists. Two approaches can be taken when attempting to reproduce the functions of natural systems or to create new molecular machines. They consist in grafting synthetic units on natural machines,[85] or in designing entirely synthetic devices.[76,79] Both approaches have been widely exploited, and a great variety of artificial molecular machine prototypes have been described.

Most of the synthetic molecular devices developed so far were studied in solution. Although rarer, molecular machines operating in the solid state open the way towards a translation of the molecular motion to the macroscopic level. If the molecules are organised anisotropically (*e.g.* in a crystal) then the controlled motion of individual molecules should result in macroscopic work observable to the unaided eye. M. Irie achieved this with a cocrystal of a dithienylethene derivative and perfluoronaphthalene that acts as a **molecular cantilever**.[86] The dithienylethene unit undergoes photoconversion to the closed-ring isomer upon irradiation with UV light, which causes a slight shape change (**Figure I.15**).

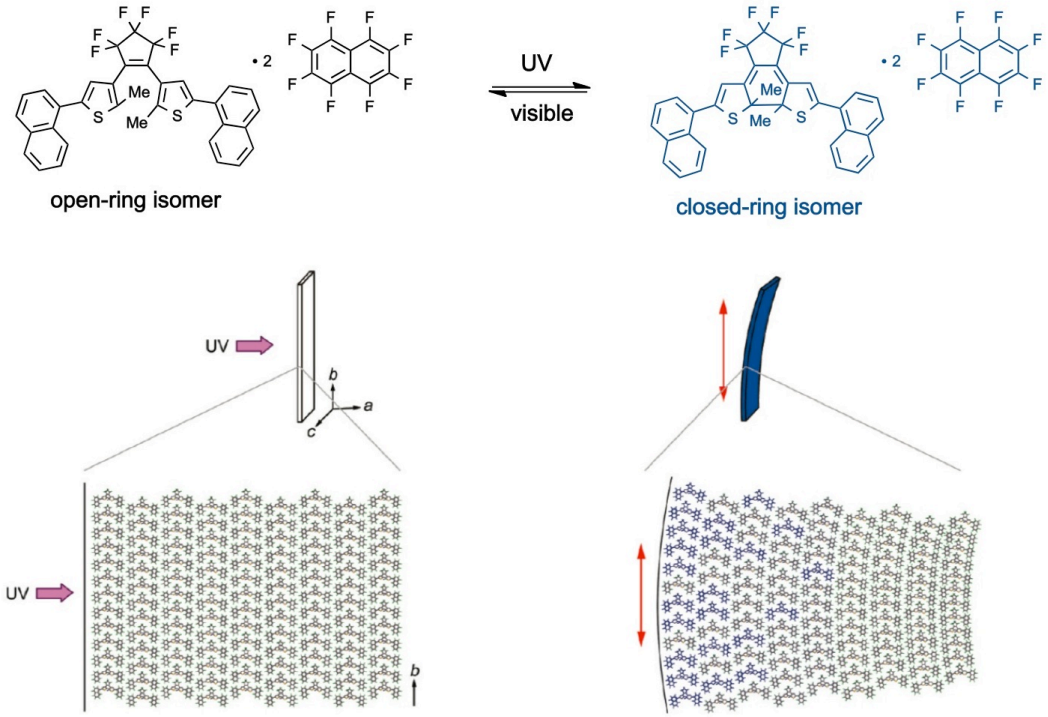

Figure I.15. Macroscopic bending motion of a cocrystal of a dithienylethene derivative and perfluoronaphthalene. The motion is due to the shape change of the dithienylethene units by photocyclisation upon irradiation with UV light.[86]

In the solid state isomerisation occurs near the surface upon irradiation with UV light from one side of the crystal. This results in a directly observable bending motion of a thin, 1-5 mm long, plate-shaped crystal. The process is reversible, and irradiation with visible light brings the system back to its initial shape. This device was successfully used as a cantilever that can lift metal balls in a stunning experiment. A rectangular plate crystal was fixed at the edge of a glass plate and a 2-mm lead ball was loaded onto the crystal. Even though the ball is 275 times heavier than the crystal, it was lifted by nearly 1 millimetre upon irradiation with UV light from below (**Figure I.16**). This experiment is a remarkable demonstration of the potential of molecular machines. A slight photoinduced motion at the molecular level generated a strong force at the macroscopic level.

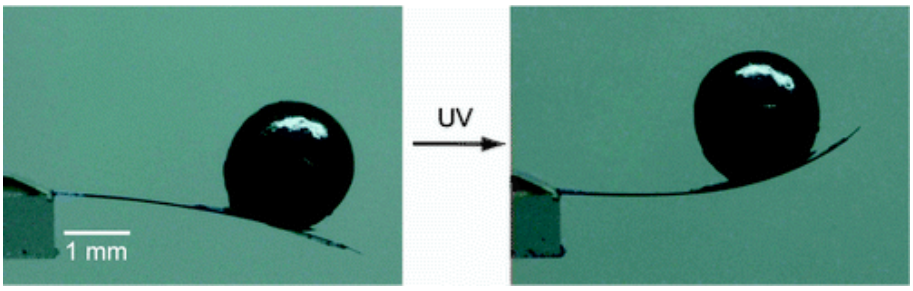

Figure I.16. A molecular crystal cantilever at work: a 0.17 mg photochromic crystal lifts a 47 mg lead ball upon irradiation with UV light.[86]

The molecular cantilever described above is a nice example of a molecular device based on a *covalently bonded* system. While a few other covalent structures have been used to make molecular rotors,[87-91] wheelbarrows,[92] scissors,[93] nanocars[94,95] and spur gears,[96] it is often advantageous to utilise the interlocked structure of **mechanically bonded systems** in the design of molecular machines. Catenanes and rotaxanes are composed of at least two components that are non-covalently but mechanically linked together. In the absence of interactions between the different constituents these will move freely in relation to each other. However, if the interactions between the components can be adjusted by external stimuli then the relative motions of the components can be monitored. Therefore, the intrinsic structure of catenanes and rotaxanes makes them excellent candidates for the construction of molecular machines, and they have indeed been extensively used in the design of various molecular devices.[97-100]

For example the rotational motion of one ring with regard to the second one in a [2]catenane can be monitored using chemical, electrochemical or photochemical stimuli.[101-107] This motion can be seen as a pirouetting motion of one ring around the other or as a sliding motion of one ring along the other. In most cases the direction of the motion can not be

monitored: the catenane can switch from one state to the other but no control is exerted on the direction of the rotation. The [3]catenane synthesised by D. A. Leigh and coworkers is an exception. The structure of this [3]catenane consists of two identical macrocycles, both threaded on a third, larger ring. **Unidirectional rotary motion** of the two small rings along the third one was achieved with this system (**Figure I.17**).[108] The large ring contains four binding sites (A, B, C, and D), which can interact with the small rings *via* hydrogen bonding. The affinity of the small macrocycles for sites A and B can be tuned by photoisomerisation of their central C=C double bond. The *Z* isomers are poor binding sites, therefore isomerisation favours binding of the small rings on sites C and D. As shown in **Figure I.17**, sequential *E* to *Z* photoisomerisation of site A, followed by *E* to *Z* photoisomerisation of site B and then thermal reconversion of sites A and B to the *E* isomers promotes successive rotary motions of the small rings. At each step the presence of the second small ring blocks rotation in one direction, forcing an overall unidirectional motion of the two small rings around the larger ring.

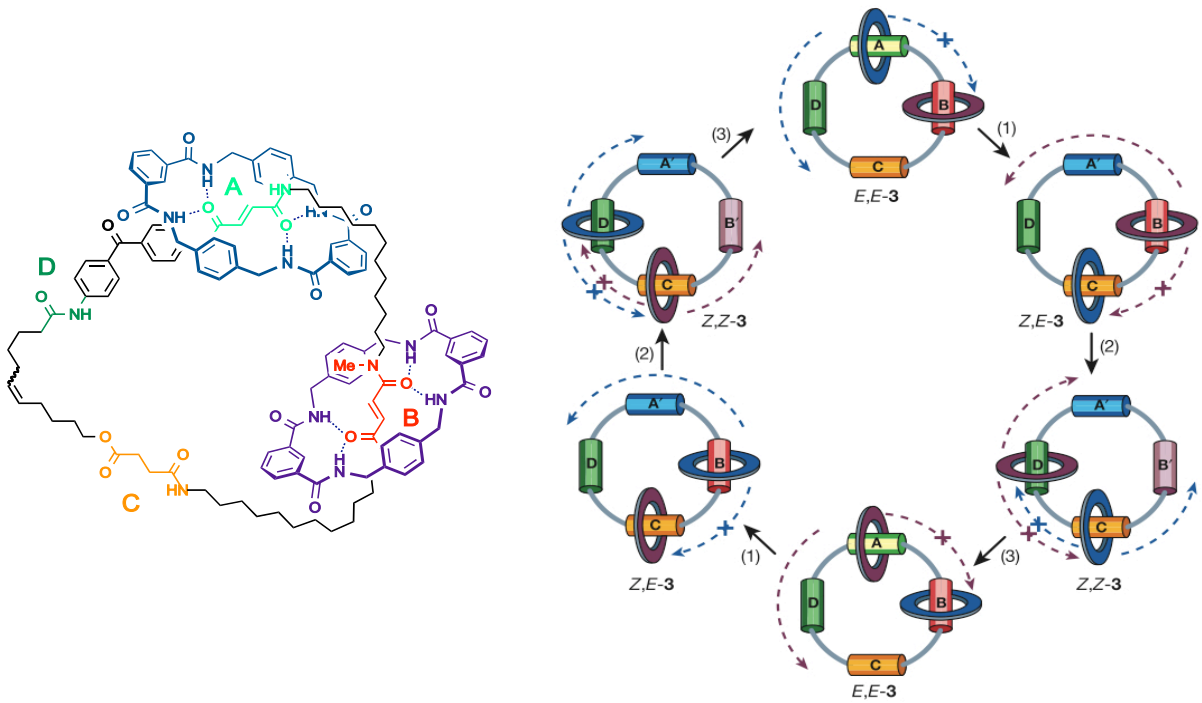

Figure I.17. A unidirectional molecular motor based on a [3]catenane structure (left). The sequential rotary motion of the two small rings around the larger ring is illustrated (right). Successive *E* to *Z* photoisomerisation of site A, followed by *E* to *Z* photoisomerisation of site B and then thermal reconversion of sites A and B to the *E* isomers promotes successive rotary motions of the small rings. The rotation direction is restricted by the presence of the second small ring. Conditions: (1) 350 nm, 5 min; (2) 254 nm, 20 min; (3) heat, 100 °C, 24h or catalytic Br_2, 400-670 nm, -78 °C, 10 min.[108]

I. 2. c) Rotaxane-based Machines

The rotaxane structure is a very interesting framework for the construction of artificial molecular machines.[76,79,109,110] The rotary motion of a catenane-based molecular motor can be translated in two different types of motion in a rotaxane: *pirouetting* of the ring around the axle; or *shuttling* of the ring along the axle. Pirouetting rotaxanes[111-114] and shuttling rotaxanes[115,116] have both been described. Particular interest has been shown in shuttling devices for their potential use as transporters.[117] The translation motion achieved in a shuttling rotaxane brings up the possibility of transport and delivery of functional substrates.

For instance, a copper-complexed [2]rotaxane that acts as a fast-moving **molecular shuttle** was recently described by the group of J.-P. Sauvage (**Figure I.18**).[118] The translation of the ring along the axle is controlled electrochemically and is based on the different coordination behaviours of copper(I) and copper(II).

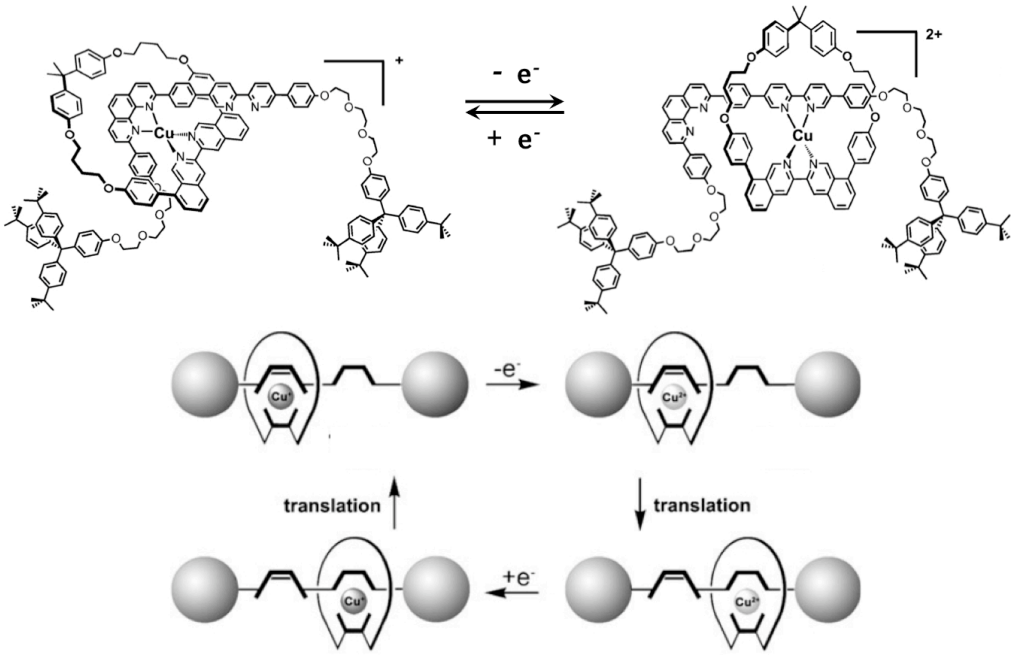

Figure I.18. A fast-moving copper-complexed [2]rotaxane shuttle. The translational motion is controlled electrochemically: copper(I) binds preferentially to the sterically hindered bidentate chelate of the axle while copper(II) binds to the less hindered bidentate site that allows coordination of an additional ligand.[118]

Copper(I) preferentially forms tetrahedral complexes and is stabilised by hindered ligands, while copper(II) can be penta-coordinated. In this new [2]rotaxane shuttle the axle contains two bidentate chelating sites, and the motion is based solely on a difference in steric hindrance between the binding sites. The copper(I) complex is located on the hindered 2,9-diphenyl-1,10-

phenanthroline site, but oxidation to copper(II) is followed by a fast translation motion resulting in complexation of the copper(II) centre on the less hindered 2,2'-bipyridine chelate. This process is reversible, and reduction of the metal centre to copper(I) brings the ring back to its initial position.

The shuttling motion of a ring along an axle has also been applied to multiply interlocked rotaxanes. J. F. Stoddart and coworkers used a rotaxane structure in the design of a **molecular elevator** whose platform goes up and down thanks to the shuttling motion of the rotaxane units. The system is based on a triply interlocked [2]rotaxane structure (**Figure I.19**). One of the components consists in three crown-ether rings linked to a central platform unit. The second component is composed of three thread-like axles connected to each other by a trifurcated triphenylbenzene derivative at one end and stoppered by di-*tert*-butylphenyl groups at the other end. Each axle is threaded through one of the rings of the platform and contains two binding stations: an ammonium (up) and a bipyridinium moiety (down). The rings slide from the upper position to the lower position and back upon deprotonation or protonation of the ammonium units, respectively; and they lift the central platform up and down in this shuttling motion.

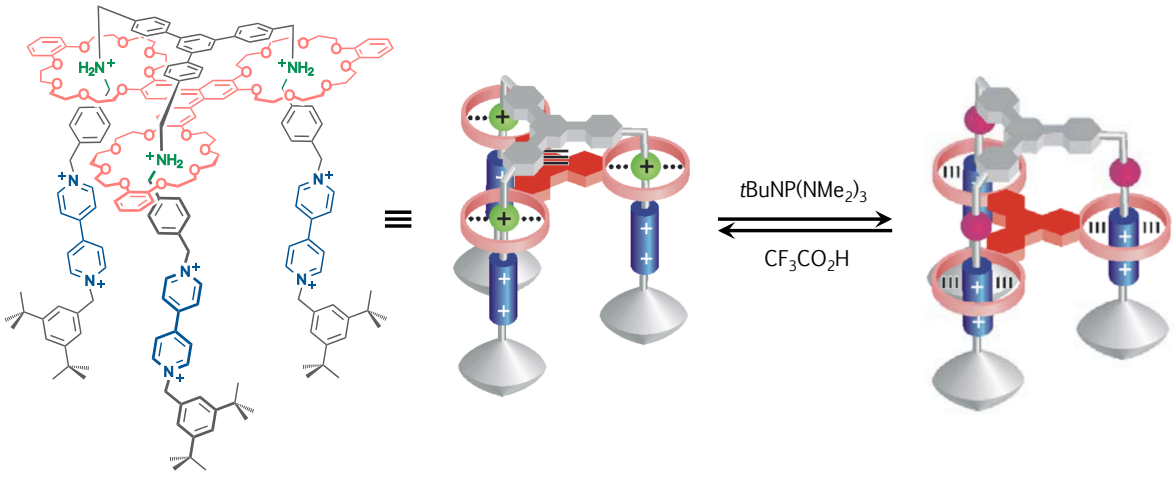

Figure I.19. A molecular elevator based on a triply interlocked [2]rotaxane structure. The interactions of the rings on the axles depend on the pH: the rings bind on the ammonium units when these are protonated and switch to the bipyridinium sites upon deprotonation of the ammonium groups. The shuttling motion of the rings along the axles lifts the central platform up and down.[119]

Of course many other molecular machines have been designed. In this introduction we do not aim to review this field exhaustively. The examples described above give a brief insight into this vast research area and point out the advantages of the rotaxane structure in the construction of molecular machines and devices.

I. 3. Porphyrins: Bright and Versatile Tools in Chemistry

Porphyrins are a class of compounds whose cores are constituted of a tetrapyrrolic macrocycle. The porphyrin ring comprises 26 π electrons, of which 18 electrons participate in a delocalised aromatic system. Due to this large aromatic system, porphyrins are intense chromophores. Related heterocycles like the chlorins and the bacteriochlorins have strong absorption on the visible region as well (**Figure I.20**). The remarkable photophysical properties of these families of molecules were utilised well before the beginning of mankind, since they are key components of the photosystem centres in plants and bacteria. They play a role as light-harvesting antennae and in the energy and electron transfer processes involved in photosynthesis.[120-122] Inspired by nature, chemists have designed many multi-porphyrin arrays as models of light-harvesting antennae and artificial photosynthetic systems.[123-128] The photophysical properties of porphyrin compounds also make them interesting as photosensitizers in photodynamic therapy and tumour imaging.[129,130]

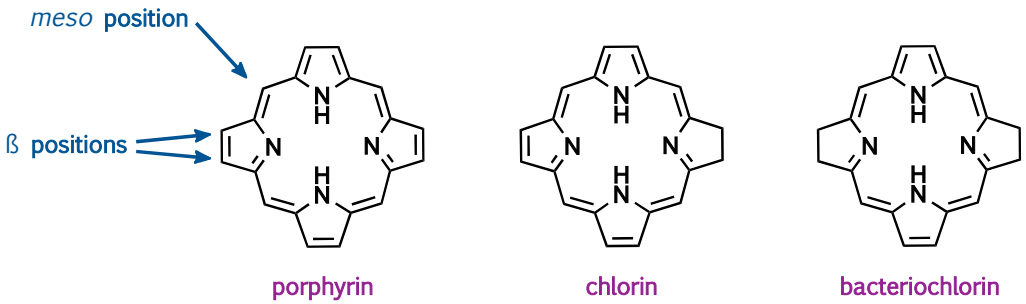

Figure I.20. Chemical structures of the porphyrin core and of two related heterocycles: the chlorin family and the bacteriochlorin family. One or two C=C double bonds are reduced in the chlorins and bacteriochlorins, respectively, compared to the porphyrin structure.

Porphyrins are excellent tetradentate chelating ligands. In its doubly deprotonated form a porphyrin can bind transition metals, which will lie either in the plane of the porphyrin or above this plane if the metal is too large to fit inside the central cavity.[131] In particular, zinc(II) ions are easily inserted in porphyrins and removed. Contrary to some other metal ions they form diamagnetic complexes with porphyrins, which facilitates their spectral characterisation by NMR. For these reasons zinc(II) porphyrins are amongst the most commonly used synthetic metalloporphyrins. Axial coordination of one or two additional ligands on a metalloporphyrin is sometimes possible, depending on the metal (**Figure I.21**). In the case of zinc, coordination of

one additional axial ligand on the zinc(II) porphyrin is favoured. The ability of metalloporphyrins to bind axial ligands offers a myriad of possibilities to assemble multi-component arrays, as will be developed later.

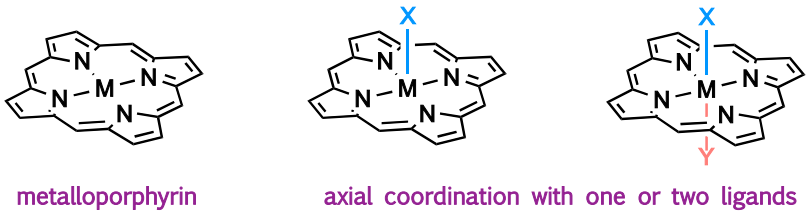

Figure I.21. Structure of metalloporphyrins and coordination of axial ligands.

Another interesting feature of porphyrins resides in the number of sites available for functionalisation. Porphyrins can be substituted at part or all of their β and *meso* positions, which makes them versatile platforms for various applications, *e.g.* in the field of molecular electronics or materials.[132-136] Several synthetic strategies have been developed for the introduction of *meso* substituents; some of these strategies will be illustrated in Chapters II and V. Extension of the π system of a porphyrin by appropriate β,β'-functionalisation is also possible. The group of M. J. Crossley developed a synthetic strategy for the connection of aromatic moieties to porphyrin cores via pyrazine bridges; this strategy will be described in Chapter IV of this thesis.

I. 3. a) Axial ligation on metalloporphyrins

As mentioned above, an interesting feature of metalated porphyrins is their ability to bind axial ligands. This interaction considerably widens the range of applications available with metalloporphyrins. In addition to the introduction of β or *meso* substituents, further functionality can arise from binding of axial substrates. Axial coordination on metalloporphyrins has been notably exploited in catalysis,[137,138] in the assembly of various porphyrin-containing multi-component structures[139,140] and in host-guest chemistry. This last topic will be detailed in part I. 3. b). Recently reported assemblies based on the coordination of axial ligands on metalloporphyrins include the formation of non-covalent [2]catenanes and the templated synthesis of a 12-porphyrin nano-ring, which are chosen as examples to illustrate this type of interaction in this introduction.

A series of [2]catenanes assembled by coordination chemistry was described by the group of J.-P. Sauvage in the recent years.[141,142] Each catenane is composed of two different sub-components: a 2,9-diphenyl-1,10-phenanthroline (dpp) chelate attached to two peripheral zinc porphyrins, and a ligand that contains two pyridyl units linked either by a phenanthroline or by a naphthalene spacer. A copper(I) template preorganises two bis-porphyrin components in an intertwined fashion by formation of a $[Cu(dpp)_2]^+$-type complex. The macrocycles are then closed by axial coordination of the bifunctional pyridyl ligands on the Zn-porphyrins to form a [2]catenane (**Figure I.22**). The geometrical fit between the components was shown to be better in the catenane containing the bis-pyridyl substituted naphthalene than in the one containing the phenanthroline units. These new non-covalent catenanes pave the way towards more complex interlocked architectures.

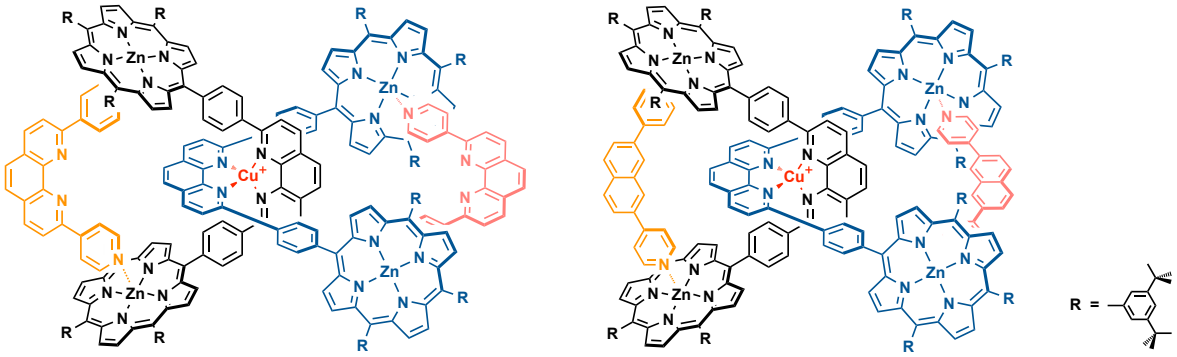

Figure I.22. [2]catenanes obtained by axial coordination of bifunctional pyridyl ligands on Zn-porphyrins.[141,142]

H. L. Anderson and coworkers recently reported the very elegant, novel synthesis of a 12-porphyrin nano-ring, whose construction involved the Zn-porphyrin/pyridine axial coordination as a key interaction.[143] Their group has developed the synthesis of linear conjugated Zn-porphyrin oligomers and studied the formation of various assemblies by axial coordination of multifunctional templates to the Zn-porphyrin wires. For example, they described ladder-shaped assemblies obtained by coordination of DABCO with two porphyrin wires.[144,145] In their recent report they used a new strategy to preorganise the building blocks. They named this strategy *Vernier templating* by analogy to the Vernier scale system and Vernier complexes.[146,147] In this type of approach two buildings blocks containing complementary binding sites are assembled. If one of the building blocks contains *n* binding sites and the second building block contains *m* sites then a multi-component assembly will be formed, where the number of bound sites is the lowest common multiple of *n* and *m*. In the system described by Anderson a six-pyridyl template interacts with a four-porphyrin oligomer by axial coordination to form a twelve-site Vernier

complex (**Figure I.23**). The novelty of the strategy resides in the use of a *cyclic* template, whereas previous Vernier complexes involved exclusively the use of linear components. The Vernier preorganisation leads to the formation of a figure-of-eight complex after covalent coupling of the linear porphyrin tetramers. Removal of the templates affords a twelve-porphyrin nano-ring. Thus, the new strategy allowed the formation of a large multi-porphyrin ring while avoiding the tedious synthesis of a twelve-site template. The method should be generalised in the future and give rise to the synthesis of functional nano-rings of a size not previously accessible.

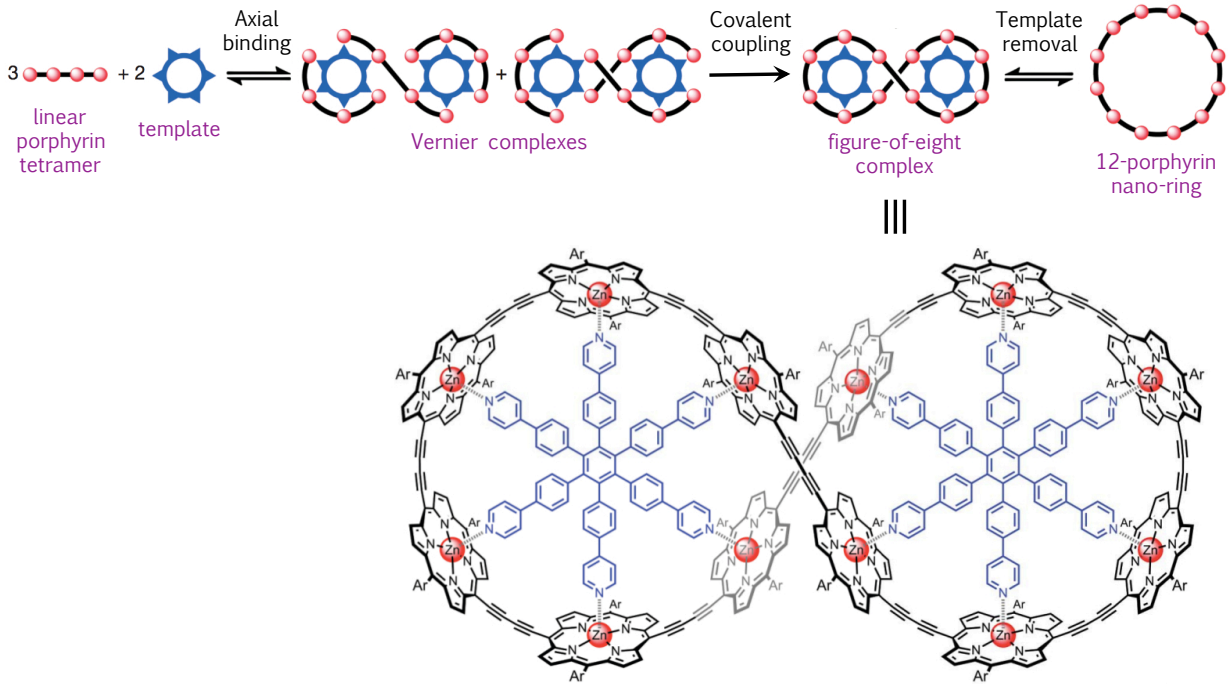

Figure I.23. A novel approach for the templated synthesis of large multi-porphyrin rings. A linear porphyrin tetramer and a cyclic six-site template with mismatched numbers of binding sites were assembled by axial porphyrin coordination to give Vernier complexes. Covalent coupling of the porphyrin oligomers followed by template removal afforded a 12-porphyrin nano-ring.[143]

As mentioned before, axial coordination on metalloporphyrins has found applications in many fields of research. An original approach was taken by M. J. Crossley and P. Thordarson, who used this interaction as a tool in the characterisation of bis-porphyrins.[148] Their system is composed of two capped porphyrins covalently linked by a rigid aromatic spacer. The reaction leading to the bis-porphyrin yields two isomers, with *syn* and *anti* orientations of the capping groups, respectively (**Figure I.24**). The isomers could be separated, but assignment of the structures using conventional spectroscopic techniques proved difficult. Axial coordination of a "molecular ruler" was used to distinguish between both isomers. The ruler is the bifunctional ligand 1,12-diaminododecane, which can bind on the unprotected faces of the Zn-porphyrin units.

The ligand is just long enough to span the Zn-Zn distance in the *syn* isomer and to form a strong intramolecular complex, but it is too short to wind itself around the *anti* isomer and to form a complex involving both faces. The isomers were thus assigned according to their binding constants with the molecular ruler (**Figure I.24**).

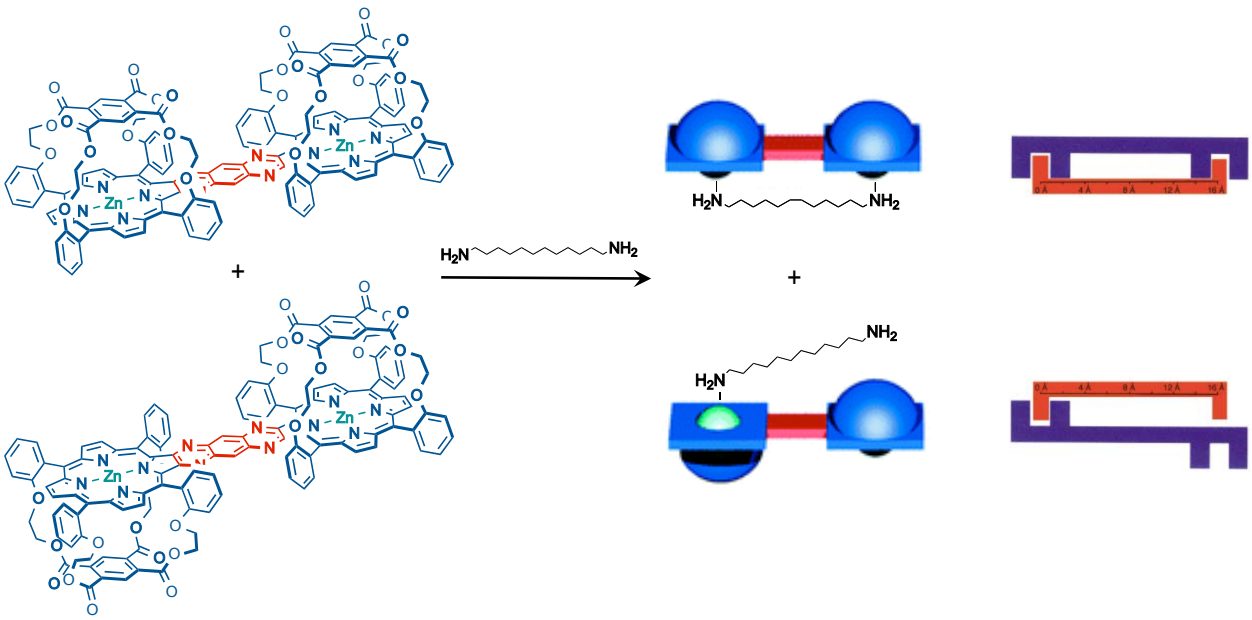

Figure I.24. Discrimination between the *syn* and *anti* isomers of a bis-porphyrin using axial coordination with a "molecular ruler". The bifunctional ruler ligand forms a strong complex with the *syn* isomer but is too short to bind both Zn-porphryin sites on the *anti* isomer.[148,149]

In a different system, the groups of K. P. Ghiggino and M. J. Crossley used axial ligation on a Zn-porphyrin to tune the energy and charge transfer properties of multi-porphyrin arrays.[150] Photoinduced charge transfer was switched on upon axial coordination of a chloride anion on a Zn-porphyrin in a porphyrin triad.

These few examples give an insight of the various applications brought up by axial coordination on metalloporphyrins. This interaction also plays a major role in host-guest systems based on porphyrins, which we will illustrate in the next part.

I. 3. b) Host-guest chemistry with porphyrins

Since the introduction of the concept of host-guest chemistry,[151] a great variety of molecular containers have been designed, and their abilities to bind guest substrates have been studied. The host-guest recognition can be based on diverse types of interactions, *e.g.* H-bonding, metal-ligand interactions or Van der Waals interactions. In particular, metalloporphyrin-containing hosts can bind substrates thanks to the axial ligation interaction described above. The group of J. M. K. Sanders contributed significantly to this field of research and published pioneering work on the synthesis of cyclic porphyrin dimers that can host ditopic guests in their central cavity.[152,153] In these systems the porphyrins are covalently linked by chains of various length and flexibility. Two of these dimers are depicted in **Figure I.25**. Both systems contain zinc porphyrins and can accommodate the aliphatic diamine 1,4-diazabicyclo[2.2.2]octane (DABCO). The association constants of the bis-porphyrin dimers with DABCO in dichloromethane (~10^7 - 10^8 M^{-1}) are two to three orders of magnitude higher than the binding constants observed for the corresponding porphyrin monomers with DABCO in the same solvent (~10^5 M^{-1}). This highlights the cooperative effect in the double binding process in the inner cavity and the stabilisation of the inclusion complex compared to 1:1 porphyrin-monomer/DABCO complexes.[153,154] The length and nature of the chains linking the porphyrins in the dimer can be varied so as to accommodate longer guests.[155] For example the dimer host closed *via* disulfide bonds (**Figure I.25**, right) has flexible chains and can bind the longer 4,4'-bipyridine guest as well as DABCO.

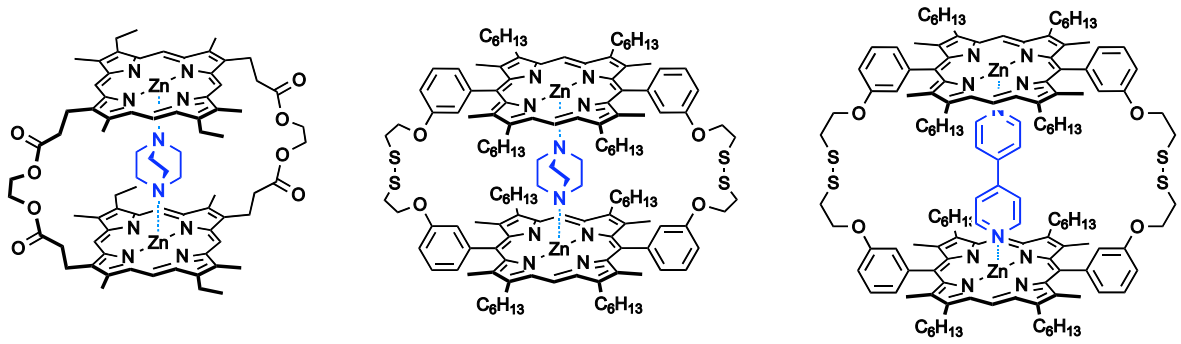

Figure I.25. Host-guest complexes of covalently linked Zn-porphyrin dimers and ditopic nitrogen ligands (DABCO or 4,4'-bipyridine) synthesised and studied in the group of J. K. M. Sanders.[153,154]

Other groups designed some tweezers-shaped bis-porphyrin hosts, in which a single bridge links the metalloporphyrins. M. J. Crossley and his group synthesised several molecular receptors constituted of two porphyrins linked by a Tröger's base bridge. The porphyrins can be

metalated with zinc(II) or tin(IV), and the bis-metalloporphyrin host binds linear diamines (in the case of zinc) or dicarboxylic acids (in the case of tin) by axial coordination on the internal faces of the porphyrins.[156-158] The templated formation of a molecular capsule by self-assembly of a Tröger's base zinc(II) bisporphyrin receptor and a dendrimer tetramine guest was also reported. The assembly is composed of two hosts encapsulating the central guest (**Figure I.26**).[159]

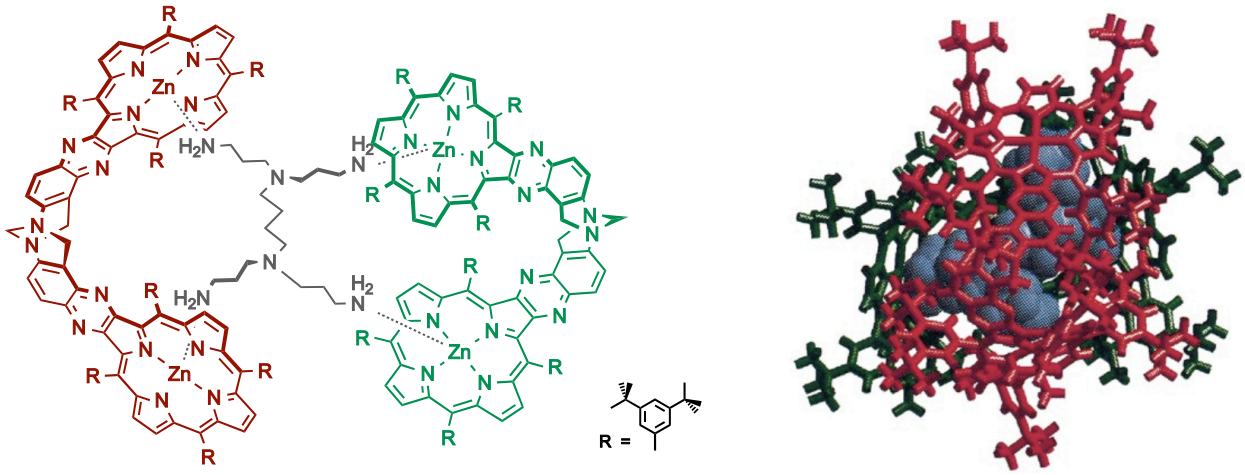

Figure I.26. Chemical structure (left) and molecular model (right) of a self-assembled capsule formed by axial coordination of a tetramine guest on the zinc(II) sites of two bis-porphyrin receptors.[159]

Host-guest recognition with porphyrin-incorporating receptors can be used to elucidate the absolute configuration of chiral guests. N. Berova and coworkers described a bis(Mg(II)-porphyrin) tweezers host that adopts a preferred helicity upon complexation of a α-chiral carboxylic acid derivative (**Figure I.27**). The helicity is determined by a circular dichroic exciton chirality method and the absolute configuration of the substrate is deduced from the data.[160]

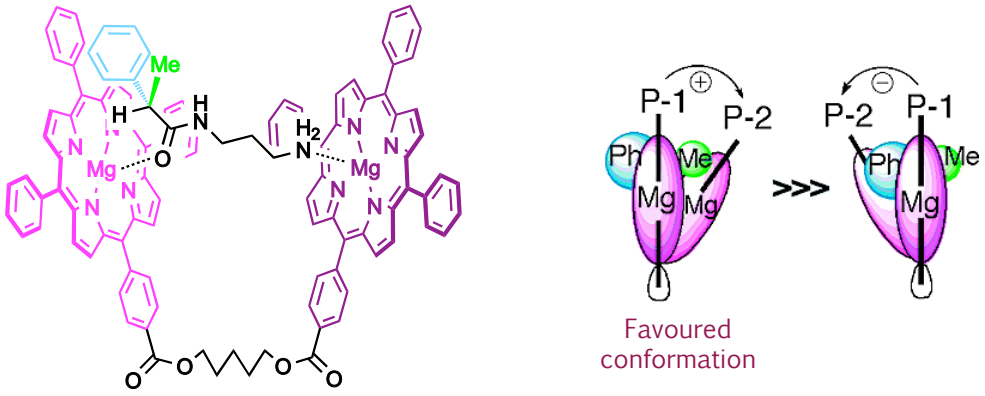

Figure I.27. Determination of the absolute configuration of α-chiral carboxylic acids with a bis-porphyrin host. Binding of the chiral guest induces a conformational change of the host with a preferred helicity, which is measured by circular dichroism.[160]

Axial coordination on metalloporphyrins gives rise to a wide range of molecular recognition possibilities. However, the host-guest chemistry of porphyrin systems is not limited to complexes formed by this type of interaction. Some cyclic porphyrin hosts form complexes with fullerene guests.[161] Inclusion of fullerenes in these systems occurs by Van der Waals interactions and in some cases *via* π-electronic charge transfer from the porphyrin moiety to the fullerene. For example, the disulfide-bonded host illustrated in **Figure I.25** is a good receptor for C_{60}.[154] J. R. Nitschke and coworkers recently described a self-assembled cubic cage whose faces incorporate nickel(II) porphyrins (**Figure I.28**. a). The cage can host large aromatic molecules like coronene and fullerenes, and shows hierarchical binding preference for the larger fullerenes (*e.g.* C_{70}) over C_{60}.[162] Another system based on aromatic donor-acceptor interactions was designed by T. Haino. His group reported the formation of a supramolecular polymer assembled by self-recognition of a hermaphroditic component (**Figure I.28**. b). The monomer is functionalised by a trinitrofluorenone moiety at one end and by a cofacially arranged bis-porphyrin unit at the other end. Host-guest recognition between the electron-acceptor trinitrofluorenone and the electron-rich bis-porphyrin leads to the formation of the supramolecular polymer.[163] Complexes of electron-donor bis-porphyrin hosts with electron-deficient guests sometimes exhibit interesting photophysical properties. S. Yagi and coworkers reported the efficient photoinduced electron transfer from a bis(Zn-porphyrin) tweezers host to a hexyl viologen guest substrate. The electron transfer can be switched off by substrate exchange of the viologen guest with DABCO.[164]

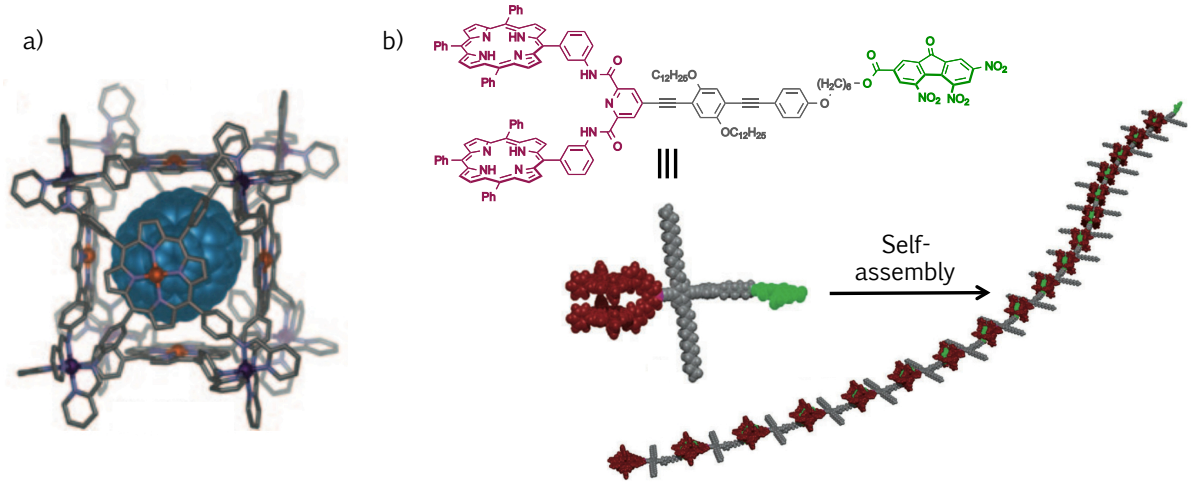

Figure I.28. a) A porphyrin-faced cubic host for C_{70} fullerene.[162] b) A supramolecular polymer formed through head-to-tail host-guest self-recognition of a hermaphroditic monomer. The host part of the monomer is an electron-rich bis-porphyrin unit, which is linked to an electron-deficient trinitrofluorenone guest moiety.[163]

Molecular receptors and cages provide a specific confined environment for guest substrates that can be very different from the environment experienced by the guests in solution. This can promote unusual reactivity and unique chemical phenomena in the cavity.[165-168] For instance folding of short peptides can be triggered by encapsulation in a porphyrin-faced cage, as reported by M. Fujita and coworkers. They designed a tris-porphyrin prism host that forms a hydrophobic pocket and accommodates short peptides (**Figure I.29**). While oligopeptides normally adopt random-coil conformations in water their encapsulation in the porphyrin prism enhances folding into hybrid α-helix/β-turn conformations.[169-171]

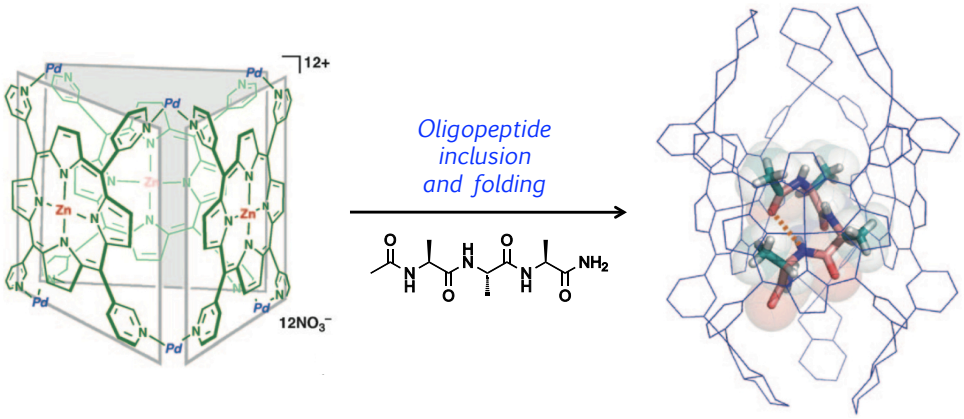

Figure I.29. A tris-porphyrin prism host that can encapsulate and fold short peptides in hybrid α-helix/β-turn conformations.[171]

I. 3. c) Porphyrins and Molecular Machines

As seen in the examples above, porphyrins are interesting for their interactions and binding properties with various substrates, which justifies their incorporation in molecular machines. To date porphyrin-containing molecular machines are not so common. The porphyrin moiety is sometimes used as a stopper or as part of the axle in rotaxane shuttling systems, where it can play a role in the trigger mechanism of the shuttling ring.[172,173]

T. Aida and coworkers designed a different molecular device whose motion is reminiscent of a **molecular pedal**, and that utilises axial coordination on Zn-porphyrins as a key interaction in the machine mechanism. The system is composed of a central ferrocene pivot substituted on one side with an azobenzene unit and on the opposite side with two cofacial zinc porphyrins arranged in a tweezers-like fashion (**Figure I.30**). The bis-porphyrin tweezers can host a ditopic nitrogen ligand like the 4,4'-biisoquinoline used in the study. The

photoisomerisation of the azobenzene unit from *trans* to *cis* and back promotes a rotary motion of the cyclopentadienyl rings of the ferrocene pivot, which in turn leads to a pedal-like conformational change of the zinc porphyrin units. This photoinduced motion of the host is then transferred to the rotary guest molecule, which undergoes twisting in a clockwise or anticlockwise fashion.[174] A photoresponsive self-locking molecule based on an analogous system was later described. The new switchable device involves the rotary motion of a ferrocene pivot and axial coordination of a ditopic guest between two porphyrins as for the previous system.[175]

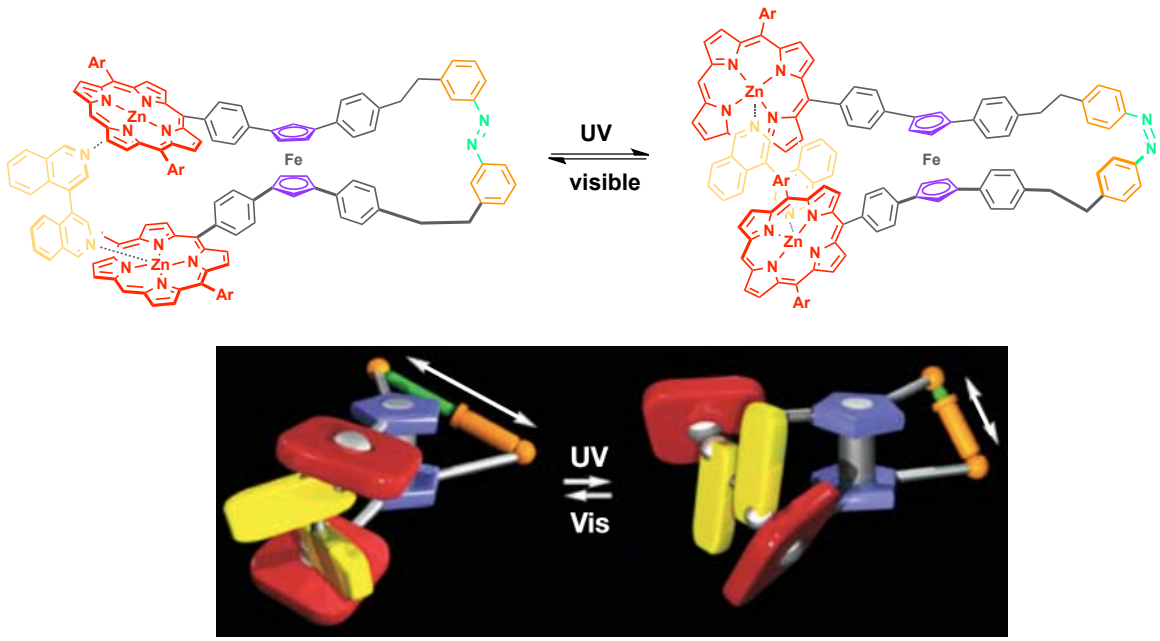

Figure I.30. A photoresponsive, porphyrin-containing molecular machine whose motion is reminiscent of a molecular pedal. Photoisomerisation of the azobenzene unit results in a rotary motion of the ferrocene pivot and of a pedal-like conformational change of the zinc porphyrin dimer. This motion is transferred to the biisoquinoline guest, which undergoes twisting around its central C-C bond.[174]

Another molecular machine involving a metalloporphyrin as a key component is the molecular gate (or turnstile) described by the group of M. W. Hosseini. The gate is composed of a handle-shaped stator linked to a Sn(IV)-porphyrin rotor by axial coordination. The tin centre serves as a hinge between the rotor and the stator components. The gate is switched from the open to the closed state by coordination of the binding sites present on the handle and on the porphyrin to silver(I) (**Figure I.31**).[176,177] The system was later improved by introduction of a tridentate coordination site on the handle or by the use of a porphyrin functionalised with two binding sites.[178-180]

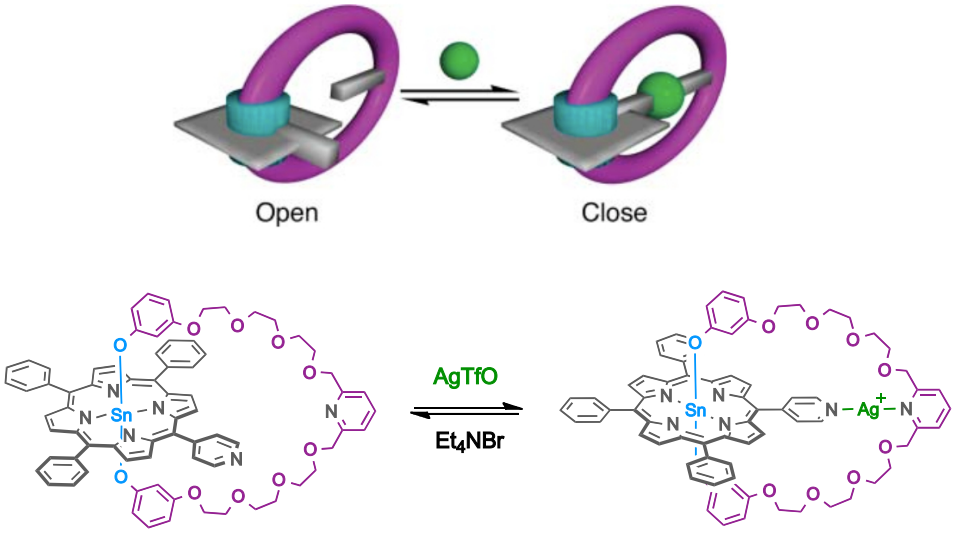

Figure I.31. A molecular gate composed of a Sn(IV)-porphyrin rotor linked to a handle stator by axial coordination. The gate is closed by coordination of silver(I) on the pyridyl sites of the handle and of the porphyrin.[176,177]

I. 4. Porphyrin-containing Rotaxanes

In the previous parts of this introduction we presented the properties of the rotaxane architectures and of the porphyrin moiety, as well as their applications, in particular in the construction of molecular machines. Here we aim to show how porphyrins and rotaxane structures can be combined in the design of functional molecular assemblies and devices.

I. 4. a) Examples of Porphyrin-containing Rotaxanes

Porphyrin units can be incorporated in a rotaxane in several ways. Due to their large size they have been used as stoppers at the end of the axle component, and they can be linked to the axle either by axial coordination[181,182] or by covalent substitution on one of the *meso* positions.[40,44,183] In some cases the porphyrin is part of the axle[173] and can be used to compartmentalise the dumbbell component in the case of a multi-rotaxane. For example [3]- and [5]rotaxanes that are constituted of two and four rings (respectively) threaded on a dumbbell have been described.[184,185] In these rotaxanes the porphyrin units incorporated in the dumbbell segregate each ring to a specific section of the axle.

Porphyrins can also be part of or covalently linked to the ring component of a rotaxane. C. A. Hunter and coworkers described a self-assembled [2]rotaxane whose ring is a zinc porphyrin dimer closed by axial coordination on the Zn-porphyrins.[186] Strapped and capped porphyrins form hollow cycles that can serve as the ring component of a rotaxane as well.[187,188] The spatial proximity between the porphyrin and the axle in such rotaxanes has been used in the catalysis of chemical transformations on the axle by the porphyrin.[71] Another possibility is to attach porphyrins to the ring component of a rotaxane. Such porphyrin-appended rotaxanes have shown interesting properties in electron and energy transfer or in host-guest chemistry.[52,73,189]

The group of J.-P. Sauvage described a [2]rotaxane that contains three porphyrin units: a gold(III)-porphyrin is incorporated in the ring component and two zinc(II)-porphyrins act as stoppers at the extremities of the dumbbell component.[190] Pirouetting of the ring around the axle is observed upon complexation/decomplexation of copper(I) (**Figure I.32**). In the presence of copper(I) the orientation of the ring is imposed by the formation of a tetrahedral complex with the bidentate sites of the macrocycle and dumbbell components, and the gold porphyrin is located far away from the zinc porphyrin stoppers. After demetalation of the copper(I) centre the ring undergoes a half-turn rotation and the rotaxane adopts a conformation where the electron-acceptor Au(III)-porphyrin is located between the electron-donor Zn(II)-porphyrins. This pirouetting rotaxane is a nice example of a molecular machine based on a porphyrin-containing rotaxane.

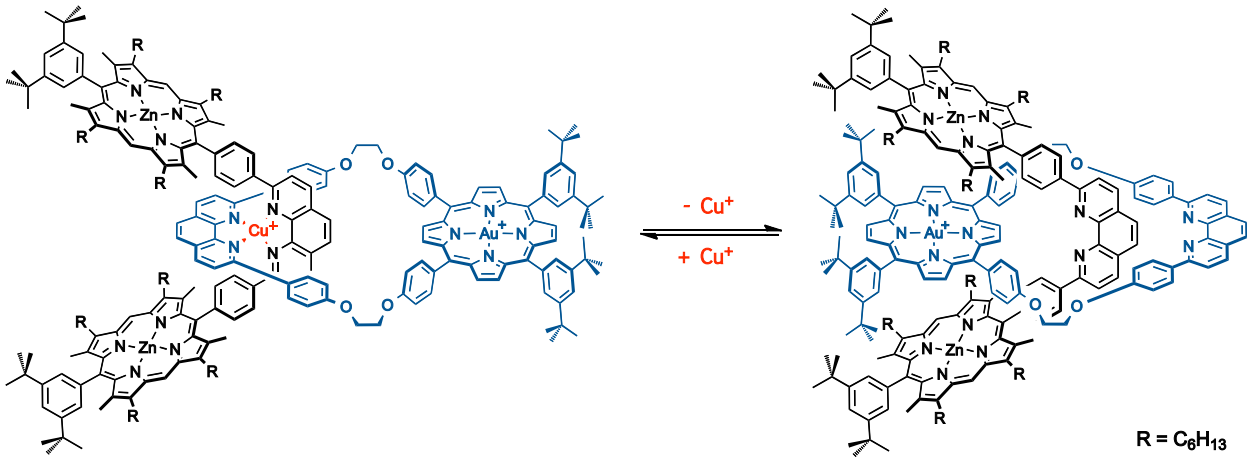

Figure I.32. Pirouetting motion of a [2]rotaxane that contains three porphyrin units. A gold(III) porphyrin is incorporated in the macrocyclic component, and the axle bears two zinc(II) porphyrins as stoppers.[190]

The geometrical features of porphyrins make them useful in the design of *multi*-rotaxanes. For example a porphyrin can be substituted with four thread-like chains at its four *meso* positions. Subsequent threading of rings and stoppering of the axles can lead to the formation of a [5]rotaxane with a central porphyrin platform, as described by D. Tuncel *et al*.[191] If the rings are large enough to enclose two threads then a [6]rotaxane structure can be formed with two face-to-face porphyrins surrounded by four doubly threaded rings. R. J. M. Nolte, J. F. Stoddart and coworkers reported the formation of this type of structure in 1997 (**Figure I.33**).[192] Their system can not strictly be called a rotaxane because the axles are not stoppered, but the interlaced structure of the [6]pseudorotaxane is maintained by the interactions between the ammonium groups of the axles and the crown-ether rings. The assembly features two slipped cofacial Cu(II) porphyrins maintained in close proximity, and parallel electron spin coupling is observed between the Cu(II) centres in the threaded assembly. The system resembles the special pair of the photosynthetic reaction centre of bacteria.

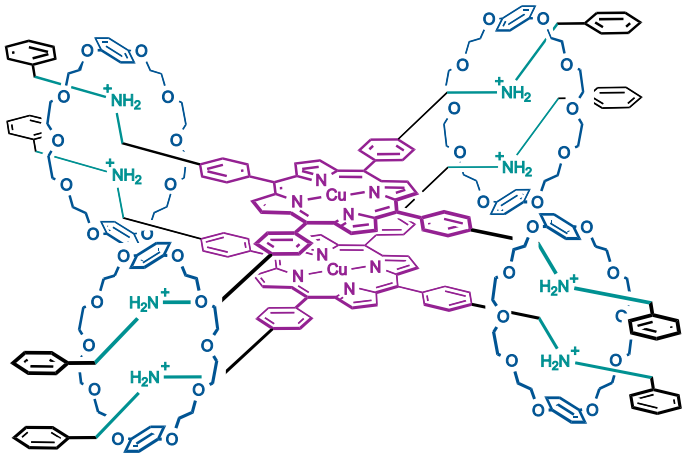

Figure I.33. A porphyrin-incorporating [6]pseudorotaxane structure reminiscent of the special pair of the photosynthetic reaction centre. Two central copper(II) porphyrins are held in a slipped cofacial arrangement by the surrounding interlocked scaffold. Parallel spin electron coupling between the Cu(II) centres results from the close proximity of the metalloporphyrins.[192]

A similar tetra-substituted porphyrin was used by the group of K. Tanaka in the design and synthesis of a tetra-interlocked [2]rotaxane.[193] The two components of this rotaxane are a copper(II) phthalocyanine tetra-substituted with four crown-ether rings and a copper(II) porphyrin with four thread-like substituents. The final [2]rotaxane consists of a metalloporphyrin and a metallophthalocyanine arranged in a face-to-face way, each axle of the porphyrin being threaded through one of the peripheral rings of the phthalocyanine (**Figure I.34**). The structure of this rotaxane is reminiscent of the molecular elevator reported by J. F. Stoddart and described in part **I. 2. c)** of this introduction. Both systems consist of rotaxane-like structures arranged

around central platforms, but the present system has four interlocked units instead of three. The position of the crown-ether rings along the threads can be monitored by protonation/deprotonation of an amine group incorporated in the axle. In the protonated state the interactions of the rings with the ammonium groups keep the Cu(II)-phthalocyanine and the Cu(II)-porphyrin relatively far from each other. As a consequence the spins of the copper(II) centres are isolated and no exchange interaction is observed. However, in the deprotonated state the phthalocyanine component is free to slide along the axles and adopt a conformation where the Cu(II)-phthalocyanine and the Cu(II)-porphyrin are in close proximity. Spin exchange between the two copper(II) centres is indeed observed in the form of an antiferromagnetic coupling. Thus, switchable spin-spin communication was achieved with this new system, which is a nice example of a functional porphyrin-incorporating rotaxane.

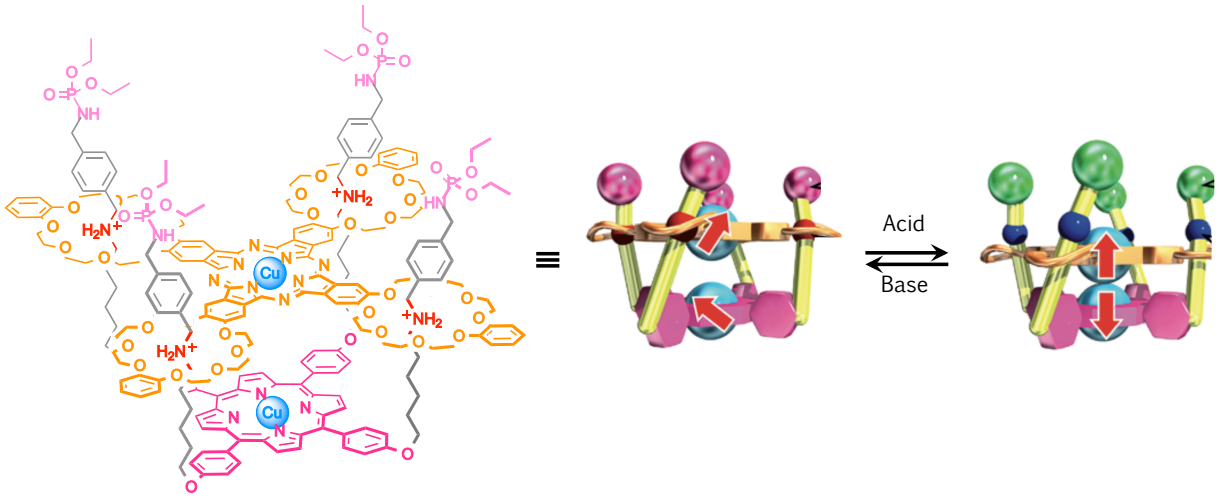

Figure I.34. A tetra-interlocked [2]rotaxane with face-to-face Cu(II)-porphyrin and Cu(II)-phthalocyanine units. The distance between the copper(II) centres is monitored by protonation/deprotonation of amine groups on the axles. Switchable spin-spin communication is achieved: the spins are isolated in the protonated state of the rotaxane whereas antiferromagnetic coupling is observed upon deprotonation.[193]

I. 4. b) Previous Work Related to this Project: Molecular Receptors Based on Rigid Bis-Porphyrinic [3]- and [4]Rotaxanes

Although the host-guest chemistry of porphyrins is well documented, examples of molecular receptors based on a porphyrin-containing rotaxane structure are rare. The first [3]rotaxane acting as a molecular receptor *via* axial coordination on two Zn-porphyrins was reported by the group of J.-P. Sauvage in 2008.[194] The rotaxane is composed of two different components: a Zn-porphyrin moiety covalently linked to a phenanthroline-containing

macrocycle through an extended aromatic system, and a dumbbell with two bidentate coordination sites. The [3]rotaxane contains two porphyrin-linked macrocycles threaded on the same axle (**Figure I.35**). It was shown to be a good receptor for various ditopic nitrogen ligands of the bipyridyl family, with flexible or rigid spacers of various lengths between the pyridyl units. The association constants measured with these guest substrates were in the range 10^{6}-$10^{7.5}$ M^{-1}. In the case of a long guest the association constant of the copper-free rotaxane was higher than that of the copper(I)-complexed rotaxane, in accordance with the expected adaptability of the copper-free host.[194,195]

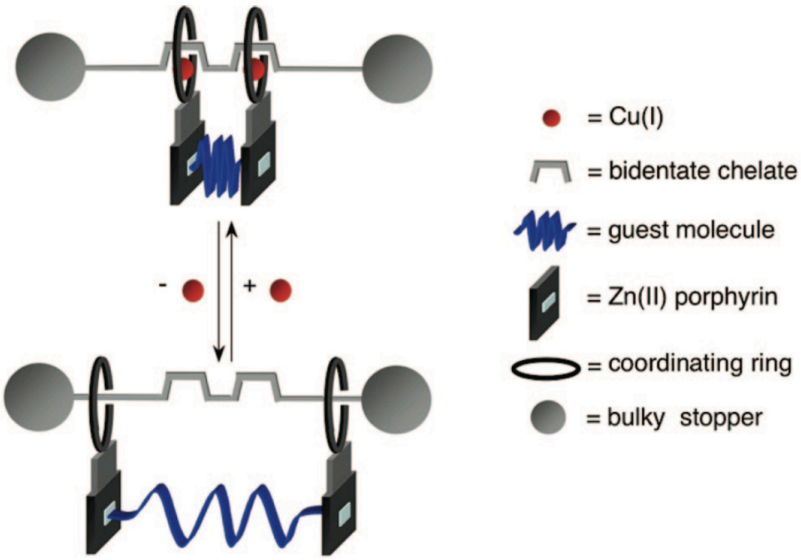

Figure I.35. Schematic views of the copper(I)-complexed (top) and copper-free (bottom) forms of a [3]rotaxane. The rotaxane is a good molecular receptor for ditopic pyridyl guests of various lengths. The copper(I)-complexed rotaxane forms stronger complexes with short guests, while the copper-free rotaxane has better affinity for long guests.[194,195]

A [4]rotaxane designed in a similar way was later described. In this rotaxane the porphyrin moieties were substituted with peripheral macrocycles at *two* antipodal positions. The coordinating macrocycle and the spacer between the ring and the porphyrin were identical to those used in the synthesis of the [3]rotaxane depicted in **Figure I.35**, except that two of these rings were attached to the porphyrin. Similar dumbbells with two bidentate sites were used to form the desired [4]rotaxane, as shown in **Figure I.36**. In the case of the copper(I)-complexed [4]rotaxane, short ditopic ligands formed guest inclusion complexes between the porphyrins, but longer guests did not fit in the central cavity.[196] Thus the copper(I)-complexed [4]rotaxane showed more selective host-guest properties than the corresponding [3]rotaxane. However, completely different behaviour was observed for the copper-free forms of the [3]- and [4]rotaxanes. While the demetalated [3]rotaxane was a good molecular receptor the [4]rotaxane

collapsed upon demetalation of the copper(I) centres and did not have any affinity for guest molecules after demetalation. This was attributed to π-stacking between the aromatic systems of the two porphyrinic bis-macrocycles and to axial coordination of the triazole groups of the dumbbells on the Zn-porphyrins.[197]

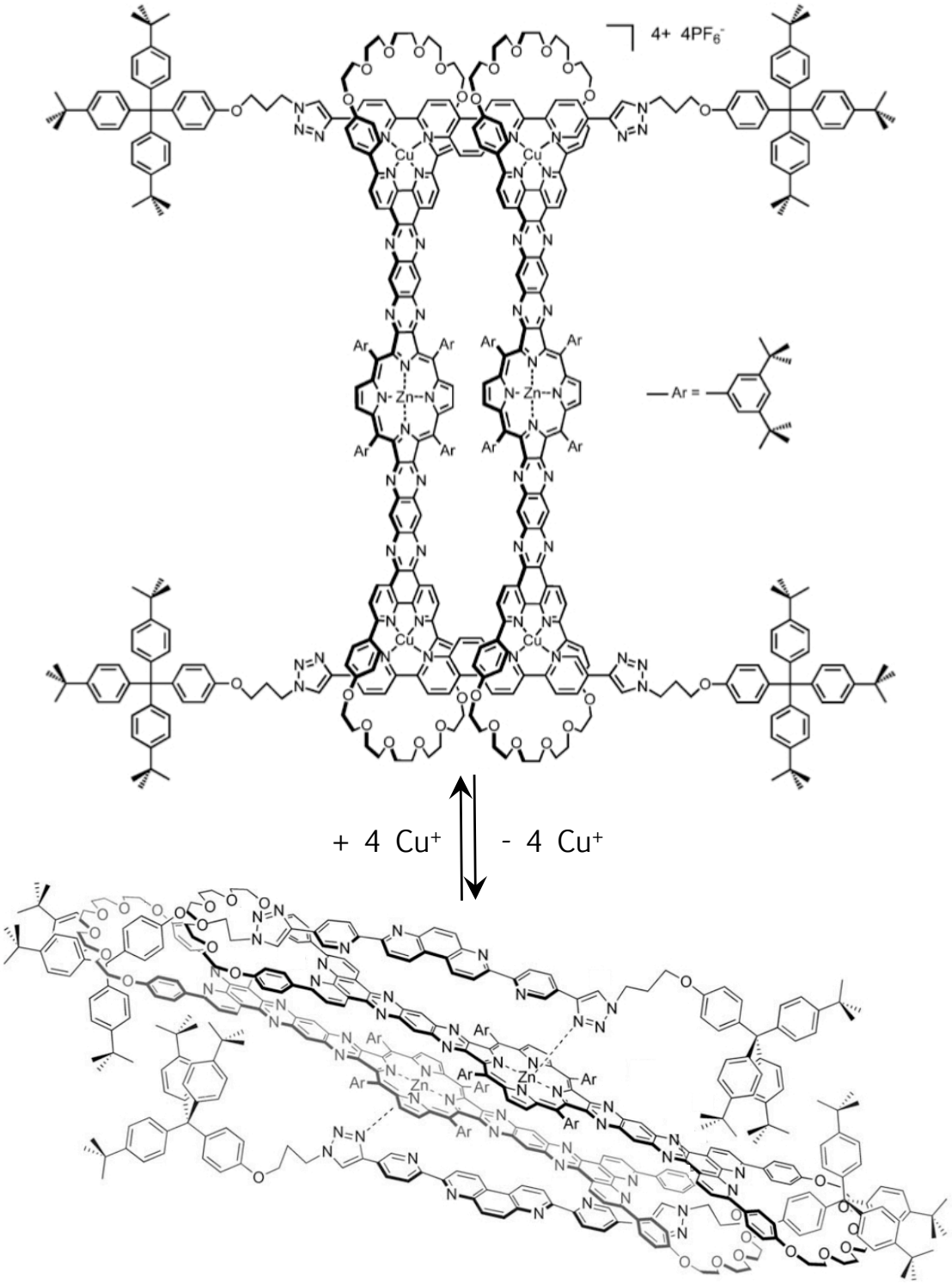

Figure I.36. A [4]rotaxane with two face-to-face porphyrins. The copper(I)-complexed rotaxane forms guest inclusion complexes with short substrates. However, the rotaxane collapses upon demetalation of the copper(I) centres and does not show any host-guest properties after demetalation.[196,197]

The [4]rotaxane described above contains a porphyrinic bis-macrocycle component whose central part is a rigid, very extended aromatic system, and whose synthesis is very lengthy and tedious. The host-guest properties of the rotaxane were limited by its rigidity and by the collapse of the system upon demetalation. This encouraged the design of a new [4]rotaxane based on a very different porphyrinic bis-macrocycle, which will be described in this thesis.

I. 4. c) Present Research Project: Design and Synthesis of Porphyrin-Based Multi-Rotaxanes as Adaptable Molecular Receptors

The main objective of this PhD research project is the design and synthesis of new adjustable molecular receptors. The theme of the project was initially inspired from the work performed by chaperone proteins. As described in part I. 2. a) of this introduction these natural molecular machines are molecular receptors for newly formed, unfolded proteins, and they assist folding of the guest proteins. Rather than trying to mimic the exact *function* of chaperonins (*i.e.* protein folding) we took inspiration from their *mechanism of action* with its three consecutive steps: capture, conformational change and release of a guest substrate. We envisioned that it could be possible to achieve the capture, conformational change and release of small organic guests with a fully synthetic receptor, which would be structurally much simpler than chaperone proteins. In particular, we envisaged the design of a molecular receptor whose internal cavity could be reduced in size upon application of an external stimulus. This receptor would be able to change the conformation of a guest substrate by *compression* and can therefore be seen as a *molecular press*.

When we designed our new molecular receptor we decided to use two cofacially arranged metalloporphyrins and to exploit their axial coordination properties to bind ditopic guest substrates in the internal cavity formed between the porphyrins. By surrounding the metalloporphyrins with a rotaxane scaffold the face-to-face arrangement of the porphyrins would be maintained. Moreover, a shuttling motion of the rings along the axles could enable to monitor the inter-porphyrin distance. The target rotaxane is schematically depicted in **Figure I.37**. It is composed of two dumbbells and of two bis-macrocycles linked by a central zinc porphyrin. Each axle contains two bidentate binding sites derived from the 2,2'-bipyridine motif. The porphyrinic component is a tetra-aryl zinc porphyrin substituted with 1,10-phenanthroline-incorporating macrocycles at two antipodal *meso* positions. The rotaxane is assembled *via* a copper(I) template

that forms complexes with the bipyridine and phenanthroline chelates of the axles and of the rings.

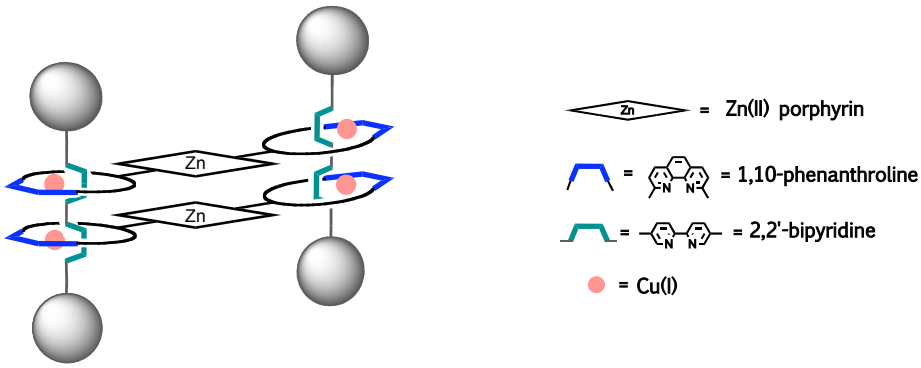

Figure I.37. Schematic view of the target [4]rotaxane. Zn-porphyrins are depicted as diamond-shaped symbols; phenanthroline and bipyridine binding sites are blue and green U-shaped symbols, respectively; copper(I) centres are pink dots and stoppers are large grey spheres.

The distance between the porphyrins in the rotaxane will be monitored by metalation/demetalation with copper(I) (**Figure I.38**). In the absence of the Cu(I) centres the macrocycles can move freely along the axles and the distance between the porphyrins can vary. However, in the presence of copper(I) the position of the macrocycles are locked by coordination with the chelates of the dumbbell components. This will bring the porphyrins in closer proximity. If a flexible guest is coordinated between the porphyrins it will adopt an elongated, thermodynamically stable conformation in the absence of Cu(I). Upon metalation of the rotaxane with Cu(I) the guest is then expected to experience conformational changes by compression between the porphyrin plates.

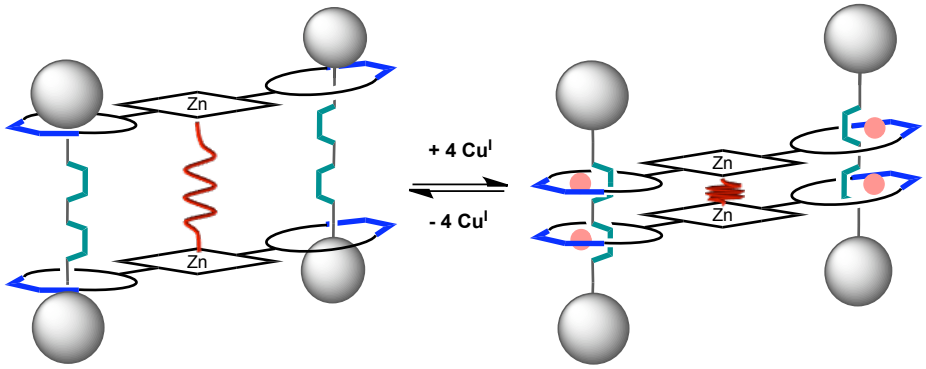

Figure I.38. Proposed mechanism of action of a molecular press based on a [4]rotaxane. A flexible guest molecule bound in the central cavity of the rotaxane by axial coordination on the Zn-porphyrins is depicted in red. In the absence of copper(I) the guest can adopt an elongated conformation. In the presence of copper(I) the porphyrins are expected to be in closer proximity and induce conformational changes on the guest.

The aromatic system of the porphyrinic bis-macrocycle component of the rotaxane will be significantly reduced in this new system by comparison with the [4]rotaxane described in part **I. 4. b)**. In the new system the macrocycles will be linked to the porphyrins *via* single C-C bonds at the *meso* positions, which should bring more flexibility to the assembly and prevent the collapse of the system upon demetalation of the copper(I) centres. The number of synthetic steps will be significantly reduced. While functionalisation of the porphyrin with *four* coordinating rings was hardy achievable with the previous design, it will be possible with the present system. The use of a porphyrinic tetra-macrocycle will open up the possibilities for the construction of architecturally interesting molecules. For example a porphyrin substituted with four coordinating macrocycles (instead of two) could give rise to a [6]rotaxane upon threading with adequate axles followed by stoppering. This rotaxane would be constituted of two face-to-face zinc porphyrins whose rings would be threaded by four dumbbells (**Figure I.39**). Thanks to the presence of two additional dumbbells a greater geometrical control over the inter-porphyrin distance could be achieved with this system compared to the system depicted in **Figure I.38**.

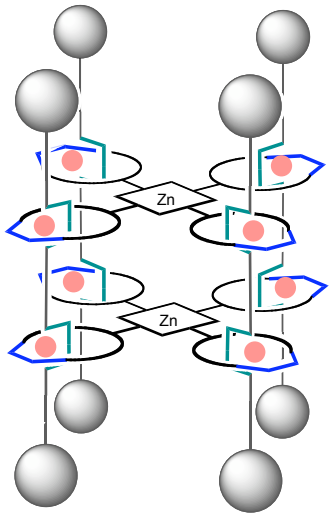

Figure I.39. Design of a [6]rotaxane composed of two porphyrinic tetra-macrocycles and of four dumbbells.

In addition to their potential as molecular receptors or presses, the rotaxanes studied in this thesis are interesting by virtue of their challenging syntheses and of the prospect of obtaining new, aesthetically attractive interlocked architectures. The project involves the syntheses of a molecular thread and stopper, as well as the syntheses of new porphyrin building blocks substituted with coordinating macrocycles, which will potentially find applications in the elaboration of other intertwined molecules in the future.

Chapter II. Rotaxane Building Blocks:

A New Zinc Porphyrin Substituted with Two Coordinating Macrocycles, a Molecular Rod and a Stopper

II. 1. Design of the System

II. 1. a) Chemical Structures of the Target Building Blocks

In this chapter we will describe the synthesis of the three building blocks needed for the formation of a [4]rotaxane that will incorporate two zinc(II) porphyrin units. A retrosynthetic scheme showing the chemical structures of the target building blocks is depicted in **Figure II.1**.

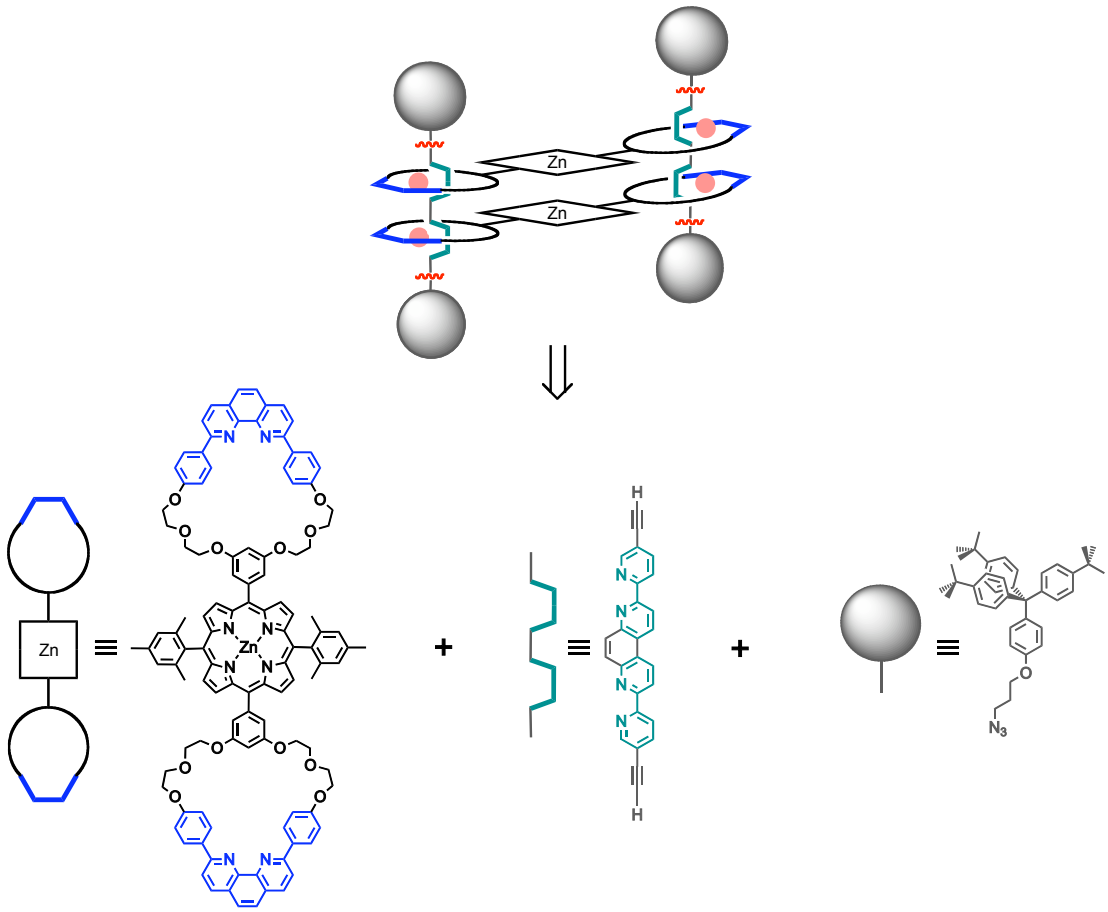

Figure II.1. Retrosynthetic scheme displaying the chemical structures of the target building blocks needed for the formation of a [4]rotaxane with two cofacial Zn-porphyrins. The pink spheres represent copper(I), the "gathering-and-threading" centre.

The target bis-macrocyclic component is a new Zn-porphyrin substituted with two dpp-containing rings at antipodal *meso* positions. The molecular rod, or axle, has a central aromatic part that forms two rigidly held bidentate chelating sites derived from the 2,2'-bipyridine motif. The porphyrinic bis-macrocycle and the axle are designed to form a [4]pseudorotaxane upon complexation with a copper(I) template, which will then be converted to the desired [4]rotaxane by introduction of stoppers at the ends of the axles. The stopper building block possesses a bulky tris(*p-tert*-butylphenyl)methane group. The axle and the stopper are functionalised with terminal acetylenic and azide groups, respectively, which makes them "clickable" *via* a Huisgen Copper(I)-catalysed Azide-Alkyne Cycloaddition (CuAAC).

II. 1. b) Comparison of the Present Porphyrinic Bis-Macrocycle with the Previous System

As mentioned in part **I. 4. c)** of the introduction the present project is related to previous work performed in our laboratory. Former PhD students and postdoctoral researchers studied a [4]rotaxane with a cyclic structure similar to that of our new target rotaxane.[196] The bis-macrocyclic component of the previously described rotaxane was a Zn-porphyrin rigidly linked to two phenanthroline-containing macrocycles. Several main differences, highlighted in **Figure II.2**, distinguish the present target bis-macrocycle from the previous system.

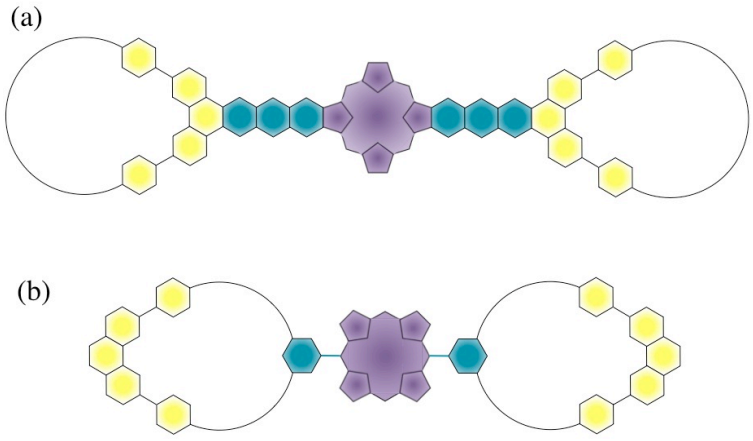

Figure II.2. Schematic view of the structural difference between two porphyrinic bis-macrocycles: (a) previously made in our group[196] and (b) described in this chapter. The main differences reside in *(i)* the nature of the bridge (highlighted in blue) between the central porphyrin (purple) and the macrocycles (rigid pyrazine-benzene-pyrazine motif *vs.* single C-C bond); *(ii)* the position of the bridge on the porphyrin (β-pyrrolic *vs. meso* substitution); *(iii)* the orientation of the coordinating dpp unit (yellow) (*exo vs. endo* coordination mode with respect to the porphyrin); and *(iv)* the electronic coupling between the dpp chelate and the porphyrin (electronically coupled *vs.* decoupled).

In the previous system the linker between the porphyrin and the dpp chelates was very rigid since the porphyrin nucleus and the chelates were fused *via* pyrazine-benzene-pyrazine bridges at antipodal β positions of the porphyrin. In addition, the porphyrin was attached to the "back" of the 1,10-phenanthroline aromatic fragment, imposing an ***exo*** coordination mode of this chelate with respect to the porphyrin. The connection mode was such that the lateral ring was rigid and could not rotate much with respect to the porphyrin plane. In the present target compound the situation is dramatically different since *(i)* the porphyrin and the coordinating rings are linked *via* single C-C bonds between the porphyrin *meso* positions and the macrocycle, making the latter susceptible to rotate with respect to the plane of the porphyrin, and *(ii)* the coordinating axis of the dpp fragment is pointing **towards** the porphyrin. In other words, the dpp unit will be located far away from the porphyrin and it will be electronically decoupled from it, contrary to the first series of porphyrin-incorporating multi-rotaxanes made in our group. These differences will introduce a greater flexibility in the rotaxanes that will be built from the new target bis-macrocycle. Consequently, original host-guest properties will be expected with the new system. Another important difference between the previous and the present systems is the number of organic steps involved in the synthesis of the porphyrinic bis-macrocycle. The synthesis of the previously described free-base porphyrin was long and tedious. It consisted in fifteen independent organic steps[196] while this number is reduced to seven for the present target compound, as will be detailed in this chapter.

II. 2. A dpp-Containing Macrocyclic Precursor

II. 2. a) Target Structure and Retrosynthesis

The macrocycle whose structure is depicted in **Figure II.3** is an important intermediate in the synthesis of the new porphyrinic building block. The macrocycle can be denominated as "m-31" according to the nomenclature traditionally used in our group because its cycle is constituted of 31 atoms. It incorporates a 2,9-diphenyl-1,10-phenanthroline (dpp) chelate and is closed by a 3,5-disubstituted benzaldehyde ring. The aldehyde function was introduced to allow the subsequent formation of a porphyrin by condensation with a pyrrolic derivative.

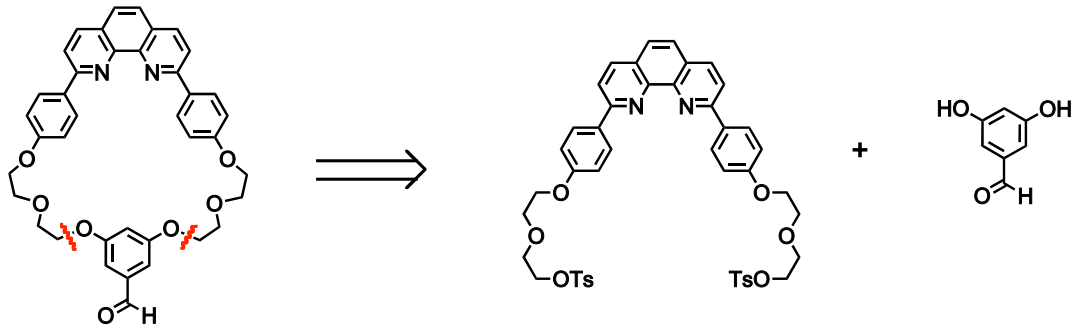

Figure II.3. Chemical structure of the macrocyclic precursor and retrosynthetic route.

The synthetic approach chosen to form the macrocycle is a double Williamson reaction between 3,5-dihydroxybenzaldehyde and a dpp-derivative functionalised with two tosylate-terminated chains.

II. 2. b) Synthesis of the dpp-Containing m-31 Macrocycle

The aldehyde-appended macrocycle **5** was synthesised in five steps from commercial compounds. The synthetic route is represented in **Figure II.4**. In a first step, 1,10-phenanthroline was functionalised with anisyl groups at positions 2 and 9. (4-methoxyphenyl)lithium was generated *in situ* by treatment of *p*-bromoanisole with butyl lithium. It was reacted with 1,10-phenanthroline, and the obtained intermediate was hydrolysed and oxidised with MnO_2 to afford 2,9-dianisyl-1,10-phenanthroline (dap) **1** in 53% yield. The phenol functions were then deprotected by treatment of dap with pyridinium chloride at 210 °C. 2,9-diphenol-1,10-

phenanthroline (dpp) **2** was obtained in 95% yield.[198,199] The dpp chelate was further functionalised with diethyleneglycol chains by Williamson reaction with 2-(2-chloroethoxy)ethanol. Tosylation of the terminal hydroxyl groups of **3** was achieved by treatment of the compound with *p*-toluenesulfonyl (tosyl) chloride.[200] Macrocycle **5** was prepared by the cyclisation reaction of ditosylate **4** with 3,5-dihydroxybenzaldehyde in the presence of cesium carbonate in high dilution conditions. After purification, the compound was obtained as a white powder in a very satisfactory 67% yield.

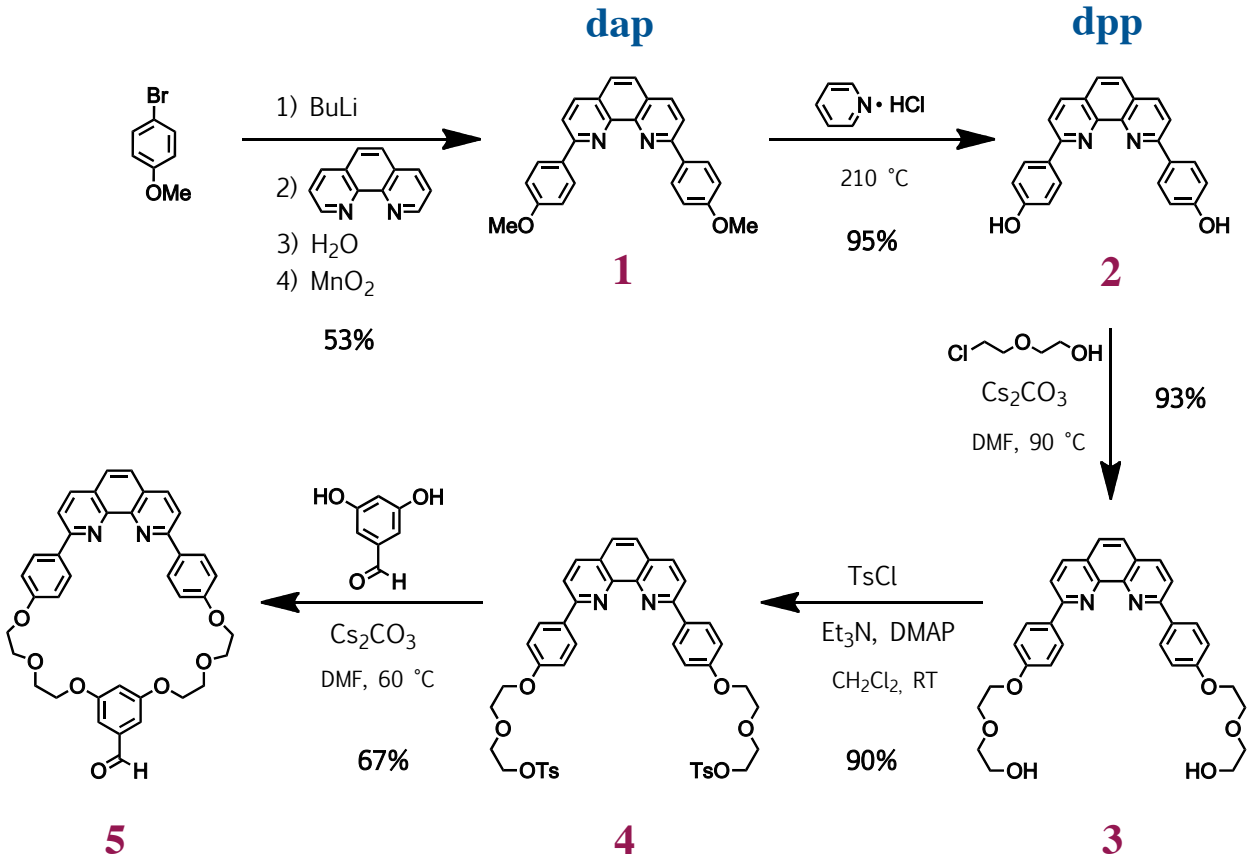

Figure II.4. Synthesis of the dpp-incorporating aldehyde-appended macrocycle **5**.

II. 2. c) Characterisation of the Macrocycle: X-Ray Crystal Structure

In addition to ^{1}H NMR spectroscopy and mass spectrometry, macrocycle **5** was characterised by X-ray diffraction. Gold-coloured prismatic single crystals suitable for X-ray crystallography were grown by recrystallisation from dichloromethane/methanol. The crystal structure of the molecule is depicted in **Figure II.5**.

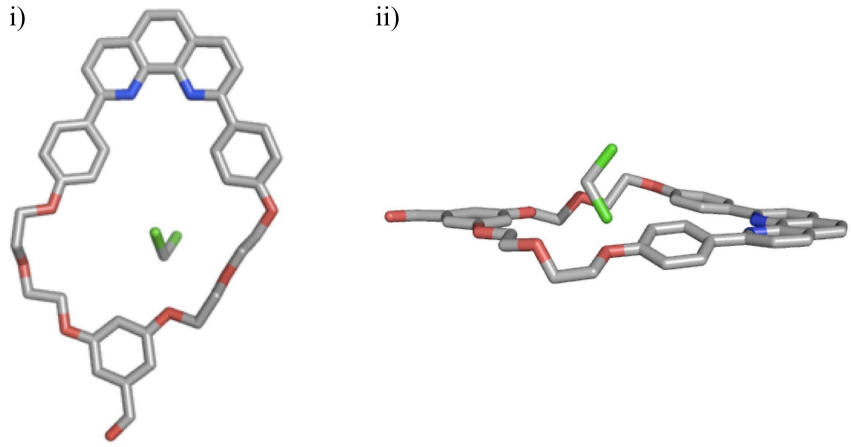

Figure II.5. X-Ray structure of the 31-membered ring **5**. A dichloromethane molecule resides in the structure (Carbon atoms are represented in grey, nitrogen atoms in blue, oxygen atoms in red, chlorine atoms in green; hydrogen atoms are omitted for clarity). (i) Top view; (ii) side view.

In the crystalline state the conformation of the macrocycle is surprisingly close to planarity, the benzaldehyde ring being nearly coplanar with the phenanthroline. The structure of **5** possesses no symmetry element, and the phenyl groups attached to the phenanthroline differ in their orientations. One of these phenyl rings is twisted by 22.45° in regard to the phenanthroline and stacks with the benzaldehyde ring of an upper molecule. Its orientation is typical of 2,9-diphenyl-1,10-phenanthroline moieties.[201] The second phenyl ring shows bending rather than twisting in regard to the phenanthroline. The torsion angle is only 3.68° but the phenyl ring points out of the mean plane of the phenanthroline. The molecules are packed in such a way that the cavities of the macrocycles form narrow channels filled with solvent molecules. A molecule of dichloromethane is present in the macrocycles, with the Cl atoms pointing towards the phenanthroline moiety.

The aldehyde-appended macrocyclic precursor **5** will be used in the synthesis of a porphyrinic bis-macrocycle, as we will detail in part **II. 3**.

II. 3. A Zn-Porphyrin Substituted with Two Lateral m-31 Rings

II. 3. a) [2+2] MacDonald Condensation for the Formation of *trans*-A_2B_2 Porphyrins

With the growing interest for porphyrin derivatives, several synthetic strategies have been developed for the formation of functionalised porphyrins. In particular, a pattern of interest in the present research project is the *trans*-A_2B_2 *meso*-substituted porphyrin. This substitution pattern can be obtained by condensation of pyrrole and a mixture of two aldehydes but this reaction would also yield important amounts of *cis*-A_2B_2, A_3B and AB_3 porphyrins, which can be difficult to separate. Thus, a different strategy known as the MacDonald condensation was developed for the synthesis of *trans*-A_2B_2 porphyrins.[202] This [2+2] condensation involves a preformed dipyrrylmethane and an aldehyde as shown on **Figure II.6**. The *trans*-A_2B_2 porphyrin is the sole porphyrin product obtained in the reaction if conditions that avoid scrambling are used.[203-205] The conditions usually employed for this condensation are similar to those of the direct condensation of aldehydes and pyrrole developed by Lindsey and his group; they involve the use of a Lewis acid or a Brønsted acid as a catalyst, typically BF_3-etherate or trifluoroacetic acid.[204,206]

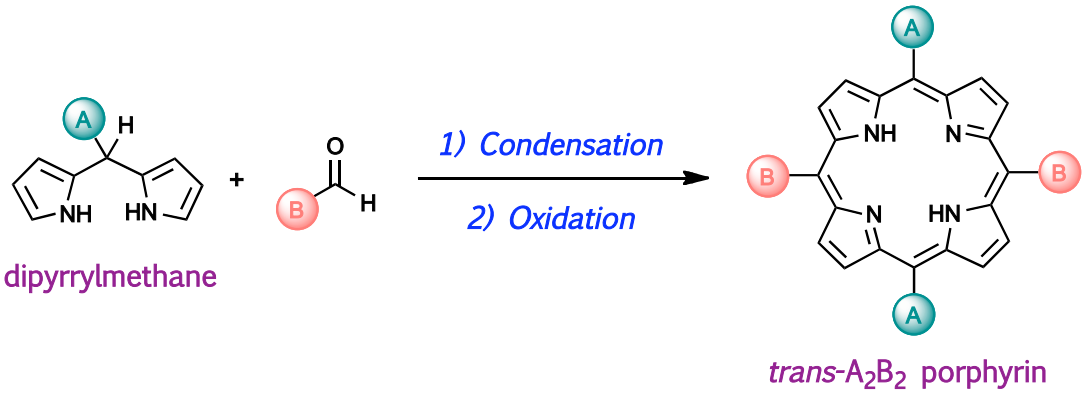

Figure II.6. [2+2] MacDonald condensation of a dipyrrylmethane and an aldehyde for the formation of *trans*-A_2B_2 porphyrins.

II. 3. b) Synthesis of the Porphyrinic Bis-Macrocycle

As seen in **Figure II.1** the target porphyrinic building block for the construction of the [4]rotaxane is a new *meso*-tetraaryl porphyrin with a *trans*-A_2B_2 substitution pattern. Consequently the MacDonald method described above was chosen for the formation of the porphyrin. The synthetic scheme is represented in **Figure II.7**.

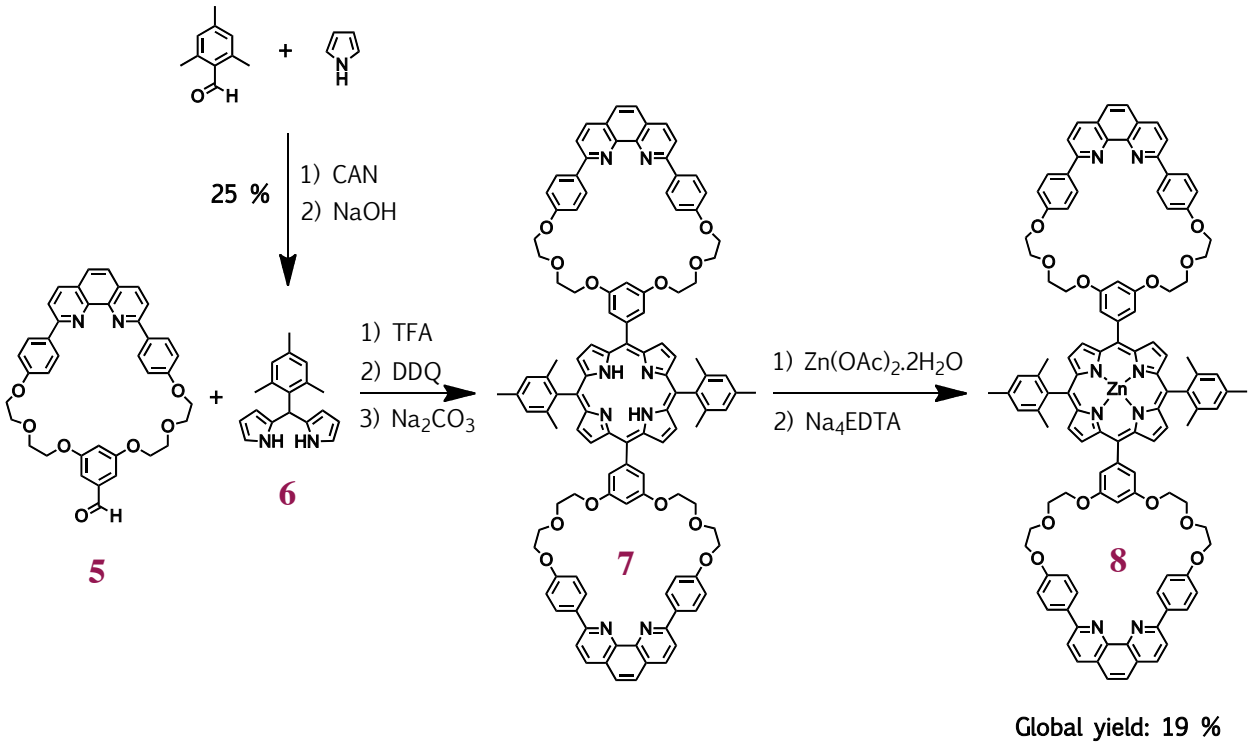

Figure II.7. Synthesis of compound **8**, a Zn-porphyrin substituted with two dpp-containing macrocycles at antipodal *meso* positions.

The free-base porphyrin **7** was formed by MacDonald condensation of macrocycle **5** with 5-mesityldipyrrylmethane **6**. The latter compound was chosen because it increases the solubility and prevents π-stacking of the corresponding porphyrin, and it reduces scrambling during the condensation reaction.[205] The dipyrrylmethane **6** was formed by condensation of mesitylaldehyde with pyrrole in the presence of a large excess of the latter reagent using ceric ammonium nitrate (CAN) as a catalyst.[207] We then followed the optimised condensation conditions described by Lindsey and coworkers for the synthesis of the porphyrin.[204] The dipyrrylmethane and the macrocyclic aldehyde (10 mM in CH_2Cl_2 containing 18 mM TFA) were stirred at room temperature. The reaction turned out to be very slow. After 20 hours we obtained the desired porphyrin in poor yield (< 2%). We performed other condensation reactions with different

concentrations of trifluoroacetic acid and observed that five equivalents of TFA were necessary to allow an efficient condensation. Chromatographic purification of the free-base porphyrin **7** proved difficult. The porphyrin could not be fully purified so the compound was treated with excess zinc acetate with the expectation that the product would be more easily isolated in its metalated form. In the course of this metalation reaction, the dpp chelates of the macrocycles formed complexes with Zn(II) as well as the porphyrin core. Purification of the product at this stage proceeded much more easily, and the porphyrinic bis-macrocycle complexed to three zinc(II) centres was obtained as an intermediate. Subsequent treatment with an EDTA solution to remove the zinc ions from the 1,10-phenanthroline chelates afforded the desired disubstituted Zn-porphyrin **8.** The global yield over the porphyrin condensation and metalation steps was 19%. Compound **8** was fully characterized by ^{1}H NMR, ES-MS and UV-visible absorption spectroscopy. The ^{1}H NMR spectrum in CD_2Cl_2 shows two doublets for the pyrrolic protons, which is in accordance with a *trans meso*-substituted porphyrin. Despite the introduction of mesityl substituents, porphyrin **8** is very poorly soluble in common organic solvents like dichloromethane or chloroform. The poor solubility may be due to intermolecular π-stacking between the phenanthroline units and the porphyrin core.

II. 4. Threading Tests with dap: Formation and Characterisation of a [3]Pseudorotaxane

II. 4. a) Threading Reaction

Bis-macrocycle **8** was designed to be a good candidate for threading. The "gathering-and-threading" effect of copper(I) was used in the synthesis of a prototypical [3]pseudorotaxane from compound **8**, in order to test its ability to form threaded assemblies. 2,9-dianisyl-1,10-phenanthroline (dap) **1** is known to thread rapidly and to form stable four-coordinate Cu(I) complexes. This chelate was thus selected as threading element. Compound **8** and $Cu(CH_3CN)_4PF_6$ (2 equiv.) were first mixed in dichloromethane/acetonitrile under argon and the dap thread **1** (2 equiv.) was subsequently added, which led to the desired pseudorotaxane $\mathbf{9}^{2+}\cdot 2PF_6$ in quantitative yield after work-up (**Figure II.8**).

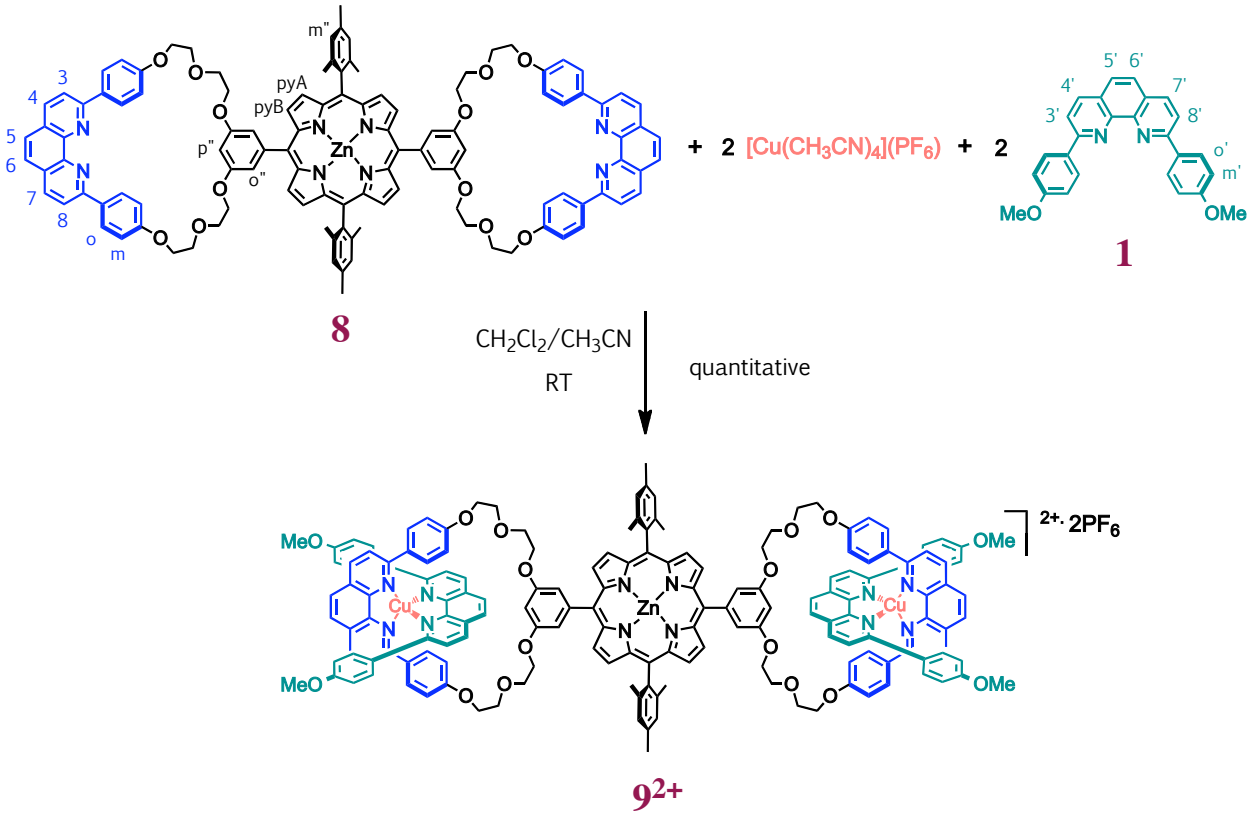

Figure II.8. Threading reaction of bis-macrocycle **8** with dap chelate **1** *via* copper(I) templating to afford the [3]pseudorotaxane $\mathbf{9}^{2+}$.

II. 4. b) NMR Characterisation of Bis-Macrocycle 8 and [3]Pseudorotaxane 9^{2+}

The [3]pseudorotaxane was characterised by electrospray mass spectrometry, ^{1}H NMR, 2D COSY and ROESY, and UV-visible absorption spectroscopy. ES-MS results are consistent with the formation of the expected complex. In the ^{1}H NMR spectrum of [3]pseudorotaxane $\mathbf{9}^{2+}\cdot 2PF_6$ most of the signals are shifted compared to bis-macrocycle **8** (**Figure II.9**). In particular, the 3, 8, o and m protons undergo a strong upfield shift, which is characteristic of threaded complexes.[25,208] These protons experience a strong ring current effect from the nearby phenanthroline moiety of the threaded dap components. Similarly, the signals of the 3', 8', o' and m' protons of the dap ligands are shifted upfield in the threaded complex due to the proximity of the phenanthroline groups incorporated in the macrocycles. The entwined structure of [3]pseudorotaxane $\mathbf{9}^{2+}$ is also confirmed by the NOE interaction observed between protons p" of the rings and protons 5', 6' of the dap ligands in the ROESY spectrum of $\mathbf{9}^{2+}$.

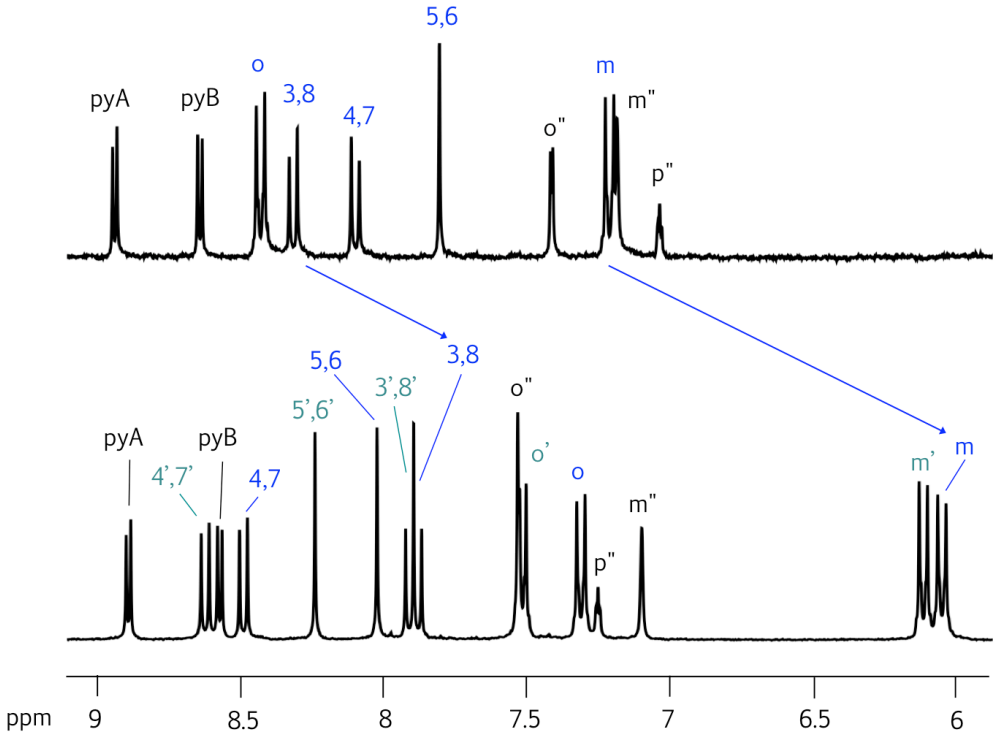

Figure II.9. ^{1}H NMR of the porphyrinic bis-macrocycle **8** and [3]pseudorotaxane $\mathbf{9}^{2+}$ (signals in the aromatic region are displayed). The chemical shifts observed for $\mathbf{9}^{2+}$ are typical of this type of threaded species. In particular, protons 3, 8 and m undergo strong upfield shifts upon threading of dap (blue arrows).

II. 4. c) UV-visible Characterisation of Bis-Macrocycle 8 and [3]Pseudorotaxane 9^{2+}

The absorption and emission spectra of compounds **8** and $\mathbf{9}^{2+}$ were measured in degassed dichloromethane at room temperature (**Figure II.10**).

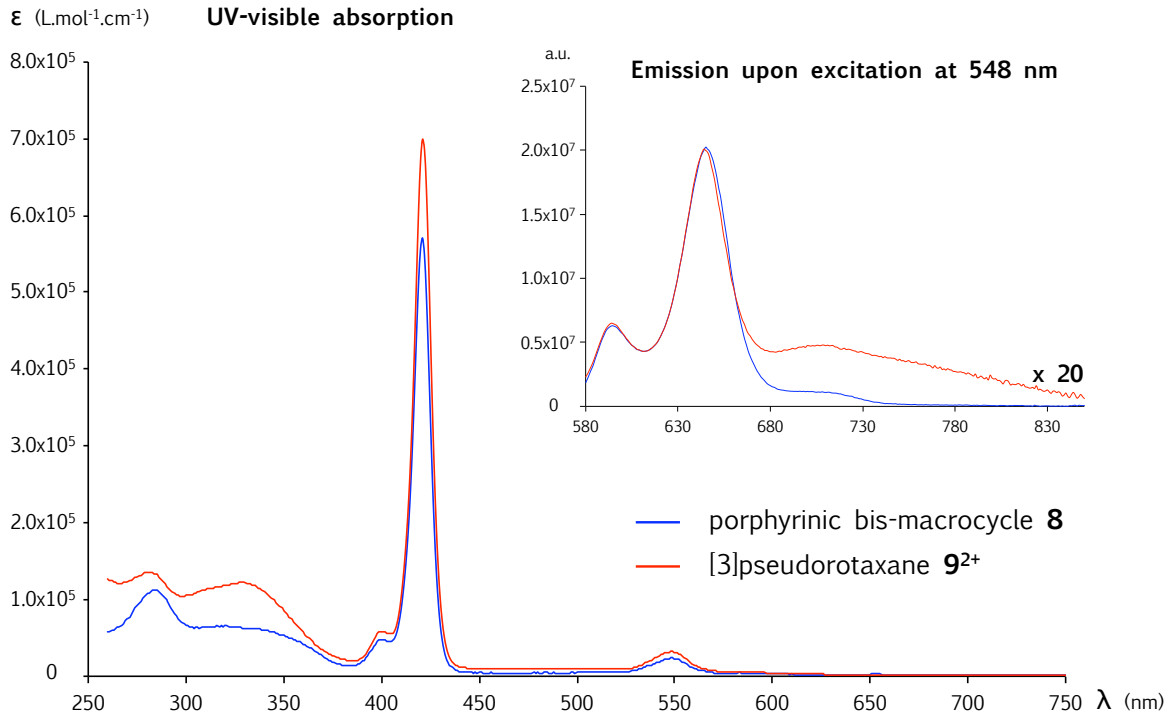

Figure II.10. UV-visible absorption and normalised emission spectra of porphyrinic bis-macrocycle **8** and [3]pseudorotaxane $\mathbf{9}^{2+}$ in CH_2Cl_2. Both compounds have a Soret band at 421 nm and Q bands at 548 and 585 nm. Emission spectra were recorded upon excitation at 548 nm. In both cases emission maxima are observed at 595 and 646 nm.

The Soret band is typically observed at 421 nm whereas the Q bands are observed at 548 and 585 nm for both compounds. The ^{1}MLCT (Metal-to-Ligand Charge Transfer) band of tetrahedral copper(I) complexes containing two ligands of the dpp family, and thus similar to the present complexes, have weak extinction coefficients (a few thousands) compared to those of zinc porphyrins (ten to hundred times more intense).[209] They are thus difficult to detect in the presence of a porphyrin due to spectral overlapping between the Soret and/or Q bands of the porphyrin and the ^{1}MLCT band. The emission maxima are also observed at a typical wavelength (646 nm after excitation at 548 nm) for both compounds. The emission lifetime of the compounds **8** and $\mathbf{9}^{2+}$ were measured at 650 nm after excitation at 370 nm (which was the only excitation source available for emission lifetime measurements). The emission lifetime of the metalloporphyrin **8** is consistent with simple zinc-complexed porphyrin monomers

(τ_1 = 1.85 ± 0.20 ns).[210] The emission lifetime of the pseudorotaxane $\mathbf{9}^{2+}$ turns out to be much shorter (τ_2 = 0.15 ± 0.05 ns) than that of the copper-free compound **8**. This observation is not especially surprising and is in line with previous work on related compounds containing zinc porphyrins and copper complexes of the $Cu(dpp)_2^+$ family.[210] The singlet excited state of the Zn porphyrin is rapidly quenched by the copper(I) complex, due to the presence of a low lying triplet MLCT.

A prototypical [3]pseudorotaxane was successfully obtained by double threading reaction of the dap chelate in the rings of porphyrinic compound **8** in the presence of a copper(I) template. This result encouraged us to continue our works towards the construction of more complex rotaxane structures.

II. 5. A Molecular Rod with Two Binding Sites and a Stopper

II. 5. a) Design of the Axle and Stopper

The construction of our target [4]rotaxane requires the synthesis of two more building blocks in addition to the porphyrinic bis-macrocycle presented above. These building blocks are a rigid **axle**, or **molecular rod**, with two chelating sites and a **stopper** possessing a bulky terminal group that will prevent unthreading in the final interlocked compound. The axle and stopper need to be appropriately functionalised to allow the attachment of the stoppers on the preformed pseudorotaxane in high yield. Ideally the stoppering reaction should proceed quantitatively and in mild conditions compatible with the presence of copper(I) complexes in the pseudorotaxane. The reactions falling into the category of *click chemistry*, as defined by K. B. Sharpless and co-authors in 2001, are excellent options for this type of reaction.[211]

Click chemistry was introduced as a new synthetic concept to generate functional molecules by joining building blocks in an easily practicable way. The reactions belonging to the family of click chemistry must meet a list of criteria, including *"be modular, wide in scope, high yielding, create only inoffensive by-products (that can be removed without chromatography), be stereospecific and simple to perform"*.[211] Click reactions comprise nucleophilic ring-opening reactions, non-aldol carbonyl chemistry, additions to carbon-carbon multiple bonds (especially thiol-ene reactions and Michael additions), and cycloadditions (*e.g.* Diels-Alder reactions and 1,3-dipolar cycloadditions). Although click chemistry was introduced as a new tool for drug discovery, it has found applications in many other fields including polymer and materials science,[212] and in the construction of supramolecular and interlocked architectures.[213] In particular the Huisgen Copper(I)-catalysed Azide-Alkyne Cycloaddition (CuAAC)[214,215] is a standard of click chemistry and is widely used in various fields.[216] The azide and alkyne precursors for this reaction are usually relatively easy to prepare, and in the presence of a copper(I) catalyst the cycloaddition proceeds with almost complete conversion and selectivity for the *anti* 1,2,3-triazole (**Figure II.11**).

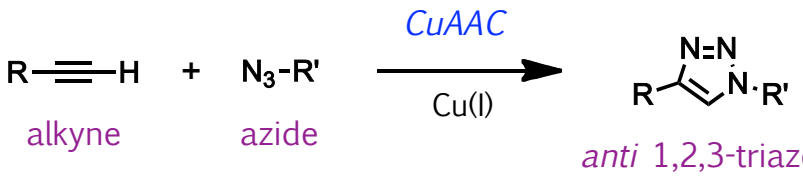

Figure II.11. The Huisgen Copper(I)-catalysed Azide-Alkyne Cycloaddition (CuAAC) reaction. With Cu(I) as a catalyst the reaction usually proceeds in high yields and the *anti* 1,2,3-triazole is formed selectively.

Given the many advantages of the CuAAC reaction it was chosen as the stoppering reaction in the formation of the new rotaxanes presented in this thesis. Consequently the axle and stopper building blocks were functionalised with terminal alkyne and azide groups, respectively (**Figure II.12**). The axle contains a central bis-3,8-(*o*-pyridyl)-4,7-phenanthroline fragment that forms two bidentate sites resembling the 2,2'-bipyridine motif. Due to the rigid linker between the chelates, they are coplanar and point in the same direction, which will result in the coordination of two metal ions on the *same* side of the axle.

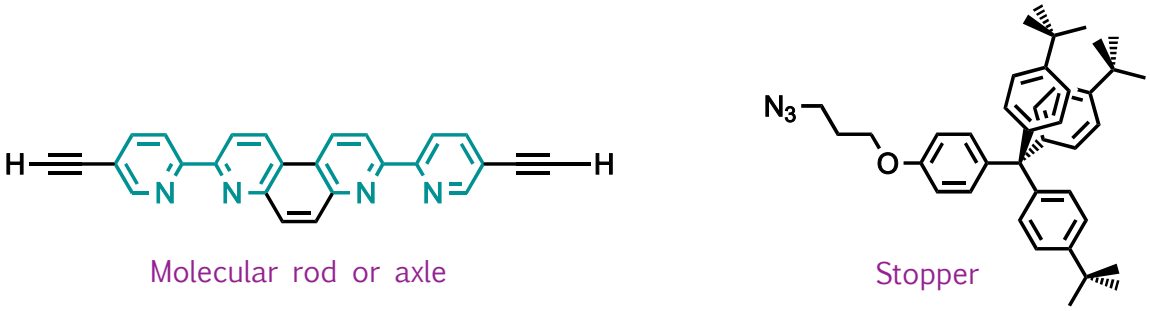

Figure II.12. Target chemical structures of the dumbbell building blocks. The molecular rod, or axle, is functionalised with two terminal alkyne groups and contains two coplanar 2,2'-bipyridine chelates facing towards the same side of the axle (left). The stopper comprises a hindering group at one end and an azide group at the other end (right).

II. 5. b) Synthesis of a Two-Station Axle terminated with Acetylenic Functions

The molecular rod represented in **Figure II.12** has already been used in the synthesis of several pseudorotaxanes and rotaxanes.[53,196,217-219] Yann Trolez, a former PhD student in Strasbourg, developed the synthetic scheme for this molecule. The alkyne-terminated bis-bidentate axle is obtained in seven steps from commercial compounds. The first five steps consist in the formation of the central brominated bis-bidentate fragment **14** (**Figure II.13**). The

3,8-dibromo-4,7-phenanthroline precursor **12** is obtained in three steps from 4,7-phenanthroline following a procedure described by the group of Lehn.[220] The procedure described in this paper is then adapted to lead to the desired dibromo-functionalised compound **14**.[221]

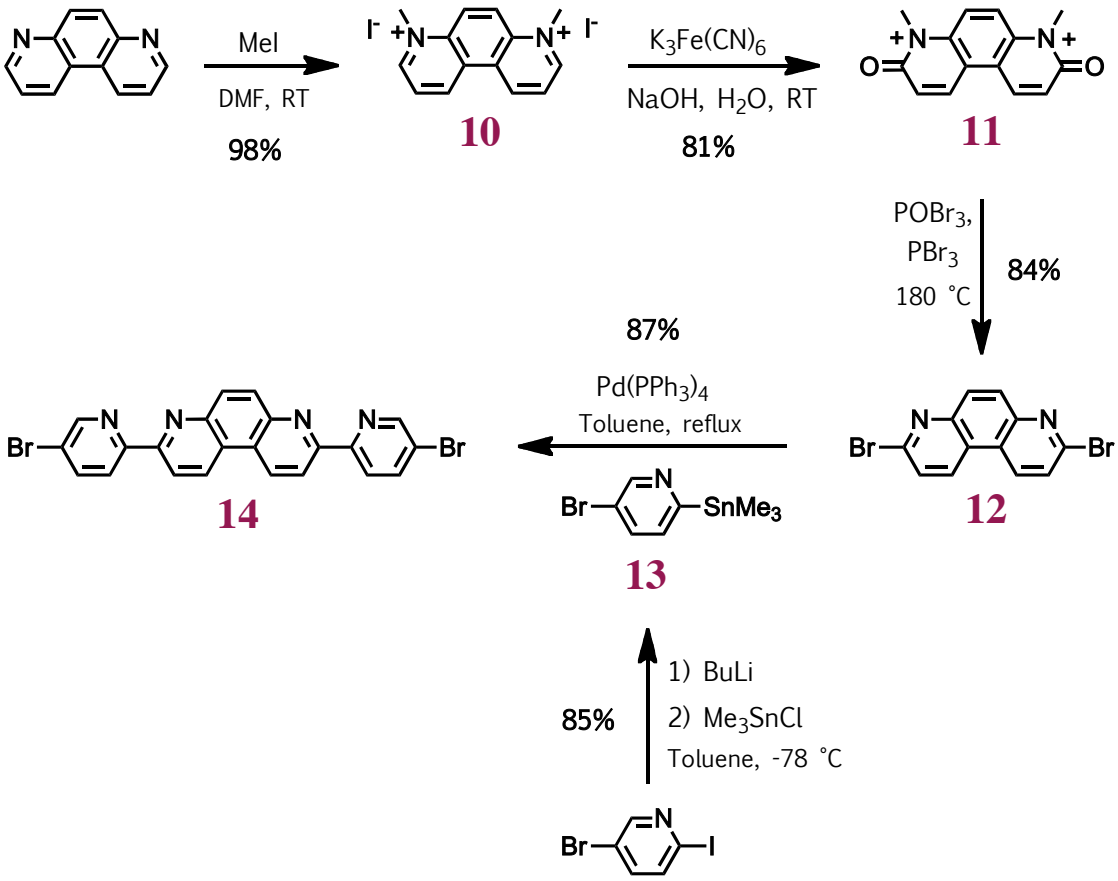

Figure II.13. Synthesis of the dibromo bis-bidentate fragment **14**.

The synthesis of the bis-bidentate ligand **14** started with the methylation of the nitrogen atoms of commercial 4,7-phenanthroline with excess iodomethane to afford compound **10** with 98% yield. The double role of this reaction is to activate the α positions of the phenanthroline (in relation to the N atoms) and to protect the nitrogen atoms in the subsequent oxidation reaction. The second step consisted in the oxidation of compound **10** with potassium ferricyanide to form a C=O double bond in α position to the N atoms of the phenanthroline moiety. Intermediate **11** is obtained in 81% yield. It was then reacted in a mixture of phosphorous tribromide and phosphorus oxybromide to yield 84% of 3,8-dibromo-4,7-phenanthroline **12**. The reaction is driven by the rearomatisation of the system and by the formation of a P=O double bond. The organotin derivative **13** needed for the following step was formed in 85% yield by reaction of 2-iodo-5-bromopyridine with butyl lithium followed by trimethyltin chloride.[222] Finally, Stille coupling of 3,8-dibromo-4,7-phenanthroline **12** and 2-trimethylstannyl-5-bromopyridine **13** was

performed using $Pd(PPh_3)_4$ as a catalyst. The dibromo bis-bidentate synthon **14** was obtained in 87% yield. The selectivity of the reaction is attributed to the electrophilic nature of the carbon located in α position relative to the nitrogen atoms of the phenanthroline moiety.

The last two steps in the synthesis of the axle building block consist in the introduction of the terminal acetylenic functions on the central bis-bidentate core (**Figure II.14**).[53] The introduction of the C≡C triple bonds was achieved by Sonogashira coupling of the dibromo precursor **14** with (triisopropylsilyl)acetylene in classical Sonogashira reaction conditions to give **15** in 59% yield after chromatographic purification. The triisopropylsilyl (TIPS) group was preferred to the trimethylsilyl group because it improves the solubility of the product. The carbon-carbon triple bonds were finally deprotected using tetrabutylammonium fluoride (TBAF), and the very poorly soluble alkyne-terminated axle **16** was obtained in 85% yield.

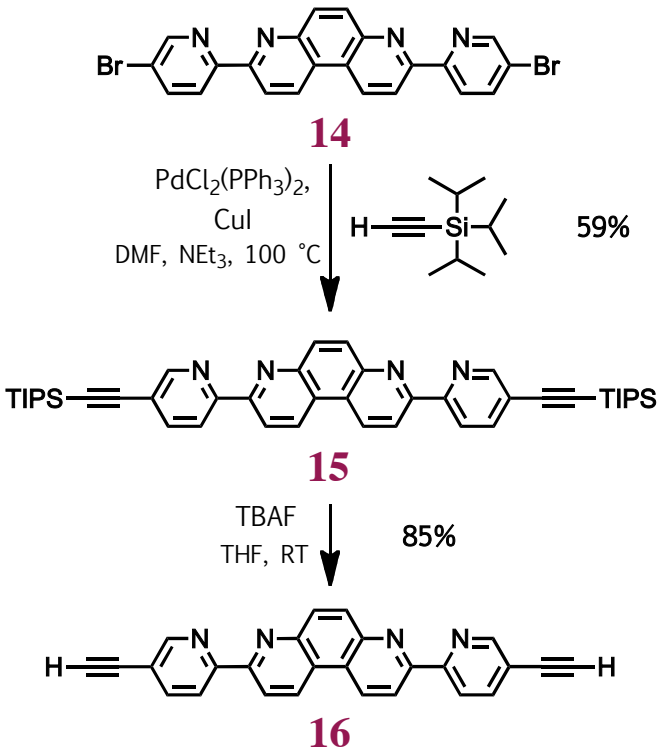

Figure II.14. Synthesis of the two-station axle **16** functionalised with acetylenic groups.

II. 5. c) Synthesis of an Azide-Functionalised Stopper

The target azide-functionalised stopper represented in **Figure II.12** was synthesised in two steps from a phenol precursor using a procedure adapted from a previously described method (**Figure II.15**).[53,223]

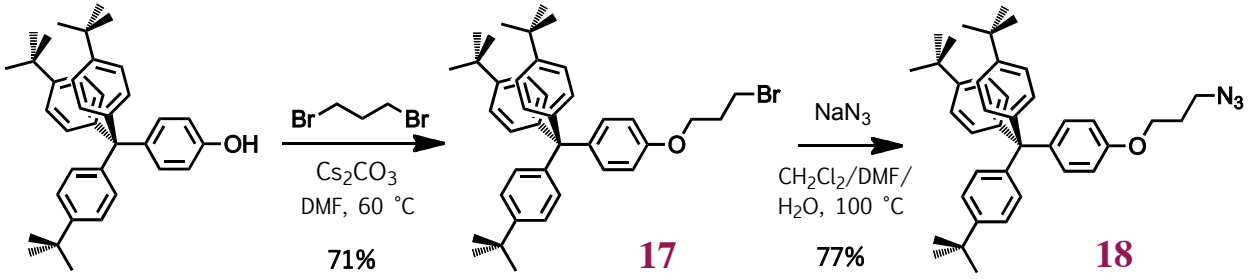

Figure II.15. Synthesis of the azide-functionalised stopper **18**.

The 4-[tris(*p*-*tert*-butylphenyl)methyl]phenol precursor was synthesised by Delphine Hatey, a former technician in our group, following a literature procedure.[224] Williamson reaction of the phenol precursor with 1,3-dibromopropane in the presence of cesium carbonate as a base yielded 71% of bromo-functionalised stopper **17**. The final azide stopper **18** was then obtained in 77% yield by nucleophilic substitution of azide anions on the bromo compound **17** using sodium azide.

In this chapter we described the syntheses of three important building blocks: a zinc porphyrin substituted with two coordinating macrocycles, a two-station rigid axle and a stopper that can be "clicked" at the ends of the axle. These building blocks were carefully designed to allow their assembly into rotaxane structures. In the next chapter we will put this concept in practice and investigate the formation of a rotaxane from the molecular bricks presented here.

Chapter III. A Cyclic [4]Rotaxane Composed of Two Dumbbells and Two Bis-Macrocycles:

A Distensible Molecular Receptor

After describing the syntheses of three building blocks we will now discuss the formation of a new rotaxane from these precursors. The rotaxane will be assembled *via* a "threading-followed-by-stoppering" strategy. Its synthesis, characterisation and molecular receptor properties will be described.

III. 1. Synthetic Approach for the Formation of a [4]rotaxane

III. 1. a) General Strategies for the Synthesis of Rotaxanes

Various synthetic approaches have been developed to assemble building blocks into rotaxane structures, in a way that makes it impossible to unthread the rings from the dumbbell components once the rotaxanes are formed. The main two strategies are the "threading-and-stoppering" and the "clipping" methods. In the **threading-and-stoppering** approach, threading of a preformed ring on an axle is followed by introduction of two bulky stoppers at the ends of the axle.[43,45,182,189,225-230] A variant of this method resides in the use of an axle bearing one stopper in the threading step. In that case only one more stopper needs to be introduced in the second step.[40] The **clipping** approach consists in the macrocyclisation of an open ring precursor around a preformed dumbbell.[58,231,232] A schematic view of these main two methods is depicted in **Figure III.1**, along with three auxiliary strategies.

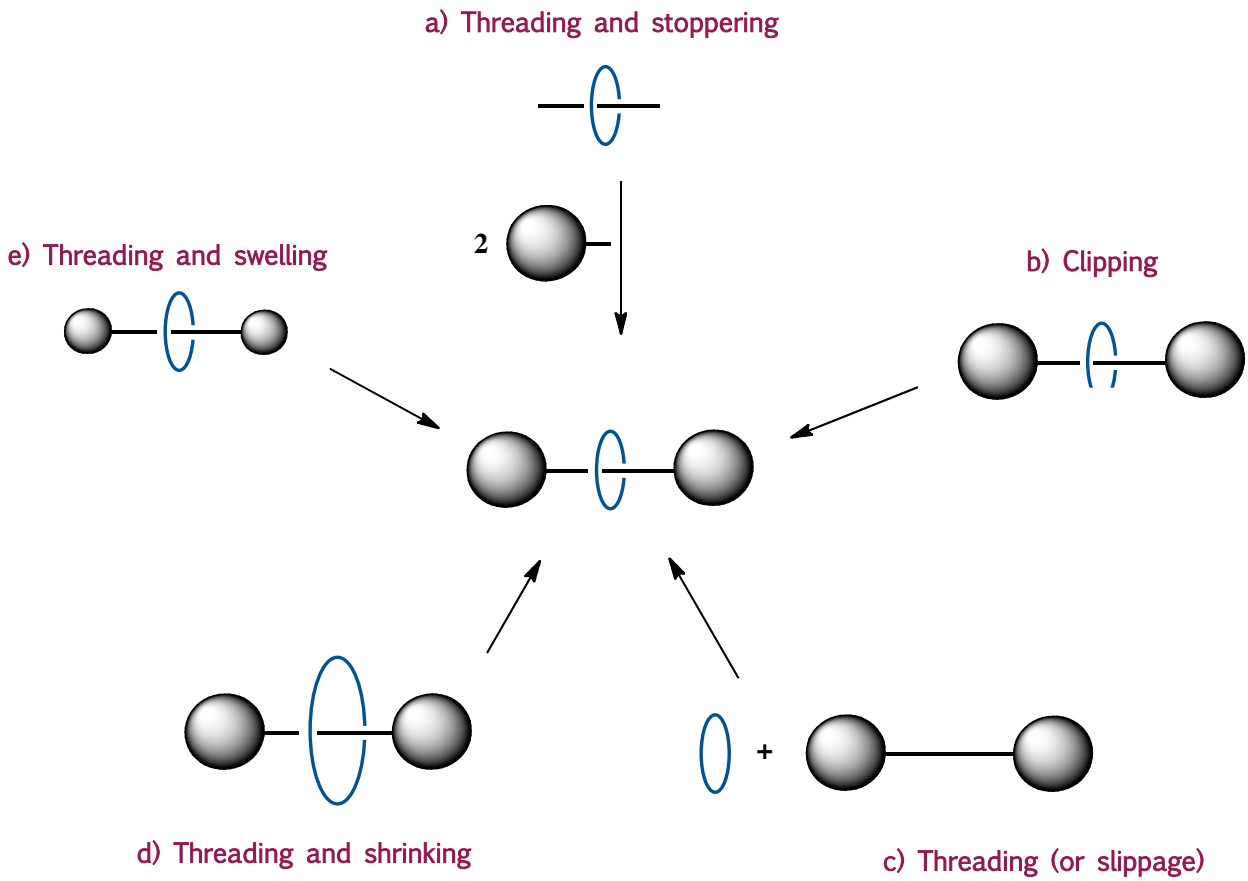

Figure III.1. Different strategies used in the assembly of rotaxanes.

Beside the "threading-and-stoppering" and "clipping" strategies, a few other methods have been reported for the formation of rotaxanes. Direct **threading** (or **slippage)** of the ring on a stoppered dumbbell can be induced at high temperature. The threaded species obtained is thermodynamically stable upon cooling to room temperature.[233,234]

Another strategy was described by M. Asakawa and coworkers. They used a macrocycle incorporating a tetradentate salophen moiety. In the absence of metal the macrocycle is big enough to slip onto the dumbbell, however a square-planar complex is formed in the presence of Pd(II), which shrinks the size of the ring formed by the complexed macrocycle and locks the system in the threaded state.[235] S.-H. Chiu recently reported a metal-free variant to this "**threading-and-shrinking**" method where ring shrinking is achieved by photoextrusion of SO_2 from a sulfone-incorporating macrocycle.[236]

The same group also took an alternative approach, which consists in making the stoppers swell instead of making the ring shrink. The end groups of the axle are *cis*-1,2-

divinylcyclopropane units, that can be converted into bulkier cycloheptadiene rings by Cope rearrangement after threading of the ring.[237,238] A similar strategy to this "**threading-and-swelling**" approach relies on the use of a stopper that can be reversibly switched between two states: an extended state that allows threading and unthreading of the ring, and a folded, bulkier state that prevents slippage. Examples of switchable stoppers include a methylstilbene unit whose extended *E* isomer is converted to the folded *Z* isomer upon photo-irradiation,[239] and an arylamide foldamer stopper.[240] This switchable-stoppering approach could find applications in the controlled release of active substances in the medicinal field.

In spite of the attractiveness of the new strategies described above we decided to opt for the more classical threading-and-stoppering approach when designing our new target rotaxanes. This method has the advantage of being well documented, versatile and efficient. A wide range of reactions for the introduction of stoppers is available, including Williamson ether synthesis,[225] C-C coupling,[43] formation of a bulky metal complex,[226] formation of porphyrins,[40] axial ligation on porphyrins,[182] Diels-Alder reaction,[189] and Huisgen Copper(I)-Catalysed Azide-Alkyne Cycloaddition (CuAAC).[45,227-230] As mentioned in the previous chapter we selected the CuAAC as the stoppering reaction for our new multi-rotaxanes. This type of click reaction has been extensively used in the synthesis of rotaxanes in recent years;[241] its mild conditions make it compatible with various rotaxane precursors.

III. 1. b) Design of the System and [4]Rotaxane Formation Strategy

The chemical structure of the target copper(I)-complexed [4]rotaxane is represented in **Figure III.2**. As previously mentioned the [4]rotaxane will consist of two dumbbells and of two bis-macrocycles that incorporate a central Zn-porphyrin. Each dumbbell will be threaded through one of the rings of each porphyrin in a cyclic structure. The dumbbells are composed of the bis-bidentate axle described in Chapter II, "clicked" to bulky stoppers stoppers at each end. The bis-macrocycle component was presented in Chapter II as well, and we showed that it could be used to form threaded assemblies in quantitative yield.

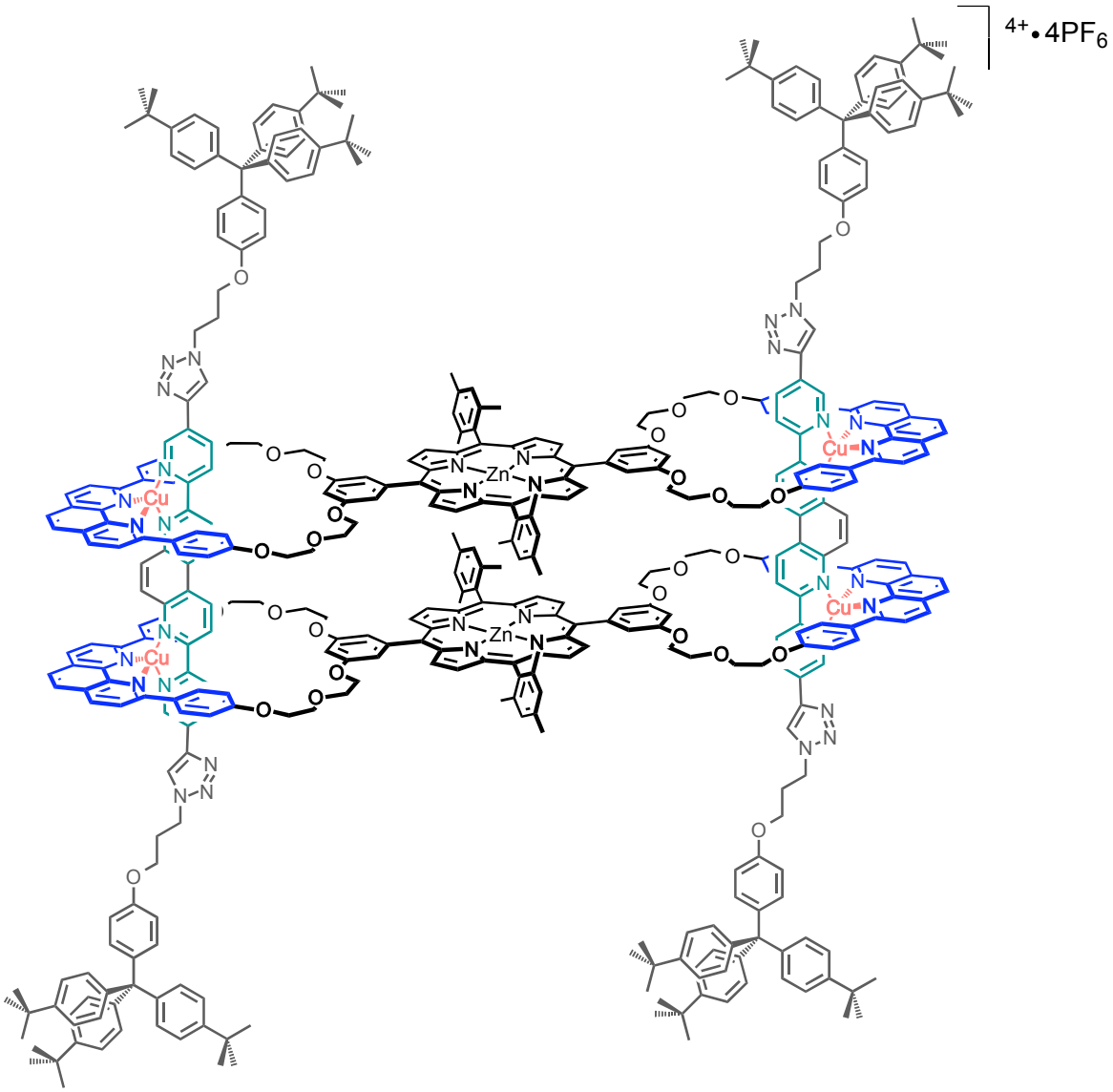

Figure III.2. Chemical structure of the target copper(I)-complexed [4]rotaxane.

The "threading-followed-by-stoppering" approach will be taken for the formation of the [4]rotaxane (**Figure III.3**). In a first step the "gathering-and-threading" effect of copper(I)[25,40,45] is utilised to form a [4]pseudorotaxane from the bis-macrocycle and axle building blocks. The stoppers are then introduced *via* a quadruple CuAAC click reaction[215] to give the [4]rotaxane.

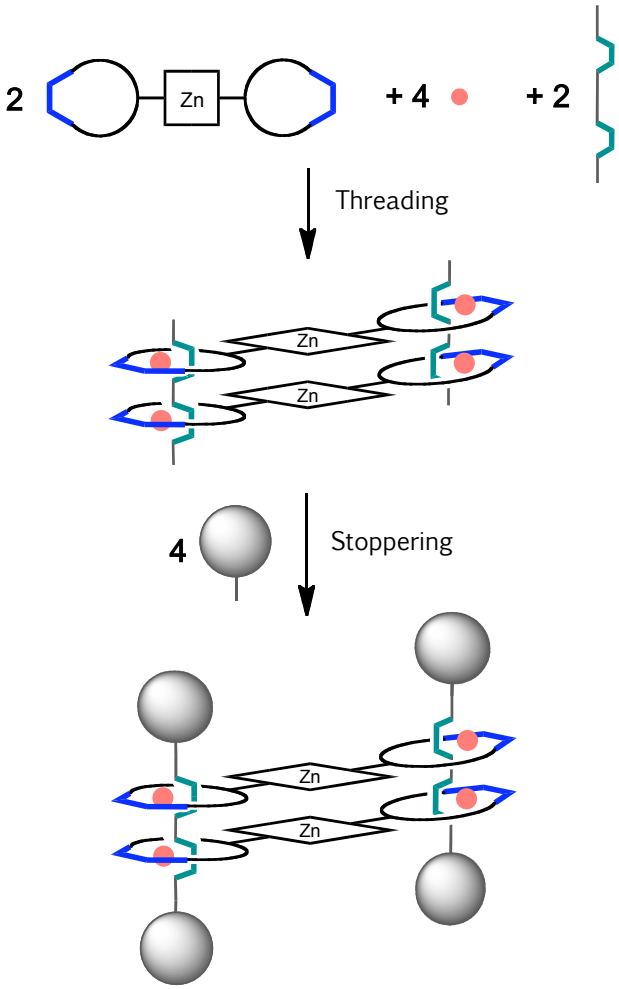

Figure III.3. Preparation of a [4]rotaxane composed of two axles and two bis-macrocycles. Each bis-macrocycle consists of two flexible rings attached to a central Zn porphyrin. The synthetic strategy is based on the "gathering-and-threading" approach using a copper(I) template, followed by stoppering. The porphyrin is represented as a square or a diamond, the bidentate chelates are indicated by green or blue U-shaped symbols and the gathering metal centre (copper(I)) is a pink dot. The stoppers are depicted as large grey spheres.

The rotaxane incorporates two central face-to-face Zn-porphyrins, which will allow for complexation of linear ditopic guests *via* axial coordination between the metalated porphyrins. The specificity of the present system is that the new bis-macrocyclic component will make the rotaxane assembly much more flexible than previously described [4]rotaxanes (see Part **I. 4. b**)).[196,197] Therefore, the new [4]rotaxane should be adaptable even in its copper-complexed form, contrary to the previous system which was more rigid and which collapsed after demetalation. Due to a higher flexibility of the connectors between the porphyrinic plates and the axles, the receptor should be "inflatable", depending on the complexed substrate, in a manner reminiscent of the induced-fit in enzymes.[242-247] As shown in previous studies the 31-membered ring can be distorted and a non-planar ring can be generated.[200,248] In this chapter we will see how this distortion ability influences the host-guest properties of the rotaxane.

III. 2. Synthesis and Characterisation of the Copper(I)-Complexed [4]Rotaxane

III. 2. a) Threading and Stoppering Reactions: [4]Rotaxane Synthesis

The synthetic approach was to form [4]rotaxane $\mathbf{19}^{4+}\bullet 4PF_6$ from bis-macrocycle **8**, thread **16** and stopper **18** in a two-step, one-pot experiment involving both the threading and stoppering reactions (**Figure III.4**). The building blocks (porphyrin-bis-macrocycle **8**, acetylenic thread **16** and azide stopper **18**) were synthesised as described in Chapter II.

The gathering-and-threading effect of copper(I) was utilised in the first step (threading), which led to the formation of a cyclic [4]pseudorotaxane consisting of two porphyrin-bis-macrocycles and two threads. First, an acetonitrile solution of $[Cu(CH_3CN)_4](PF_6)$ was added to a suspension of the poorly soluble porphyrin **8** in dichloromethane to give a deep red solution of bis-macrocycle **8** complexed to two copper(I) ions at the dpp chelating sites. This solution was then added to a suspension of acetylenic thread **16** (stoichiometric amount) in dichloromethane. This resulted in the formation of the [4]pseudorotaxane with four tetrahedral copper(I) complexes linking the dpp sites of the macrocycles and the bipyridine-type sites of the threads.

In a second step, bulky azide-functionalised stopper precursors were introduced at each acetylenic end of the threads *via* a CuAAC click reaction. Stopper **18**, catalytic $[Cu(CH_3CN)_4](PF_6)$ and base (Na_2CO_3) were added to the reaction mixture containing the [4]pseudorotaxane. The resulting stoppered [4]rotaxane $\mathbf{19}^{4+}\bullet 4PF_6$ was obtained as a deep purple solid after purification by consecutive alumina, size-exclusion and silica column chromatographies. The global yield over two steps (threading and quadruple stoppering) was 50%.

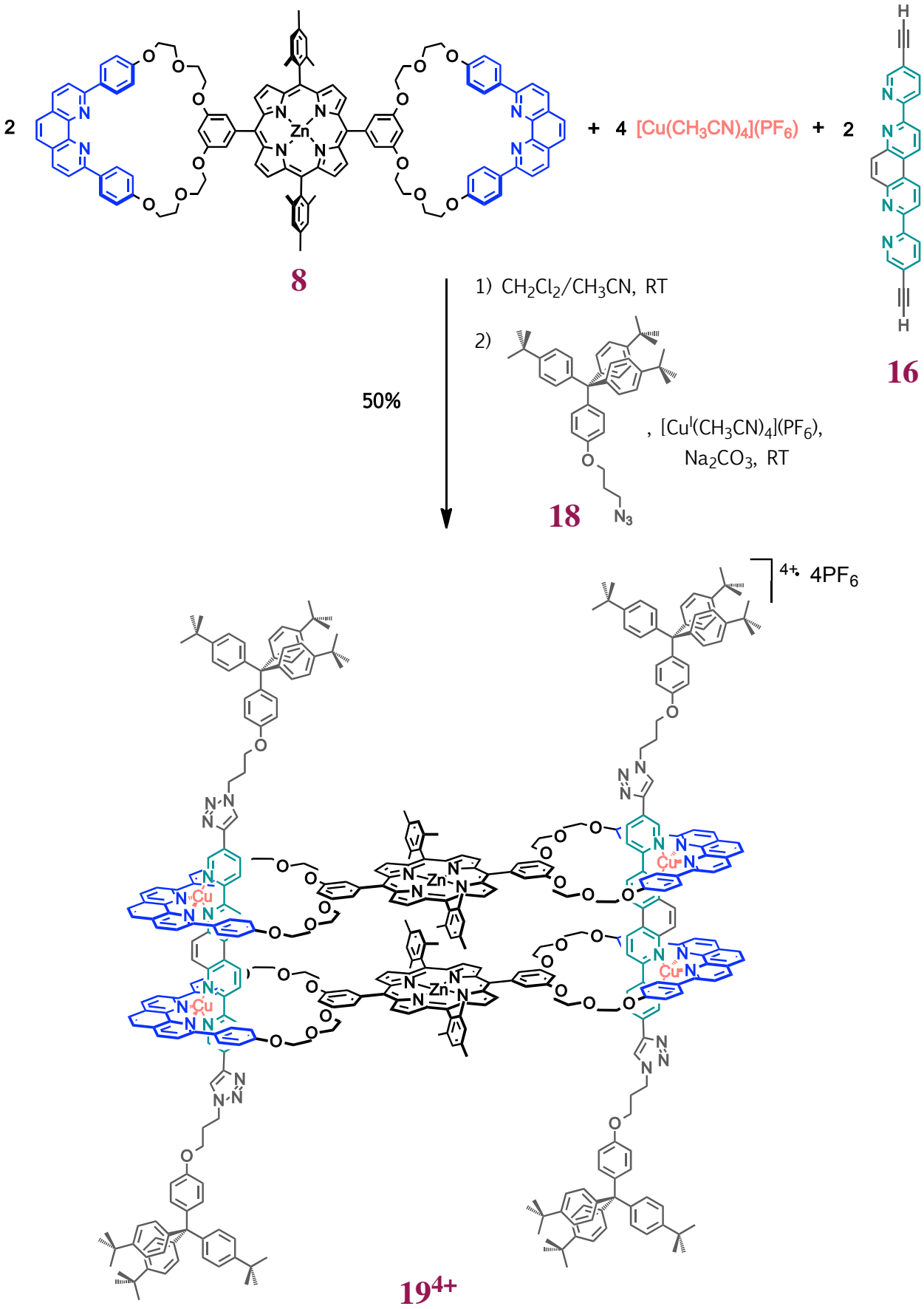

Figure III.4. Two-step, one-pot synthesis of [4]rotaxane **19**$^{4+}$ in 50% yield by (1) threading of bis-macrocycle **8** and axle **16** into a [4]pseudorotaxane and (2) quadruple CuAAC stoppering reaction with azide stopper **18**.

III. 2. b) HRES-MS Characterisation of the [4]Rotaxane

The [4]rotaxane $\mathbf{19}^{4+}\bullet 4PF_6$ was characterised by high-resolution electrospray mass spectrometry (HRES-MS), ^{1}H and ^{13}C NMR (1D and 2D experiments) and UV-visible absorption spectroscopy. The HRES-MS analysis resulted in a very clean spectrum with a major peak at *m/z* = 1760.169, the calculated value for rotaxane $\mathbf{19}^{4+}$ being 1760.202 (**Figure III.5**).

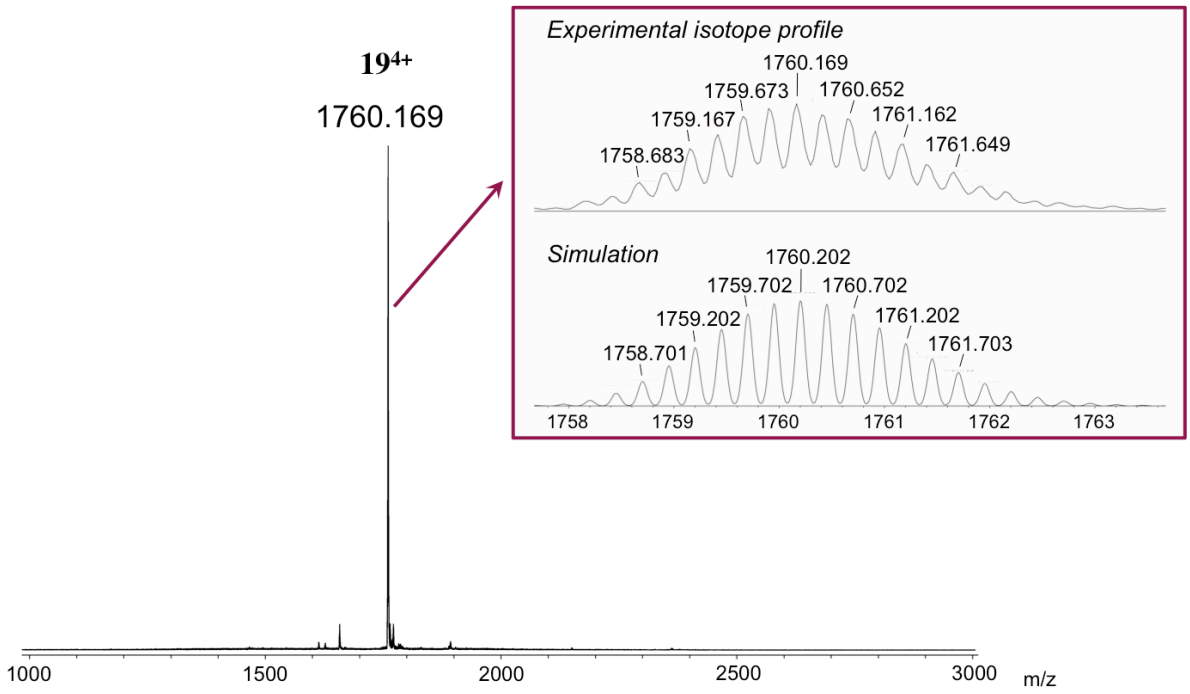

Figure III.5. High resolution electrospray mass spectrum of rotaxane $\mathbf{19}^{4+}$. The main signal is magnified to show the isotope profile (top right); this profile fits well with the calculated spectrum (bottom).

The isotope profile confirms that the [4]rotaxane obtained has four positive charges and consists of two dumbbells and two bis-macrocycles (2:2 species), linked by Cu(I) cations. A different threading scheme could have been expected where a single axle would be threaded through both rings of the same bis-macrocycle. This would have led to a doubly charged [2]rotaxane consisting of one dumbbell and one bis-macrocycle (1:1 species) (**Figure III.6**). The 1:1 species would have had the same *m/z* value as the 2:2 species, but the isotope profile would have been different, with a larger gap between two signals, which was not observed experimentally. Therefore, the observed profile confirms that the isolated product is a [4]rotaxane, not a [2]rotaxane.

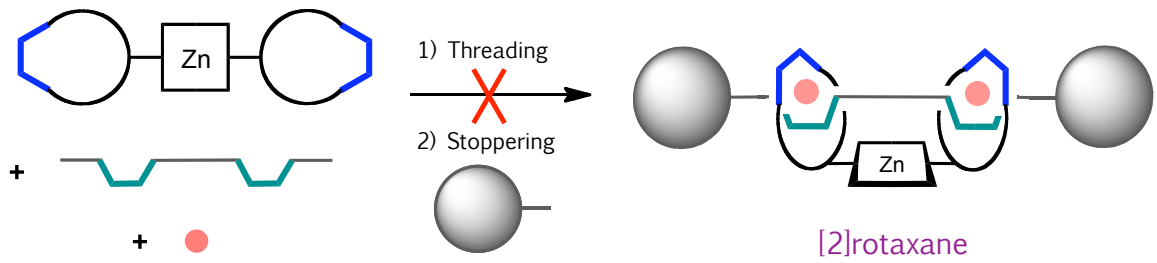

Figure III.6. Hypothetical threading and stoppering scheme leading to a [2]rotaxane. Mass spectrometry results indicated that this threading scheme is not favoured. The isotope profile is consistent with a [4]rotaxane containing four copper(I) centres

III. 2. c) NMR Characterisation of the [4]Rotaxane

NMR characterisation of the [4]rotaxane was not as straightforward as mass spectrometry characterisation. ^{1}H NMR spectra were recorded in a series of deuterated solvents ($CDCl_3$, CD_2Cl_2, $C_2D_2Cl_4$, CD_3CN, CD_3NO_2, C_6D_6 and DMSO-d_6). In most of these solvents very broad signals were observed at room temperature. However, the signals sharpened and shifted upon heating to higher temperatures, as observed in particular with nitromethane as solvent (**Figure III.7**).

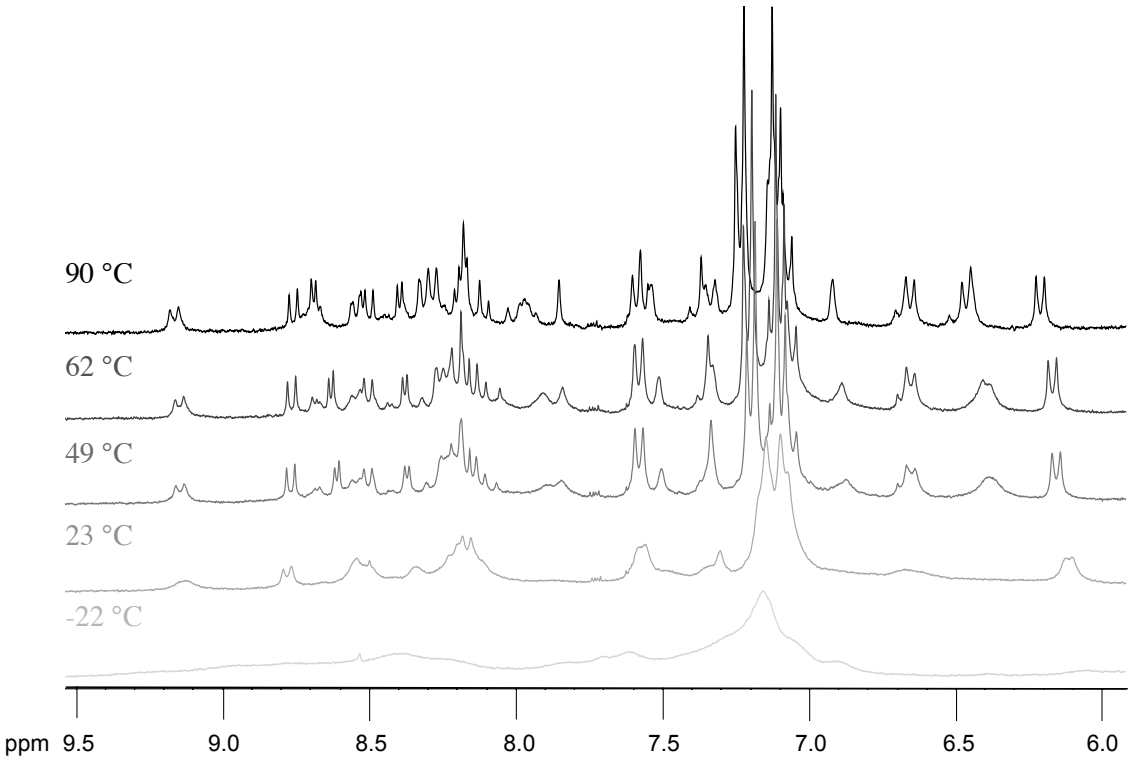

Figure III.7. Variable temperature ^{1}H NMR spectra of [4]rotaxane **19**$^{4+}$ in CD_3NO_2. Signals in the aromatic region are displayed.

These results seem to indicate that several conformers of the rotaxane are in slow equilibrium in solution at low temperature with a solvent-dependent exchange rate. However, in the case of CD_2Cl_2 the proton NMR spectrum was well resolved even at room temperature as shown on **Figure III.8**. Consequently, the ^{13}C spectrum and 2D NMR experiments (COSY, NOESY, HSQC, HMBC and DOSY) were recorded in this solvent and assignment of the signals was possible after close scrutiny of the data.

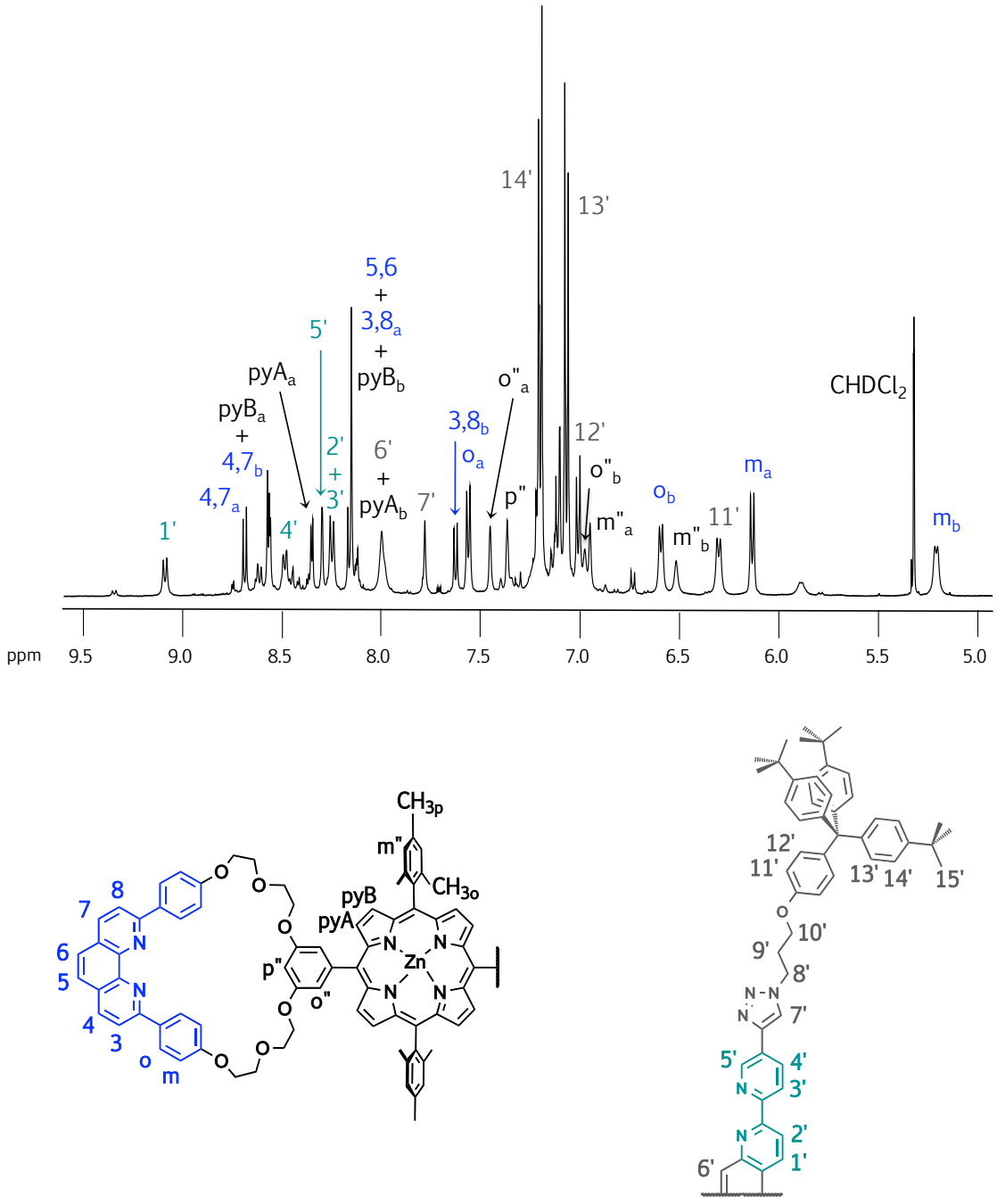

Figure III.8. ^1H NMR spectrum of rotaxane **19**$^{4+}$ in CD_2Cl_2 at room temperature. Signals in the aromatic region are displayed (top), as well as proton assignments on the bis-macrocycle and dumbbell components of the rotaxane (bottom). Split signals are annotated with "a" and "b" subscripts. Signals were assigned using COSY, NOESY, HSQC and HMBC data.

The ^{1}H NMR data confirm the interlocked structure of the rotaxane. This is evidenced by characteristic chemical shifts in the rotaxane compared to the free porphyrinic bis-macrocycle **8**, for example the upfield shift of the phenyl protons of the dpp units (protons o and m on **Figure III.8**). In addition, many NOE interactions are observed between the ethyleneglycol chains of the macrocycles and the central bis-3,8-(o-pyridyl)-4,7-phenanthroline moiety of the axle on the NOESY spectrum (**Figure III.9**).

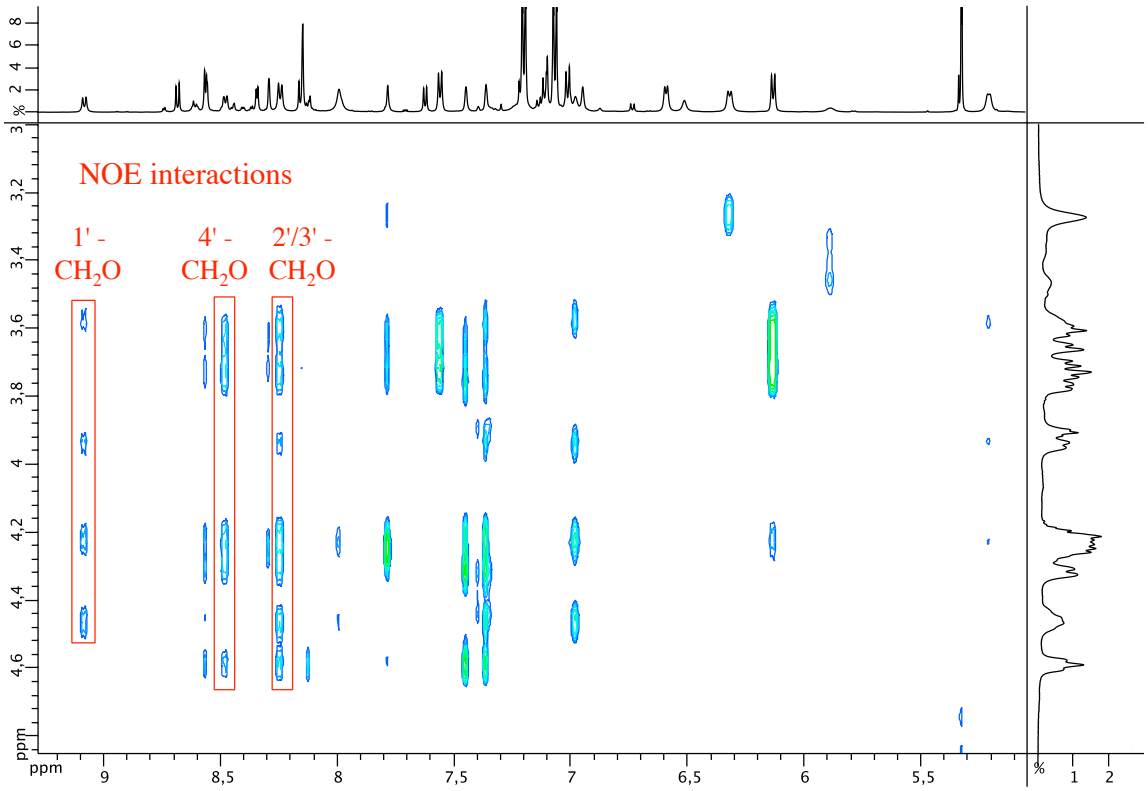

Figure III.9. Part of the NOESY spectrum of rotaxane **19**$^{4+}$ displaying NOE interactions between the central part of the dumbbell (protons 1' - 4') and the ethyleneglycol chains of the macrocycles.

Considerable loss of symmetry was observed in the proton spectrum of rotaxane **1**$^{4+}$ compared to its components taken independently. The signals belonging to the protons of the bis-macrocyclic component **8** were split in two signals in the NMR of the rotaxane (see signals annotated with "a" and "b" subscripts in **Figure III.8**). Yet the number of signals assigned to the dumbbell component of the rotaxane reflects the same degree of symmetry as its free precursors (axle **16** and stopper **18**): six different proton signals are observed for the central bis-3,8-(o-pyridyl)-4,7-phenanthroline moiety in axle **16** and in the rotaxane (protons 1' to 6' in **Figure III.8**). Based on the NMR data we propose a potential geometry for the rotaxane in CD_2Cl_2 solution, which accounts for the loss of symmetry observed by NMR. This geometry is schematically depicted in **Figure III.10**. If the rotaxane adopts a twisted, pro-helical

conformation as proposed then both halves of the dumbbells will have the same chemical environments, hence the number of signals observed in the proton NMR. On the contrary the protons of the bis-macrocyclic components will have different environments depending on their positions relative to the second bis-macrocycle. Protons pointing towards the inside of the rotaxane and located in closer proximity to the second bis-macrocycle will experience larger ring current effects than those pointing outwards, hence the splitting observed. To illustrate this we can examine the signals observed for the CH_3 groups *ortho* to the porphyrin on the mesityl substituents. These methyl groups give a single signal at 1.75 ppm in porphyrin **8**, which splits into two singlets at 1.47 and 0.64 ppm, respectively, in rotaxane $\mathbf{19^{4+}}$. The CH_3 protons are shielded due to the closeness of the second porphyrin moiety, with a stronger shielding effect on the internal methyl group than the external one. The relative integrations of signals assigned to the dumbbell and to the bis-macrocycles are consistent with the above interpretations. The ratio of the bis-macrocycle signals integrations (total integration for both split signals) to the integrations of the dumbbell signals corroborates a 1:1 dumbbell/bis-macrocycle stoichiometry in the rotaxane.

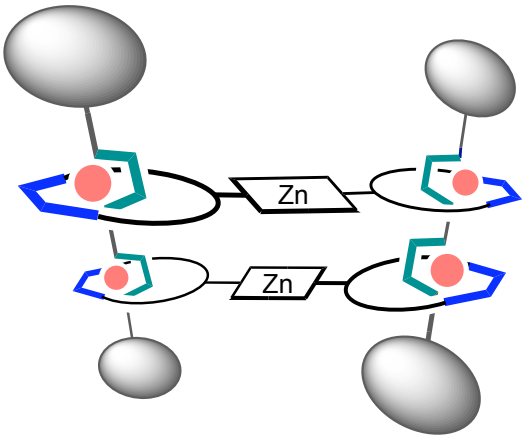

Figure III.10. Schematic view of the proposed geometry of rotaxane $\mathbf{19^{4+}}$ in solution deduced from the NMR data.

Besides the major set of signals discussed above, a second, minor set of signals is observed in the ^{1}H NMR spectrum of rotaxane $\mathbf{19^{4+}}$. These minor signals were consistently observed in the same ratio to the major signals even after repeated chromatographic purification of the compound. In addition, diffusion-ordered spectroscopy (DOSY) NMR – an experiment that differentiates NMR signals of different species according to their diffusion coefficient[249,250] – shows that only *one species* is present in solution (**Figure III.11**). Indeed, all signals are on the same line, which means that all protons belong to molecules that diffuse at the same rate. Some of the minor peaks are too small and fall under the detection limit for the DOSY experiment, but

the signals integrating for a larger number of protons among the minor peaks are a good probe for this experiment. For instance, the protons corresponding to the signals at 8.60, 7.11 and 6.73 ppm (belonging to the minor set of signals) are on the same line as as other protons. Consequently, we tend to believe that the minor signals observed do not correspond to an impurity but to a different conformer of the [4]rotaxane. This conformer does not seem to exchange fast with the major conformer in CD_2Cl_2 solution. Unfortunately, we were not able to identify what the structure of the minor conformation is.

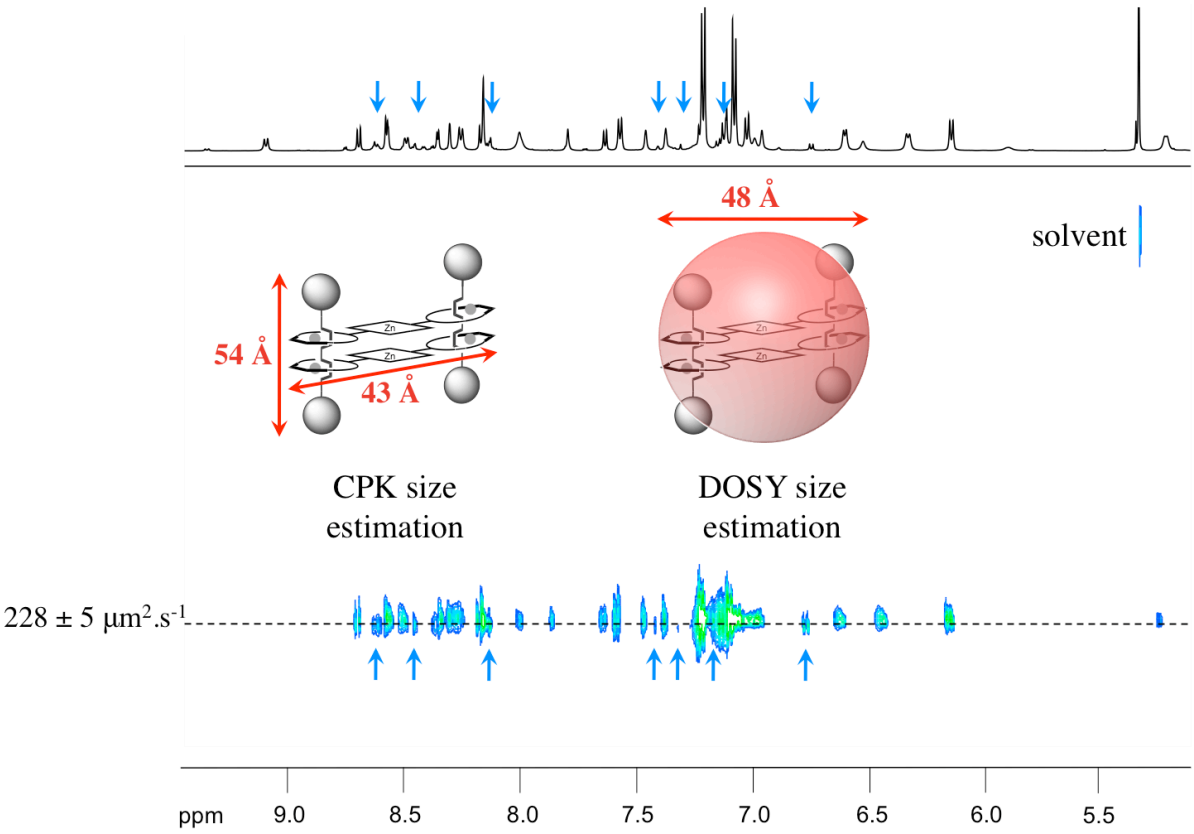

Figure III.11. DOSY spectrum of rotaxane **19**$^{4+}$ in CD_2Cl_2, displaying signals in the aromatic region. The DOSY data show the presence of a single chemical species in solution; arrows point at minor signals that belong to a second, minor conformer of the [4]rotaxane in very slow exchange with the major conformer. This minor conformer diffuses at the same rate as the major conformer. A good fit is obtained for the estimated size of the rotaxane using CPK models and the diffusion coefficient measured by DOSY NMR. The rotaxane approximates to a 48 Å sphere.

The DOSY experiment can provide an estimation of the size of the species in solution as well as sorting them out according to their diffusion coefficient. The Stokes-Einstein equation links the diffusion coefficient to the hydrodynamic radius of molecules.[251] In the case of rotaxane **19**$^{4+}$ a diffusion coefficient of 228 ± 5 $\mu m^2.s^{-1}$ was measured by DOSY NMR in CD_2Cl_2 at 25 °C. Using the Stokes-Einstein equation applied to a spherical model we deduce a diameter of 48 Å for the rotaxane. This is consistent with the formation of the [4]rotaxane **19**$^{4+}$ whose size was

estimated using CPK models. According to the CPK model the length of the porphyrinic bis-macrocycle approximates to 43 Å and the length of the dumbbell component in fully extended conformation approximates to 54 Å. Given that the linker between the central part of the dumbbell and the stopper is flexible, we can assume that the conformation of the dumbbell is not fully extended in solution and that its length averages shorter values. In conclusion, the CPK-estimated size fits well with an experimentally measured ball-shaped model of 48 Å.

III. 2. d) UV-visible Absorption Characterisation of the [4]rotaxane

Finally, the [4]rotaxane was characterised by UV-visible absorption spectroscopy. The spectrum of **19**$^{4+}$ shows a Soret band at 420 nm and Q bands at 551 and 591 nm in dichloromethane. The absorption spectra of rotaxane **19**$^{4+}$ and its precursor, porphyrin **8** were recorded in CH_2Cl_2 solutions at the same concentration in porphyrin units ([**19**$^{4+}$] = 0.95*10^{-6} M and [**8**] = 1.9*10^{-6} M) for comparison (**Figure III.12**).

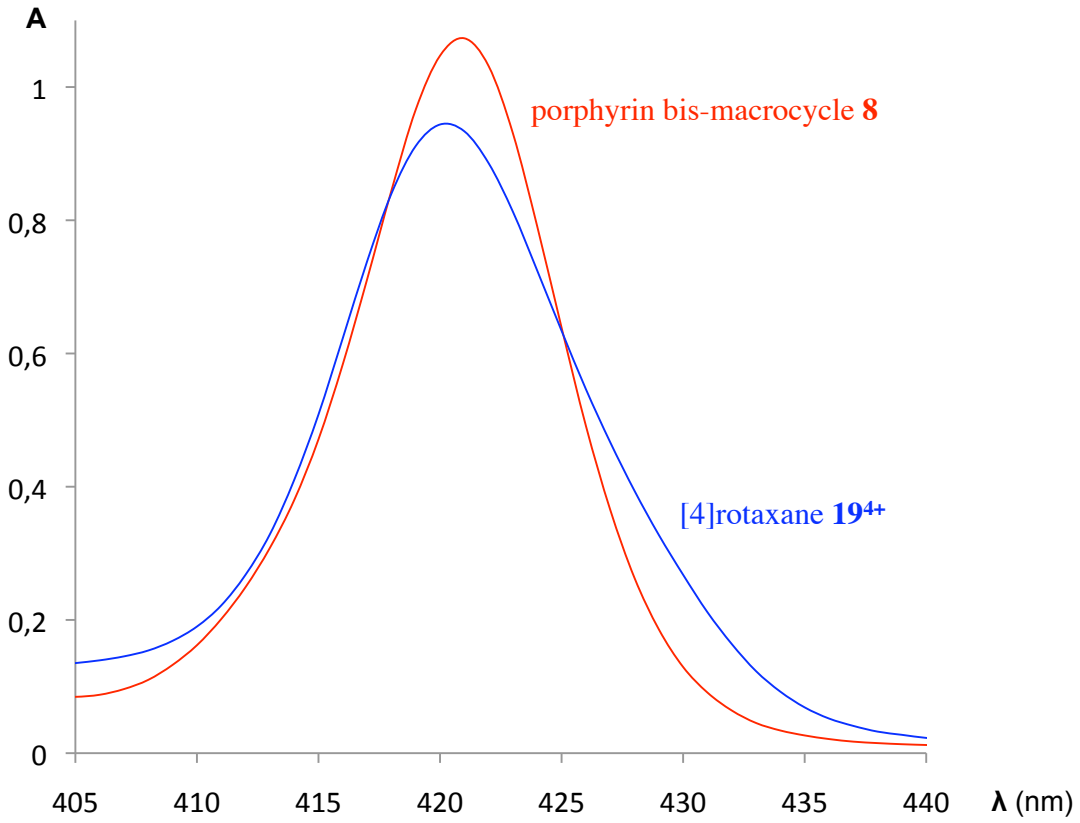

Figure III.12. UV-visible absorption spectra (Soret band) of [4]rotaxane **19**$^{4+}$ and its precursor, porphyrinic bis-macrocycle **8** in CH_2Cl_2 with [porphyrin] = 1.9*10^{-6} M. The blue shift and broadening of the Soret band of the rotaxane is attributed to exciton coupling between the two central porphyrins.

The rotaxane has a slightly blue-shifted and significantly broadened Soret band compared to the free porphyrin. A half-band width of 13 nm is measured for the rotaxane, as opposed to 10 nm for porphyrin **8**. These changes are typical of an excitonic coupling between two parallel porphyrins and suggest that the two porphyrins are in close proximity in the rotaxane.[252-256] Other potential causes for a shift of the absorption band might have been the impact of the nearby Cu(I) complexes and of the dumbbell. Nevertheless, these possibilities can be ruled out by comparison with the UV-visible absorption properties of similar (pseudo)rotaxanes built with either the same bis-macrocycle or the same dumbbell as rotaxane $\mathbf{19}^{4+}$. The [3]pseudorotaxane $\mathbf{9}^{2+}$ (Chapter II) was built with the same porphyrinic component **8** as the [4]rotaxane $\mathbf{19}^{4+}$, and it incorporates tetrahedral Cu(I) complexes analogous to those of the [4]rotaxane. No shift or broadening of the Soret band was observed for the pseudorotaxane $\mathbf{9}^{2+}$ compared to compound **8**. By analogy, we conclude that complexation with Cu(I) is not likely to be responsible for the variations observed in the present study. Influence of the dumbbell component can be estimated by comparison with another rotaxane built with the same axle as $\mathbf{19}^{4+}$. In Chapter V, we will describe a [3]rotaxane whose porphyrinic component is substituted with four macrocycles instead of two. This [3]rotaxane contains the same Cu(I) complexes and the same dumbbell (resulting from click reaction of two stoppers **18** on the axle **16**) as rotaxane $\mathbf{19}^{4+}$, but it incorporates only *one* porphyrin as opposed to *two* cofacial porphyrins in the case of $\mathbf{19}^{4+}$ (**Figure III.13**).

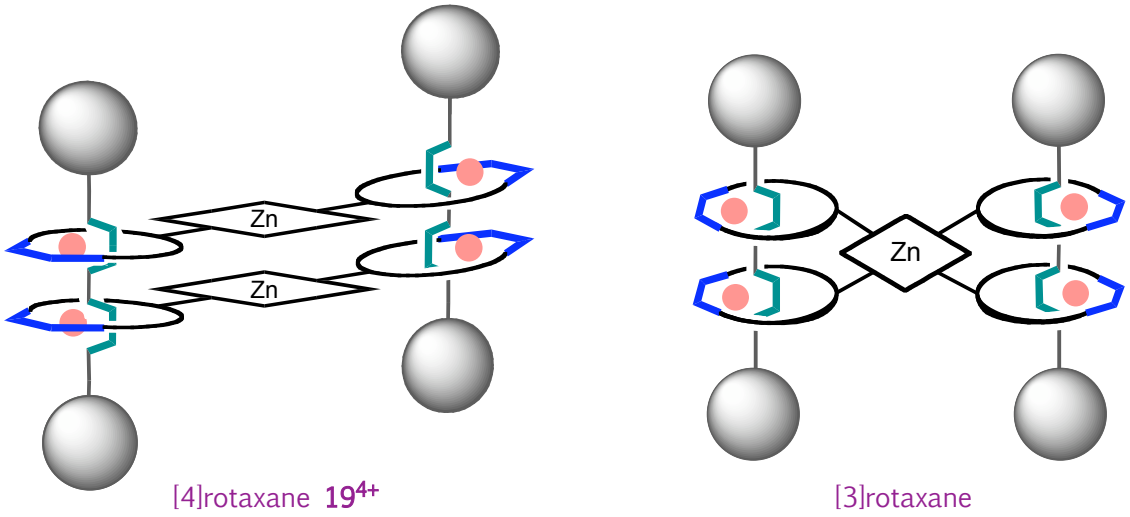

Figure III.13. Scheme highlighting the similarities and differences between the present [4]rotaxane $\mathbf{19}^{4+}$ and the [3]rotaxane that will be described in Chapter V. Both rotaxanes comprise exactly the *same dumbbell* resulting from the click reaction of two stoppers **18** on the axle **16**, and are complexed to four Cu(I) centres. However, only *one* porphyrin is incorporated in the [3]rotaxane while the [4]rotaxane contains *two* cofacial porphyrins.

A 3 nm *red* shift was observed for the Soret band of the [3]rotaxane compared to its porphyrinic precursor. Although the same axle and stopper were used to form the [4]rotaxane, the Soret band was shifted in the *opposite direction*. This is clear evidence that other factors are prevailing in the case of the [4]rotaxane and are strong enough to counterbalance the influence of the dumbbells. A major difference between the [3]rotaxane described in Chapter IV and the present [4]rotaxane is the number of porphyrins: the [3]rotaxane contains only one porphyrin whereas the [4]rotaxane contains two cofacially arranged porphyrin units. This supports the idea that the variations in the absorption spectrum are the result of an exciton coupling between the porphyrins of the [4]rotaxane, as proposed above. Excitonic coupling between chromophores may lead to hypso- or bathochromic shifts depending on the relative orientation of the transition dipoles.[252-256] Thus, exciton coupling in a face-to-face bis-porphyrin leads to a hypsochromic shift of the Soret band (parallel transition dipoles), whereas a bathochromic shift is observed in the case of linear, head-to-tail bis-porphyrins (in-line transition dipoles). As for oblique bis-porphyrin dimers, splitting of the Soret band is typically observed. The hypsochromic shift observed for the present bis-porphyrinic rotaxane is consistent with a face-to-face, parallel orientation of the porphyrins.

III. 2. e) Demetalation of the Copper(I)-Complexed [4]Rotaxane

Attempts to demetalate the copper(I)-complexed [4]rotaxane with potassium cyanide gave mixtures of products. A very small amount (~ 1 mg) of copper-free rotaxane was isolated, yet its characterisation proved difficult. MALDI-TOF mass spectrometry gave a signal at m/z = 6788.327 (calculated for $[M+H]^+$: m/z = 6788.198), but proton NMR showed broad signals that were difficult to interpret. Consequently, we did not proceed with further studies of the demetalated, copper-free rotaxane.

III. 3. The [4]Rotaxane used as a Host for Guest Molecules of Different Lengths

III. 3. a) Presentation and Synthesis of the Guest Molecules

The coordination mode and association constant of rotaxane **19^{4+}** with four guest substrates were investigated by UV-visible absorption titration in toluene. The guests are depicted in **Figure III.14**. Guest **G1** is the aliphatic diamine 1,4-diazabicyclo[2.2.2]octane (DABCO) whereas guests **G2** - **G4** are bifunctional pyridine-type ligands with phenylene spacers between the pyridyl units (0, 1 and 2 phenylene spacers, respectively).

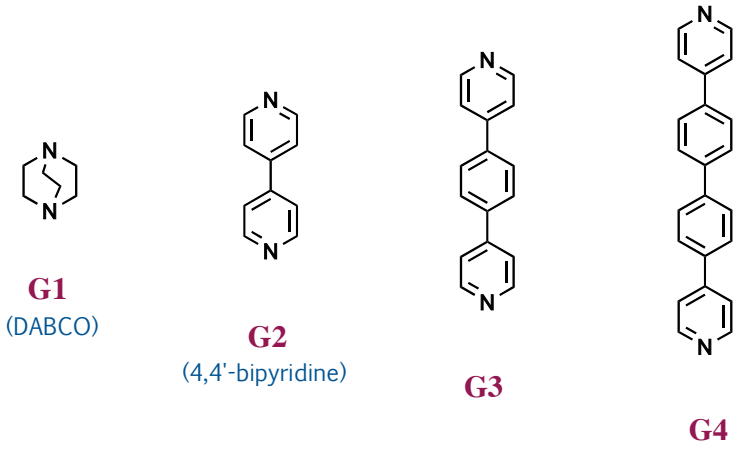

Figure III.14. Chemical structures of guests **G1** - **G4**.

All four guests are rigid, with a N-N distance varying from 2.6 to 15.8 Å according to crystallographic data.[257,258] They are known to form axial complexes with zinc porphyrins.[131,153,155,195,196,259,260] While DABCO **G1** and 4,4'-bipyridine **G2** are commercial compounds, the extended bipyridines **G3** and **G4** are not commercially available and were synthesised according to published procedures (**Figure III.15**).[261]

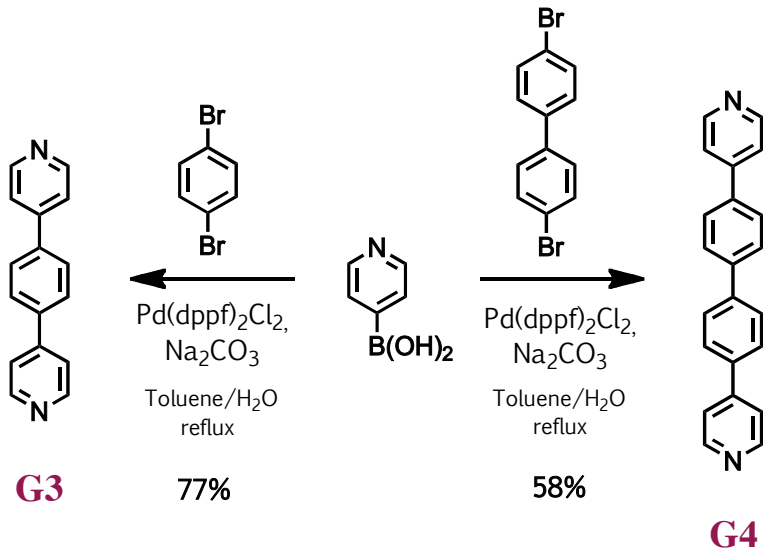

Figure III.15. Synthesis of guests **G3** and **G4**.[261]

The 1,4-bis(4-pyridyl)benzene guest **G3** was synthesised in 77% yield by Suzuki coupling of pyridine-4-boronic acid and *p*-dibromobenzene. The 4,4′-bis(4-pyridyl)biphenyl guest **G4** was prepared from a 4,4'-dibromobiphenyl precursor following the same procedure.

We performed host-guest titrations with the rigid substrates **G1** - **G4** of increasing length in order to measure their association constants with the host rotaxane $\mathbf{19^{4+}}$. The Soret band of Zn-porphyrins has been shown to undergo a bathochromic shift upon axial coordination of nitrogen ligands.[131] This makes UV-visible titration an excellent method for assessing the host-guest interactions between the [4]rotaxane and substrates **G1** - **G4**. In the titration experiment 0.1 equivalent aliquots of the guest were added to a 10^{-6} M solution of the [4]rotaxane in toluene and the absorbance of the Soret band (400 to 450 nm) was recorded after stirring for 2 minutes. Several coordination modes between the rotaxane host $\mathbf{19^{4+}}$ and the ditopic guests can potentially be considered with internal and/or external binding of the guest(s) (**Figure III.16**). Coordination of two axial ligands on the same Zn(II) porphyrin was excluded because zinc porphyrins are preferentially penta-coordinated with only one axial ligand. In each titration experiment the host/guest stoichiometry was determined by mathematical treatment of the titration data with the Specfit/32 software. Guest inclusion complexes were distinguished from external complexes by comparison of the association constant with values reported in the literature for similar host/guest systems.

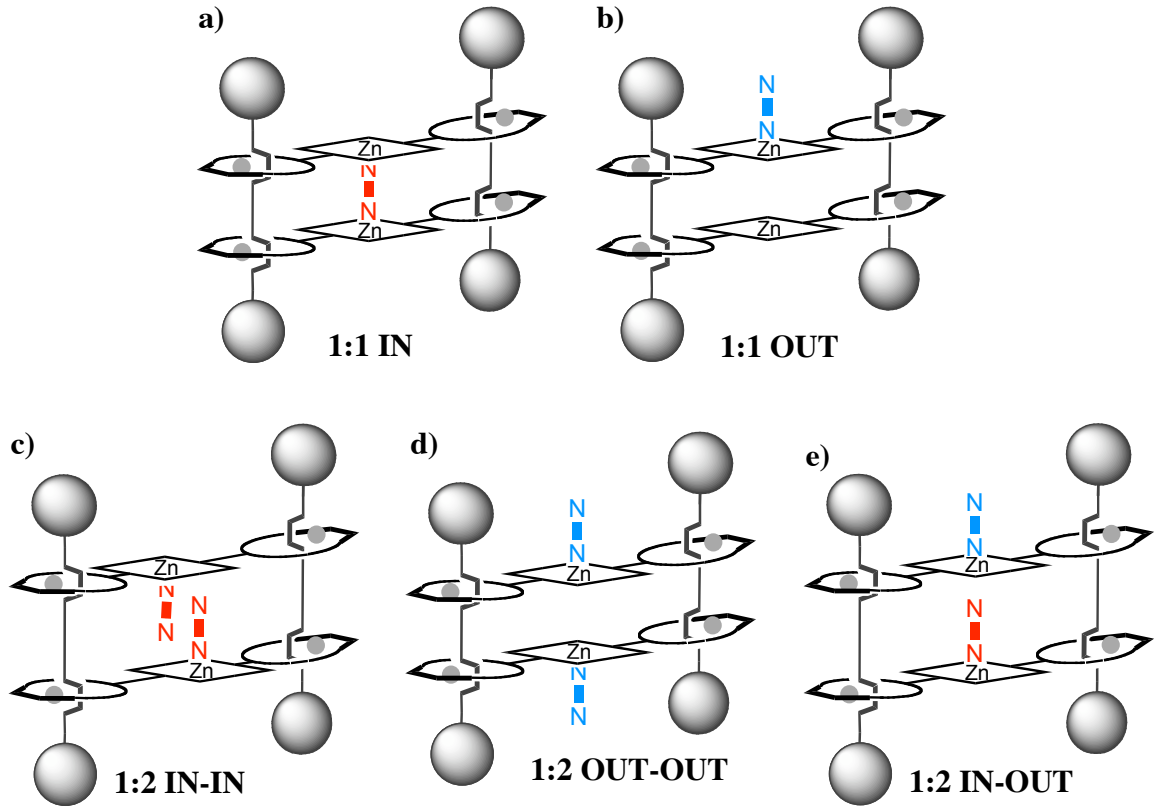

Figure III.16. Possible coordination modes of guests **G1** - **G4** with rotaxane host $\mathbf{19^{4+}}$. a) 1:1 host-guest stoichiometry, internal complex (guest inclusion); b) 1:1 stoichiometry, external complex; c) 1:2 host-guest stoichiometry, internal complexes; d) 1:2 stoichiometry, external complexes, e) 1:2 stoichiometry with one internal and one external guest.

III. 3. b) Titration with the DABCO Guest G1

The data obtained in the case of the short DABCO guest **G1** indicated the coexistence of several host-guest species. A bathochromic shift of the Soret band of the host was observed upon addition of the guest. Superimposition of the absorption spectra obtained upon addition of 0.0 to 0.7 equivalents of DABCO brought up an isosbestic point (**Figure III.17**). Mathematical treatment of the data with the Specfit/32 software corroborated a 1:1 host-guest stoichiometry with an association constant of log K_{a1} = 8.1 ± 0.5 (see Eq. 1). The binding constant is consistent with an internal coordination mode where the guest is complexed between the porphyrins, inside the cavity of the rotaxane. Indeed, DABCO typically binds simple zinc porphyrins with an association constant of 10^5 mol.L^{-1} in toluene.[131] The high affinity observed here reflects the cooperative effect of the coordination of the ditopic ligand between *two* zinc porphyrins. The association constant of the very short DABCO guest with rotaxane host $\mathbf{19^{4+}}$ is slightly higher than that observed with the more rigid [4]rotaxane described previously in the Sauvage group,[196]

which could be explained by the greater adaptability of the present host compared to the previous system. Due to the flexible anchoring points between the porphyrinic component and the axles of the rotaxane, the two porphyrins can come to relatively close proximity so as to adjust the Zn…Zn distance to the small DABCO guest.

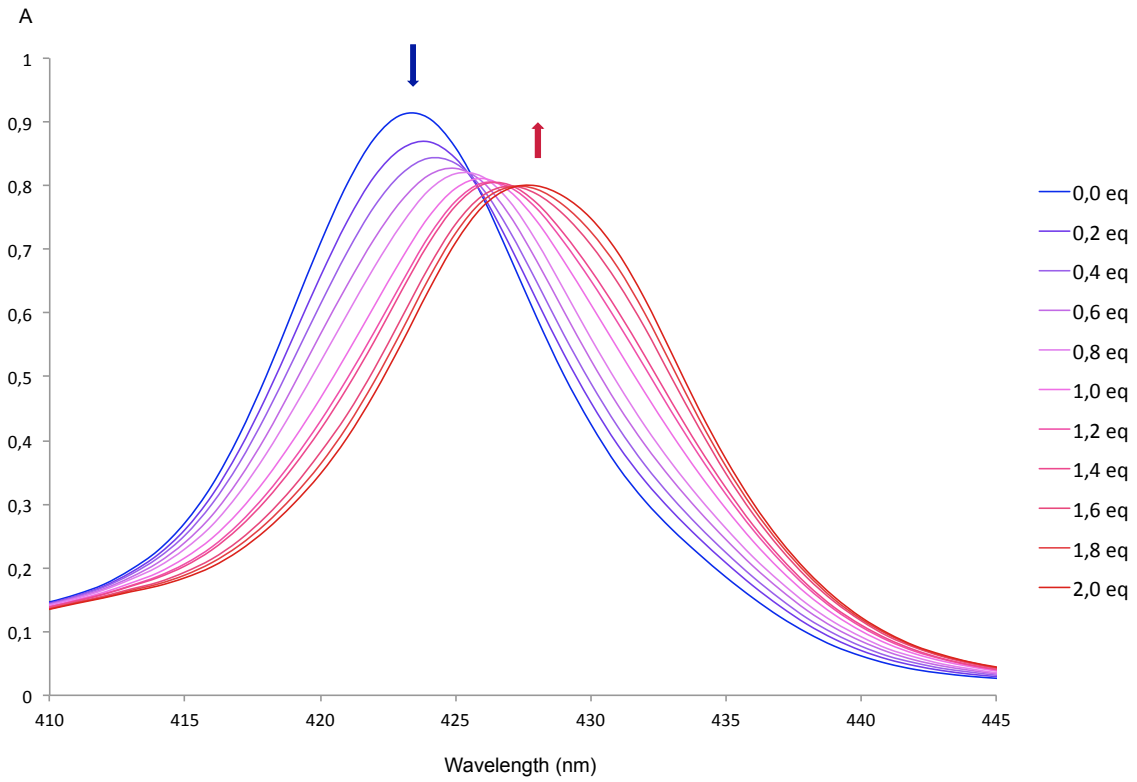

Figure III.17. UV-visible titration spectra in toluene (Soret band) of rotaxane **19**$^{4+}$ (0.92 x 10^{-6} M) with DABCO guest **G1** (2.8 x 10^{-5} M) from 0.0 to 2.0 equiv. Arrows show changes in the host spectrum with increasing guest concentration; a 6 nm red shift from 423 to 429 nm is observed.

Beyond one equivalent of DABCO a different coordination behaviour arises with disappearance of the isosbestic point. The data indicate that several equilibria are to be taken into account with several species coexisting in solution in significant proportions. Given that Zn-porphyrins preferentially bind a single axial ligand the most significant species are likely to be the 1:1 internal complex formed initially (**Figure III.16**.a) and 1:2 coordination species (**Figure III.16**.c-e). The following equilibria account for the formation of the host (H) - guest (G) species.

$$H + G \rightleftharpoons H{\bullet}G \qquad K_{a1} = \frac{[H{\bullet}G]}{[H]*[G]} \qquad \text{Eq. 1}$$

$$H + 2\,G \rightleftharpoons G{\bullet}H{\bullet}G \qquad K_{a2} = \frac{[G{\bullet}H{\bullet}G]}{[H]*[G]^2} \qquad \text{Eq. 2}$$

Both equilibria were considered simultaneously in the mathematical treatment with log K_{a1} = 8.1 ± 0.5 for the formation of the 1:1 host-guest complex. The data fitted with an association constant of log K_{a2} = 14.5 ± 0.2 for the formation of the 1:2 complex. We can conclude that the 1:1 guest inclusion complex is predominantly formed with a high association constant in the presence of substoichiometric amounts of DABCO whereas additional binding of ligand is observed in the presence of excess guest.

III. 3. c) Titration with the 4,4'-Bipy Guest G2

In the case of the 4,4'-bipyridine guest **G2** a clear isosbestic point was observed (**Figure III.18**). This indicates that only one equilibrium is to be considered and that *a single complex* is formed. Mathematical treatment of the spectra fits with the formation of a 1:1 host : guest complex with an association constant of log K_{a1} = 6.2 ± 0.1. Other stoichiometries between host and guest (*e.g.* 1:2 or 2:1) were not corroborated by the mathematical treatment. The high binding constant is consistent with an internal coordination mode where the guest is complexed between the porphyrins. Indeed, a pyridyl ligand typically binds a zinc porphyrin with a relatively low association constant of 10^3 mol.L^{-1} in toluene. Higher binding constants with bipyridine ligands usually reflect a cooperative effect of ligand binding between two cofacial metalloporphyrins.[131] The association constant observed here is one order of magnitude lower than that obtained with the related bis-porphyrin system previously studied in our group, with log K_{a1} = 7.3. In the present system, the porphyrin is a classical tetraaryl tetrapyrrolic compound whereas in the previous system investigated, electron withdrawing groups were attached on two pyrrole rings of the porphyrin. Lewis acidity of the zinc(II) centre is thus less pronounced in the present system than in the previous case reported by our group,[196] which could explain the lower binding constant observed.

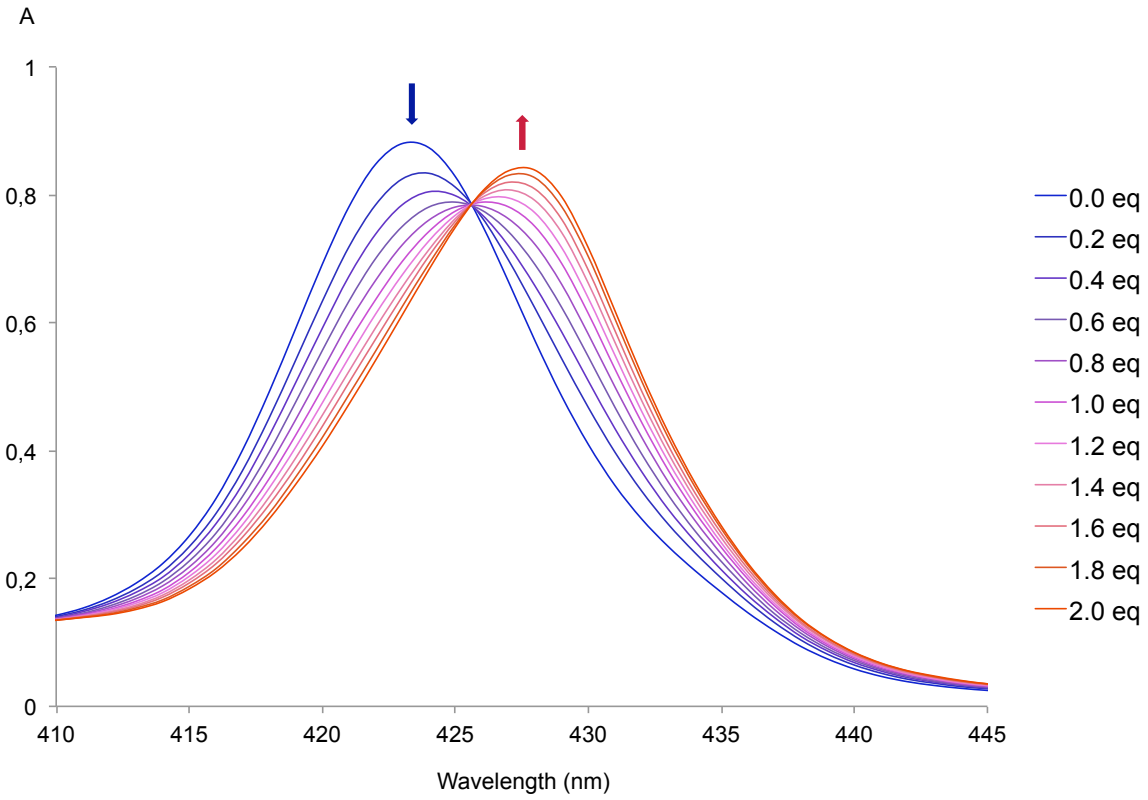

Figure III.18. UV-visible titration spectra in toluene (Soret band) of rotaxane $\mathbf{19}^{4+}$ (0.92 x 10^{-6} M) with 4,4'-bipyridine guest **G2** (2.8 x 10^{-5} M) from 0.0 to 2.0 equiv. Arrows show changes in the host spectrum with increasing guest concentration; a 5 nm red shift from 423 to 428 nm is observed.

The absorbance change at λ_{max} = 423 nm upon titration with guests **G1** and **G2** is depicted in **Figure III.19**. The graph highlights the difference in behaviour of the two guests towards complexation with rotaxane $\mathbf{19}^{4+}$. At the start of the titration 1:1 host/guest complexes are formed in both cases. However, a gradient change is then observed in the case of the DABCO guest **G1**, which is a clear indication that other species are formed with this substrate.

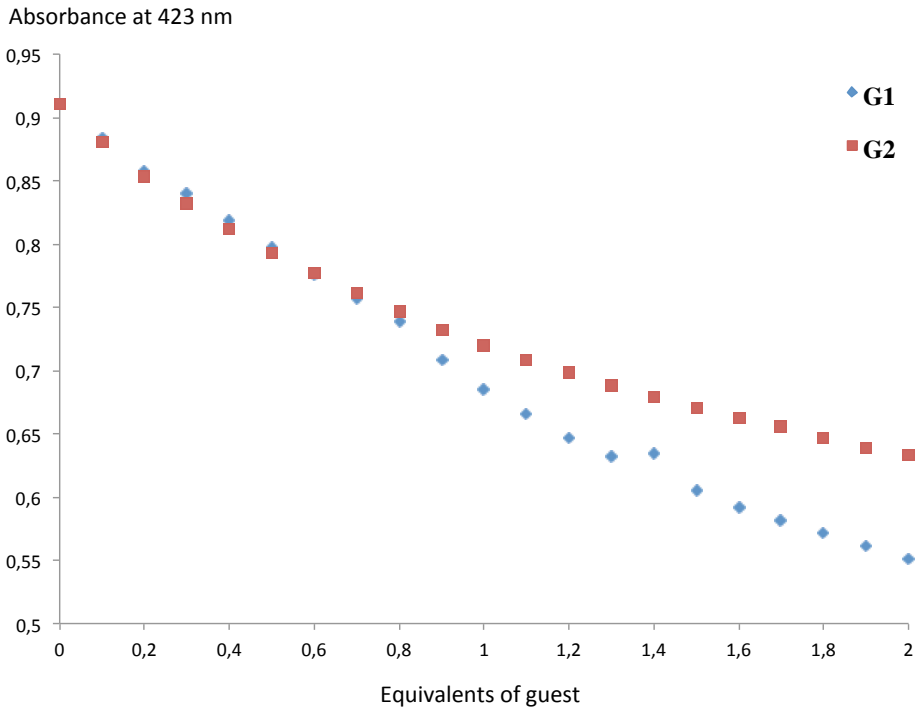

Figure III.19. UV-visible titration of rotaxane $\mathbf{19}^{4+}$ with guests **G1** and **G2** in toluene. Absorbance plotted against the added guest equivalents at λ_{max} = 423 nm.

III. 3. d) Titrations with Guests G3 and G4

Similar results were obtained with guests **G3** and **G4** upon addition of 0.1 to 2.0 equivalents of guest to the rotaxane solution. In both cases a bathochromic shift of the Soret band was observed as expected and superimposition of the spectra showed isosbestic points (**Figures III.20** and **III.21**). The data fit with the formation of 1:1 complexes with an association constant of log K_{a1} = 6.1 ± 0.1 and log K_{a1} = 5.6 ± 0.1 for **G3** and **G4**, respectively. These values are two to three orders of magnitude higher than the expected binding constant for the mono-complexation of a bipyridine-type ligand on a single porphyrin, which evidences a cooperative effect and hence internal binding of the guest inside the cyclic rotaxane.

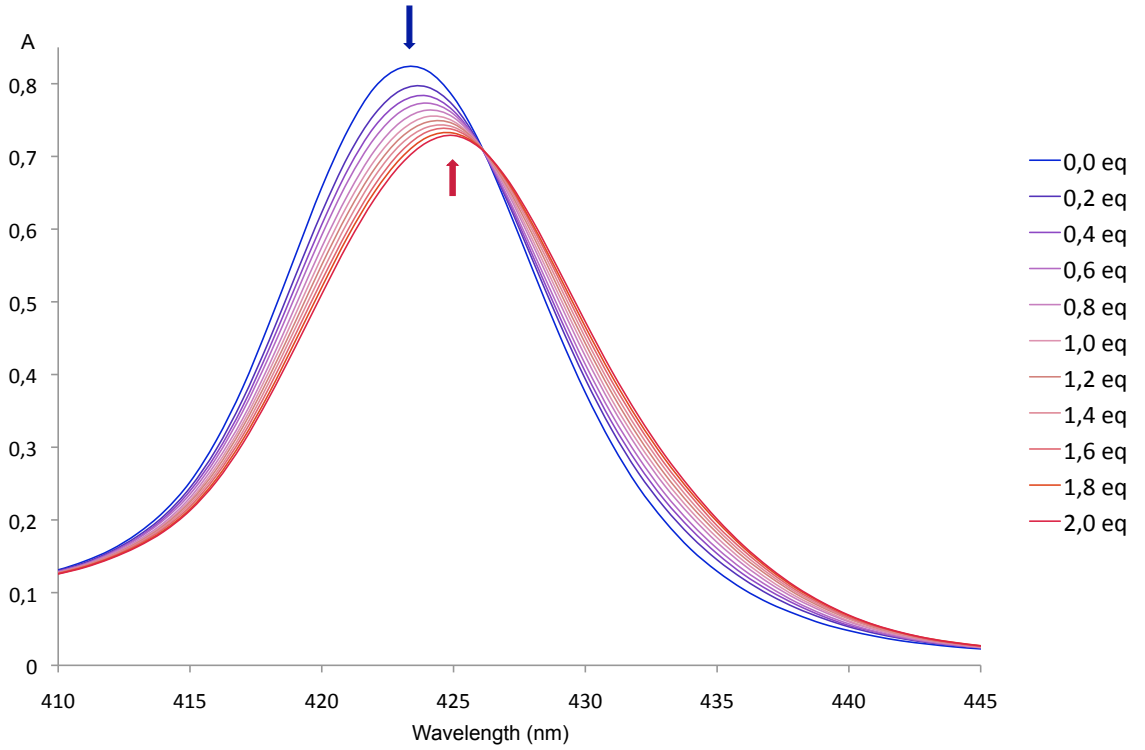

Figure III.20. UV-visible titration spectra in toluene (Soret band) of rotaxane **19**$^{4+}$ (0.92 x 10^{-6} M) with guest **G3** (2.8 x 10^{-5} M) from 0.0 to 2.0 equiv. Arrows show changes in the host spectrum with increasing guest concentration; a 2 nm red shift from 423 to 425 nm is observed.

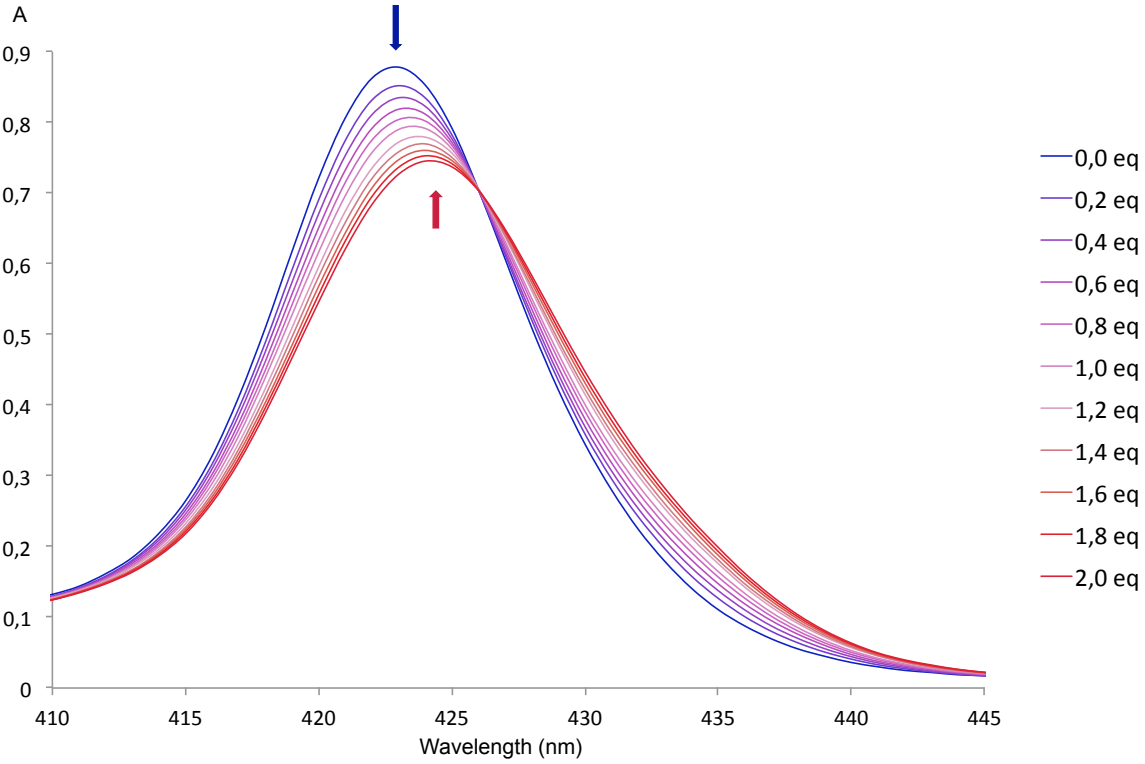

Figure III.21. UV-visible titration spectra in toluene (Soret band) of rotaxane **19**$^{4+}$ (0.92 x 10^{-6} M) with guest **G4** (2.8 x 10^{-5} M) from 0.0 to 2.0 equiv. Arrows show changes in the host spectrum with increasing guest concentration; a 1 nm red shift from 423 to 424 nm is observed.

III. 3. e) Titration Results Analysis: A Distensible Molecular Host

Very close binding constants were obtained for guests **G2** and **G3**; this attests for the flexibility of the rotaxane that can equally accommodate these two guests of increasing lengths (7.1 and 11.4 Å, respectively). The exceptional flexibility of the rotaxane is confirmed by the binding constant obtained for the extended guest **G4**. The constant is slightly lower – presumably due to steric constraints – yet consistent with guest inclusion into the central cavity of the rotaxane. The results are summarised in **Table 1**.

Table III.1. Association constants of guests **G1** - **G4** with rotaxane host $\mathbf{19^{4+}}$ and lengths of the ligands.

Guest	log K_{a1}*	N-N distance in Å (from crystallographic data)[257,258]
G1	8.1 ± 0.5	2.6
G2	6.2 ± 0.1	7.1
G3	6.1 ± 0.1	11.4
G4	5.6 ± 0.1	15.8

*for the 1:1 host/guest complexes. In the case of DABCO (**G1**), 1:2 host/guest complexes were also formed with an association constant of log K_{a2} = 14.5 ± 0.2.

The titrations point out the remarkable adaptability of the rotaxane host, which "inflates" or "deflates" depending on the guest substrate, as illustrated in **Figure III.22**. Rotaxane $\mathbf{19^{4+}}$ is one of very few reported bis-porphyrinic systems able to accommodate guests **G3** and **G4**.[195,262] This adaptability differentiates the present rotaxane $\mathbf{19^{4+}}$ from the [4]rotaxane host previously reported in the Sauvage group.[196] In the previous system the guest **G4** was too long to fit between the porphyrins. Only 1:2 host/guest species were observed where the guests were bound externally. An intermediate situation was observed in the case of **G3**, which suggested that guest **G3** had a critical size and that several complexes coexisted in solution. The previous rotaxane was unable to adjust its conformation to the size of the guest because of the rigidity of the porphyrinic bis-macrocycle component. Moreover, this rotaxane collapsed upon demetalation of the copper(I) centres and did not exhibit any host/guest recognition properties after demetalation.[197] On the contrary, the spacer between the porphyrin units and the copper(I) anchoring points in rotaxane $\mathbf{19^{4+}}$ is very flexible, which allows for inclusion of a large range of

guests in the rotaxane. An analogy can be drawn between rotaxane host **19**$^{4+}$ and the induced fit of substrates in enzymes: both systems are flexible and can adjust their conformation to the size and the shape –for enzymes– of the substrate to be recognised.

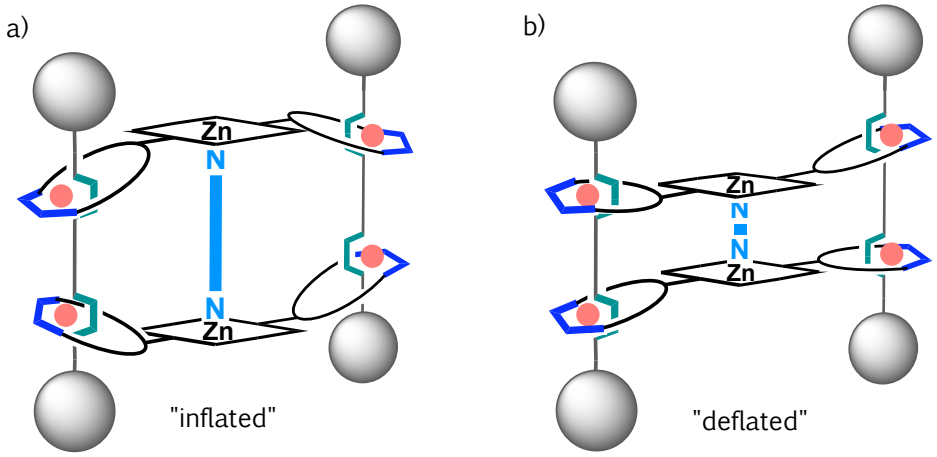

Figure III.22. a) "inflated" and b) "deflated" conformations of the host **19**$^{4+}$. The rotaxane can adjust its geometry to accommodate either extended guests (*e.g.* **G4**) or very short guests (*e.g.* DABCO).

In conclusion, the now well-established "gathering-and-threading" principle based on copper(I) and bidentate ligand-containing cyclic and acyclic fragments turned out to be remarkably efficient for preparing a new [4]rotaxane that consists of two bis-macrocycles and two rigid axles. Each bis-ring fragment contains a central zinc porphyrin. Two flexible coordinating rings are attached *via* single C-C bonds on two antipodal *meso* carbon atoms of the porphyrin. The final rotaxane has been characterised by high-resolution electrospray mass spectrometry, ^{1}H and ^{13}C NMR and UV-visible absorption spectroscopy.

The new [4]rotaxane described in here incorporates two face-to-face zinc-complexed porphyrins, making it an interesting receptor for a variety of substrates. It shows structural similarities with previously described compounds[196,197] in the sense that it also belongs to the family of [4]rotaxanes consisting of two axles and two bis-macrocycles. However, the greater flexibility of the system, originating from the totally different connections between the threads and the rings, leads to very different host-guest properties. Interestingly, rod-like guests of extremely different lengths could be accommodated between the two porphyrins, affording complexes of similar stability constants, thus demonstrating that the present [4]rotaxane behaves as a distensible receptor, able to inflate or deflate at will to adjust to the guest size. This property is well illustrated by the fact that exotopic guests of the 4,4'-bipyridine family with overall lengths varying from 7.1 Å to 15.8 Å form complexes of comparable stability.

The photophysical porperties of the [4]rotaxane could be studied in the future. Its electronic properties should be very different from those of the previously reported [4]rotaxane since the two porphyrins incorporated in the present compound are "normal" porphyrins of the tetra-aryl series whereas they were π-extended porphyrins in the previous system.

Chapter IV. Towards A New Porphyrinic Bis-Macrocycle:

Two Coordinating Rings Linked to a Central Porphyrin via an Extended Aromatic System

IV. 1. Design of the New Porphyrinic Bis-Macrocycle and Retrosynthetic Strategies

IV. 1. a) Design of the System

The results described in the previous chapter prompted us to design a new, *more rigid* porphyrinic bis-macrocycle in order to improve our model of a molecular press. In particular, a key point in the new design is to rigidify the bridge between the porphyrin and the rings.

In Chapter III, we showed that the [4]rotaxane $\mathbf{19^{4+}}$ is a good molecular receptor for ditopic guests. However, no comparison between the host-guest properties of the copper-free rotaxane and of the copper(I)-complexed rotaxane could be drawn because of difficulties encountered with the demetalation of the copper-complexed rotaxane. Furthermore the [4]rotaxane proved to be very flexible in its metalated form. It can adjust its shape and the distance between the porphyrin sites to the size of the guest to be complexed. Complexation with flexible guests was not tested but the great adaptability of the rotaxane suggests that no significant constraint would be applied on the conformation of the guest molecule. Moreover the characterisation of a potential conformational change of the guest by NMR spectroscopy would be difficult because of the complexity of the ^{1}H NMR spectrum of the rotaxane. A more rigid bis-macrocyclic structure is likely to lead to a more symmetrical rotaxane in solution, as observed with other [4]pseudorotaxane and [4]rotaxane structures.[196,217,221] It should also limit the adaptability of the rotaxane in its copper(I)-complexed form, which will have a greater impact on the conformation of a flexible guest molecule. We conclude from these observations that a

rotaxane based on a more rigid bis-macrocycle should be a better candidate as a molecular press. The new target building block is schematically depicted in **Figure IV.1**.b.

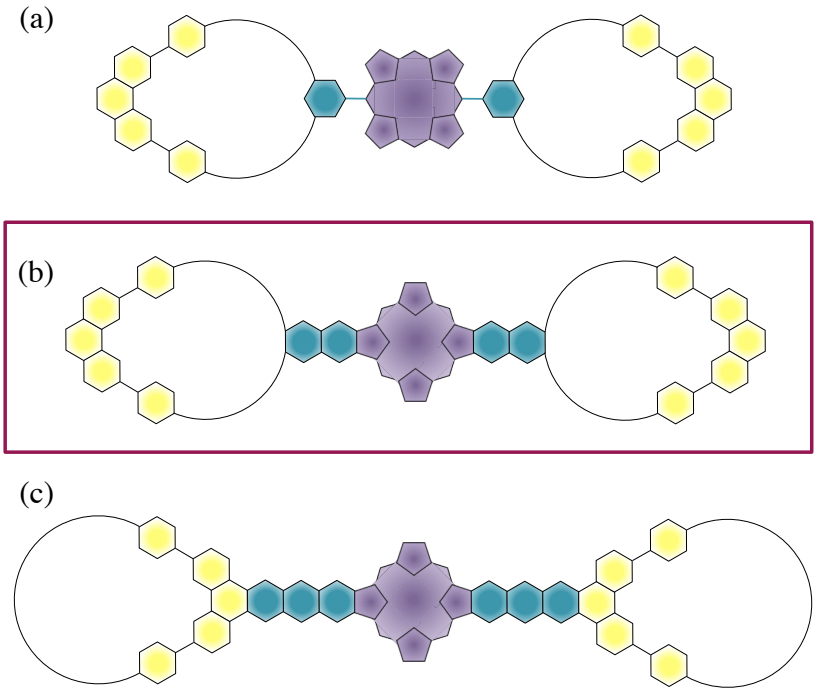

Figure IV.1. Schematic view of the structural differences between three porphyrinic bis-macrocycles: (a) compound **8** described in Chapters II and III of this thesis; (b) new target compound; (c) compound used in previous studies.[196,197,217] The rigidity of the new system will be intermediate between the very flexible bis-macrocycle **8** and the very rigid bis-macrocycle studied by former members of the Sauvage group.

The main differences between the new target (**Figure IV.1**.b) and the porphyrinic bis-macrocycle **8** (**Figure IV.1**.a) reside in the nature and the position of the bridges between the porphyrin moiety and the macrocycles. In the previous system single C-C bonds were linking the rings to the porphyrin core at the *meso* positions. The single-bonded bridge allowed free rotation of the macrocycles in relation to the plane of the porphyrin. In the new system a quinoxaline spacer will link the macrocycles to the β positions of the porphyrin. This aromatic bridge will restrict the rotational freedom of the rings. The macrocycles will be m-30 rings composed of the same dpp chelates and diethyleneglycol chains as in the case of compound **8**. By comparison with the porphyrinic bis-macrocycle previously studied in the Sauvage group (**Figure V.1**.c, Part **I. 4. b)**),[196,197,217] the π system of the new target compound will be significantly reduced. The dpp units of the macrocycles will be electronically decoupled from the extended porphyrin core, while they were coupled in the previously studied system. This is to avoid the collapse of the corresponding rotaxane and the π-stacking interactions observed upon demetalation of the copper(I) centres in the case of the rotaxane studied before.[197]

IV. 1. b) The Crossley Method for β,β'-Functionalisation of Porphyrins

The synthesis of the new target bis-macrocycle involves the functionalisation of the porphyrin core at its β positions. M. J. Crossley and his group developed a synthetic strategy that enables the attachment of various moieties to the β,β'-pyrrolic sites of a porphyrin *via* an extended π system (**Figure IV.2**).[263-265]

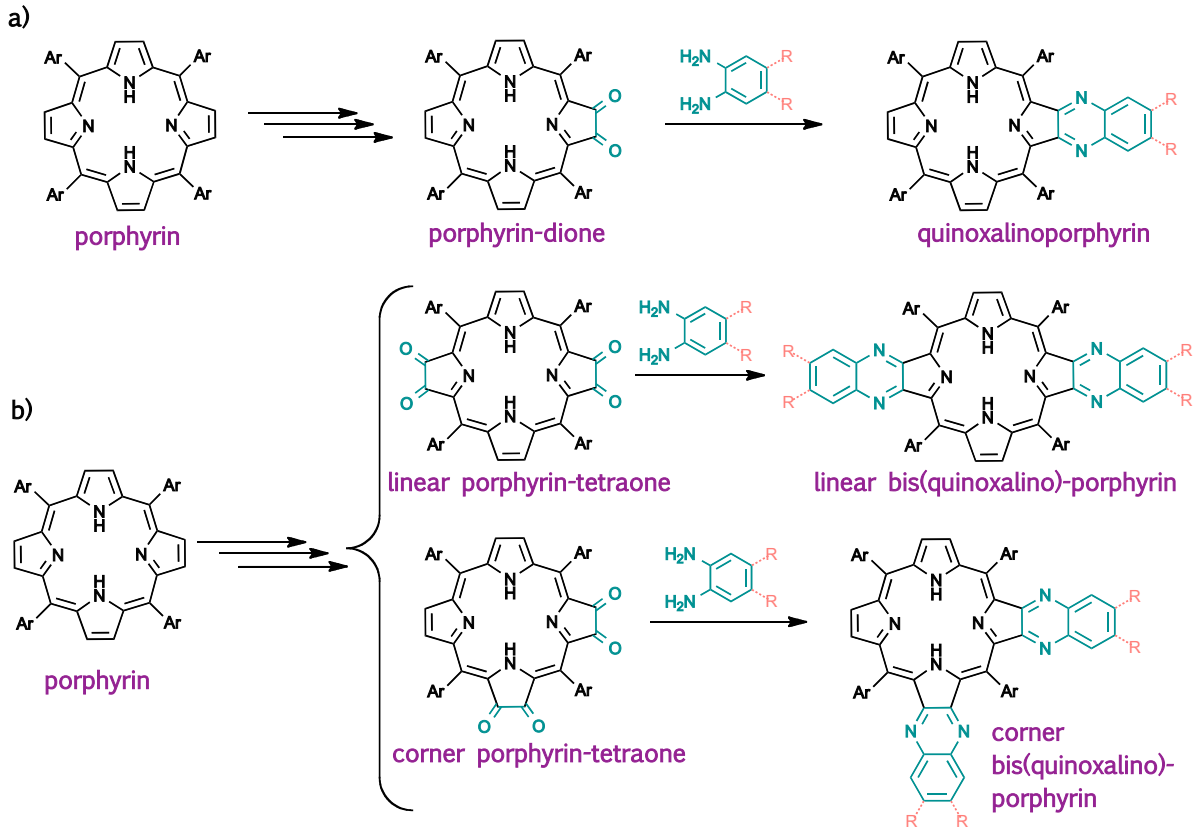

Figure IV.2. The Crossley synthetic approach for the functionalisation of porphyrins at the β positions. The method involves the formation of porphyrin-dione (a) or tetraone (b) derivatives, followed by condensation with a (substituted) 1,2-phenylenediamine unit. It allows the formation of linear or "corner" planar multifunctional systems, whose functional groups are covalently linked to the porphyrin via an extended aromatic system (Ar = aryl group).[265]

The approach consists in introducing two vicinal ketone groups on the β and β' positions of one or two of the pyrrole rings on the porphyrin core. Subsequent condensation with a 1,2-phenylenediamine leads to a quinoxalino- or bis(quinoxalino)-porphyrin derivative by ring annulation at the β,β' pyrrolic sites (**Figure IV.2**). The condensation is compatible with the presence of a wide range of substituents on the 1,2-benzenediamine unit, allowing the construction of multi-functional systems. This approach has notably been used in the synthesis of covalently linked multi-porphyrin arrays.[124,264-268] It was later extended to the stepwise annulation

of three[269] or four[270] pyrrolic rings of a porphyrin. In the present study the target compound is a porphyrin substituted with two macrocycles at antipodal β,β'-pyrrolic sites; we will use the ring annulation on a linear porphyrin-tetraone for this synthesis.

IV. 1. c) Retrosynthetic Strategies

The chemical structure of the target porphyrinic bis-macrocycle is depicted in **Figure IV.3**. As mentioned above the central part of the molecule is an extended porphyrin. The dpp-containing macrocycles are linked to the porphyrin core *via* rigid quinoxaline spacers.

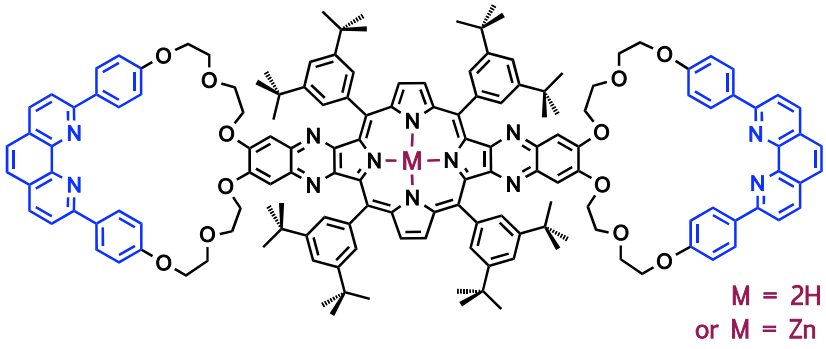

Figure IV.3. Chemical structure of the target extended porphyrin substituted with two coordinating macrocycles.

Two main retrosynthetic strategies can be envisaged for the synthesis of the new porphyrinic building block (**Figure IV.4**). **Strategy A** consists in a double macrocyclisation on an appropriately functionalised porphyrin derivative. This strategy involves a bis(dihydroxyquinoxalino)-porphyrin as an intermediate in the retrosynthetic scheme, which should be accessible *via* the Crossley method for the β,β'-functionalisation of porphyrins. Williamson reaction of this intermediate with the ditosylate **4** (described in Chapter II) in high dilution conditions is expected to give the desired bis-macrocycle. **Strategy B** is based on the attachment of preformed macrocycles to a porphyrin derivative. This alternative approach requires the preliminary synthesis of a dpp-containing macrocycle functionalised with a 1,2-benzenediamine group. Ring annulation on a linear porphyrin-tetraone would then afford the target bis-macrocycle.

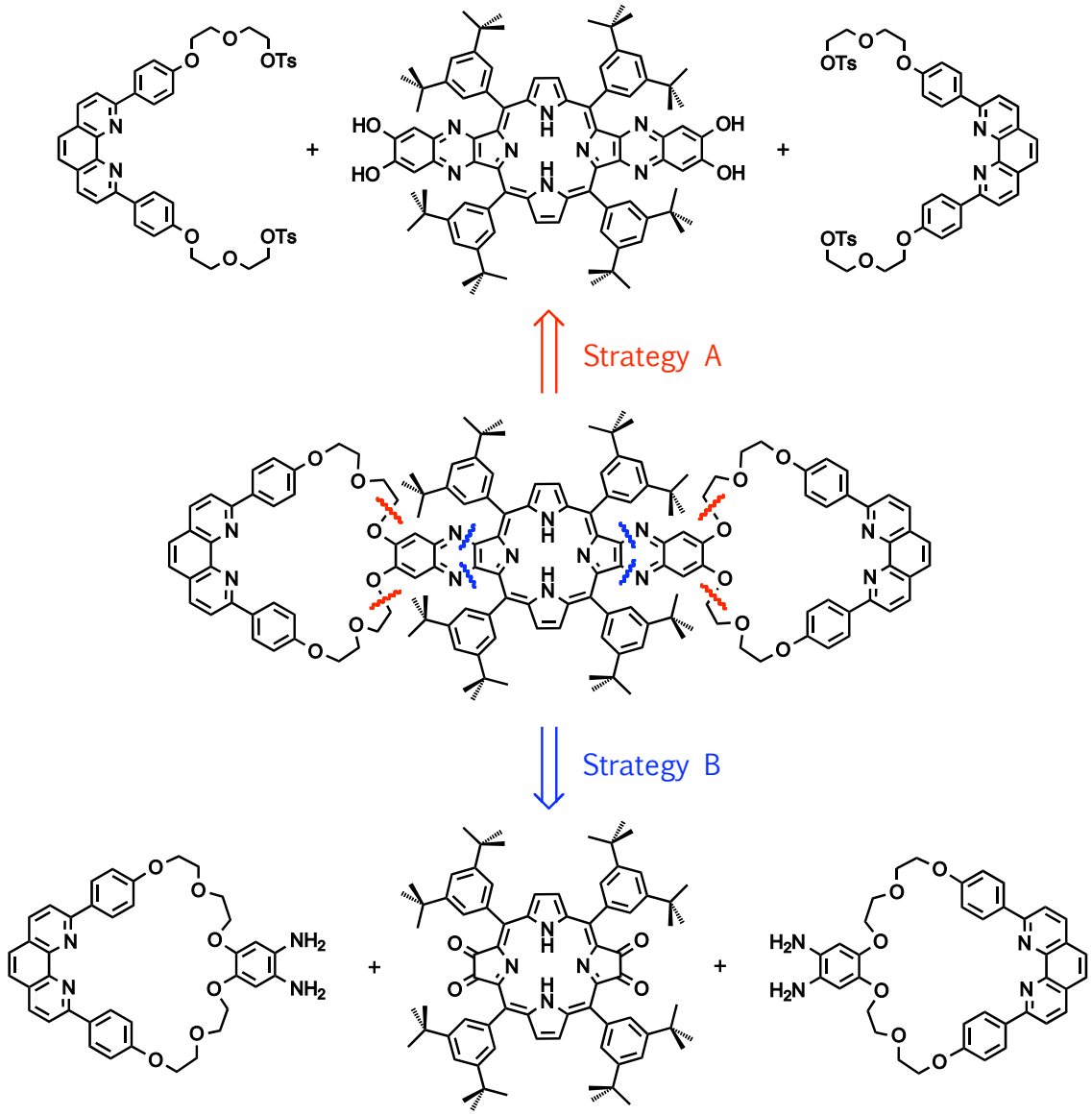

Figure IV.4. Two retrosynthetic strategies for the synthesis of the target porphyrinic bis-macrocycle. **Strategy A**: double macrocyclisation on a bis(dihydroxyquinoxalino)-porphyrin. **Strategy B**: condensation of a porphyrin-tetraone with a diamino-substituted macrocycle.

Strategies A and **B** toward the new porphyrinic bis-macrocycle were both tested. Both approaches involve an important intermediate: the linear porphyrin-tetraone derived from tetrakis(3,5-di-*tert*-butylphenyl)porphyrin. We will now describe the synthesis of this intermediate. Attempts to synthesise the target bis-macrocycle using strategies A and B will then be detailed in parts IV. 2. and IV. 3, respectively.

IV. 1. d) Synthesis of a Linear Porphyrin Tetraone

As explained above, the linear tetrakis(3,5-di-*tert*-butylphenyl)porphyrin-tetraone **25** is a key intermediate in both possible strategies towards the formation of our target bis-macrocycle. This intermediate will then be further functionalised by ring annulation at the pyrrolic sites using appropriately functionalised 1,2-benzenediamine derivatives. The linear porphyrin-tetraone was synthesised following a literature procedure;[265] the synthetic scheme is represented in **Figure IV.5**.

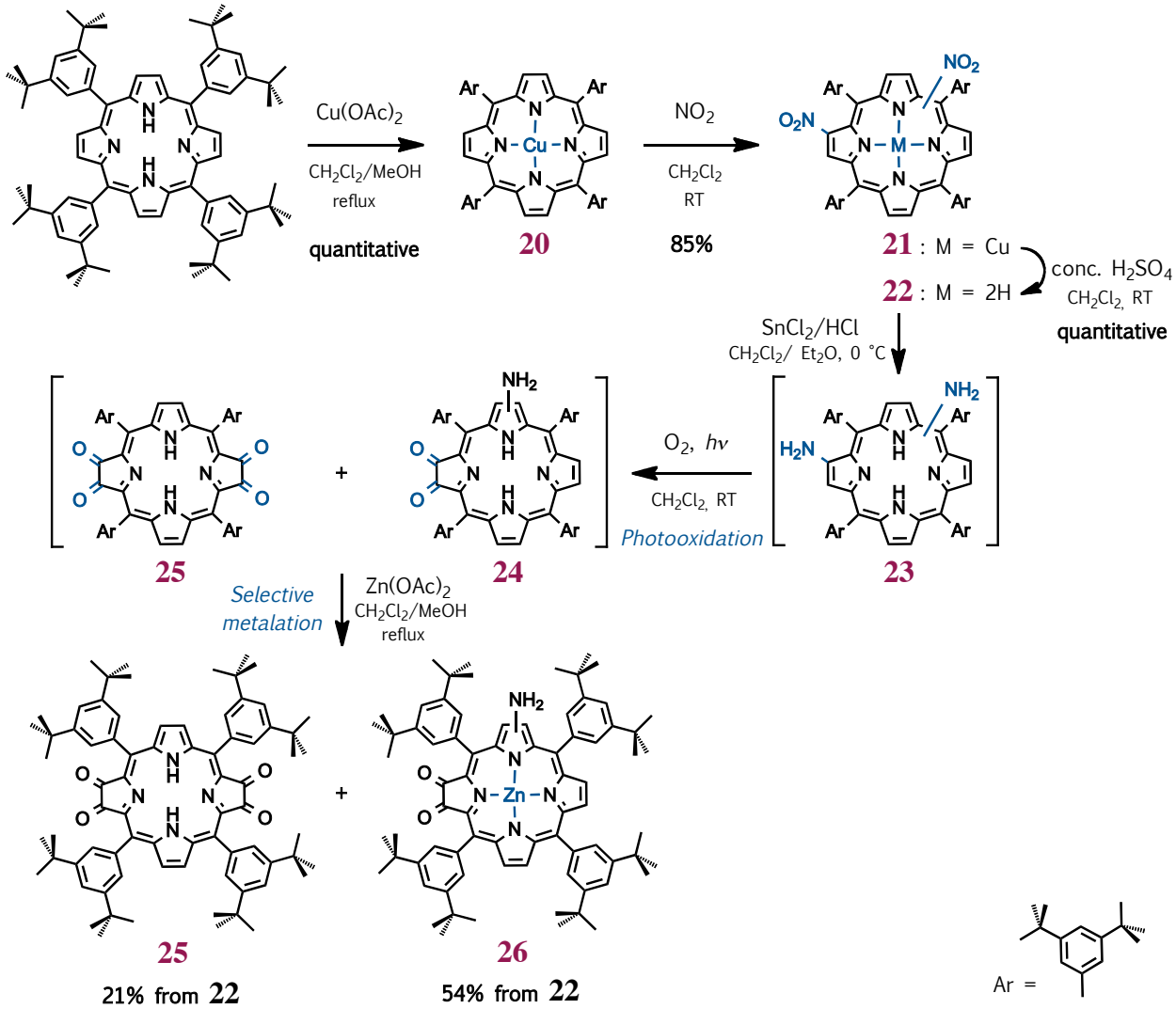

Figure IV.5. Six-step synthesis of linear porphyrin-tetraone **25** *via* a literature procedure.[265]

The linear porphyrin-tetraone **25** was obtained in six steps from 5,10,15,20-tetrakis(3,5-di-*tert*-butylphenyl)porphyrin. This porphyrinic starting material can easily be synthesised by condensation of 3,5-di-*tert*-butylbenzaldehyde and pyrrole in Adler-Rothemund conditions. In a first step, the free-base porphyrin was quantitatively metalated using copper(II) acetate. Double

nitration of the copper(II)-porphyrin **20** was achieved by addition of a solution of nitrogen dioxide in light petroleum to a solution of **20** in dichloromethane. The mononitrated adduct formed first; the dinitrated compound was obtained upon further treatment with NO_2. Chromatographic purification afforded the dinitrated copper(II)-porphyrin **21** as a mixture of isomers in 85% yield. Demetalation of **21** with concentrated sulphuric acid yielded dinitrated free-base porphyrin isomers **22** quantitatively. The nitro groups of **22** were reduced with tin(II) chloride in the presence of hydrochloric acid to give the diamino compounds **23**. A modification of the literature procedure was followed in this step. In the literature procedure the reaction is run in a biphasic system of **22** in dichloromethane and aqueous hydrochloric acid. Instead of this biphasic reaction mixture, we used a solution of hydrochloric acid in ether, which was added to the dichlomethane solution of **22**. This resulted in a monophasic system and reduced the reaction time from three days to two hours. Then, the diamino isomers **23** were immediately photooxidised to afford a mixture of corner 7- and 8-aminoporphyrin-diones **24** and linear 2,3, 12,13-porphyrin-tetraone **25**. Due to the very difficult separation of the free-base porphyrin derivatives **24** and **25**, the mixture of compounds was further reacted with zinc(II) acetate. The aminoporphyrin-diones were selectively metalated to give the corresponding zinc(II) porphyrins **26** while the porphyrin tetraone **25** remained unchanged. The products were separated by column chromatography; the linear free-base porphyrin-tetraone **25** was isolated in 21% yield and the zinc(II) aminoporphyrin-diones **26** were obtained in 54% yield from the dinitrated adducts **22**.

IV. 2. Synthetic Strategy A: Double Macrocyclisation on a Bis(dihydroxyquinoxalino)-Porphyrin

IV. 2. a) Retrosynthetic Routes to the Bis(dihydroxyquinoxalino)-Porphyrin

As presented in **Figure IV.4**, two organic synthons are needed for the synthesis of the desired porphyrinic bis-macrocycle following **Strategy A**. One of the synthons is the dpp derivative **4** functionalised with two terminal tosylate groups, already synthesised and described in Chapter II. The second synthon is a linear extended porphyrin adduct with two terminal catechol moieties. Retrosynthetically, two different routes can be considered for the formation of this bis(dihydroxyquinoxalino)-porphyrin derivative (**Figure IV.6**). **Route A.1** involves the tetramethoxyl equivalent of the desired synthon as an intermediate. A sample of this tetramethoxyl-substituted extended porphyrin was available in the laboratory. Consequently, **Route A.1** was tested first. **Route A.2** consists in the direct condensation of 4,5-diaminocatechol with linear porphyrin-tetraone **25**.

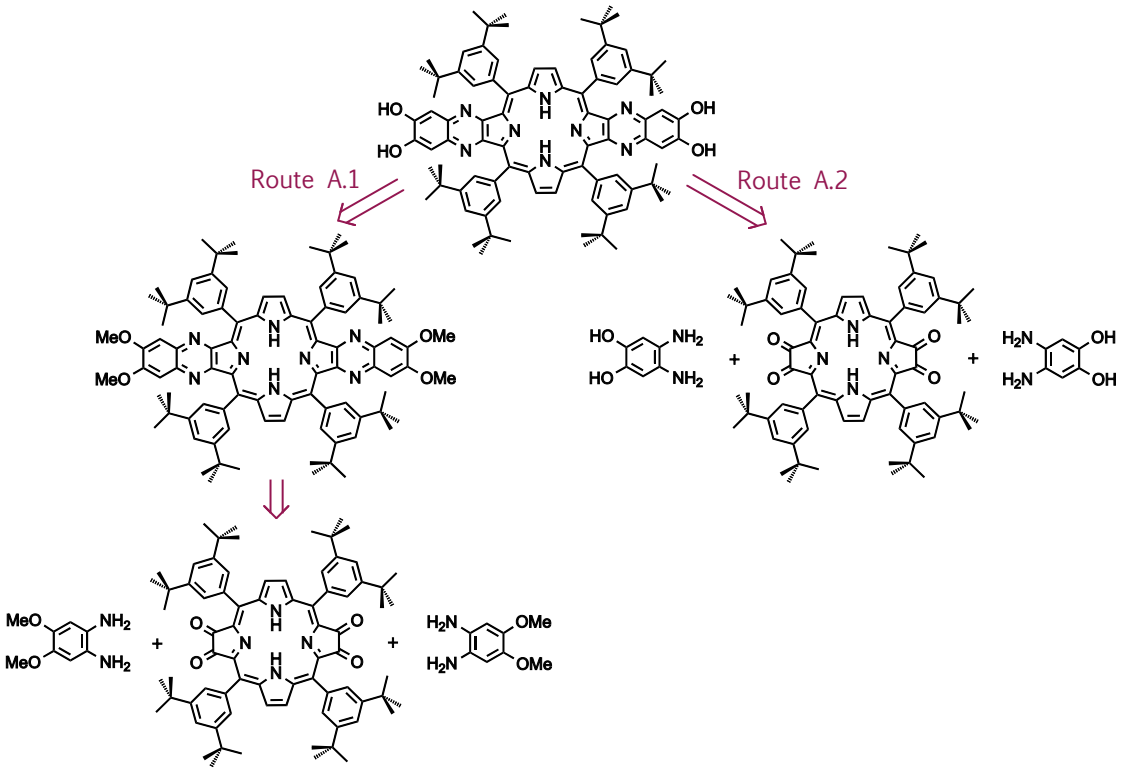

Figure IV.6. Two retrosynthetic routes for the formation of a linear bis(dihydroxyquinoxalino)-porphyrin derivative.

IV. 2. b) Route A.1: Attempted Deprotection of a Linear Bis(dimethoxyquinoxalino)-Porphyrin

Route A.1 was tested on a sample of the tetramethoxyl-substituted precursor available in the laboratory. This compound was synthesised by Linda J. Govenlock, a former PhD student in the Crossley group. It was obtained in high yield by reaction of 4,5-diaminoveratrole (4,5-dimethoxybenzene-1,2-diamine) with the porphyrin-tetraone **25**.[271] Several sets of conditions were tested for the cleavage of the methyl ether groups of the extended porphyrin (**Figure IV.7**). Surprisingly, no reaction occurred upon treatment of the starting material with boron tribromide, even in the presence of a large excess of BBr_3. Heating to 220 °C in pyridinium chloride[272] proved equally inefficient, and the unreacted starting material was recovered. Demethylation of the methyl ethers was then attempted by treatment with aluminium trichloride and ethanethiol.[273] These conditions have been successfully used in the synthesis of a dicatechol ligand where other deprotection conditions had only led to partial cleavage of the methyl ethers.[274] In our case disappearance of the starting material and formation of a very polar species was observed by TLC. However, attempts to characterise the product of the reaction were unsuccessful. Extremely broad signals were observed by NMR spectroscopy, and mass spectrometry analyses gave no peak. The tetra-hydroxyl product might have formed coordination polymers with Al(III), which would not ionise very easily in electrospray or other mass spectrometry techniques.

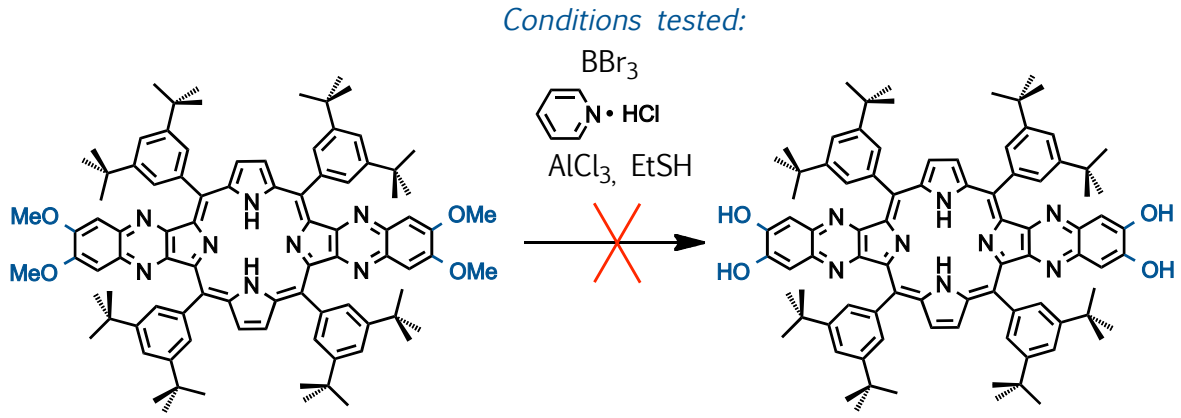

Figure IV.7. Attempted deprotection of the methoxyl groups of a bis(dimethoxyquinoxalino)-porphyrin.

Given the difficulties encountered with the deprotection of the tetramethoxyl compound, we decided to abandon **Route A.1** and to test **Route A.2**.

IV. 2. c) Route A.2: Formation of a Bis-Catechol Extended Porphyrin and Attempted Bis-Macrocyclisation

As shown in **Figure IV.6**, **Route A.2** involves a double ring annulation of 4,5-diaminocatechol on the linear porphyrin-tetraone **25**. The catechol derivative was synthesised in three steps from commercial veratrole (1,2-dimethoxybenzene) following a literature procedure.[275] Nitration of veratrole with nitric acid afforded 4,5-dinitroveratrole **27** in 81% yield after recrystallisation. Reduction of the nitro groups was performed using hydrazine and catalytic palladium on charcoal to yield 4,5-diaminoveratrole **28** quantitatively. Finally, demethylation was achieved in 89% yield by treatment with boron tribromide. 4,5-Diaminocatechol is highly sensitive to air and decomposes readily; it was isolated in the form of the more stable hydrobromide salt **29**.

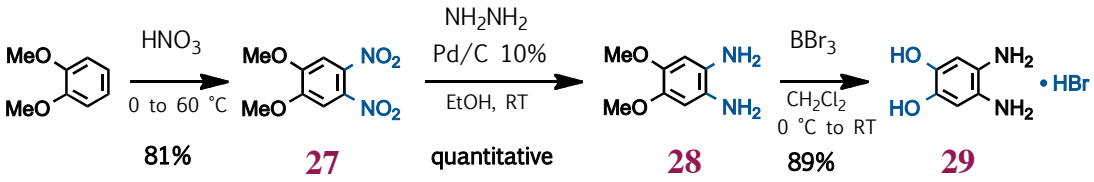

Figure IV.8. Synthesis of 4,5-diaminocatechol hydrobromide **29**.[275]

Porphyrin-tetraone **25** and diaminocatechol hydrobromide **29** were then condensed in refluxing pyridine to afford the desired bis(dihydroxyquinoxalino)-porphyrin **30** in 85% yield after recrystallisation (**Figure IV.9**).

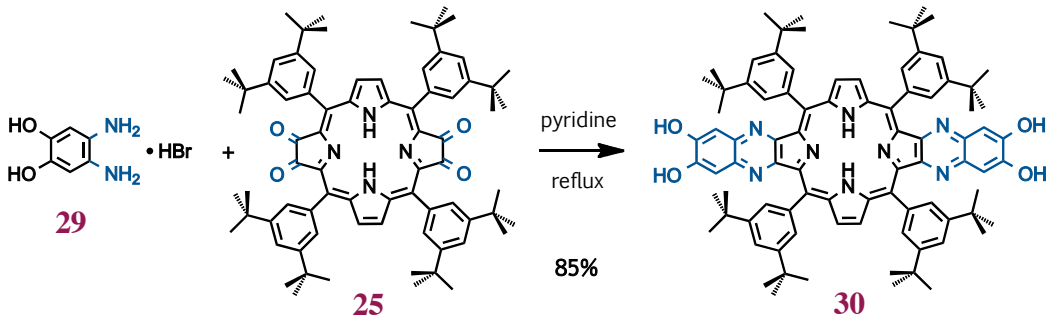

Figure IV.9. Synthesis of the linear bis(dihydroxyquinoxalino)-porphyrin **30**.

The structure of the product was confirmed by a clean mass spectrum with a single peak at m/z = 1331.93 in positive mode (calculated for **30** + H^+: m/z = 1331.78) and m/z = 1329.93 in negative mode (calculated for **30** - H^+: m/z = 1329.76). Very broad signals were observed by ^1H NMR in $CDCl_3$, which made the interpretation of the spectrum difficult. The poor resolution of

the spectrum is probably due to an equilibrium between tautomers in solution (**Figure IV.10**). Even though compound **30** could not be fully characterised, the clean mass spectrum prompted us to proceed with the following macrocyclisation step.

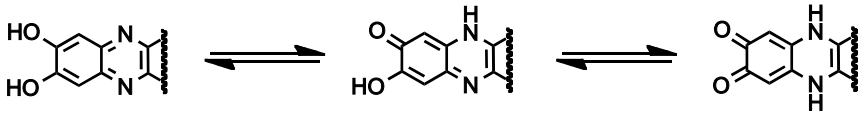

Figure IV.10. Tautomerisation of the dihydroxyquinoxaline moieties of compound **30**.

Double macrocyclisation between the porphyrinic bis-catechol derivative **30** and the ditosylate **4** was then attempted (**Figure IV.11**). Compound **30** was reacted with two equivalents of **4** in DMF in high dilution conditions identical to those used for the formation of macrocycle **5** (Chapter II). Unfortunately a mixture of compounds was obtained, and the desired product was not detected by mass spectrometry. The seemingly low reactivity of compound **30** could be explained by a poor nucleophilicity of the phenolate groups, due to the tautomerisation of the compound.

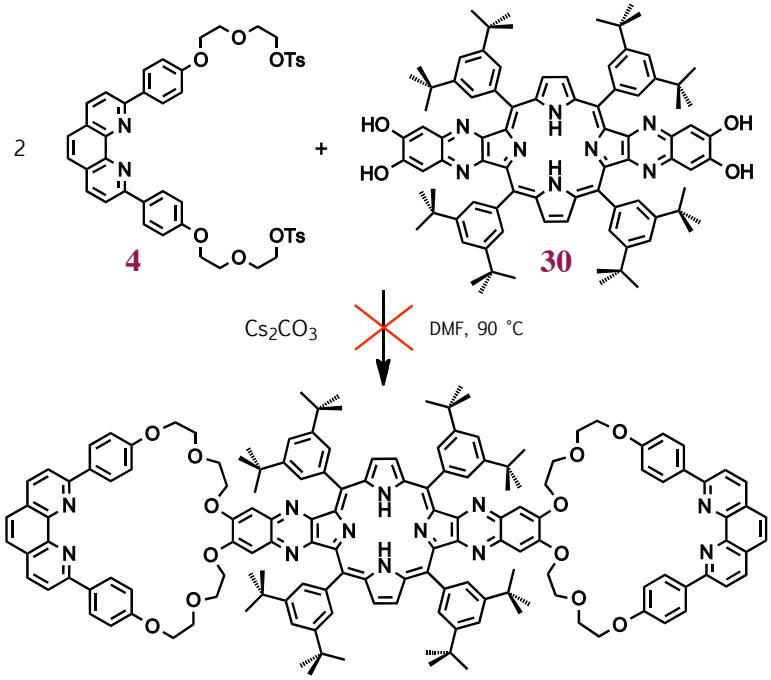

Figure IV.11. Attempted synthesis of the target porphyrinic bis-macrocycle.

The multiple difficulties encountered incited us to follow another synthetic strategy towards the synthesis of the desired porphyrinic bis-macrocycle. Attempts to synthesise the target bis-macrocycle by means of **Strategy B** will be described in the next section of this chapter.

IV. 3. Synthetic Strategy B: Condensation of a Porphyrin-Tetraone with a Diamino-Substituted Macrocycle

The new synthetic approach relies on the retrosynthetic **Strategy B** presented in **Figure IV.4**. In this approach the final synthetic step consists in the condensation of two macrocycles on the linear porphyrin-tetraone **25**. A macrocyclic precursor functionalised with two vicinal aromatic amines is needed for this condensation. Here we will describe attempts to synthesise this diamino-substituted macrocycle using several routes.

IV. 3. a) Route B.1: Attempted Synthesis of a Dinitro-Substituted Macrocycle

The first attempted route towards the formation of the diamino macrocyclic precursor is represented in **Figure IV.12**. The synthetic scheme consists in the macrocyclisation of ditosylate **4** with 4,5-dinitrocatechol **31** to form a dinitro-substituted macrocycle, followed by reduction of the nitro groups to amines.

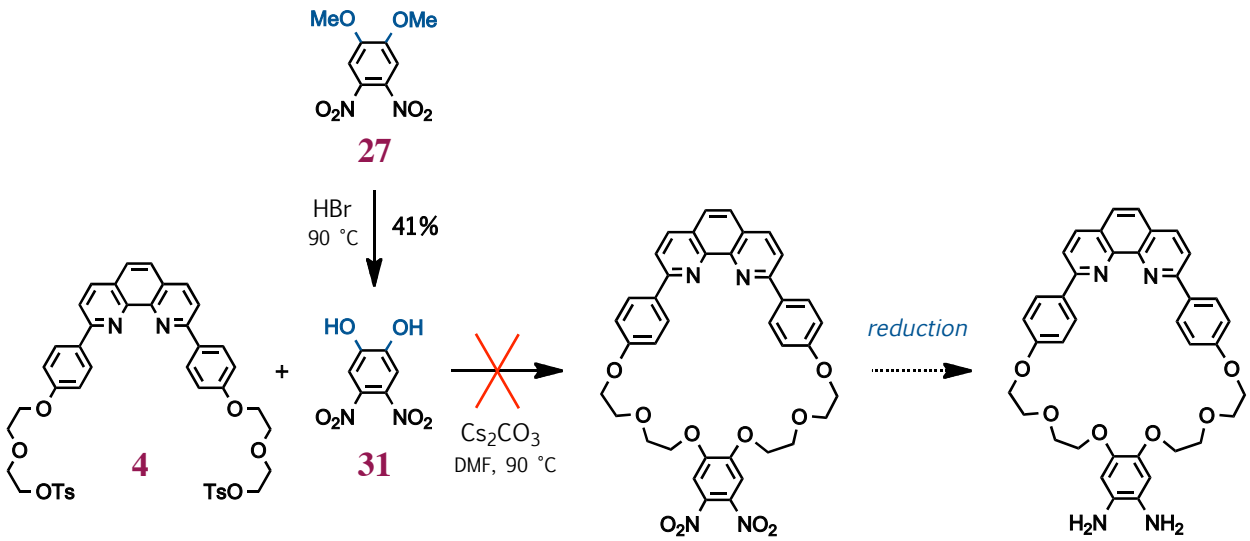

Figure IV.12. Route B.1: Attempted synthesis of a dinitro-substituted macrocycle.

4,5-Dinitrocatechol **31** was obtained in one step by cleavage of the methyl ethers of 4,5-dinitroveratrole **27** following a published procedure.[276] Compound **27** was heated to 90 °C for two days in hydrobromic acid (48%) to afford the deprotected 4,5-dinitrocatechol in 41% yield.

The substituted catechol **31** was then reacted with ditosylate **4** in classical macrocyclisation conditions in DMF. However, TLC analysis showed that a mixture of products was obtained. The products were isolated by column chromatography but the desired dinitro-substituted macrocycle could not be identified. This negative result could be explained by the presence of electron-withdrawing nitro substituents on compound **31**, which significantly reduce the nucleophilicity of the phenolate groups in the macrocyclisation reaction.

IV. 3. b) Route B.2: Attempted Synthesis of a Boc-Protected Diamino-Macrocycle

A second synthetic route was considered in the light of the results obtained with Route B.1. We reasoned that reduction of the nitro groups to electron-donating amines prior to the macrocyclisation should favour the reaction. The phenolate groups of diaminocatechol **29** should be significantly more nucleophilic than the corresponding dinitrocatechol **31**. Nonetheless, we decided to protect the amine groups of compound **29** in order to avoid any competition between the phenolate and the amine nucleophiles in the macrocyclisation reaction. *t*-Butyloxycarbonyl (Boc) was chosen as a protective group for its ease of introduction and compatibility with the macrocyclisation reaction conditions (**Figure IV.13**).[277]

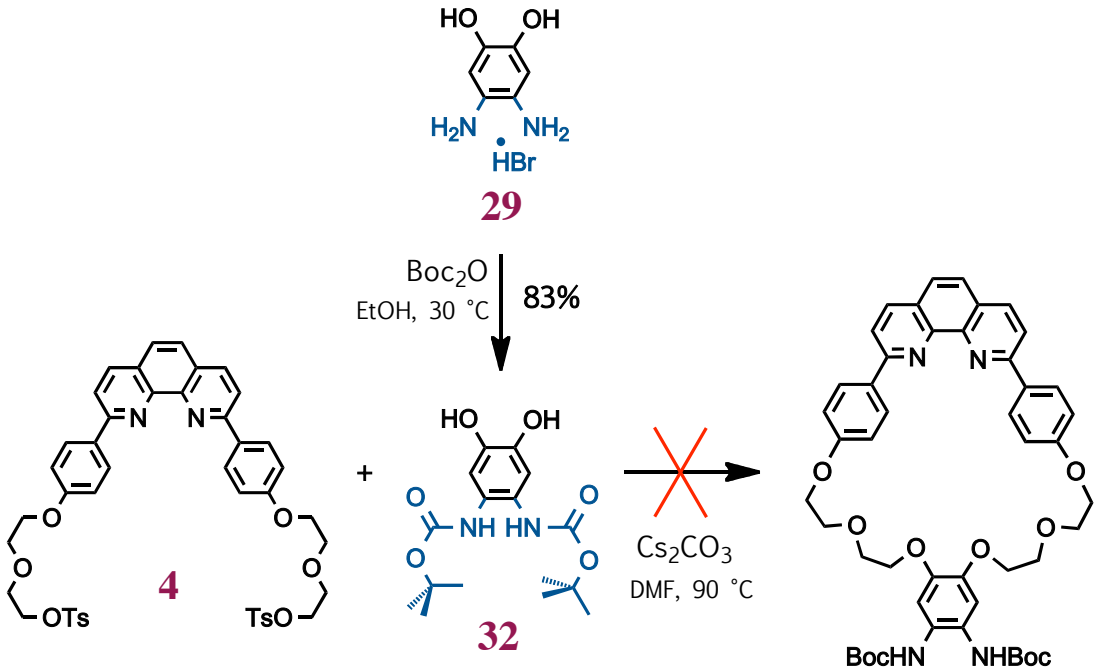

Figure IV.13. Route B.2: Attempted synthesis of a Boc-protected diamino-macrocycle.

The protection reaction was achieved by neutralisation of diaminocatechol hydrobromide **29** with pyridine and immediate treatment with di-*tert*-butyl dicarbonate (Boc_2O) in conditions described in the literature.[278] Carbamate formation at the amine sites occurred selectively, and the Boc-protected diaminocatechol **32** was obtained in 83% yield after recrystallisation. Identification of the product was confirmed by mass spectrometry and NMR. Surprisingly, macrocyclisation attempts using ditosylate **4** and catechol derivative **32** did not yield the expected compound. The products of the reaction could not be clearly identified. The ^1H NMR spectra seemed to indicate the loss of the Boc groups. Consequently, we decided to use a different protecting group.

IV. 3. c) Route B.3: Protection of the Amine Groups using Anisaldehyde

After the unsuccessful macrocyclisation with the Boc-protected compound **32** an alternative protecting group was sought for the amine functions of the diaminocatechol **29**. We decided to exploit the ability of primary amines to form imines reversibly by condensation with aldehydes. Aromatic aldehydes are the most widely used reagents for this type of protection.[277] Anisaldehyde was used in the present study; *p*-methoxyl groups were introduced to increase the electron-donating character of the protective group and the reactivity of the protected catechol derivative towards nucleophilic substitution in the subsequent macrocyclisation reaction.

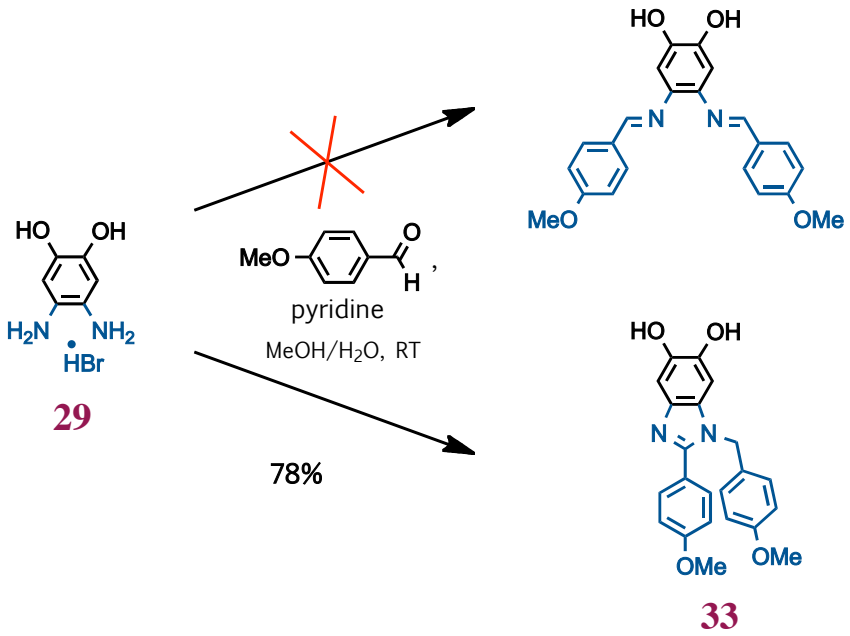

Figure IV.14. Condensation reaction of 4,5-diaminocatechol **29** with anisaldehyde. The 1-benzyl-2-phenylbenzimidazole derivative **33** was obtained instead of the expected bis(N-anisylidenamine) species.

4,5-diaminocatechol hydrobromide **29** was neutralised with pyridine and condensed with two equivalents of anisaldehyde at room temperature in conditions similar to those reported by the group of D. Coucouvanis for the formation of salphen ligands from compound **29** and salicylaldehyde derivatives (**Figure IV.14**).[275] An off-white solid precipitated out of the reaction mixture, and was filtered off and recrystallised from hot ethanol. Analysis of a sample by electrospray mass spectrometry gave a signal at m/z = 376.80 as expected for the desired bis(*N*-anisylidenamine) derivative (calculated value for **M** + H^+: m/z = 377.15). However, the ^{1}H NMR spectrum indicated the formation of an asymmetrical species (**Figure IV.15**). We performed further NMR analyses in order to identify the product of the reaction. The DEPT-135 spectrum indicated the presence of a secondary carbon atom in the molecule, which is not consistent with the expected structure. A literature search revealed that the formation of 1-benzyl-2-phenylbenzimidazole derivatives has been observed from the reaction of *o*-phenylenediamine with aldehydes in some cases.[279-281] This type of structure would be consistent with the observation of a -CH_2- signal in the DEPT spectrum. Consequently, we propose the substituted benzimidazole structure **33** for the product isolated here (**Figure IV.14**). Compound **33** is an isomer of the expected bis-imine product, which explains that the expected mass was found by ES-MS. Complete assignment of the ^{1}H and ^{13}C NMR spectra using COSY, ROESY, HSQC and HMBC data supports the proposed structure (**Figure IV.15**). The molecule contains two non-equivalent anisyl groups with two distinct sets of protons. The chemical shift of the CH_2 signal at 5.31 ppm is typical of benzylic protons in this type of structure.[281-283] The asymmetry of the structure results in splitting of the signals of the catechol protons (c_1, c_2, OH_1 and OH_2).

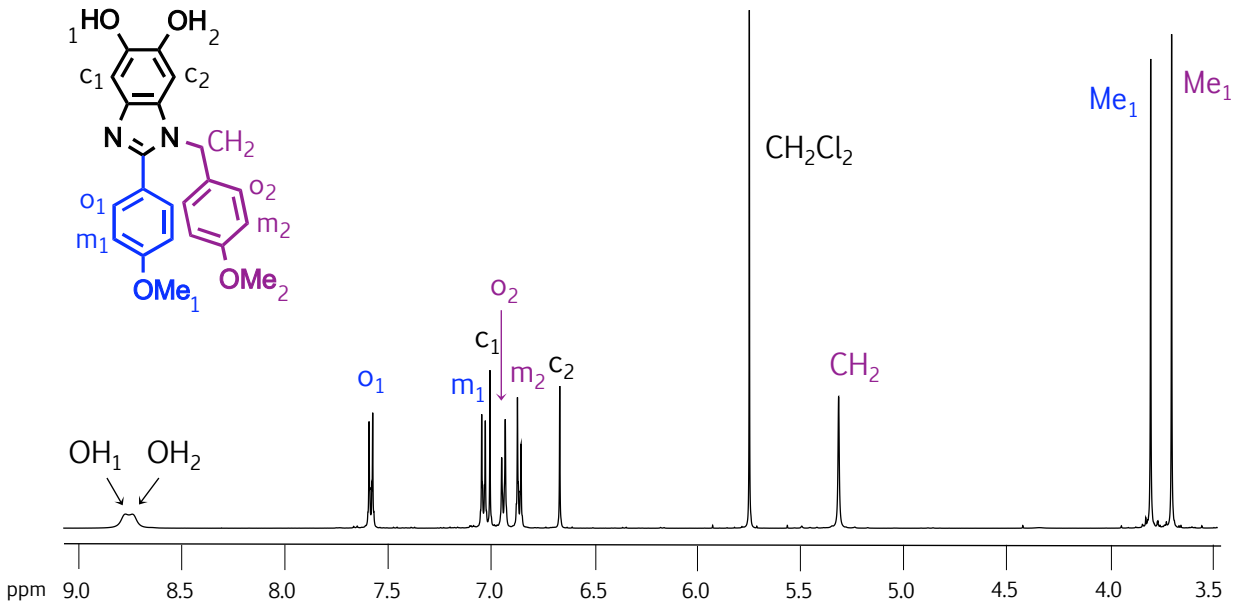

Figure IV.15. Proton NMR spectrum of the 1-benzyl-2-phenylbenzimidazole derivative **33** in DMSO-d_6 (500 MHz). Signals were assigned using COSY, ROESY, HSQC and HMBC data.

Several reaction mechanisms have been proposed in the literature for the formation of 1-benzyl-2-phenylbenzimidazoles from 1,2-phenylenediamine derivatives.[279,281,282] All of these mechanisms involve an inter- or intramolecular hydride transfer step. However, hydride shifts are high energy processes and are not very likely in the mild conditions used here (the reaction was run at room temperature in methanol/water as solvent). The mechanism depicted in **Figure IV.16** seems more plausible. This mechanism involves the initial formation of the expected bis-imine compound. Pyridinium bromide is present in solution as a result of the neutralisation of the hydrobromide salt **29** with pyridine; it provides a source of protons. Protonation at one of the nitrogen sites favours cyclisation to a five-membered ring. A tautomerism equilibrium can then take place, and the final deprotonation is driven by the rearomatisation of the system. We did not perform any additional experiment to validate the proposed mechanism.

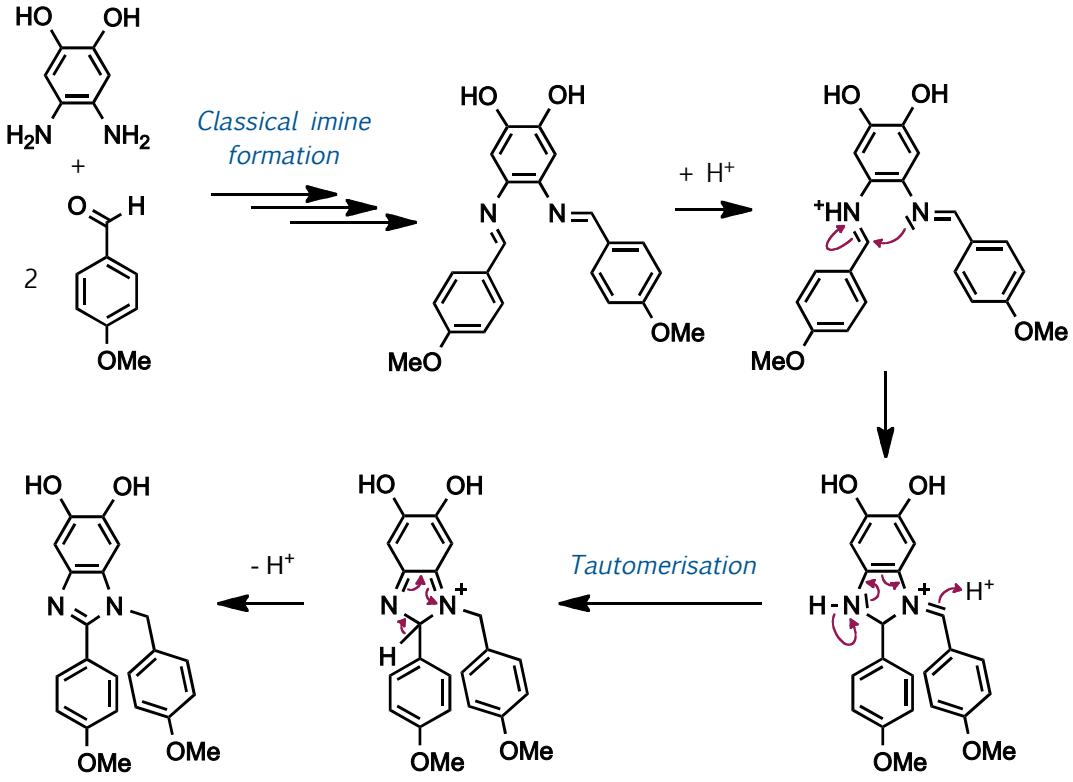

Figure IV.16. Possible mechanism for the formation of **33** in the presence of catalytic acid.

The outcome of the reaction presented here with the formation of a benzimidazole derivative as a major product differs from the results obtained by D. Coucouvanis and coworkers. In their study, the diaminocatechol **29** is condensed with substituted salicylaldehyde derivatives, and the bis-Schiff bases are the major products.[275] The bis-imine adducts obtained from these aldehydes are stabilised by intramolecular hydrogen bonds between the *ortho* -OH groups of the salicylidene moieties and the N atoms of the imines. This could explain the different reactivity

observed with these aldehydes compared to aldehydes that do not incorporate hydrogen bond donors in *ortho* position, *e.g.* anisaldehyde.

The formation of the benzimidazole derivative **33** is unfortunate because it impairs the subsequent deprotection of the amine groups. The macrocyclisation reaction was nevertheless tested with compound **33** (The reaction was run before the structure of **33** was completely elucidated). Williamson reaction of the catechol derivative **33** with the ditosylate **4** in high dilution conditions afforded the expected macrocycle **34** in 60% yield (**Figure IV.17**). The product was characterised by ES-MS and ^{1}H and ^{13}C NMR. The NMR spectra were fully assigned thanks to 2D ^{1}H-^{1}H and ^{1}H-^{13}C correlation experiments. The asymmetry of the 1-benzyl-2-phenylbenzimidazole moiety is conveyed to the macrocyclic part of the molecule. Splitting of almost all signals was observed in the proton NMR spectrum compared to a symmetrical macrocycle like compound **5**; only the 5,6 protons of the phenanthroline unit came out as a single signal.

Cleavage of the aromatic benzimidazole moiety is supposedly very difficult. Yet we estimated that it might be possible to convert it to the corresponding phenylenediamine by palladium-catalysed reduction under high pressure of hydrogen. All attempts were unsuccessful. Treatment of macrocycle **34** with catalytic palladium on charcoal under hydrogen pressure of up to 40 bars yielded mixtures of products; the desired diamino-macrocycle could not be isolated from these mixtures.

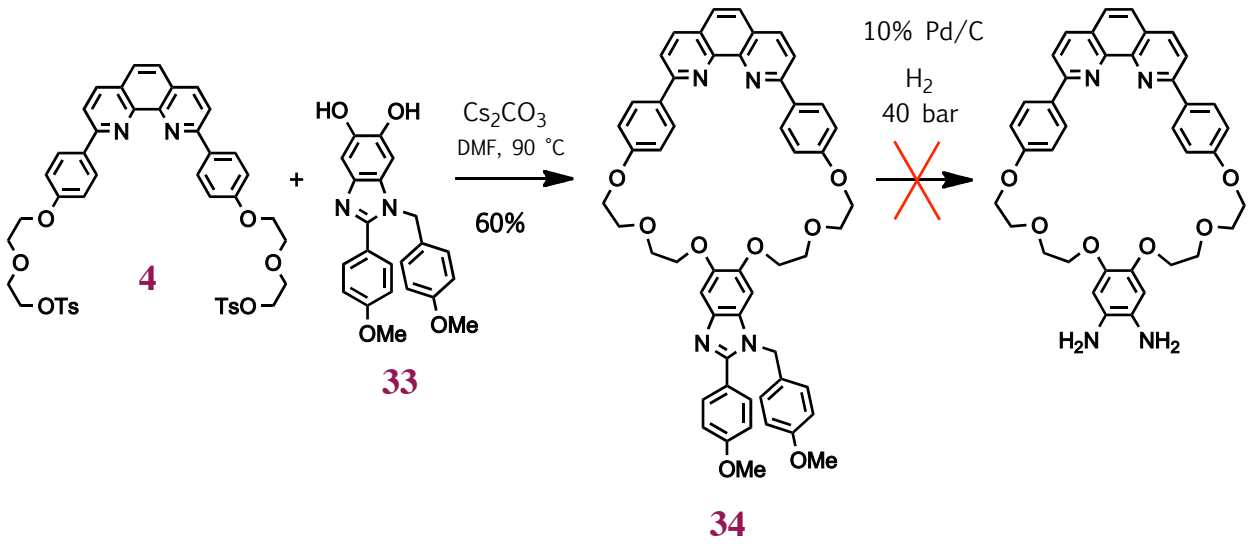

Figure IV.17. Synthesis of macrocycle **34** and attempted deprotection of the amine groups.

IV. 3. d) Route B.4: Post-Macrocyclisation Introduction of Amine Groups

Given the difficulties faced with the synthesis of a macrocycle that incorporates protected amine groups, we designed a fourth synthetic route towards the formation of the desired diamino-macrocycle. We considered that the macrocyclic structure could be formed first, and that the amine functions could be subsequently introduced. The synthetic route relies on the formation of a dibromo-functionalised macrocycle, whose bromo substituents will then be converted to amine functions *via* Hartwig-Buchwald amination.[284-287]

The synthetic scheme leading to the formation of the dibromo-substituted macrocycle **36** is depicted in **Figure IV.18**. First, catechol is converted to 4,5-dibromocatechol **35** in 53% yield by treatment with bromine in chloroform, following a published procedure.[288] Double Williamson reaction between the dibromocatechol **35** and the ditosylate **4** in high dilution was successful and gave the expected macrocycle **36** in 36% yield. The structure of compound **36** was confirmed by ES-MS and NMR.

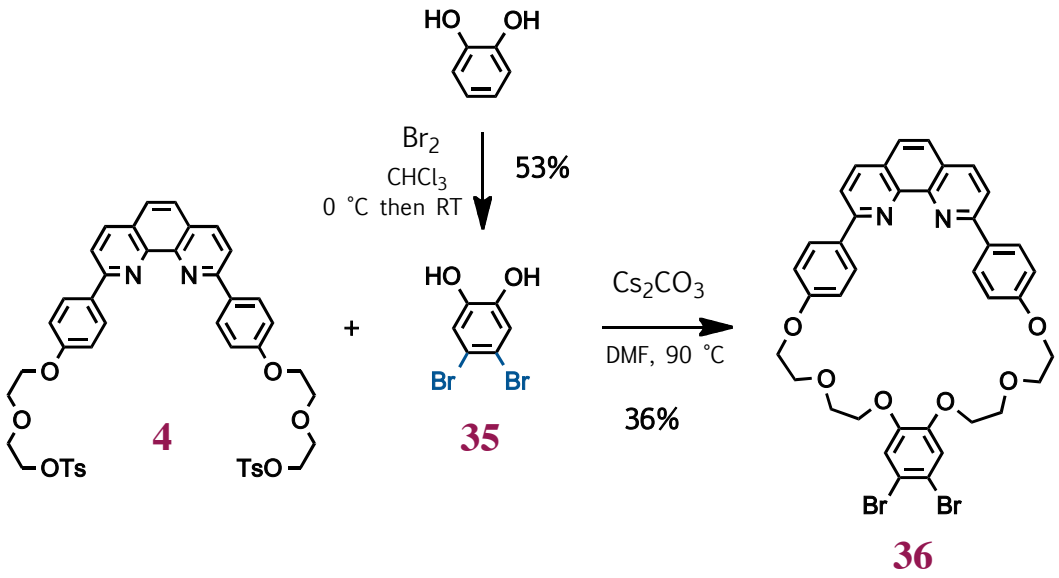

Figure IV.18. Synthesis of the dibromo-substituted macrocycle **36**.

Macrocycle **36** was then coupled to an ammonia equivalent in order to form the desired C-N bonds. Benzophenone imine was chosen as the ammonia equivalent because it results in adducts that are stable to chromatographic purification after coupling. We followed a procedure developed by the group of S. L. Buchwald[289] and later used by D. Jiang and coworkers for the six-fold amination of a hexabromo-triphenylene derivative.[290] Dibromo-macrocycle **36** was

refluxed with benzophenone imine, sodium *tert*-butoxide and catalytic amounts of $Pd_2(dba)_3$ and racemic BINAP in toluene (**Figure IV.19**). The expected bis-imine macrocycle **37** was formed in the reaction as evidenced by mass spectrometry. However, we faced purification problems and the product could not be isolated for the time being. Once the macrocycle is isolated the imines will be cleaved to give the desired diamino-macrocycle. Several methods are available for this cleavage reaction (transamination, hydrogenolysis or acidic hydrolysis).[289,290] The target porphyrinic bis-macrocycle presented at the start of this chapter should then be accessible by condensation of the diamino-macrocycle with the linear porphyrin-tetraone **25**.

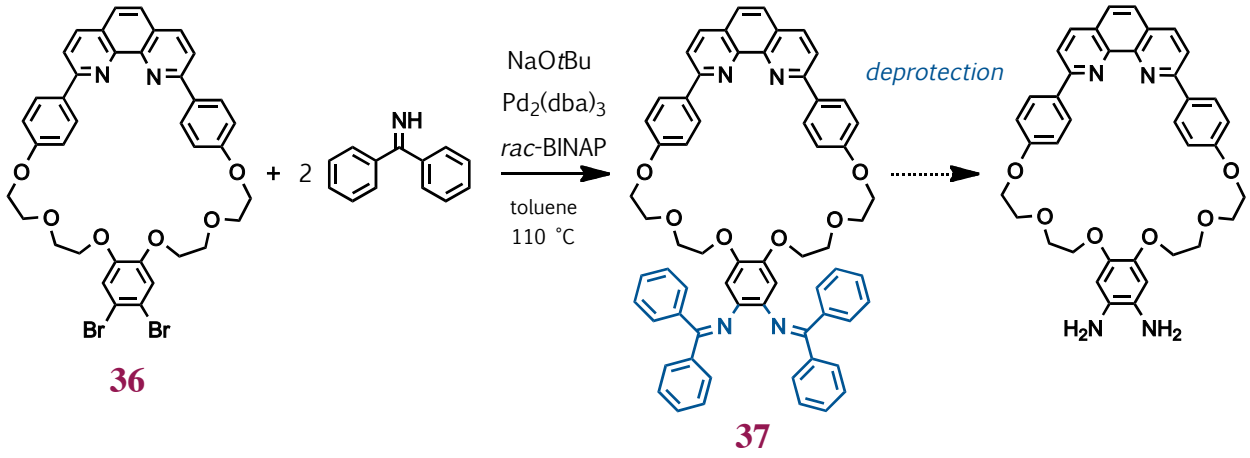

Figure IV.19. Synthesis of bis-imine macrocycle **37** by Buchwald-Hartwig reaction with benzophenone imine.[289]

In conclusion, numerous difficulties were met towards the formation of a new, rigid porphyrinic bis-macrocycle. The synthetic strategy had to be redesigned several times, and the target molecule has not been obtained yet. However, the last synthetic route presented here gave encouraging results. Overcoming the purification problems with precursor **37** should give access to the desired bis-macrocycle. This building block could then be tested in a threading-followed-by-stoppering reaction with axle **16** and stopper **18**. The formation of a cyclic [4]rotaxane with a structure similar to that of rotaxane $\mathbf{19}^{4+}$ is expected. The ability of the rotaxane to bind guest substrates and compress them upon complexation with copper(I) could be studied. The molecular press properties of the rotaxane would thus be tested.

Chapter V. A [3]Rotaxane of Novel Architecture and its Precursor:

A New Zinc Porphyrin Substituted with Four Coordinating Macrocycles

In the previous chapters we described the synthesis and attempted synthesis of porphyrins substituted with two macrocycles, and the formation and host-guest properties of a [4]rotaxane that incorporates one of these porphyrinic bis-macrocycles. In order to obtain more elaborate structures we then designed a new porphyrin substituted with *four* coordinating macrocycles. In this chapter we will describe the synthesis of a tetra-substituted porphyrin and investigate the formation of multi-rotaxanes from this new porphyrinic building block.

V. 1. A Zinc Porphyrin Substituted with Four Coordinating Macrocycles

V. 1. a) Design of the system

After the study of our new [4]rotaxane based on a porphyrinic bis-macrocycle, we decided to further functionalise our building blocks in order to gain access to higher order rotaxanes. The new target is a porphyrin linked to four peripheral rings instead of two, which should widen the range of threading options. We envisioned that a [6]rotaxane could be obtained from this new tetra-macrocyclic building block (**Figure V.1**). A templated assembly with a two-station axle could lead to this [6]rotaxane following a threading scheme similar to that observed for the formation of the [4]rotaxane described in Chapter III. The final [6]rotaxane would be constituted of two face-to-face zinc porphyrins mechanically linked to four dumbbell components. This architecture is reminiscent of the [6]pseudorotaxane described by the groups of J. F. Stoddart and R. J. M. Nolte (see part **I. 4. a)**). However in this system the porphyrins were attached to the *thread* components of the pseudorotaxane while in the present system the

porphyrins will be covalently linked to the *ring* components. The cofacial arrangement of the porphyrins in the [6]rotaxane should allow the complexation of various guest molecules between the two porphyrins. **Figure V.1** shows a schematic view of the target [6]rotaxane and the retrosynthetic route for its formation, as well as the chemical structure of the target porphyrinic tetra-macrocycle building block. The structure consists of four coordinating rings attached to the *meso* positions of a central zinc porphyrin *via* single C-C bonds. The macrocycles are identical to those incorporated in the porphyrinic bis-macrocycle described in Chapter II; they are 31-membered rings that contain 2,9-diphenyl-1,10-phenanthroline fragments located relatively far away from the porphyrin nucleus. The free rotation around the single carbon-carbon bond linking the rings and the porphyrin allows the rings to be tilted in relation to the plane of the porphyrin. It is also noteworthy that these rings are flexible enough to fold up and adopt a non-planar geometry without imposing a significant strain onto the whole molecular system. After a few generalities on the synthesis of porphyrins, we will now describe the synthesis of the target tetra-macrocycle.

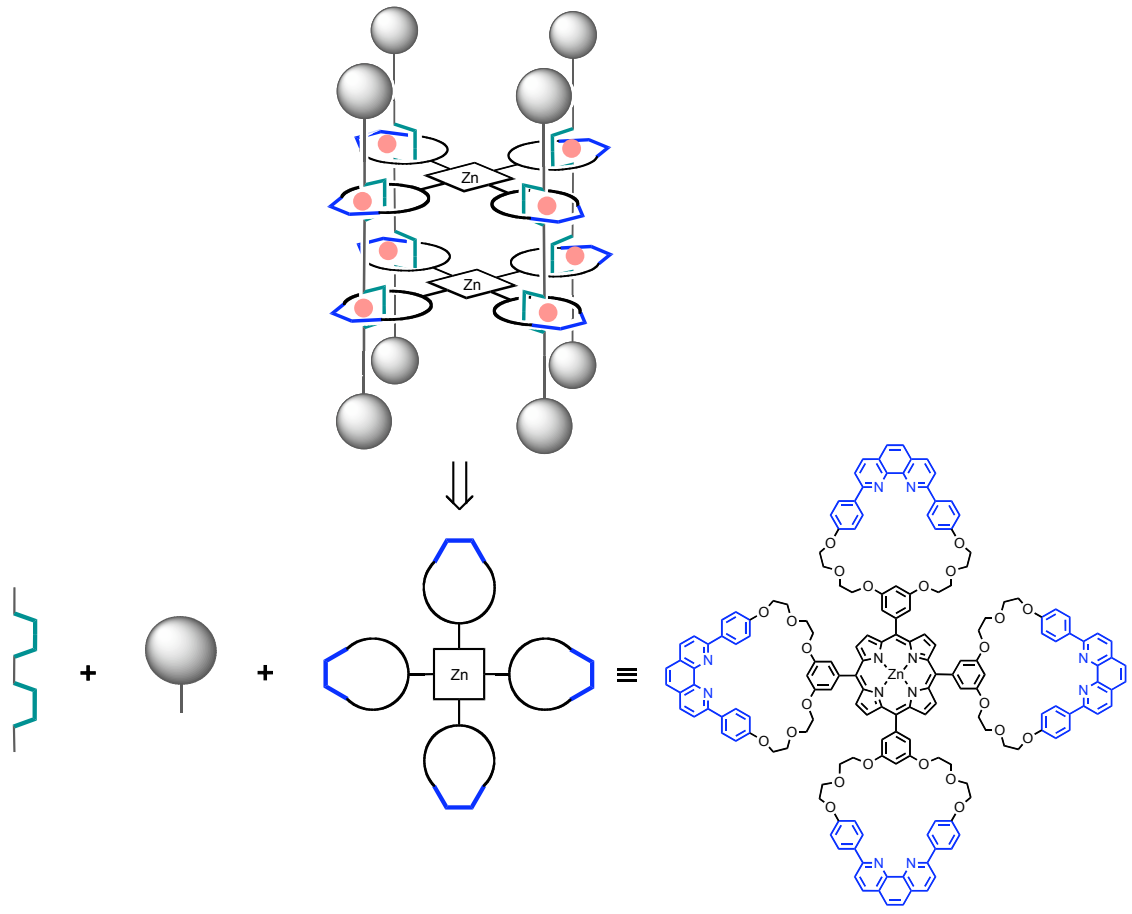

Figure V.1. Schematic view of the target [6]rotaxane constituted of two face-to-face porphyrins, each of them covalently linked to four coordinating macrocycles and mechanically linked to four dumbbells. The retrosynthetic route for the formation of this [6]rotaxane involves the use of a two-station axle, a stopper and a new porphyrinic tetra-macrocycle whose target chemical structure is depicted.

V. 1. b) Synthetic Approaches for the Formation of Porphyrins

With the growing interest for porphyrin derivatives several synthetic strategies have been developed for their formation. The present target molecule is a symmetrical tetra-aryl porphyrin. The most straightforward strategy for the synthesis of this type of porphyrin consists in condensing pyrrole with an aldehyde, and oxidising the intermediate porphyrinogen to the aromatic porphyrin ring (**Figure V.2**).[291] Symmetrical *meso* tetra-substituted porphyrins are accessible *via* this method, the *meso* substituent depending on the starting aldehyde used in the condensation. Mixtures of aldehydes afford unsymmetrical *meso*-substituted porphyrins; however the relative positions of the different substituents cannot be monitored and statistical mixtures are obtained. β-substituted porphyrins can also by synthesised with this method if the starting material is a substituted pyrrole.

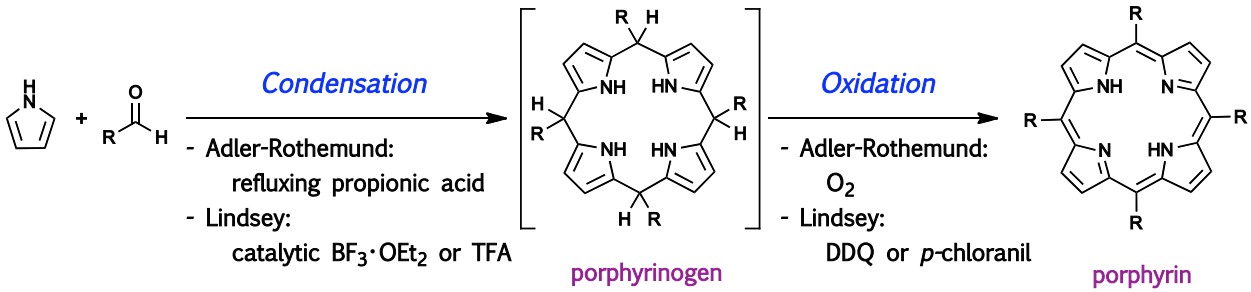

Figure V.2. Porphyrin synthesis by condensation of an aldehyde and pyrrole to a porphyrinogen intermediate, followed by oxidation to form the aromatic porphyrin ring. The conditions for the Adler-Rothemund and the Lindsey procedures are given.

Two main sets of conditions are typically used in the condensation-followed-by-oxidation process. In the Adler-Rothemund method the aldehyde and pyrrole are condensed in refluxing propionic acid; and exposure of the reaction mixture to air allows *in situ* oxidation by molecular oxygen.[292,293] In the Lindsey procedure the condensation is catalysed by an acid, typically trifluoroacetic acid (TFA) or trifluoroborate-etherate (BF_3•OEt_2); and a chemical oxidant like 2,3-dichloro-5,6-dicyano-1,4-benzoquinone (DDQ) or *p*-chloranil is used to obtain the aromatic ring (**Figure V.2**).[294,295] Condensation of an aldehyde with pyrrole never affords the desired porphyrin in quantitative yield because side products are formed in the reaction (*e.g.* open-chain oligomers). The porphyrin yield is typically around 20 to 25% and depends a lot on the -R substituent of the aldehyde and on the conditions of the reaction. Alternatives to the Adler-Rothemund and Lindsey conditions for the synthesis of symmetrical tetra-substituted porphyrins have been described and give good results in some cases.[296-300] Some of these alternatives will be discussed in this chapter.

Porphyrins functionalised with polydentate nitrogen ligands (*e.g.* 1,10-phenanthroline or 2,2'-biypridine chelates) are useful building blocks for the construction of functional assemblies. Two main routes can be considered for the synthesis of this type of porphyrins. The chelate can be introduced on the preformed porphyrin ring by appropriate coupling; or it can be attached to the aldehyde precursor used in the condensation, leading directly to the functionalised porphyrin. This last route can reduce the number of synthetic steps. However, reports describing the formation of chelate-functionalised porphyrins following this direct strategy are rare, probably owing to synthetic difficulties.[301-304] Here we will present our optimisation of the reaction conditions in the case of an aldehyde attached to a dpp unit.

V. 1. c) Synthesis of the New Porphyrinic Tetra-Macrocycle

The strategy adopted for the synthesis of the new tetra-substituted porphyrin depicted in **Figure V.1** involves condensation of a macrocyclic aldehyde with pyrrole, as shown in **Figure V.3**, followed by metalation with zinc acetate.

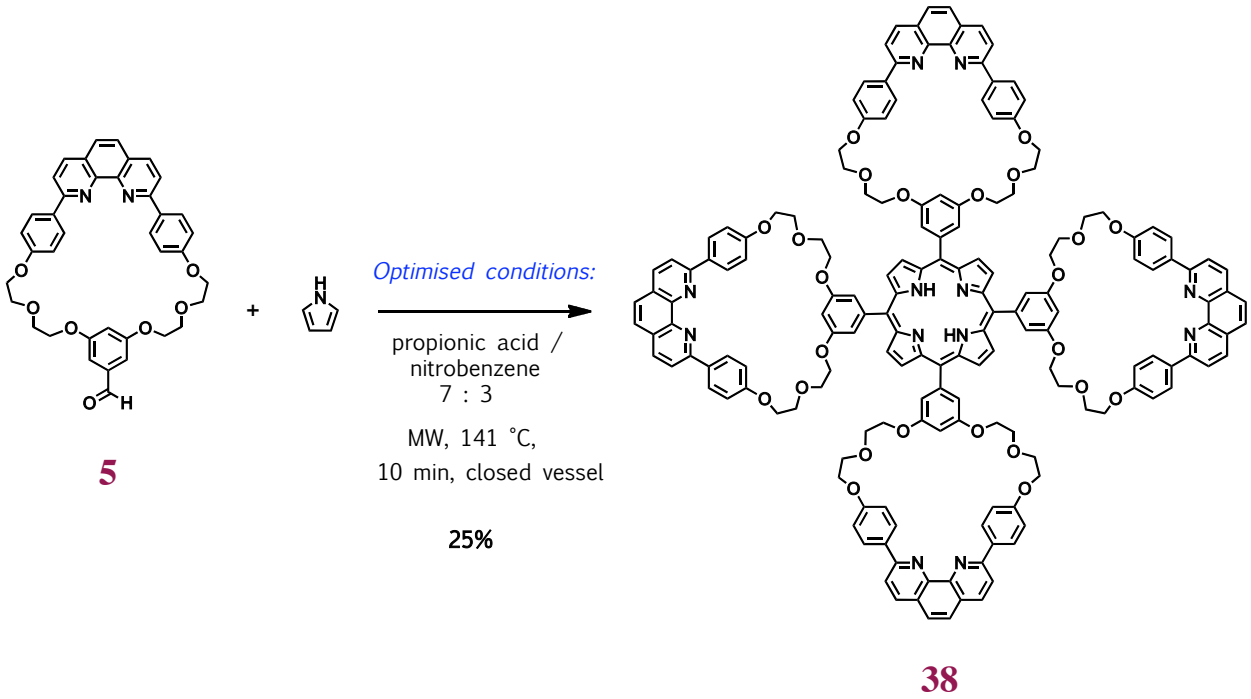

Figure V.3. Synthesis of tetra-substituted free-base porphyrin **38**. Optimised conditions for the condensation: **5** (1 eq., 200 mM), pyrrole (1 eq., 200 mM), propionic acid/nitrobenzene 7:3, microwaves, 141°C, 10 min (25%).

The aldehyde precursor used in the condensation reaction is the macrocycle **5**, which was prepared in gram amounts as described in Chapter II. The chemical structure of the target free-base porphyrin **38** is depicted in **Figure V.3** as well as the optimised conditions leading to its preparation. A series of different reaction conditions were tested in order to improve the porphyrin yield, which was initially very low. First, equimolar amounts of pyrrole and aldehyde **5** were condensed in classical Lindsey conditions using boron trifluoride etherate as a catalyst, followed by oxidation with DDQ.[294] Porphyrin **38** was obtained in a very low yield of 3%. Use of trifluoroacetic acid (TFA) instead of boron trifluoride etherate gave similar results (**Table V.1**, Entries 1-2). In an attempt to increase the yield of this challenging synthesis, various alternative methods were then tested. Crossley *et al*. developed a procedure for the synthesis of porphyrins using *p*-toluenesulfonic acid as a catalyst with azeotropic removal of water.[296] Low yields (2-4%) of porphyrin **38** were obtained with this method, possibly due to poor solubility of macrocycle **5** in toluene in the presence of *p*-toluenesulfonic acid (**Table V.1**, Entry 3). Use of equimolar amounts of CF_3SO_2Cl or catalytic amounts of iodine were reported to yield 25-64% of various *meso*-tetraarylporphyrins[297,298] but absolutely no reaction occurred between aldehyde **5** and pyrrole under these conditions (**Table V.1**, Entries 4-5). This indicated that mild conditions were not adequate for the synthesis of porphyrin **38**, presumably due to the presence of a 1,10-phenanthroline moiety in the macrocycle. Our results incited us to try harsher conditions.

Table V.1. Synthesis of free-base porphyrin **38** in classical Lindsey conditions or mild conditions.

Entry	Catalyst	Solvent	Temperature	Reaction time	Yield	Ref.
1	$BF_3{\cdot}OEt_2$ (0.1 eq.)	$CHCl_3$	RT	1 h	3%	294
2	TFA (0.1 eq.)	CH_2Cl_2	RT	1 h	4%	294
3	*p*TsOH (0.2 eq.)	Toluene	Reflux (Dean-Stark)	40 h	4%	296
4	Iodine (0.2 eq.)	CH_2Cl_2	Reflux (Microwaves)	30 min	0%	297
5	CF_3SO_2Cl (1 eq.)	$CHCl_3$	RT	4 h	0%	298

We then tested reaction conditions derived from the Adler-Rothemund method (**Table V.2**).[292,293] Refluxing pyrrole and aldehyde **5** in propionic acid afforded porphyrin **38** in an encouraging yield of 9% (**Table V.2**, Entry 1). Based upon the observation by Newkome and coworkers that a microwave-enhanced synthesis led to an improved yield in the synthesis of a terpyridine-containing porphyrin,[304] we tested the microwave activation effect on our reaction. Indeed, the reaction time went from 2 h to 30 min and the yield was increased to 12% when the reaction was run in a microwave reactor (**Table V.2**, Entry 2). Use of nitrobenzene as cosolvent and oxidising agent in this type of reaction has been reported to give rise to higher yields.[300] In our case it increased the solubility of the starting material in the reaction mixture and free-base porphyrin **38** was obtained in 15% yield after 10 minutes of microwave irradiation (**Table V.2**, Entry 3). Temperature and concentration also proved to be critical parameters in this reaction (**Table V.2**, Entries 4-6). Temperatures below 140 °C led to incomplete conversion and longer reaction times while increasing the temperature to 190°C led to partial decomposition of the product. Increasing the concentration of the starting materials from 50 to 200 mM improved the yield of the reaction considerably, and target porphyrin **38** was obtained in 25% yield. Thus, reacting 200 mM aldehyde and pyrrole at 141 °C for 10 minutes in a 7:3 mixture of propionic acid and nitrobenzene under microwave irradiation were found to be the best conditions for the synthesis of porphyrin **38**. Purification by sequential silica and size-exclusion chromatographies gave pure free-base porphyrin **38** as a purple solid in 25% yield using these conditions.

Table V.2. Synthesis of free-base porphyrin **38** in conditions derived from the Adler-Rothemund method.

Entry	Solvent	Microwaves	Temperature	Reaction time	Concentration (mM)	Yield
1	Propionic acid	No	141 °C	2 h	50	9%
2	Propionic acid	Yes	141 °C	30 min	50	12%
3	Propionic acid / nitrobenzene 7:3	Yes	141 °C	10 min	50	15%
4	Propionic acid / nitrobenzene 7:3	Yes	190 °C	10 min	50	9%
5	Propionic acid / nitrobenzene 7:3	Yes	141 °C	10 min	200	25%
6	Propionic acid / nitrobenzene 7:3	Yes	100 °C	40 min	200	20%

Metalation of the porphyrinic site was carried out by adding excess zinc acetate in methanol to a refluxing solution of **38** in chloroform. Further treatment with EDTA to remove zinc(II) from the phenanthroline chelates afforded zinc porphyrin **39** as a purple solid in quantitative yield (**Figure V.4**). By using the optimal experimental procedure based on the above-described study, it was possible to prepare batches of the tetra-substituted Zn-porphyrin **39** on the 100 mg scale.

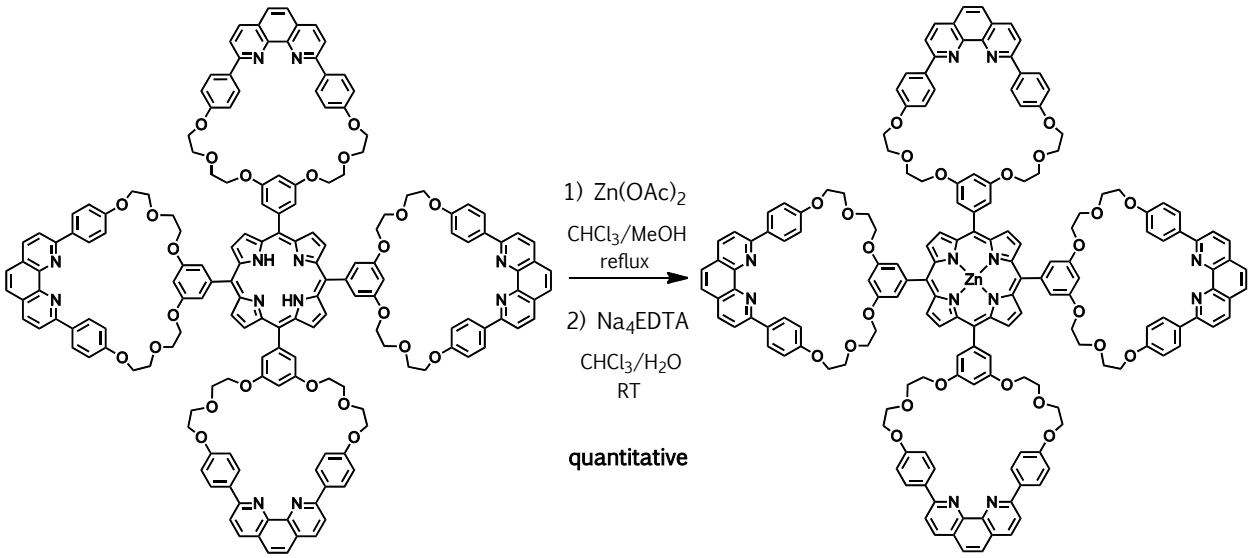

Figure V.4. Synthesis of tetra-substituted zinc(II) porphyrin **39** (quantitative yield).

The condensation conditions and their optimisation presented here might lead to real advances in the synthesis of porphyrins incorporating polypyridine chelates or other polydentate ligands. These porphyrins are typically obtained in poor yields (5-12%) when they are formed by the direct condensation of pyrrole and chelate-appended aldehydes.[302-304] The reaction conditions developed here could afford better yields in the syntheses of this type of porphyrins.

V. 2. A [3]Rotaxane Composed of a Porphyrinic Tetra-Macrocycle and Two Dumbbells

V. 2. a) Threading and Stoppering Reactions: Formation of a [3]Rotaxane

Once the zinc porphyrin **39** substituted with four coordinating rings was obtained, it was used as a building block in the templated assembly of a copper(I)-complexed multi-rotaxane. As explained at the start of this chapter, the formation of a [6]rotaxane was expected by threading of two-station axles through the rings of compound **39** followed by the introduction of stoppers. We used the alkyne-functionalised bis-bidentate ligand **16** and the azide-functionalised derivative **18** (both described in Chapter II) as the axle and the stopper, respectively, in the reaction of formation of the rotaxane. However, a different threading scheme is prevailing in this case, as evidenced by the formation of a [3]rotaxane instead of the expected [6]rotaxane (**Figure V.5**). This is explained by the flexibility of the dpp-containing macrocycles and by the free rotation allowed by the single-bonded connector between the rings and the porphyrin core. The tetra-macrocycle can adopt a conformation where the orientation of the rings is perpendicular to the plane of the central porphyrin; this enables threading of the same axle through two adjacent rings of the same porphyrin. The double threading of two axles through the rings of the tetra-macrocyclic component **39** leads to the formation of a [3]rotaxane as schematically depicted in **Figure V.5**. Although its formation was not expected, the [3]rotaxane is far from being devoid of interest. Its architecture is novel and is reminiscent of two "simple" [3]rotaxanes (consisting of a dumbbell and two threaded rings) whose rings are linked together by a central porphyrinic plate.

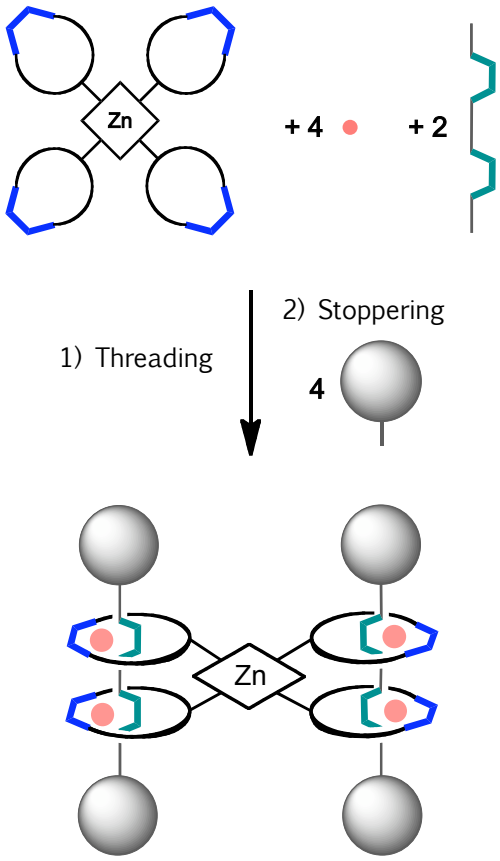

Figure V.5. Preparation of a [3]rotaxane whose central fragment consists of a Zn-complexed porphyrin bearing four coordinating rings. The synthetic strategy is based on the "gathering-and-threading" approach followed by stoppering. The threading scheme that prevails in this case differs from that observed for the formation of the [4]rotaxane in Chapter III. Free rotation of the rings in relation to the porphyrin allows threading of the axles through two adjacent rings of the porphyrin.

Figure V.6 shows the reaction conditions leading to the formation of the new [3]rotaxane $\mathbf{40^{4+}\cdot 4PF_6}$. The rotaxane was obtained *via* a two-step, one-pot synthesis consisting of *(i)* formation of a [3]pseudorotaxane and *(ii)* stoppering reaction. In a first step, the [3]pseudorotaxane was formed by mixing tetra-macrocycle **39** and $[Cu(CH_3CN)_4](PF_6)$ in chloroform/acetonitrile, and then transferring the resulting solution to a suspension of acetylenic thread **16** in chloroform and stirring under argon for 24 h. The classical threading procedure adopted here involves complexation of Cu(I) with the dpp units of the macrocycle and then addition of the rod, threading through the macrocycles and formation of tetrahedral complexes with Cu(I) to give a [3]pseudorotaxane as an intermediate. In a second step, azide stopper precursor **18** and catalytic $[Cu(CH_3CN)_4](PF_6)$ and Na_2CO_3 were added to the reaction mixture, which was subsequently stirred under argon for six days. In this step the stoppers were introduced by formation of triazoles at the end of the threads via a Huisgen copper-catalysed azide-alkyne cycloaddition (CuAAC). After chromatographic purification, the [3]rotaxane $\mathbf{40^{4+}}$ was obtained as a dark red solid in 44% yield (threading and quadruple stoppering steps).

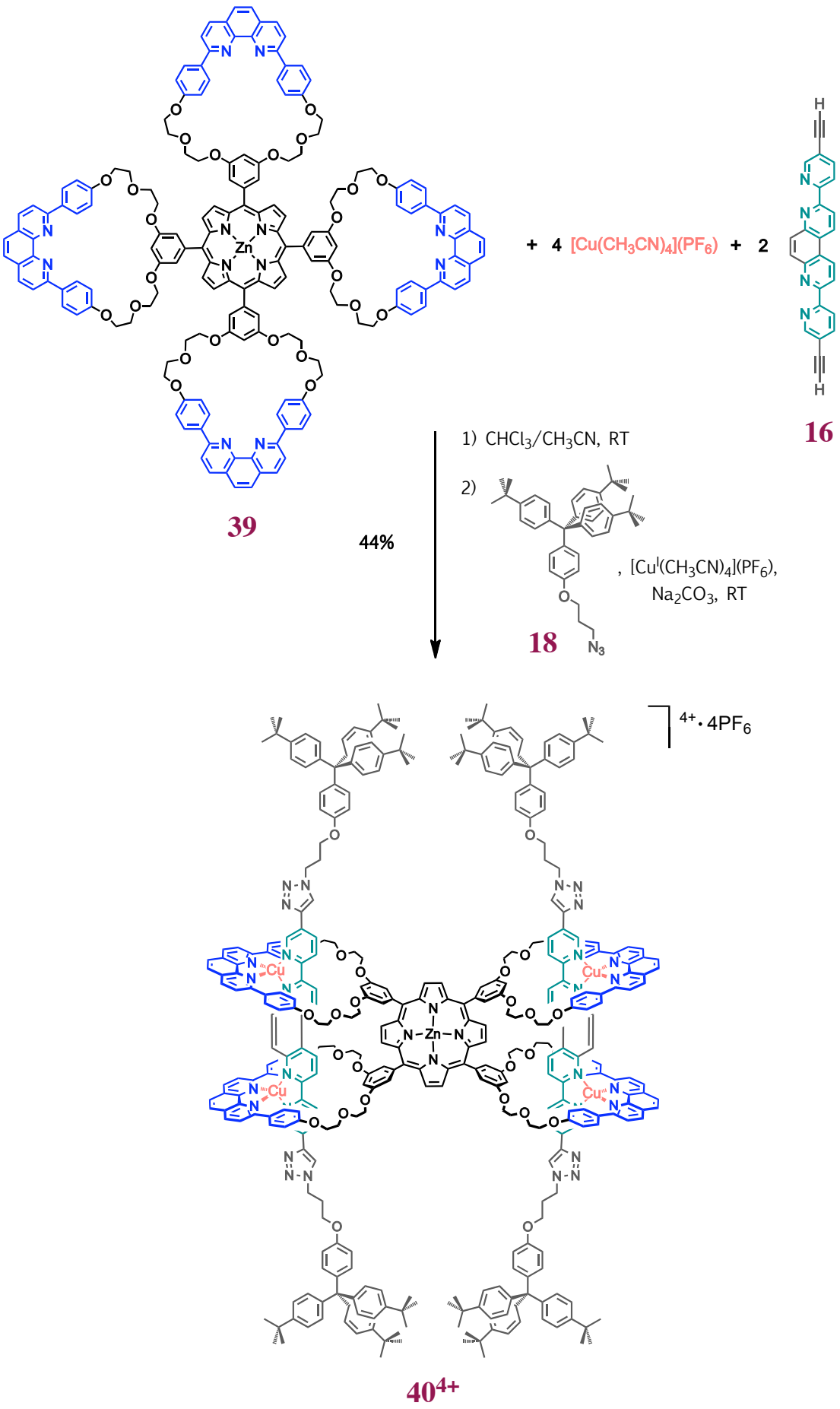

Figure V.6. Two-step, one-pot synthesis of rotaxane **40**$^{4+}$ by (1) formation of a [3]pseudorotaxane and (2) quadruple CuAAC stoppering reaction.

V. 2. b) HRES-MS Characterisation of the [3]Rotaxane

The [3]rotaxane $\mathbf{40^{4+}\cdot 4PF_6}$ was characterised by high resolution electrospray ionisation mass spectrometry (HRES-MS), ^{1}H NMR (1D, COSY, NOESY), ^{13}C NMR and UV-visible absorption spectroscopy. The mass spectrum gave the first proof of the formation of a [3]rotaxane. A largely major peak was observed at m/z = 1548.606 in high resolution ES-MS, in accordance with the calculated value for the [3]rotaxane complexed to four copper(I) centres at m/z = 1548.615 (**Figure V.7**). However, the m/z value does not enable to distinguish between the expected [6]rotaxane and the obtained [3]rotaxane. Indeed, the [6]rotaxane would have had twice the molecular mass and twice as many positive charges as the [3]rotaxane, which would have resulted in the same m/z value. Observation of the isotope profile is needed to discriminate between both multi-rotaxanes. The gap between signals observed in the experimental isotope profile is characteristic of a species bearing four positive charges. This gap would have been twice as small for a [6]rotaxane with eight Cu(I) centres. In a whole the experimental isotopic profile fits perfectly with the simulation (**Figure V.7**). Two minor peaks are also observed at m/z = 2043.501 and m/z = 2112.134 in the mass spectrum. Both peaks correspond to triply charged species according to their isotope profiles. Simulations showed that the peak at m/z = 2112.134 corresponds to [3]rotaxane $\mathbf{40^{4+}}$ with one PF_6^- counterion while the peak at m/z = 2043.501 corresponds to [3]rotaxane $\mathbf{40^{4+}}$ with one missing Cu(I) centre. Decomplexation of a copper ion probably occurred during the electrospray ionisation process. These ES-MS results are in agreement with the formation and isolation of the [3]rotaxane structure $\mathbf{40^{4+}}$.

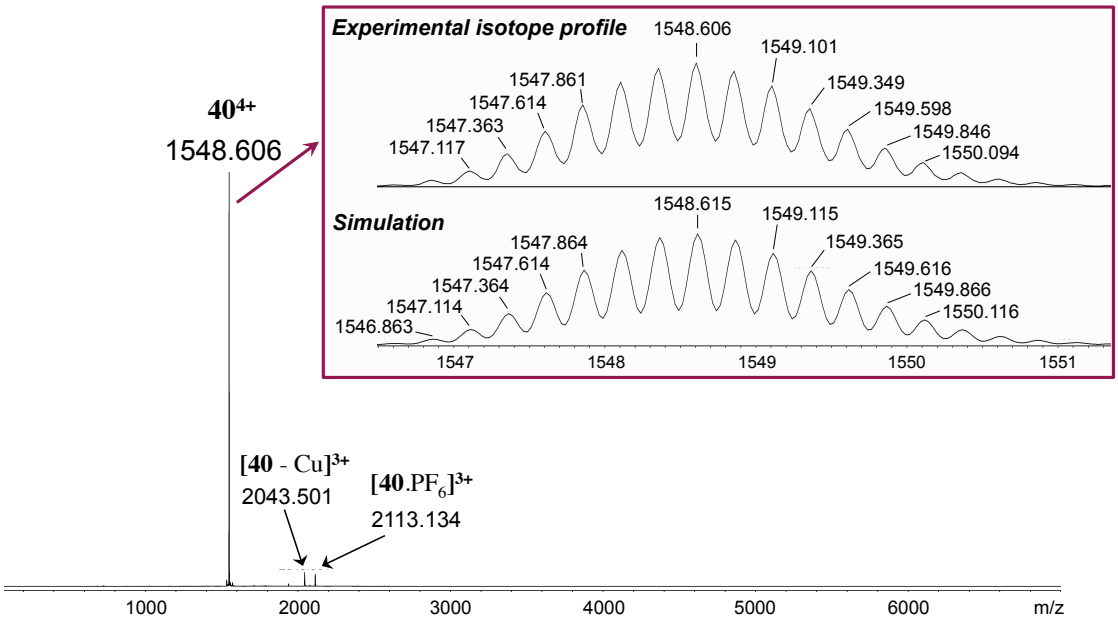

Figure V.7. HRES-MS spectrum of [3]rotaxane $\mathbf{40^{4+}}$ and isotope profile evidencing the 1:2 porphyrin/rod stoichiometry.

V. 2. c) NMR Characterisation of the [3]Rotaxane

The aromatic region of the ^{1}H NMR spectra of rotaxane **40**$^{4+}$, Zn-porphyrin **39** and rod **15** is presented in **Figure V.8**.

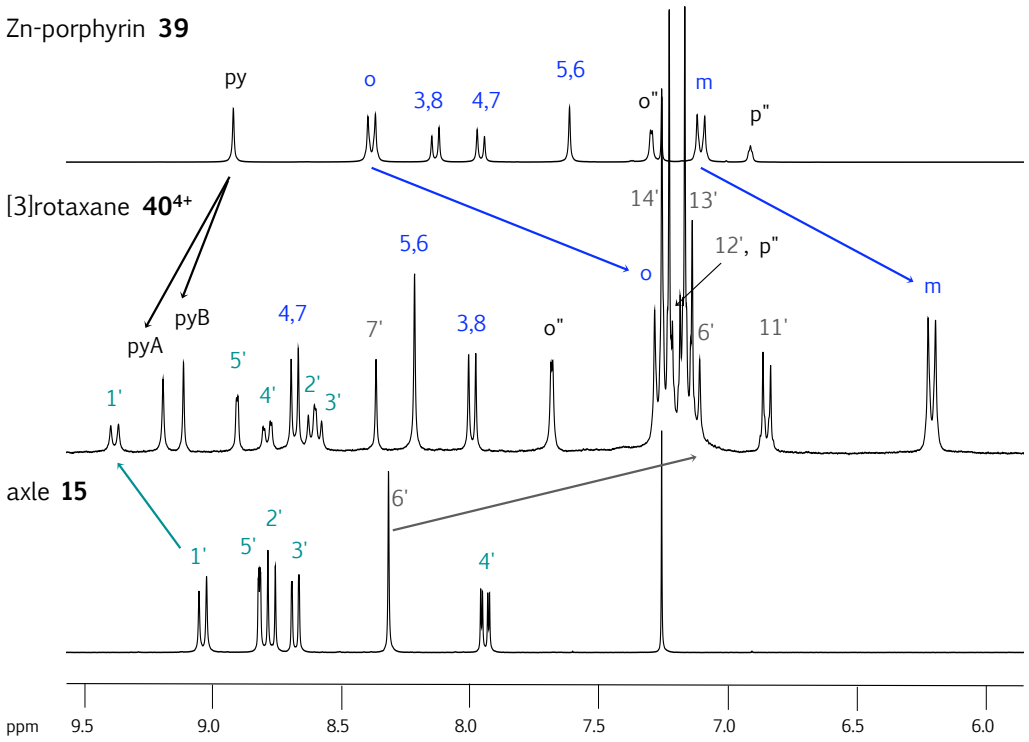

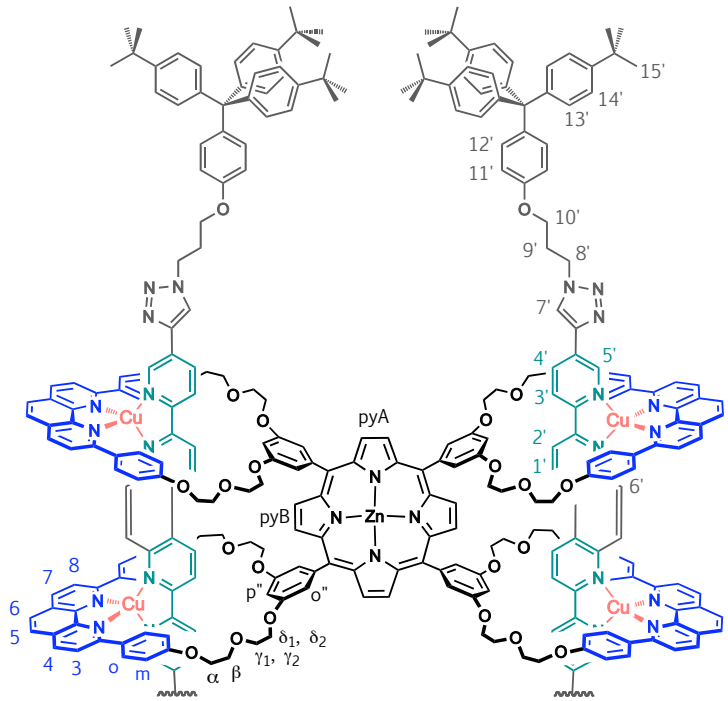

Figure V.8. ^{1}H NMR spectra of rotaxane **40**$^{4+}$, Zn-porphyrin **39** and rod **15**; signals in the aromatic region are displayed (top). NMR assignments of the [3]rotaxane **40**$^{4+}$ (bottom).

The interlocked structure of rotaxane **40**$^{4+}$ was confirmed by the characteristic upfield chemical shift of the aromatic o and m protons of the porphyrinic component **39** and of protons 6' of the rod component **16**. Downfield chemical shifts of protons 1' and 4' in rod **15** were also observed upon copper(I) complexation and threading. Furthermore, NOESY NMR showed NOE interactions between $H_{2'}$ and $H_{3'}$ from the rod and $H_{p''}$ belonging to the macrocycle. It also showed strong NOE interactions between $H_{1'}$ from the rod and H_{pyB} belonging to the porphyrin (**Figure V.9**). These observations are clear evidence that the two axles are threaded through the macrocycles of the porphyrin. The peak integrations corresponding to the zinc porphyrin and the rod in compound **40**$^{4+}$ support a 1:2 porphyrin/rod stoichiometry. Another characteristic feature of the [3]rotaxane is given by the signals of the pyrrolic protons of the porphyrin moiety. The pyrrolic protons were equivalent in compound **39** and appeared as a singlet at 8.92 ppm, whereas they are observed as two singlets at 9.20 and 9.12 ppm in the rotaxane. This splitting is consistent with the proposed chemical structure of rotaxane **40**$^{4+}$, where protons pyA and pyB experience different chemical environments.

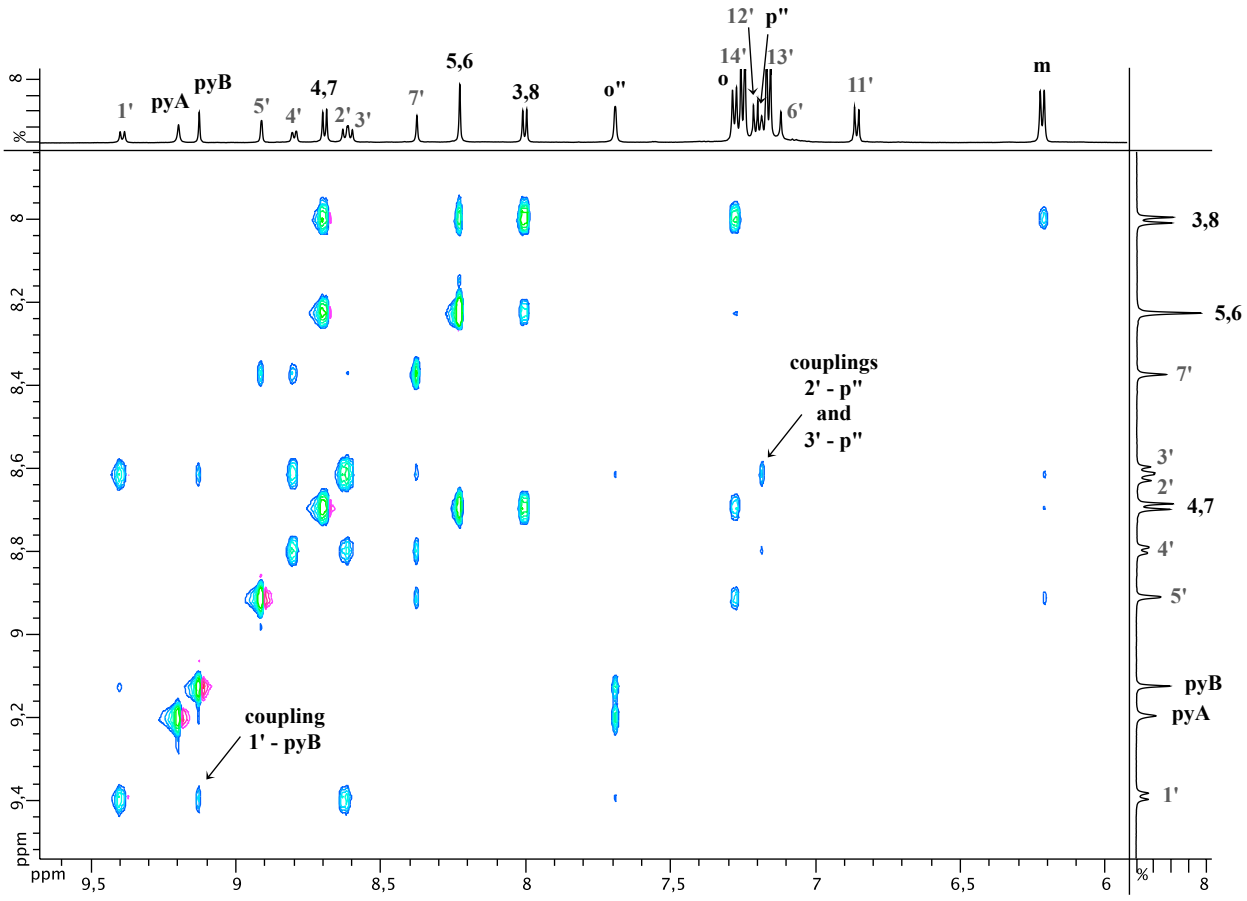

Figure V.9. Aromatic region of the ^{1}H-^{1}H NOESY (600 MHz) spectrum of rotaxane **40**$^{4+}$. NOE correlations between the rod and the tetra-macrocycle in the aromatic region are highlighted.

V. 2. d) UV-visible Characterisation of the [3]Rotaxane

The UV-visible absorption spectrum of free-base porphyrin **38** measured in dichloromethane shows a porphyrin Soret band at 421 nm and four Q bands at 515, 550, 588, and 645 nm in the visible region. In the case of the zinc porphyrin **39** the Soret band is observed at 424 nm and two Q bands are observed at 550 and 590 nm. The threading induces a 3 to 5 nm red shift of the B and Q bands with the Soret band appearing at 427 nm for [3]rotaxane $\mathbf{40}^{4+}$ (**Figure V.10**). It is noteworthy that a *bathochromic* shift is observed upon threading of the axles in this case, while a *hypsochromic* shift occurred in the case of the [4]rotaxane $\mathbf{19}^{4+}$ (Chapter III). The hypsochromic shift of $\mathbf{19}^{4+}$ was attributed to excitonic coupling between two face-to-face porphyrins, which can not occur in [3]rotaxane $\mathbf{40}^{4+}$ that contains a single porphyrin unit. The red shift observed here did not occur upon complexation of Cu(I) and threading of dap chelates through the rings of bis-macrocycle **8** to form the [3]pseudorotaxane $\mathbf{9}^{2+}$ (Chapter II). The absorption maxima were observed at 421, 548 and 585 nm for $\mathbf{9}^{2+}$, with no shift compared to the copper-free porphyrin precursor **8**. This seems to indicate that the MLCT absorbance of the Cu(I) complexes do not induce any shift of the absorption bands of the porphyrin. Consequently, the bathochromic shift observed in the present case is not likely to be due to the presence of the Cu(I) centres and might be the result of a distortion of the porphyrin in the [3]rotaxane.

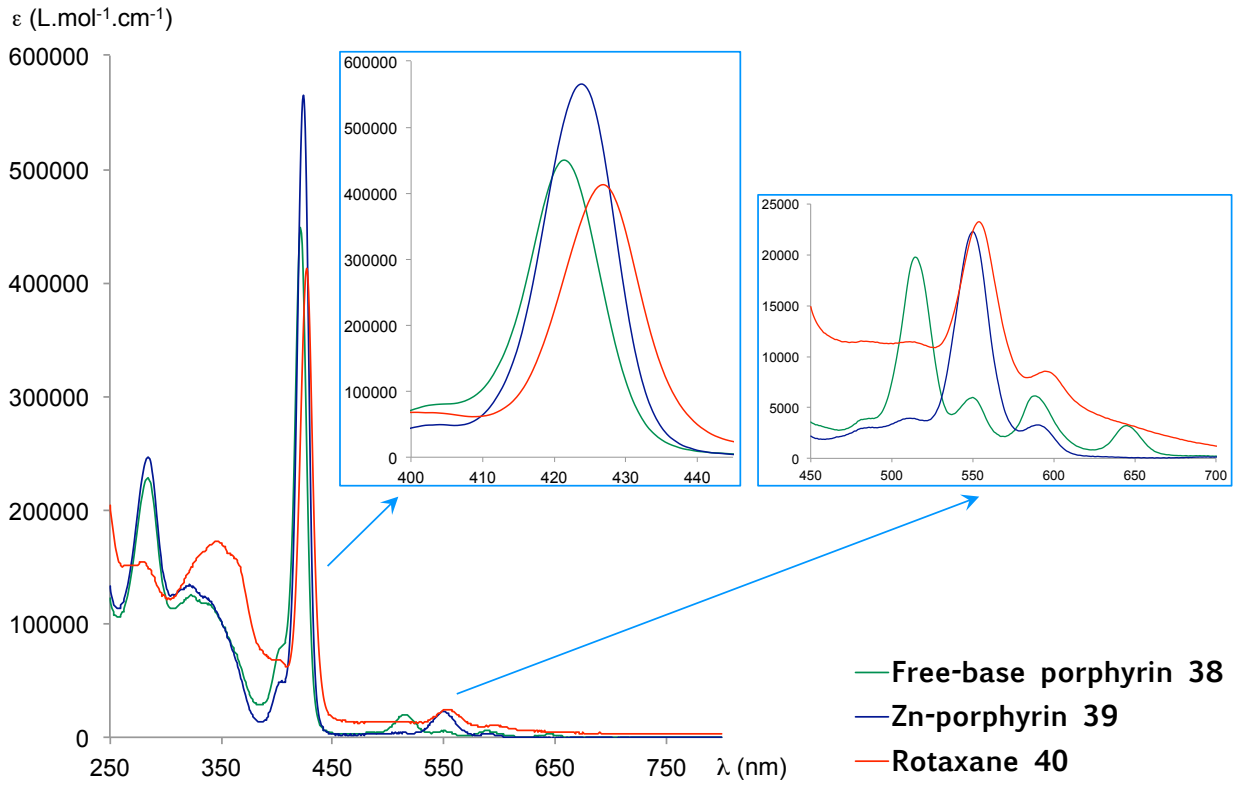

Figure V.10. UV-visible absorption spectra of free-base porphyrin **38**, Zn-porphyrin **39** and rotaxane $\mathbf{40}^{4+}$ in CH_2Cl_2.

In conclusion we synthesised and fully characterised a [3]rotaxane that consists of a zinc porphyrin component substituted with four coordinating macrocycles and of two dumbbell components. Each dumbbell is threaded through two adjacent rings of the porphyrin in a novel architecture. We then modified the design of the system with the aim of forming a [6]rotaxane.

V. 3. Towards a [6]Rotaxane: Design of a New Axle

V. 3. a) Strategy for the Formation of a [6]Rotaxane

After the description of a novel [3]rotaxane structure obtained from our new porphyrinic tetra-macrocycle, we decided to pursue our efforts towards the formation of a [6]rotaxane as described at the beginning of this chapter. The [6]rotaxane structure would be novel as well, and could present interesting host-guest properties.

Our strategy towards the formation of a [6]rotaxane composed of two porphyrinic tetra-macrocycles and four dumbbells is based on the use of porphyrin **39** as the tetra-macrocyclic component and of an axle that differs from axle **16** as the dumbbell precursor. We envisioned that the introduction of a longer spacer between the bidentate sites of the axle would force the system towards the formation of a [6]pseudorotaxane instead of a [3]pseudorotaxane in the threading step (**Figure V.11**). If the bidentate sites are far apart on the axle then the formation of tetrahedral copper(I) complexes with the phenanthroline sites of two adjacent rings of the porphyrin will not be possible. Consequently, the formation of a [3]pseudorotaxane will not be favoured because not all binding sites will be occupied. Other threaded assemblies allowing maximal occupancy of the binding sites will be thermodynamically favoured, and the [6]pseudorotaxane will most likely be the most stable interlocking species.

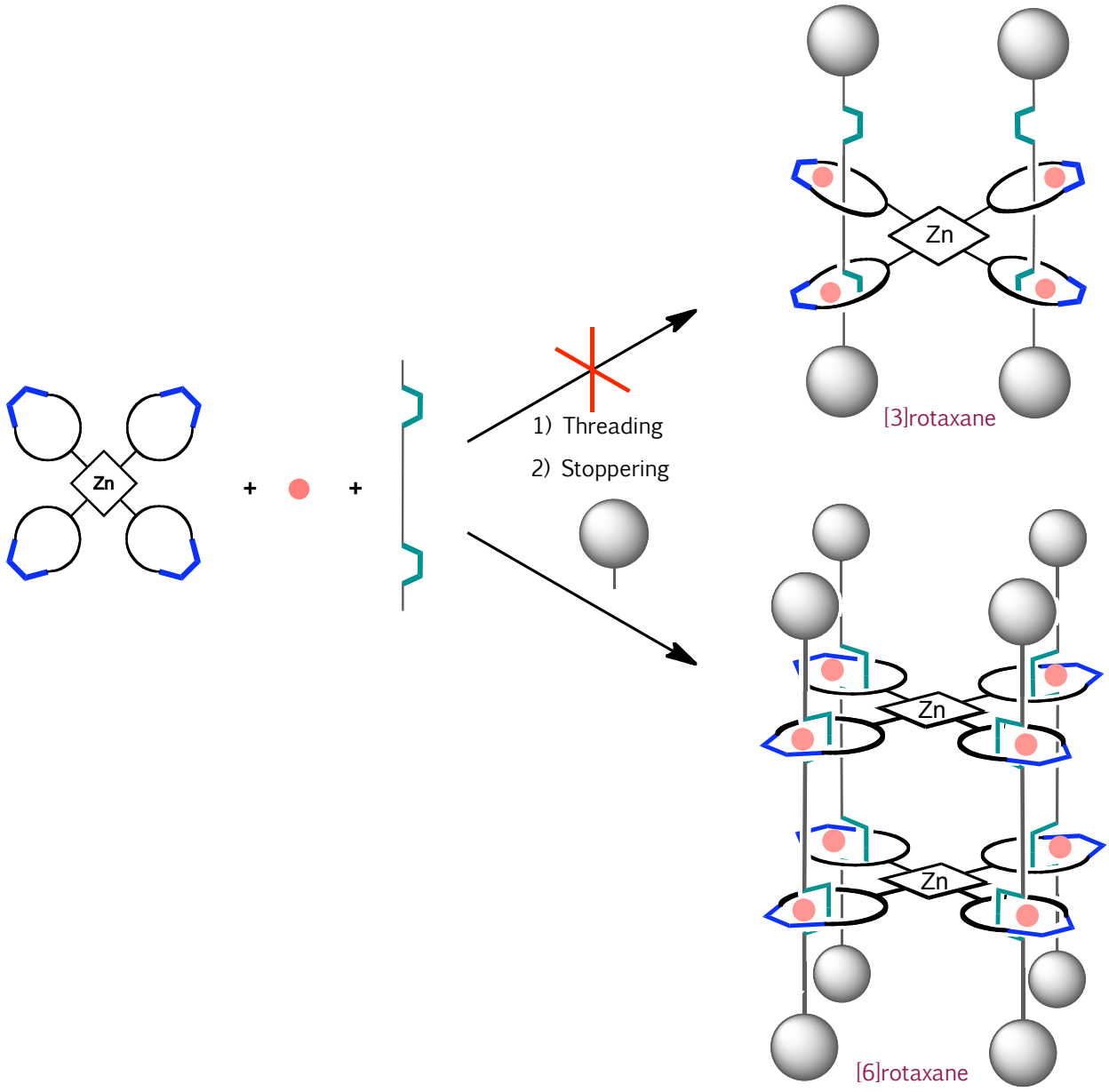

Figure V.11. Introduction of a longer spacer between the bidentate sites of the axle to avoid the formation of a [3]rotaxane and consequently favour the formation of a [6]rotaxane.

V. 3. b) Design of the Axle and First Results

As explained above, our strategy toward the construction of the desired [6]rotaxane structure relies on the synthesis of a new axle building block that incorporates a longer spacer between the bidentate chelates. This project forms part of a collaboration with **Nathan L. Strutt**, who was previously a student in the Sauvage group in Strasbourg and who is now a PhD candidate with J. F. Stoddart at Northwestern University. Nathan is carrying out the syntheses of the new axles and corresponding rotaxanes.

The chemical structures of rod **16** used in the previous studies and of the new target axles are depicted in **Figure V.12**. Rod **16** was very short with a single chemical bond between the bidentate sites. Several new rods with spacers of various lengths were then designed. The first target structure is composed of two 3,8-disubstituted-1,10-phenanthroline units separated by two phenylene rings (**Figure V.12**.b). The syntheses of the non-symmetrical phenanthroline precursors needed as intermediates for this rod proved difficult and low yielding. Therefore the synthesis of this rod was abandoned and new rods were designed.

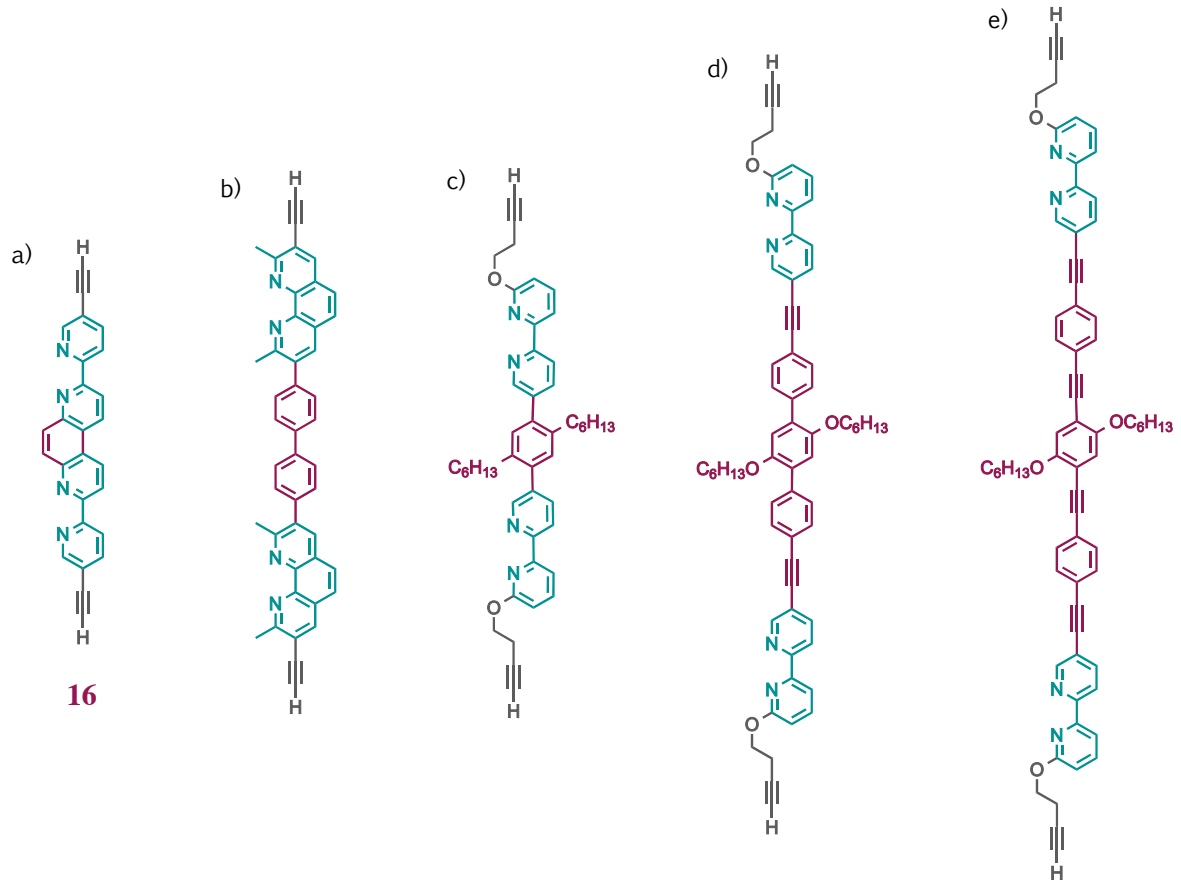

Figure V.12. Chemical structures of bis-bidentate molecular rods. a) Rod **16** used in the previous studies, with a very short spacer between the coordination sites. b) Design of a rod with two phenylene spacers, abandoned due to synthetic problems. c) New rod with one phenylene spacer. A threading test with a precursor of this rod gave the [3]pseudorotaxane. d) and e) Target structures of rods with very long spacers between the bidentate sites.

The phenanthroline chelates were replaced with 2,2'-bipyridine units in the new rods because these units can be more easily functionalised in a non-symmetrical way. The first bis-bipy rod contains one phenylene spacer substituted with hexyl chains to improve the solubility of the compound (**Figure V.12**.c). An intermediate in the synthesis of this rod is the bis-bipy

precursor substituted with two terminal methoxyl groups located in α position to the nitrogen atoms. This intermediate was used in a preliminary threading test with the porphyrinic tetra-macrocycle. However, only the [3]pseudorotaxane was observed in mass spectrometry and no trace of [6]pseudorotaxane was detected.

Subsequently, molecular modelling studies were performed with the Avogadro software. Structure minimisations using force-field calculations suggested that the porphyrinic tetra-macrocycle is flexible enough for the [3]pseudorotaxane to form upon threading of a rod that contains up to three phenylene spacers between the bidentate sites. Therefore, a linear spacer with more than three aryl rings is probably needed in order to favour the formation of the [6]pseudorotaxane. Two new rods were then designed; their target chemical structures are depicted in **Figure V.12**.d and e. Rod d contains three aryl and two alkyne groups as a spacer; molecular modelling shows that the formation of a [3]pseudorotaxane might still be possible with this rod but the system would be sterically constrained and the copper(I) complexes would most likely be distorted and destabilised. Rod e contains three aryl and four alkyne groups as a spacer. Threading of the rods and complexation with the Cu(I) template into a [3]pseudorotaxane structure would not be possible with this rod according to the molecular model. Consequently, these last two rods appear to be good candidates for the formation of a [6]rotaxane; they will be synthesised and tested in the near future.

In conclusion, we prepared a tetra-substituted porphyrin bearing macrocycles at its four *meso* positions. A large variety of experimental conditions were explored to prepare the free-base porphyrin, which gradually led to a remarkable improvement of the yield. Under the best experimental conditions, a 25% yield was obtained, affording the desired compound at the 0.1 g scale. More generally, the reaction conditions developed here could be useful for the synthesis of porphyrins incorporating polypyridine chelates or other polydentate ligands.

In a copper(I)-driven multi "gathering-and-threading" step followed by a stoppering reaction, a [3]rotaxane was obtained in good yield. The structure of this [3]rotaxane is novel: it consists of two dumbbell components, each of them threaded through two adjacent rings of a central porphyrinic tetra-macrocycle. The synthesis principle described in this chapter should be generalised in the future so as to afford related porphyrinic multi-rotaxanes displaying several possible geometries, in relation to molecular machines and receptors. The design and synthesis of a new axle for the elaboration of a [6]rotaxane is under way in a collaboration with Nathan Strutt and Fraser Stoddart. As well as a novel architecture, the target [6]rotaxane should display interesting properties as a molecular receptor. The formation of other types of interlocked structures can also be envisaged from our new porphyrinic tetra-macrocycle. For example, the extremities of the rods could be joined in the [3]pseudorotaxane formed by threading of axle **16** through the rings of porphyrin **39**. This would result in the formation of a [2]catenane composed of one large ring threaded through all four rings of the porphyrinic tetra-macrocycle (**Figure V.13**).

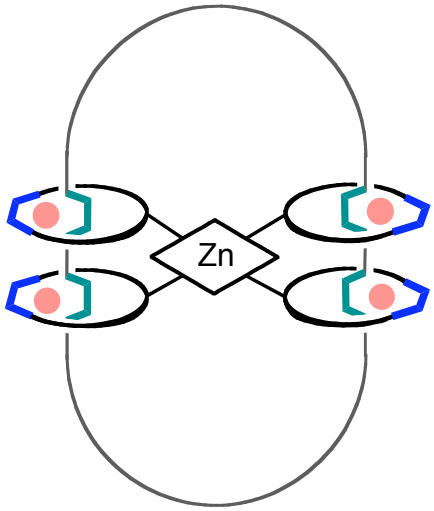

Figure V.13. Schematic view of a new topologically interesting [2]catenane. This type of structure could be obtained by junction of the axle ends of the [3]pseudorotaxane resulting from threading of rods **16** with tetra-macrocycle **39**.

Conclusion

The work presented in this thesis focuses on the design of multiply interlocking assemblies and molecular receptors. The features and properties of the porphyrin core and of the rotaxane structure were exploited and combined in the elaboration of novel porphyrin-based multi-rotaxanes, whose syntheses constitute interesting challenges. New porphyrinic multi-macrocycles and the corresponding [3]- and [4]rotaxanes were obtained and fully characterised, and the host-guest properties of the [4]rotaxane were studied. The synthesis of a new bis-macrocyclic system is under way. This last system was designed to be a better molecular press model, which should be able to change the conformation of a guest substrate by compression.

The design of the systems presented here involved the incorporation of bidentate ligands in the building blocks and the use of the "gathering-and-threading" effect of copper(I) to interlace the components into rotaxane structures. The syntheses of three rotaxane building blocks were described first. A bis-bidentate molecular thread (or axle), a stopper and a new zinc(II) porphyrin linked to two dpp-containing rings were prepared. The molecular thread and stopper were needed as precursors of the "dumbbell" part of the rotaxanes. The new porphyrinic bis-macrocycle contains two rings linked to antipodal *meso* positions of a Zn-porphyrin *via* single C-C bonds. It was obtained in good yield by [2+2] MacDonald condensation of mesityldipyrrylmethane with a new aldehyde-functionalised macrocyclic precursor. This precursor, whose structure was confirmed by X-ray diffraction crystallography, was later used in the synthesis of a porphyrin substituted with four lateral rings. The ability of the porphyrinic bis-macrocycle to form threaded assemblies was tested *via* the formation of a prototypical [3]pseudorotaxane. Complexation with copper(I) and two dap chelates led to the quantitative formation of a doubly threaded species as expected.

A new copper(I)-complexed [4]rotaxane was obtained in good yield from the porphyrinic bis-macrocycle, molecular axle and stopper described above. The building blocks were assembled in a two-step, one-pot reaction involving *(i)* Cu(I)-templated formation of a [4]pseudorotaxane and *(ii)* quadruple CuAAC stoppering reaction. The [4]rotaxane has a *very flexible structure* and contains two central face-to-face Zn-porphyrins. Detailed NMR studies suggested that the rotaxane adopts an asymmetrical, twisted geometry in dichloromethane

solution. Observation of an excitonic coupling confirmed the cofacial arrangement of the metalloporphyrins, which form an internal cavity suitable for complexation of guest substrates. Indeed, host-guest studies with linear ditopic nitrogen ligands showed that the rotaxane is a good molecular receptor. Rigid guests substrates of various lengths were tested, and high association constants were observed in all cases. The complexation of 2.6 to 15.8 Å-long rod-like guests within the internal cavity attests the exceptional adaptability of the rotaxane, which can adjust its shape to the size of the guest substrate. The [4]rotaxane can be described as a *distensible molecular receptor*, which can adopt an "inflated" or a "deflated" conformation depending on the guest. Complexation with chiral diamines could be attempted in the future. Chirogenesis could be observed upon binding of a chiral guest, which would make the rotaxane host a good chiral sensor for this type of molecules. The photophysical properties of the [4]rotaxane could also be studied.

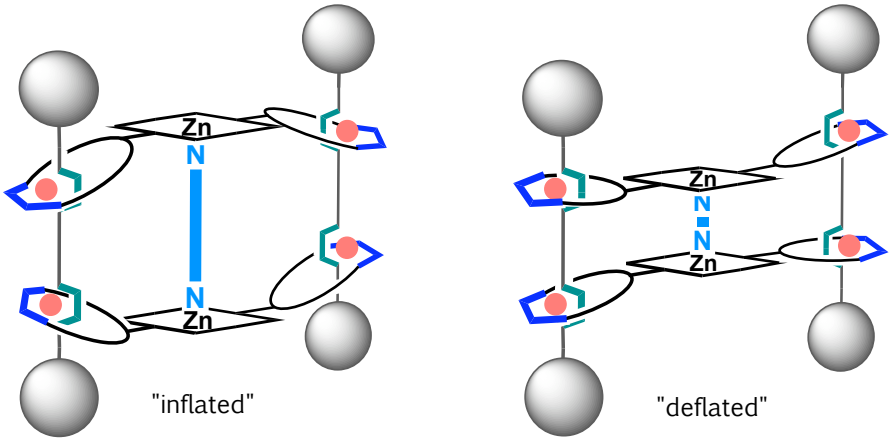

A new porphyrinic bis-macrocycle was then designed towards the formation of a more rigid [4]rotaxane host. An aromatic bridge will be introduced between the porphyrin moiety and the macrocycles to lock the rings in a coplanar orientation to the porphyrin core. The resulting [4]rotaxane would be less adaptable than that described above. The complexation of flexible guest molecules and the impact of the [4]rotaxane host on the conformation of the guest could be tested to check if the host acts as a molecular press. Several synthetic routes were envisaged for the formation of the new target bis-macrocycle. Difficulties were faced with some of the synthetic steps, and the synthesis of the target molecule is still in progress. However, the latest results are encouraging, and interesting macrocyclic intermediates could be obtained. Only two more steps should be required to obtain the desired extended porphyrin. In the future, the formation of the corresponding [4]rotaxane could be tested, and its receptor properties could be studied. Comparative host-guest studies between the copper-free rotaxane and the copper(I)-

complexed rotaxane could be performed to assess the ability of the host to "compress" guest substrates upon complexation with Cu(I). We could then envisage to replace one of the zinc(II) centres with another metal, which would enable the axial coordination of oxygen ligands (*e.g.* tin(IV)). The rotaxane would then be a host for amino acids and small peptides. The ability of the rotaxane to change the conformation of a peptide guest would make it a new synthetic prototype of a chaperone protein.

Finally, a porphyrinic tetra-macrocycle was designed and synthesised from the aldehyde-functionalised macrocyclic precursor used in the first study. In this new structure the central porphyrin is linked to lateral dpp-containing rings at its four *meso* positions. While the classical porphyrin condensation conditions afforded the desired tetra-substituted porphyrin in very poor amounts, optimisation of the reaction conditions led to a significant increase of the yield. The optimised conditions are derived from the Adler-Rothemund method; we showed that the combined use of nitrobenzene as a cosolvent and of microwave activation favoured the formation of the porphyrin product. More generally, the condensation conditions developed here could prove useful for the synthesis of other porphyrins substituted with polydentate ligands. A multiply-interlocked, copper(I)-complexed [3]rotaxane was obtained by threading of bis-bidentate axles through the rings of the porphyrinic tetra-macrocycle, followed by stoppering. The structure of this rotaxane is novel: it contains two dumbbell components, each of them threaded through two adjacent rings of the central porphyrin unit. The formation of this [3]rotaxane attests the remarkable flexibility of the tetra-macrocyclic precursor, whose dpp chelates can rotate in relation to the plane of the porphyrin to allow the threading of axles through neighbouring rings. Future work could deal with the synthesis of a novel [2]catenane structure from the porphyrinic tetra-macrocycle. Instead of clicking stoppers to the [3]pseudorotaxane precursor, the ends of the axles could be joined *via* an appropriate spacer, forming a large ring threaded through all four rings of the porphyrinic tetra-macrocycle. The design and synthesis of longer axles is also under way in a collaboration with Nathan Strutt and Fraser Stoddart at Northwestern University. The formation of a [6]rotaxane is expected after threading with the tetra-macrocycle. This novel structure could exhibit interesting molecular receptor properties.

Experimental Part

General

Dry CH_2Cl_2, $CHCl_3$ and CH_3CN were distilled from CaH_2 as drying agent. Dry toluene and THF were distilled over sodium and benzophenone. Commercial chemicals were at the best available grade and used without further purification, except pyrrole. Pyrrole was passed through a plug of alumina immediately prior to use. $[Cu(CH_3CN)_4](PF_6)$ was purified according to a literature procedure.[305] Preparative column chromatography was carried out using silica gel (Merck Kieselgel, silica gel 60, 0.063-0.200 mm), neutral alumina (Merck aluminium oxide 90, 0.063-0.200 mm), or size-exclusion Biobeads S-X1 support (Bio-Rad).

NMR spectra for ^1H were acquired on Bruker AVANCE 600, 500, 400 or 300 MHz or on Bruker AC-200 (200 MHz) spectrometers. The spectra were referenced to residual proton-solvent references (CD_2Cl_2 at 5.32 ppm (^1H) and 53.84 ppm (^{13}C); $CDCl_3$ at 7.26 ppm (^1H) and 77.16 ppm (^{13}C); DMSO-d_6 at 2.50 ppm (^1H) and 39.52 ppm (^{13}C)). In the assignments, the chemical shift (in ppm) is given first, followed, in brackets, by the multiplicity of the signal (s, singlet; d, doublet; t, triplet; ; q, quintuplet; dd, doublet of doublets; m, multiplet; br, broad signal), the value of the coupling constants in Hz if applicable, the number of protons implied and finally the assignment. Mass spectra (ES-MS) were recorded on a Bruker MicroTOF spectrometer by the Service de Spectrométrie de Masse (Université de Strasbourg). UV-visible absorption spectra were recorded with a Kontron Instruments UVIKON 860 spectrometer at 21°C with a 1 cm path cell. Titration spectra were measured in 0.92 x 10^{-6} M toluene solutions of rotaxane **19**$^{4+}$. Guest solutions (2.8 x 10^{-5} M) were added to the rotaxane sample in 10 μL (0.1 equivalent) aliquots using a 100 μL Hamilton syringe. UV-visible spectrophotometric titrations were analyzed by fitting the series of spectra at 1 nm intervals by using the SPECFIT/32 3.0 software (Spectrum Software Associates), which takes into account the changes in volume during the titration.[306] Emission spectra were recorded using a Fluorolog FL3-22 de HORIBA Jobin Yvon spectrophotometer. Lifetime measurements were detected by a TCSPC (time-correlated single-photon counting) technique with a NanoLED-370 electroluminescent diode as the excitation source. X-ray diffraction studies were performed by Dr. Lydia Brelot, Service de Radiocristallographie (Université de Strasbourg). CCDC-823860 contains the supplementary crystallographic data for macrocycle **5**. These data can be obtained free of charge from The Cambridge Crystallographic Data Centre via www.ccdc.cam.ac.uk/data_request/cif.

2,9-Dianisyl-1,10-phenanthroline (dap) 1 [198,199]

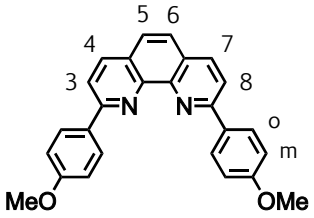

A solution of 4-bromoanisole (10 mL, 80 mmol) in dry THF (100 mL) was degassed with argon and cooled down to -78 °C. A 1.6 M solution of BuLi in hexanes (100 mL, 0.16 mol) was added dropwise. The reaction mixture was then stirred for 3 h at - 78 °C under argon. It was allowed to warm up to -10 °C, then transferred by cannula to a solution of pre-dried 1,10-phenanthroline (5.8 g, 32 mmol) in 150 mL of dry, degassed toluene at 0 °C. The reaction mixture was allowed to warm up to room temperature and stirred under argon for 20 hours. The solution was hydrolysed with 50 mL of water. After evaporation of the solvents the solid was dissolved in CH_2Cl_2 (250 mL) and washed three times with water (250 mL). The organic layer was rearomatised by successive additions of MnO_2 under effective magnetic stirring The rearomatisation was followed by TLC and disappearance of the yellow colour, and was ended after addition of 60 g MnO_2. The mixture was dried over $MgSO_4$ and filtered on Celite. The solvent was evaporated and the solid was recrystallised from hot toluene. Final purification was achieved by silica column chromatography using dichloromethane/methanol (100:1) as eluent to yield 6.7 g of dap **1** (53%) as a pale yellow solid.

^{1}H NMR (300 MHz, $CDCl_3$): δ = 8.44 (d, ^3J = 8.7 Hz, 4H, H_o), 8.26 (d, ^3J = 8.4 Hz, 2H, $H_{3,8}$), 8.09 (d, ^3J = 8.4 Hz, 2H, $H_{4,7}$), 7.74 (s, 2H, $H_{5,6}$), 7.12 (d, ^3J = 8.7 Hz, 4H, H_m), 3.93 ppm (s, 6H, OMe).

2,9-Diphenol-1,10-phenanthroline (dpp) 2 [198,199]

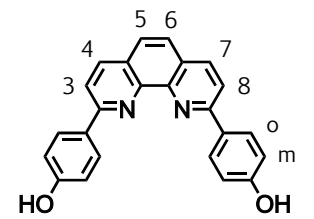

Anhydrous pyridine (10.2 mL) was placed in a 50 mL three-necked round-bottomed flask fitted with a thermometer and a magnetic stirrer. With rapid stirring concentrated hydrochloric acid (11.2 mL) was added. The flask was equipped for distillation, and water was distilled from the mixture until its internal temperature rose to 210 °C. After cooling to 140 °C, dap **1** (4.00 g, 10.2 mmol) was added as a solid and the reaction flask was fitted with a reflux condenser

connected to a source of argon. The yellow mixture was stirred and refluxed for three hours (200-220 °C). The reaction mixture was allowed to cool to 120 °C, diluted with 15 mL of warm water and slowly poured into 75 mL of warm water. The resulting bright yellow suspension was refrigerated overnight. After cooling, the precipitated solid was filtered by suction, and washed with cold water. Crude acidic diphenol **2** was suspended (it dissolves partially) in an ethanol-water mixture (75 mL/50 mL) and neutralised with a dilute NaOH solution to pH = 7. The solution was diluted with hot water (300 mL), and neutral **2** precipitated as a beige solid upon cooling. The precipitate was filtered off and dried overnight to yield 3.53 g of dpp **2** (95%) as a red solid, which could be used without further purification.

^{1}H NMR (200 MHz, DMSO-d_6): δ = 8.38 (d, ^3J = 8.6 Hz, 2H, $H_{3,8}$), 8.30 (d, ^3J = 8.6 Hz, 4H, H_o), 8.19 (d, ^3J = 8.6 Hz, 2H, $H_{4,7}$), 7.82 (s, 2H, $H_{5,6}$), 6.92 (d, ^3J = 8.6 Hz, 4H, H_m).

Dpp diol 3 [200]

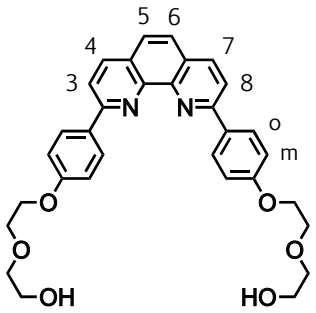

2,9-Diphenol-1,10-phenanthroline **2** (2.20 g, 6.04 mmol) was added to a suspension of Cs_2CO_3 (5.90 g, 18.1 mmol) in DMF (220 mL) under argon. 2-(2-chloroethoxy)ethanol (3.2 mL, 30 mmol) was then added and the mixture was stirred at 90 °C under argon. After 12 h, 0.64 mL of 2-(2-chloroethoxy)ethanol were added. The solution was stirred at 90 °C for 4 h. After filtration and evaporation of the solvent, the remaining solid was dissolved in dichloromethane/methanol 1:1 (500 mL). The solution was washed with water (3 × 500 mL). The organic layer was dried over Na_2SO_4 and concentrated in vacuo. The product was purified by column chromatography on silica with dichloromethane/methanol (100:2) to yield the diol **3** as a yellow solid (3.04 g, 93%).

^{1}H NMR (300 MHz, $CDCl_3$): δ = 8.43 (d, ^3J = 9.0 Hz, 4H, H_o), 8.27 (d, ^3J = 8.7 Hz, 2H, $H_{3,8}$), 8.09 (d, ^3J = 8.7 Hz, 2H, $H_{4,7}$), 7.75 (s, 2H, $H_{5,6}$), 7.14 (d, ^3J = 9.0 Hz, 4H, H_m), 4.27 (t, ^3J = 4.5 Hz, 4H, CH_2), 3.94 (t, ^3J = 4.5 Hz, 4H, CH_2), 3.81 (m, 4H, CH_2), 3.72 ppm (m, 4H, CH_2).

Ditosylate 4 [200]

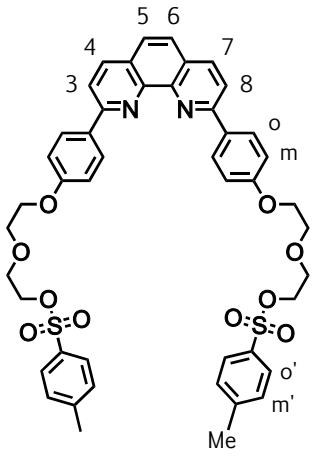

The diol **3** (3.04 g, 5.62 mmol) was partly dissolved in dry dichloromethane (200 mL). The solution was cooled to 0 °C in an ice-bath under argon. Triethylamine (4.7 mL, 34 mmol) and DMAP (4-dimethylaminopyridine) (56 mg, 0.46 mmol) were added to the cooled mixture. Tosyl chloride (4.68 g, 24.6 mmol) was slowly added. The solution was stirred under argon at 0°C for 2 h, then at room temperature for 12 h. Additional 1.07 g of tosyl chloride were added to the reaction mixture and the solution was stirred at room temperature overnight. The solution was then poured onto a mixture of ice (200 g) and HCl (1% aq., 50 mL). The aqueous layer was neutralised to pH 7 with aqueous NaOH. The organic layer was separated and the aqueous layer was washed with dichloromethane (2 × 250 mL). The organic layers were combined, washed with water (200mL), and dried with Na_2SO_4. The solvent was removed in vacuo. The resulting yellow oil was subjected to silica gel chromatography using dichloromethane/methanol (100:1) as an eluent to yield the ditosylate **4** (4.29 g, 90%) as a yellow solid.

^{1}H NMR (300 MHz, $CDCl_3$): δ = 8.41 (d, ^3J = 8.7 Hz, 4H, H_o), 8.28 (d, ^3J = 8.4 Hz, 2H, $H_{3,8}$), 8.09 (d, ^3J = 8.4 Hz, 2H, $H_{4,7}$), 7.81 (d, ^3J = 8.4 Hz, 4H, $H_{o'}$), 7.75 (s, 2H, $H_{5,6}$), 7.31 (d, ^3J = 8.1 Hz, 4H, $H_{m'}$), 7.09 (d, ^3J = 9.0 Hz, 4H, H_m), 4.22 (t, ^3J = 4.8 Hz, 4H, CH_2), 4.16 (t, ^3J = 4.5 Hz, 4H, CH_2), 3.84 (t, ^3J = 4.8 Hz, 4H, CH_2), 3.79 (t, ^3J = 4.8 Hz, 4H, CH_2), 2.40 ppm (s, 6H, Me).

m-31 Macrocycle 5

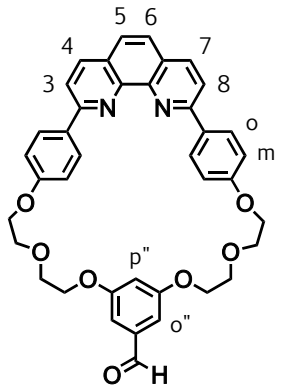

A solution of the ditosylate phenanthroline derivative **4** (4.18 g, 4.92 mmol) and 3,5-dihydroxybenzaldehyde (0.680 g, 4.92 mmol) in DMF (400 mL) was degassed, transferred to an addition funnel, and added dropwise to a suspension of Cs_2CO_3 (8.02 g, 24.6 mmol) in DMF (600 mL) over a period of 4 h. The mixture was then heated to 60 °C and stirred under argon for 16 h. The warm mixture was filtered and the solid residue was washed with DMF (100 mL). After evaporation of the solvent, the remaining solid was dissolved in dichloromethane (300 mL), washed with water (3 × 300mL) and dried over Na_2SO_4. The organic layer was evaporated, and the crude product was purified by silica gel chromatography in dichloromethane/methanol (100:1) to yield the macrocycle **5** as a pale yellow solid (2.10 g, 67%).

^{1}H NMR (300 MHz, $CDCl_3$): δ = 9.84 (s, 1H, aldehyde H), 8.41 (d, ^3J = 9.0 Hz, 4H, H_o), 8.26 (d, ^3J = 8.4 Hz, 2H, $H_{3,8}$), 8.07 (d, ^3J = 8.4 Hz, 2H, $H_{4,7}$), 7.75 (s, 2H, $H_{5,6}$), 7.14 (d, ^3J = 9.0 Hz, 4H, H_m), 7.03 (d, ^4J = 2.4 Hz, 2H, $H_{o"}$), 6.91 (t, ^4J = 2.3 Hz, 1H, $H_{p"}$), 4.32-4.36 (m, 4H, CH_2), 4.20-4.23 (m, 4H, CH_2), 3.93-3.97 ppm (m, 8H, CH_2). **ES-MS**: calcd for $C_{39}H_{35}N_2O_7$ [**5**+H]$^+$ 643.24; found 643.25. **Elemental analysis**: $C_{39}H_{34}N_2O_7 \cdot 0.5H_2O \cdot CH_2Cl_2$ (736.64): calcd. C 65.22, H 5.07, N 3.80; found C 65.38, H 5.05, N 3.56.

5-Mesityldipyrrylmethane 6 [207]

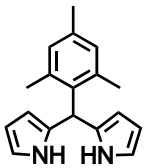

Pyrrole (10 mL, 0.14 mol) and mesitylaldehyde (0.85 mL, 5.7 mmol) were added to a dry round-bottomed flask and degassed with a stream of Ar for 5 min. Ceric ammonium nitrate (0.31 g, 0.57 mmol) was added, and the solution was stirred under Ar at room temperature for 25 min. Ethyl acetate (20 mL) was then added, and the reaction was quenched by neutralisation with 0.1 M NaOH. The organic phase was washed with water (2 × 25 mL) and dried with

Na_2SO_4. The solvent was evaporated to yield a dark green oil. The crude product was purified by flash column chromatography (petroleum ether/ethyl acetate/triethylamine, 80 : 20 : 1). Removal of the solvent under vacuum gave a solid that was washed with cold cyclohexane to dissolve the green impurities. The product was dried overnight to give 5-mesityldipyrrylmethane **6** (0.41 g, 27%) as an off-white solid.

^{1}H NMR (300 MHz, $CDCl_3$): δ = 8.01 (br s, 2H, H_{NH}), 6.87 (s, 2H, H_m), 6.65 (m, 2H, H_{py}), 6.12 (m, 2H, H_{py}), 5.92 (m, 2H, H_{py}), 5.91 (s, 1H, H_{meso}), 2.27 (s, 3H, Me_p), 2.06 ppm (s, 6H, Me_o).

Free-base porphyrin bis-macrocycle 7

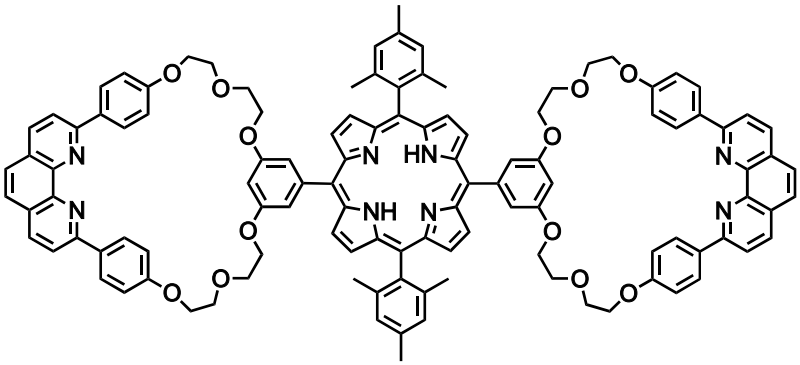

To a solution of the macrocyclic aldehyde **5** (313 mg, 0.487 mmol) in dry dichloromethane (50 mL) was added trifluoroacetic acid (181 µL, 2.44 mmol) and 5-mesityldipyrrylmethane **6** (135 mg, 0.511 mmol). The flask was protected from light and the solution was stirred for 2 h under argon. DDQ (2,3-dichloro-5,6-dicyanobenzoquinone) (177 mg, 0.779 mmol) was added and the solution was stirred under argon for an additional hour. A solution of Na_2CO_3 (1.0 g) in water (50 mL) was added and the solution was stirred vigorously for 30 min. The two phases were separated and the aqueous layer was washed twice with dichloromethane. The organic solvents were evaporated and the compound was purified by silica gel chromatography using dichloromethane/methanol (100:0.5) as eluent. Complete purification of the product at this stage was difficult, so the partially purified free-base porphyrin (109 mg) was directly metalated.

Zinc porphyrin bis-macrocycle 8

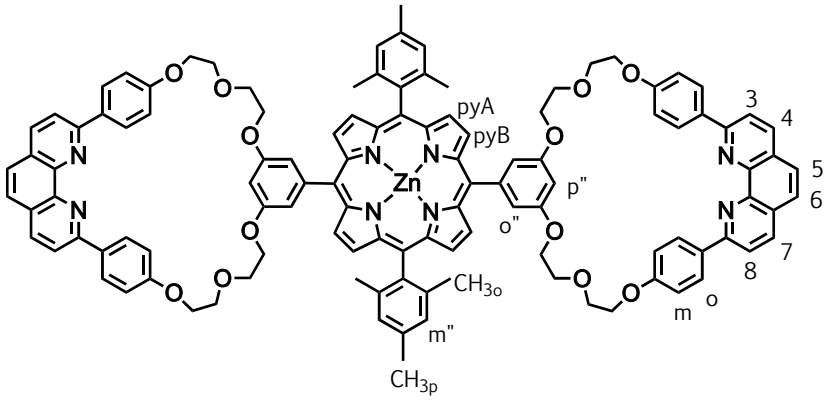

The partially purified free-base porphyrin **7** (109 mg) was dissolved in chloroform (95 mL) and a saturated solution of $Zn(OAc)_2.2H_2O$ in methanol (5 mL) was added. The mixture was refluxed for 5 h. The solvent was evaporated and the resulting solid was purified by alumina column chromatography with dichloromethane as eluent. The product was dissolved in CH_2Cl_2 (100 mL) and treated with an aqueous solution of Na_4EDTA (0.02 M, 100 mL). The biphasic mixture was vigorously stirred for 24 hours at room temperature. The organic layer was separated, washed three times with water. After evaporation, compound **8** was obtained as a purple solid (84 mg, 19%).

^{1}H NMR (300 MHz, CD_2Cl_2): δ = 8.92 (d, ^3J = 4.7 Hz, 4H, H_{pyA}), 8.67 (d, ^3J = 4.6 Hz, 4H, H_{pyB}), 8.45 (d, ^3J = 8.8 Hz, 8H, H_o), 8.28 (d, ^3J = 8.4 Hz, 4H, $H_{3,8}$), 8.08 (d, ^3J = 8.4 Hz, 4H, $H_{4,7}$), 7.77 (s, 4H, $H_{5,6}$), 7.42 (d, ^4J = 2.4 Hz, 4H, $H_{o"}$), 7.20 (d, ^3J = 8.8 Hz, 8H, H_m), 7.19 (s, 4H, $H_{m"}$), 7.04 (t, ^4J = 2.4 Hz, 2H, $H_{p"}$), 4.31 (m, 16H, OCH_2), 3.91 (m, 16H, OCH_2), 2.58 (s, 6H, CH_{3p}), 1.75 (s, 12H, CH_{3o}) ppm. **ES-MS**: calcd for $C_{114}H_{97}N_8O_{12}Zn$ (**8** + H^+) 1833.65; found 1833.51. **UV-visible absorption** (CH_2Cl_2) : λ_{max} (logε) = 421 (5.76), 549 (4.37), 585 (3.63) nm.

[3]Pseudorotaxane 9^{2+}

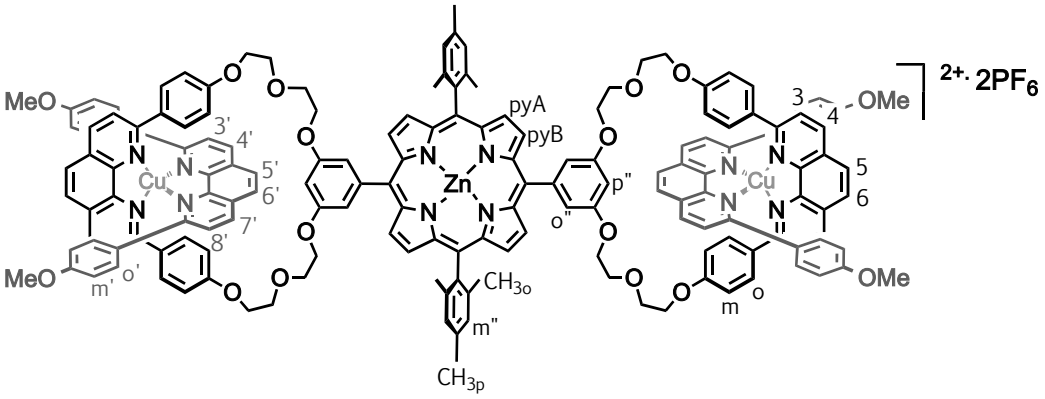

A degassed solution of $[Cu(MeCN)_4](PF_6)$ (5.15 mg, 13.8 μmol) in CH_3CN (3 mL) was added by cannula to a degassed suspension of zinc porphyrin **8** (12.2 mg, 6.65 μmol) in CH_2Cl_2

(10 mL), and the resulting deep red solution was stirred under argon for 30 min. A degassed solution of 2,9-dianisyl-1,10-phenanthroline **1** (5.42 mg, 13.8 μmol) in CH_2Cl_2 (5 mL) was then added by cannula. After stirring for 3 h at room temperature, the solvent was evaporated. The solid was dissolved in acetonitrile and the solution was filtered. The solvent was then evaporated to dryness giving the pseudorotaxane $\mathbf{9^{2+}}.2PF_6$ as a purple solid in quantitative yield (18.0 mg).

^{1}H NMR (300 MHz, CD_2Cl_2): δ = 8.90 (d, ^3J = 4.8 Hz, 4H, H_{pyA}), 8.64 (d, ^3J = 8.4 Hz, 4H, $H_{4',7'}$), 8.58 (d, ^3J = 4.6 Hz, 4H, H_{pyB}), 8.50 (d, ^3J = 8.2 Hz, 4H, $H_{4,7}$), 8.25 (s, 4H, $H_{5',6'}$), 8.04 (s, 4H, $H_{5,6}$), 7.92 (d, ^3J = 8.3 Hz, 4H, $H_{3',8'}$), 7.89 (d, ^3J = 8.0 Hz, 4H, $H_{3,8}$), 7.53 (s, 4H, $H_{o''}$), 7.52 (d, ^3J = 8.6 Hz, 8H, $H_{o'}$), 7.32 (d, 8.4 Hz, 8H, H_o), 7.29 (m, 2H, $H_{p''}$), 7.09 (s, 4H, $H_{m''}$), 6.12 (d, ^3J = 8.6 Hz, 8H, $H_{m'}$), 6.05 (d, ^3J = 8.6 Hz, 8H, H_m), 4.43 (m, 8H, OCH_2), 3.97 (m, 8H, OCH_2), 3.72 (m, 8H, OCH_2), 3.67 (m, 8H, OCH_2), 3.52 (s, 12H, OMe), 2.35 (s, 6H, CH_{3p}), 1.68 (s, 12H, CH_{3o}) ppm. **ES-MS**: calcd for $C_{166}H_{136}Cu_2N_{12}O_{16}Zn^{2+}$ ($\mathbf{9^{2+}}$/2) 1371.41; found 1371.37. **UV-visible absorption** (CH_2Cl_2) : λ_{max} (logε) = 421 (5.84), 548 (4.51), 585 (3.79) nm.

4,7-Phenanthroline derivative 10 [220]

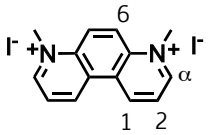

A large excess of MeI (21 mL, 0.34 mol) was added to a solution of 4,7-phenanthroline (1.84 g, 10.2 mmol) in DMF (250 mL) and the resulting reaction mixture was stirred at room temperature for 48 h. The precipitate formed was collected by filtration and dried under vacuum. More MeI (10 mL, 0.16 mol) was added to the filtrate and the reaction further stirred for 24 h. The precipitate formed was again collected by filtration and dried under vacuum. Product **10** was isolated as an orange crystalline solid (4.83 g, 98%).

^{1}H NMR (300 MHz, D_2O): δ = 10.07 (dd, ^3J = 8.4 Hz, ^4J = 0.6 Hz, 2H, H_α), 9.49 (dd, ^3J = 6.0 Hz, ^4J = 0.6 Hz, 2H, H_1), 9.04 (s, 2H, H_6), 8.43 (dd, ^3J = 8.4 Hz, ^3J = 6.0 Hz, 2H, H_2), 4.80 ppm (s, 6H, Me).

4,7-Phenanthroline derivative 11 [220]

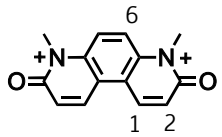

Compound **10** (4.82 g, 10.4 mmol) was dissolved in distilled water (200 mL). 5 drops of aqueous NaOH (1 M) were added. An aqueous solution of $K_3Fe(CN)_6$ (405 mM, 128 mL) was then added to the stirred solution dropwise over a period of 1 h. The pH was adjusted to pH 8 by addition of 1 M NaOH. 72 mL of the aq. $K_3Fe(CN)_6$ were added dropwise and the solution was stirred for 4 h. The solution was concentrated and extracted with CH_2Cl_2 (5 × 250 mL). The organic layers were combined and the solvent was evaporated to give 2.01 g (81%) of **11** as a brown solid.

^{1}H NMR (300 MHz, CDCl3): δ = 8.25 (d, ^3J = 9.9 Hz, 2H, H_1), 7.65 (s, 2H, H_6), 6.92 (d, ^3J = 9.9 Hz, 2H, H_2), 3.81 ppm (s, 6H, Me).

3,8-Dibromo-4,7-phenanthroline 12 [220]

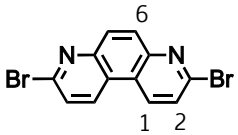

Compound **11** (1.28 g, 5.34 mmol), $POBr_3$ (44 g, 0.15 mol) and PBr_3 (7.5 g, 22 mmol) were placed in a round bottom flask fitted with an air condenser under argon. The mixture was heated at 180 °C for 48 hours. After cooling to about 60 °C, the black residue formed was added to excess ice/water (600 mL) and was vigorously stirred until hydrolysis of the remaining phosphorous halides was complete. Further ice was added and the mixture adjusted to pH 13 by dropwise addition of 20 % aq. NaOH. The final mixture was stirred for 30 min and then cooled down in an ice bath. The precipitate formed was collected by filtration, and then washed with hot $CHCl_3$ (8 × 100 mL). The aqueous filtrate was extracted with $CHCl_3$ (4 × 250 mL). The combined organic layers were evaporated to afford **12** as a pale yellow solid (1.51 g, 84%).

^{1}H NMR (300 MHz, $CDCl_3$): δ = 8.69 (d, ^3J = 8.7 Hz, 2H, H_1), 8.22 (s, 2H, H_6), 7.78 ppm (d, ^3J = 8.7 Hz, 2H, H_2).

5-Bromo-2-(trimethylstannyl)pyridine 13 [222]

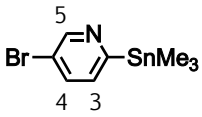

BuLi (9.2 mL of a 1.65 M solution in hexane, 15 mmol) was added dropwise to a solution of 5-bromo-2-iodopyridine (4.01 g, 14.1 mmol) in dry toluene (130 mL) at -20 °C. During the addition, the temperature was progressively lowered to -78 °C. After the end of the addition, the reaction mixture was further stirred for 2 h at -78 °C. A solution of trimethyltin chloride (3.41 g, 16.8 mmol) in dry toluene (40 mL) was added and the resulting yellow solution was stirred for 1 h at -78 °C. It was then allowed to warm up to room temperature. The solvent was evaporated and the resulting solid was taken up in CH_2Cl_2. Insoluble salts were filtered off and the filtrate was evaporated to dryness. The resulting yellow oil was submitted to column chromatography on alumina with pentane as an eluent to afford compound **13** as a yellow oil (3.82 g, 85%).

^{1}H NMR (300 MHz, $CDCl_3$): δ = 8.80 (d, ^4J = 2.1 Hz, 1H, H_5), 7.65 (dd, ^3J = 8.1 Hz, J = 2.4 Hz, 1H, H_4), 7.33 (d, ^3J = 8.1 Hz, 1H, H_3), 0.34 ppm (s with Sn satellites, 9H, Me).

Dibromo bis-bidentate ligand 14 [221]

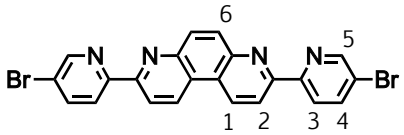

3,8-Dibromo-4,7-phenanthroline **12** (2.20 g, 3.56 mmol) and 5-bromo-2-trimethyltin pyridine **13** (2.35 g, 7.30 mmol) were suspended in dry toluene (150 mL) and the mixture was degassed with argon. $Pd(PPh_3)_4$ (0.23 g, 0.24 mmol) was added. The resulting reaction mixture was again degassed, and then refluxed under argon for 18 h. More $Pd(PPh_3)_4$ (0.19 g) was added and the reaction stirred for another 48 h under reflux. The solvent was evaporated to afford the crude product as a grey solid that was washed with MeOH (100 mL) and Et_2O (3 × 100 mL). The solid was placed in a soxhlet and extracted with chloroform for 10 days to afford compound **14** (1.52 g, 87%) as a yellow/grey solid.

^{1}H NMR (300 MHz, $CDCl_3$): δ = 9.05 (d, ^3J = 8.7 Hz, 2H, H_1), 8.80 (d, ^4J = 1.8 Hz, 2H, H_5), 8.74 (d, ^3J = 8.7 Hz, 2H, H_2), 8.64 (d, ^3J = 8.7 Hz, 2H, H_3), 8.31 (s, 2H, H_6), 8.03 ppm (dd, ^3J = 8.7 Hz, ^4J = 1.8 Hz, 2H, H_4).

TIPS bis-bidentate axle 15 [53]

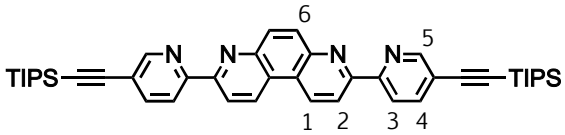

Compound **14** (787 mg, 1.60 mmol), triisopropylsilylacetylene (1.6 mL, 7.0 mmol), CuI (45 mg, 0.24 mmol) and $PdCl_2(PPh_3)_2$ (0.12 mg, 0.18 mmol) were introduced in an oven-dried flask. A degassed mixture of anhydrous DMF (30 mL) and distilled NEt_3 (3 mL) was subsequently added. The reaction mixture was further degassed with argon, and was then stirred for 18 h at 100 °C under argon. The reaction mixture was cooled down to room temperature and 40 mg of $PdCl_2(PPh_3)_2$ were added. The solution was stirred at 100 °C for 5 h, and then cooled down to room temperature. The solvents were evaporated and the crude product was purified by column chromatography on silica (eluent: dichloromethane) and then washed with pentane to afford 655 mg of compound **15** (59%) as a pale yellow solid.

^{1}H-NMR (300 MHz, $CDCl_3$): δ = 9.05 (d, ^3J = 8.7 Hz, 2H, H_1), 8.82 (dd, ^4J = 2.1 Hz, ^5J = 0.6 Hz, 2H, H_5), 8.78 (d, ^3J = 8.7 Hz, 2H, H_2), 8.69 (dd, ^3J = 8.1 Hz, ^5J = 0.6, 2H, H_3), 8.32 (s, 2H, H_6), 7.95 (dd, ^3J = 8.1 Hz, ^4J = 2.1 Hz, 2H, H_4), 1.18 ppm (s, 42H, H_{TIPS}).

Alkyne bis-bidentate axle 16 [53]

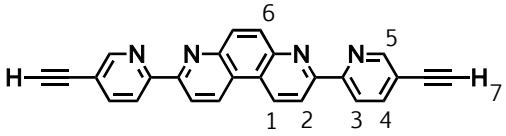

TIPS derivative **15** (150 mg, 0.216 mmol) were suspended in THF (10 mL). A 1 M solution of TBAF (0.60 mL, 0.60 mmol) in THF was then added, and a fine precipitate immediately formed. The reaction mixture was stirred for 30 min at room temperature. The solvent was evaporated, and the residual brown precipitate was washed with water, diethylether and pentane, and filtered over a Millipore filter. Compound **16** (70 mg, 85%) was obtained as a light brown powder.

^{1}H-NMR (300 MHz, $CDCl_3$): δ = 9.07 (d, ^3J = 8.7 Hz, 2H, H_1), 8.85 (dd, ^4J = 2.1 Hz, ^5J = 0.6 Hz, 2H, H_5), 8.78 (d, ^3J = 8.7 Hz, 2H, H_2), 8.72 (dd, ^3J = 8.1 Hz, ^5J = 0.6, 2H, H_3), 8.33 (s, 2H, H_6), 7.99 (dd, ^3J = 8.1 Hz, ^4J = 2.1 Hz, 2H, H_4), 3.34 ppm (s, 2H, H_7).

Bromo stopper 17 [223]

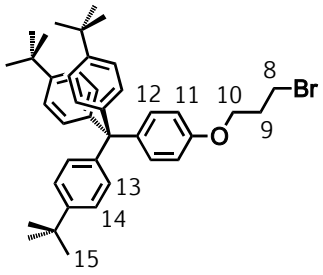

Pre-dried 4-[tris(*p-tert*-butylphenyl)methyl]phenol (1.00 g, 1.98 mmol) and Cs_2CO_3 (1.29 g, 3.96 mmol) were introduced in an oven dried round-bottom flask and 30 mL of degassed anhydrous DMF were added. The reaction mixture was heated to 60 °C under argon and 1,3-dibromopropanol (2.0 mL, 20 mmol) was then added. The reaction mixture was stirred under argon at 60 °C for 24 h. The solvent was evaporated and the resulting solid was taken up with CH_2Cl_2 (200 mL). The solution was washed with water (3 × 200 mL), then the organic layer was evaporated and the resulting solid was purified by silica column chromatography with CH_2Cl_2/pentane 1:1 as an eluent. Bromo stopper **17** (882 mg, 71%) was obtained as a white solid.
^{1}H-NMR (300 MHz, $CDCl_3$): δ = 7.23 (d, ^3J = 8.7 Hz, 6H, H_{13}), 7.09 (d, ^3J = 9.0 Hz, 2H, H_{12}), 7.08 (d, ^3J = 8.7 Hz, 6H, H_{14}), 6.77 (d, ^3J = 9.0 Hz, 2H, H_{11}), 4.08 (t, ^3J = 5.7 Hz, 2H, H_8), 3.60 (t, ^3J = 6.3 Hz, 2H, H_{10}), 2.31 (q, ^3J = 6.0 Hz, 2H, H_9), 1.30 ppm (s, 27H, H_{15}).

Azide stopper 18 [53]

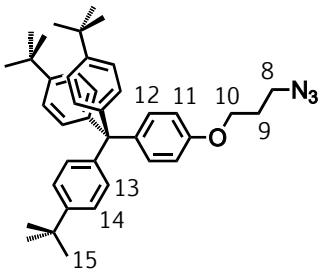

Bromo stopper **16** (882 mg, 1.41 mmol) was dissolved in 10 mL of CH_2Cl_2. A solution of sodium azide in water (3 mL) and DMF (10 mL) was added, and the reaction mixture was stirred at 100 °C for 24 h. The solvents were evaporated and the resulting solid was taken up in CH_2Cl_2 (150 mL). The solution was washed with water (3 × 150 mL), then the organic layer was evaporated and the resulting solid was purified by silica column chromatography with CH_2Cl_2/pentane 1:1 as an eluent. Azide stopper **18** (638 mg, 77%) was obtained as a white solid.
^{1}H-NMR (300 MHz, $CDCl_3$): δ = 7.23 (d, ^3J = 8.7 Hz, 6H, H_{13}), 7.09 (d, ^3J = 9.0 Hz, 2H, H_{12}), 7.08 (d, ^3J = 8.7 Hz, 6H, H_{14}), 6.76 (d, ^3J = 9.0 Hz, 2H, H_{11}), 4.02 (t, ^3J = 5.7 Hz, 2H, H_8), 3.51 (t, ^3J = 6.6 Hz, 2H, H_{10}), 2.04 (q, ^3J = 6.3 Hz, 2H, H_9), 1.30 ppm (s, 27H, H_{15}).

[4]Rotaxane 19^{4+}

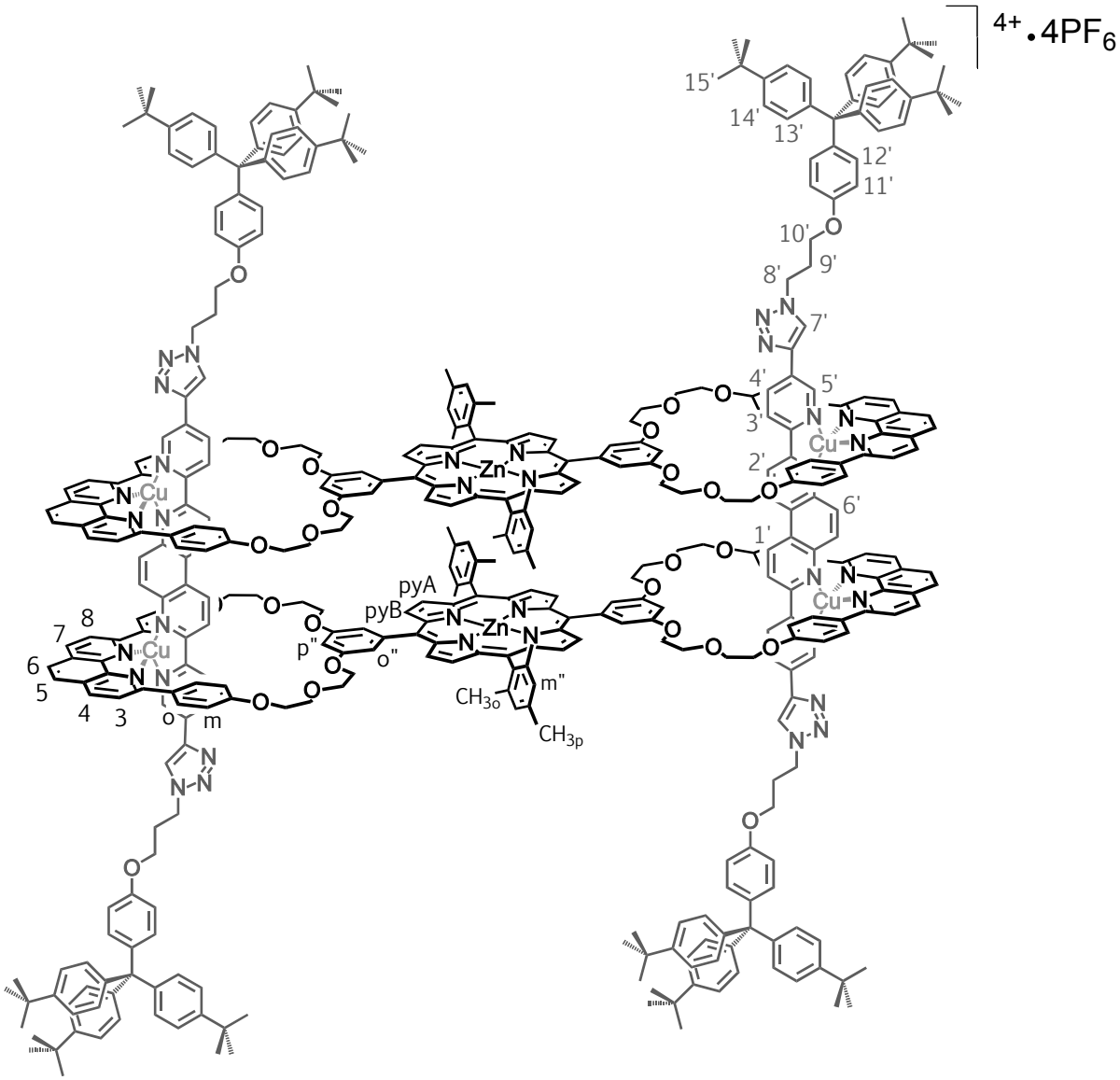

A degassed solution of $[Cu(CH_3CN)_4](PF_6)$ (10 mg, 28 μmol) in CH_3CN (3 mL) was added by cannula to a degassed suspension of Zn-porphyrin **8** (25 mg, 14 μmol) in CH_2Cl_2 (3 mL). The mixture was stirred under argon for 30 min, resulting in a dark red solution. This solution was then added to a degassed suspension of acetylenic thread **16** (5.2 mg, 14 μmol) in CH_2Cl_2 (3 mL). The mixture was stirred for 24 h under argon. Azide stopper **18** (24 mg, 41 μmol), $[Cu(CH_3CN)_4](PF_6)$ (5.1 mg, 14 μmol), Na_2CO_3 (0.6 mg, 5.4 μmol) and sodium ascorbate (1.1 mg, 5.4 μmol) were then added to the solution. The mixture was stirred under argon during 5 days. The solvents were then evaporated and the resulting deep red solid was purified by column chromatography. Consecutive alumina chromatography (using a gradient of elution from CH_2Cl_2/MeOH 100:0 to 92:8), size-exclusion Biobeads S-X1 chromatography in distilled THF and silica chromatography (using a gradient of elution from CH_2Cl_2/MeOH 98:2 to 94:6) gave 26 mg of rotaxane $\mathbf{19^{4+}}\cdot 4PF_6$ (50%) as a dark red solid.

^{1}H NMR (600 MHz, CD_2Cl_2): δ = 9.08 (d, ^3J = 8.4 Hz, 4H, $H_{1'}$), 8.68 (d, ^3J = 7.8 Hz, 4H, $H_{4,7a}$), 8.56 (d, ^3J = 4.8 Hz, 4H, H_{pyBa}), 8.55 (d, ^3J = 7.8 Hz, 4H, $H_{4,7b}$), 8.47 (d, ^3J = 7.8 Hz, 4H, $H_{4'}$), 8.34 (d, ^3J = 4.2 Hz, 4H, H_{pyAa}), 8.29 (s, 4H, $H_{5'}$), 8.24 (d, ^3J = 8.4 Hz, 8H, $H_{2'}$ + $H_{3'}$), 8.15 (d, ^3J = 7.8 Hz, 4H, $H_{3,8a}$), 8.14 (s, 8H, $H_{5,6}$), 8.12 (d, ^3J = 4.8 Hz, 4H, H_{pyBb}), 7.99 (s, 4H, $H_{6'}$), 7.98 (m, 4H, H_{pyAb}), 7.77 (s, 4H, $H_{7'}$), 7.62 (d, ^3J = 7.8 Hz, 4H, $H_{3,8b}$), 7.55 (d, ^3J = 8.4 Hz, 8H, H_{oa}), 7.44 (s, 4H, $H_{o"a}$), 7.36 (s, 4H, $H_{p"}$), 7.19 (d, ^3J = 8.4 Hz, 24H, $H_{14'}$), 7.06 (d, ^3J = 8.4 Hz, 24 H, $H_{13'}$), 7.00 (d, ^3J = 8.4 Hz, 8H, $H_{12'}$), 6.97 (s, 4H, $H_{o"b}$), 6.94 (s, 4H, $H_{m"a}$), 6.58 (d, ^3J = 7.8 Hz, 8H, H_{ob}), 6.51 (s, 4H, $H_{m"b}$), 6.29 (d, ^3J = 8.4 Hz, 8H, $H_{11'}$), 6.12 (d, ^3J = 8.4 Hz, 8H, H_{ma}), 5.20 (d, ^3J = 7.8 Hz, 8H, H_{mb}), 4.60-4.19 (m, 24H, OCH_2), 4.24 (m, 8H, $H_{8'}$), 3.95-3.89 (m, 8H, OCH_2), 3.77-3.59 (m, 24H, OCH_2), 3.24 (m, 8H, $H_{10'}$), 2.77-2.60 (m, 8H, OCH_2), 2.00 (s, 12H, CH_{3p}), 1.85 (m, 8H, $H_{9'}$), 1.47 (s, 12H, CH_{3oa}), 1.26 (s, 108H, $H_{15'}$), 0.64 (s, 12H, CH_{3ob}) ppm. **^{13}C NMR** (75 MHz, CD_2Cl_2): 159.85, 158.98, 158.63, 158.46, 158.34, 157.65, 155.93, 152.99, 150.22, 149.95, 149.83, 149.65, 149.36, 148.81, 146.14, 145.52, 144.77, 144.70, 144.28, 144.08, 143.36, 140.74, 139.02, 138.97, 138.52, 138.32, 138.20, 137.68, 134.89, 133.06, 132.46, 132.39, 132.17, 131.65, 131.23, 130.72, 130.35, 129.90, 129.74, 128.60, 128.40, 127.77, 127.25, 126.92, 126.83, 125.73, 125.36, 124.67, 124.54, 122.32, 121.69, 119.62, 119.32, 114.29, 113.77, 113.66, 113.55, 112.35, 101.97, 70.29, 69.66, 69.35, 68.85, 68.51, 68.42, 67.80, 67.20, 64.16, 63.42, 34.57, 31.47, 29.66, 25.21, 21.53, 21.09, 21.06 ppm. **HRES-MS**: calcd for $[C_{440}H_{416}Cu_4N_{36}O_{28}Zn_2]^{4+}/4$ (**19^{4+}**/4) *m/z* = 1760.202; found 1760.169. **UV-visible absorption** (CH_2Cl_2): λ_{max} (log ε) = 280 (5.31), 339 (5.34), 420 (6.00), 551 (4.68), 591 nm (4.09).

Guest G3 [261]

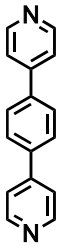

1,4-Dibromobenzene (235 mg, 1.00 mmol), pyridine 4-boronic acid (430 mg, 3.50 mmol), $Pd(dppf)_2Cl_2$ (82 mg, 0.10 mmol), and Na_2CO_3 (0.21 g, 2.0 mmol) were introduced in a 10 mL round-bottom flask, and a mixture of toluene/water 1:1 (5 mL) was added. The mixture was degassed for 10 min and allowed to reflux for 72 h under argon atmosphere. The solvent was evaporated, and the residue was extracted with ethyl acetate (50 mL). The solution was washed with water (3 × 50 mL). The organic layer was dried over anhydrous $MgSO_4$ and evaporated to afford a brown solid, which was purified by silica gel column chromatography in ethyl acetate/pentane/triethylamine 8:5:1 to afford pure 1,4-bis(4-pyridyl)benzene **G3** as an off-white solid (180 mg, 77%).

^{1}H-NMR (400 MHz, $CDCl_3$): δ = 8.72 (br d, 4H), 7.78 (s, 4H), 7.57 ppm (br d, 4H).

Guest G4 [261]

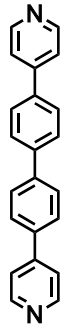

4,4'-Dibromobiphenylene (312 mg, 1.00 mmol), pyridine 4-boronic acid (430 mg, 3.50 mmol), $Pd(dppf)_2Cl_2$ (82 mg, 0.10 mmol), and Na_2CO_3 (0.21 g, 2.0 mmol) were introduced in a 10 mL round-bottom flask, and a mixture of toluene/water 1:1 (5 mL) was added. The mixture was degassed for 10 min and allowed to reflux for 72 h under argon atmosphere. The solvent was evaporated, and the residue was extracted with ethyl acetate (50 mL). The solution was washed with water (3 × 50 mL). The organic layer was dried over anhydrous $MgSO_4$ and evaporated to afford a brown solid, which was purified by silica gel column chromatography in ethyl acetate/pentane/triethylamine 8:5:1 to afford pure 1,4-bis(4-pyridyl)benzene **G3** as an off-white solid (179 mg, 58%).

^{1}H-NMR (400 MHz, $CDCl_3$): δ = 8.70 (d, ^3J = 6.4 Hz, 4H), 7.77 (s, 8H), 7.57 ppm (d, ^3J = 6.4 Hz, 4H).

Copper(II) porphyrin 20 [265]

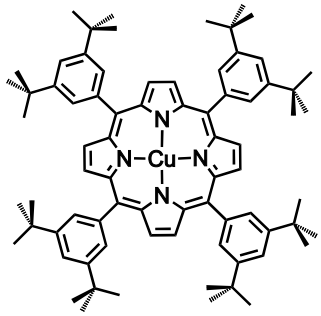

A solution of copper(II) acetate monohydrate (0.78 g, 3.9 mmol) in methanol (30 mL) was added to a solution of free-base 5,10,15,20-tetrakis(3,5-di-*tert*-butylphenyl)porphyrin (2.08 g, 1.96 mmol) in dichloromethane (100 mL). The reaction mixture was allowed to reflux for 1.5 h. After cooling, the solvent was evaporated. The residue was passed through a plug of silica using dichloromethane as eluent. The main fraction was collected and the solvent was evaporated to give copper(II) porphyrin **20** (2.20 g, quantitative) as a red-purple solid.

Identification of the product was confirmed by comparison of the TLC and UV-visible absorption spectrum with those of an authentic sample.

UV-visible absorption ($CHCl_3$): λ_{max} (log ε) = 420 (5.69), 541 nm (4.30).

Dinitro copper(II) porphyrins 21 [265]

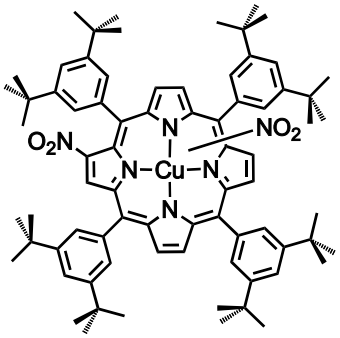

A solution of nitrogen dioxide in light petroleum (0.5 M, 10 mL) was added in small aliquots to a solution of copper(II) porphyrin **20** (2.20 g, 1.96 mmol) in dichloromethane (100 mL). The reaction was followed by TLC (dichloromethane/light petroleum 1:4). A new spot corresponding to the mono-nitrated adduct appeared on TLC, followed by appearance of other spots corresponding to dinitrated porphyrins. When conversion to the dinitrated species was complete according to TLC, the mixture was immediately passed through a plug of silica gel using dichloromethane as eluent. The solvent was evaporated to give a purple residue, which was further purified by column chromatography over silica using dichloromethane/light petroleum (1:4) as eluent. A mixture of dinitro copper(II) porphyrin isomers **21** was obtained as a red-purple solid (2.02 g, 85%). Identification of the product was confirmed by comparison of the TLC and UV-visible absorption spectrum with those of an authentic sample.

UV-visible absorption ($CHCl_3$): λ_{max} (log ε) = 438 (5.19), 559 (4.08), 601 nm (4.03).

Dinitro free-base porphyrins 22 [265]

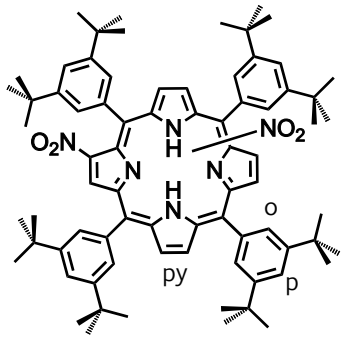

Concentrated sulphuric acid (5 mL) was added dropwise to a solution of **21** (2.02 g, 1.67 mmol) in dichloromethane (60 mL). The reaction mixture was stirred at room temperature for 15 min and then poured into an ice–water mixture (100 mL). The organic layer was washed with water (100 mL), 10 % aqueous sodium carbonate (100 mL), water (100 mL), dried over Na_2SO_4, and filtered. The solvent was evaporated to give a purple solid, which was purified by column chromatography on silica gel using dichloromethane–light petroleum 1:4 as eluent. Dinitro free-base porphyrin isomers **24** were obtained as a purple solid (1.92 g, quantitative).

^{1}H NMR (300 MHz, $CDCl_3$,): δ = 8.77-9.11 (m, 6H, H_{py}), 8.00-8.14 (m, 8H, H_o), 7.80-7.88 (m, 4H, H_p), 1.50-1.56 (72H, $H_{t\mathrm{Bu}}$), -2.09 to -2.18 and -2.40 to -2.48 ppm (6H, NH). **UV-visible absorption** ($CHCl_3$): λ_{max} (log ε) = 442 (5.32), 539 (4.13), 583 (3.96), 618 (3.76), 683 nm (4.04).

Diamino free-base porphyrins 23 [265]

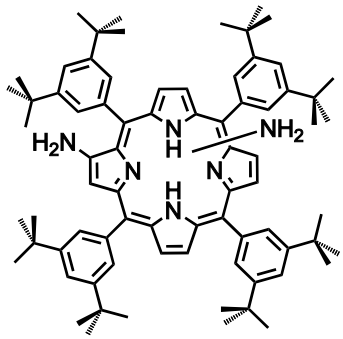

Isomers **22** (1.92 g, 1.67 mmol) and tin(II) chloride dihydrate (4.52 g, 20.0 mmol) were dissolved in dichloromethane/diethylether 1:1 (40 mL) and the solution was cooled in an ice bath. A solution of hydrochloric acid in diethylether (~2 M, 10 mL) was slowly added. The solution was allowed to warm up to room temperature and stirred for 2 h. It was washed with water (50 mL), 10 % aqueous $NaHCO_3$ (50 mL) and water (50 mL). The organic layer was evaporated to give the crude diamino free-base porphyrins **23** (1.77 g), which were immediately photooxidised.

Corner amino free-base porphyrin-diones 24 and linear free-base porphyrin-tetraone 25 [265]

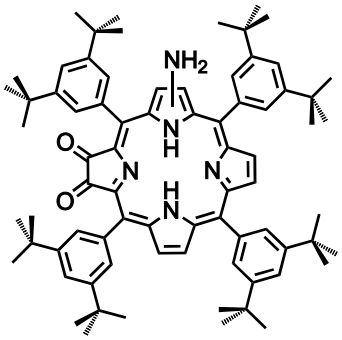

24

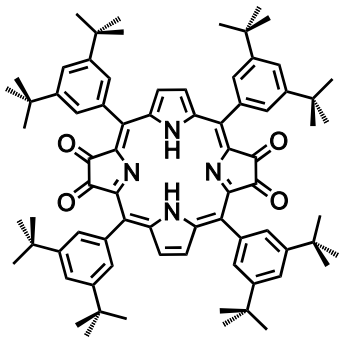

25

The crude diamino free-base porphyrins **23** (1.77 g) were dissolved in dichloromethane. Photooxidation was achieved by irradiation with UV-light and bubbling of oxygen through the solution for 3.5 h. The solvent was evaporated to give a mixture of 7- and 8-aminoporphyrin diones **24** and linear porphyrin-tetraone **25**, which were subjected to selective metalation.

Corner amino zinc porphyrin-diones 26 and linear free-base porphyrin-tetraone 25 [265]

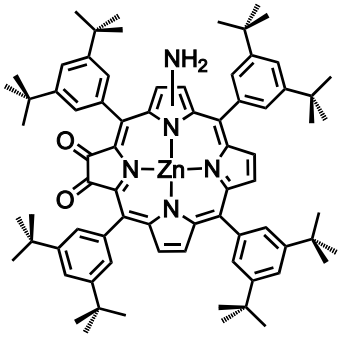

26

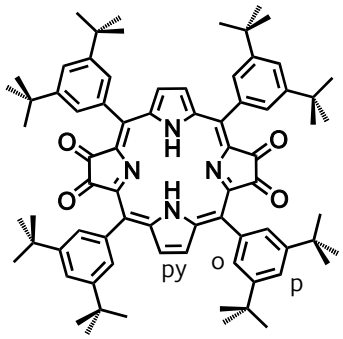

25

The mixture of 27 and 28 was dissolved in dichloromethane (100 mL), and a solution of zinc acetate dihydrate (1.42 g, 6.46 mmol) in methanol (15 mL) was added. The reaction mixture was refluxed for 2 h, and the solvents were then evaporated. The resulting solid was subjected to silica column chromatography in dichloromethane/hexane 1:1 to isolate the linear free-base porphyrin-tetraone **25** (453 mg, 21% from dinitro isomers **22**) and the corner zinc(II) aminoporphyrin-diones **26** (1.26 g, 54% from dinitro isomers **22**).

25: ^{1}H NMR (400 MHz, $CDCl_3$): δ = 8.50 (s, 4H, H_{py}), 7.74 (t, ^4J = 1.7 Hz, 4H, H_p), 7.65 (t, ^4J = 1.7 Hz, 8H, H_o), 1.44 (s, 72H, H_{tBu}), -1.32 ppm (br s, 2H, NH).

4,5-Dinitroveratrole 27 [275]

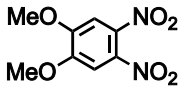

1,2-Dimethoxybenzene (veratrole) (20 mL, 0.16 mol) was added dropwise over 1 h to a vigorously stirred mixture of concentrated HNO_3 (50 mL) and H_2O (5 mL) at 0 °C. The resulting yellow slurry was then warmed to 60 °C to liberate NO_2 as a brown gas. After gas evolution ceased (4 h), the solution was poured into 500 mL of ice water and the yellow solid was isolated by suction filtration. The solid was washed thoroughly with a saturated solution of $NaHCO_3$ followed by H_2O. After drying, the product was recrystallised from hot ethanol. 4,5-Dinitroveratrole was isolated as a crystalline yellow solid (29 g, 81%).

^{1}H NMR (300 MHz, $CDCl_3$): δ = 7.33 (s, 2H, H_{Ar}), 4.01 ppm (s, 6H, H_{Me}).

4,5-Diaminoveratrole 28 [275]

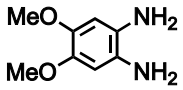

4,5-Dinitroveratrole **27** (5.05 g, 22.1 mmol) and 10% Pd/C (0.20 g) were placed under argon and degassed absolute ethanol (115 mL) was added. Hydrazine monohydrate (11 mL, 0.23 mol) was added slowly and the reaction was stirred at room temperature under argon. A vigorous exothermic reaction occurred within the first 30 min. The reaction was then set to reflux. The colour of the reaction solution proceeded from orange through yellow to colourless within 2 h. The slurry was filtered through Celite and the filtrate was evaporated to yield 4,5-diaminoveratrole **28** as an off-white solid (3.71 g, quantitative).

^{1}H NMR (200 MHz, $CDCl_3$): δ = 6.38 (s, 2H, H_{Ar}), 3.79 (s, 6H, Me), 2.20 ppm (br s, 4H, NH_2).

4,5-Diaminocatechol hydrobromide 29 [275]

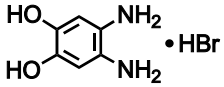

4,5-Diaminoveratrole **28** (3.71 g, 22.1 mmol) was dissolved in degassed CH_2Cl_2 (50 mL) and the solution was cooled to 0 °C. BBr_3 (50 mL of a 1.0 M CH_2Cl_2 solution, 50 mmol) was added slowly via cannula to the stirred solution. The resulting grey slurry was allowed to warm to room temperature and was stirred for 16 h under argon. Methanol (100 mL) was added slowly,

producing a purple solution. The solvent was evaporated, and the methanol treatment was repeated twice. The final crude purple residue was recrystallised from MeOH/THF (1:9) to yield 4,5-diaminocatechol hydrobromide **29** as a purple crystalline solid (4.35 g, 89%).

^{1}H NMR (300 MHz, CD_3OD): δ = 6.96 (s, 2H, H_{Ar}), 5.01 ppm (br s, 5H, NH_2).

Linear bis(dihydroxyquinoxalino)porphyrin 30

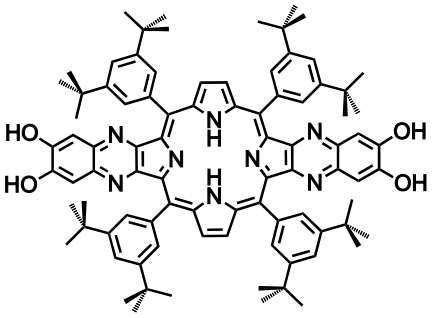

Linear porphyrin-tetraone **25** (50 mg, 45 μmol) and 4,5-diaminocatechol hydrobromide **29** (39 mg, 0.11 mmol) were dissolved in degassed distilled pyridine, and the reaction mixture was refluxed under argon for 20 h. The solvent was evaporated, and the resulting solid was dissolved in dichloromethane (50 mL) and washed with water (50 mL), 10 % aqueous $NaHCO_3$ (50 mL) and water (50 mL). The solvent was evaporated and the solid was recrystallised from dichloromethane/methanol to give compound **30** as a dark red solid (50 mg, 85%).

HRES-MS: calcd for $C_{88}H_{99}N_8O_4^+$ (**30** + H^+) *m/z* = 1331.78; found 1331.93; calcd for $C_{88}H_{97}N_8O_4^-$ (**30** - H^+) *m/z* = 1329.77; found 1329.93.

^{1}H NMR (300 MHz, $CDCl_3$): broad signals.

4,5-Dinitrocatechol 31 [276]

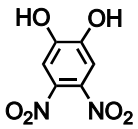

4,5-Dinitroveratrole **27** (8.5 g, 37 mmol) and hydrobromic acid (48%, 50 mL) were heated to 90 °C for 48 h. A brown solid precipitated. It was filtered off, and the product was extracted from the filtrate with diethylether (3 × 100 mL). The organic layers were combined and the solvent was evaporated to give 4,5-dinitrocatechol **31** as an orange solid (3.0 g, 41%).

^{1}H NMR (300 MHz, DMSO-d_6): δ = 11.18 (br s, 2H, OH), 7.42 ppm (s, 2H, H_{Ar}).

Boc-protected 4,5-diaminocatechol 32

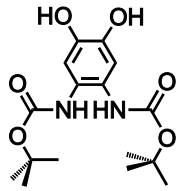

4,5-Diaminocatechol hydrobromide **29** (430 mg, 1.94 mmol) was dissolved in degassed absolute ethanol (5 mL). Pyridine (0.32 mL, 3.9 mmol) and di-*tert*-butyl dicarbonate (Boc_2O) (1.70 g, 7.8 mmol) were added. The reaction mixture was stirred at 30 °C under argon for 20 h. The solvent was evaporated and the product was recrystallised in THF to give the Boc-protected compound **32** as a purple solid (548 mg, 83%).

^{1}H NMR (200 MHz, DMSO-d_6): δ = 8.86 (br s, 2H, NH), 8.10 (br s, 2H, OH), 6.81 (s, 2H, H_{Ar}), 1.43 ppm (s, 18H, H_{tBu}). **ES-MS**: calcd for $C_{16}H_{24}N_2NaO_6^+$ (**32** + Na^+) *m/z* = 383.15; found 362.67.

1-Benzyl-2-phenylbenzimidazole derivative 33

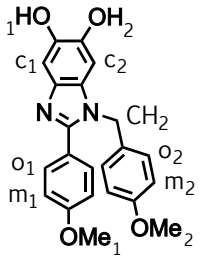

4,5-Diaminocatechol hydrobromide (2.15 g, 9.71 mmol) was dissolved in a carefully degassed mixture of ethanol and water 1:2 (90 mL) to produce a dark purple solution. Pyridine (3.6 mL, 44 mmol) was added to neutralise the hydrobromic acid, and the solution turned red. Anisaldehyde (2.7 mL, 22 mmol) was added, and the solution was stirred at room temperature under argon for 4 h. A pale pink solid precipitated, it was filtered off and washed with diethylether. After recrystallisation from hot ethanol, compound **33** was obtained as an off-white solid (2.85 g, 78%).

^{1}H NMR (500 MHz, DMSO-d_6): δ = 8.78 (br s, 1H, OH_2), 8.74 (br s, 1H, OH_1), 7.58 (d, 2H, ^3J = 9.0 Hz, H_{o1}), 7.04 (d, 2H, ^3J = 9.0 Hz, H_{m1}), 7.01 (s, 1H, H_{c1}), 6.94 (d, 2H, ^3J = 8.5 Hz, H_{o2}), 6.86 (d, 2H, ^3J = 8.5 Hz, H_{m2}), 6.67 (s, 1H, H_{c2}), 5.31 (s, 2H, CH_2), 3.80 (s, 3H, Me_1), 3.70 ppm (s, 3H, Me_2). **^{13}C NMR** (125 MHz, DMSO-d_6): δ = 159.82, 158.44, 150.90, 143.18, 142.63, 135.84, 129.99, 129.28, 128.97, 127.20, 122.98, 114.12, 114.07, 103.99, 96.40, 55.20, 55.01, 46.89 ppm. **ES-MS**: calcd for $C_{22}H_{21}N_2O_4^+$ (**33** + H^+) *m/z* = 377.15; found 376.80.

Benzimidazole macrocycle 34

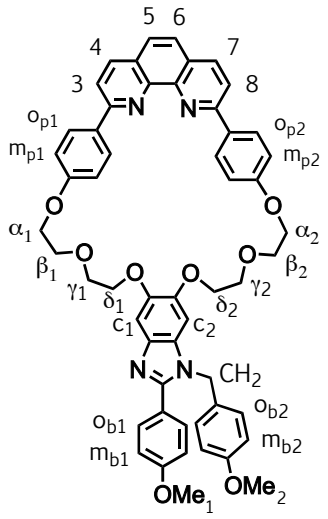

A mixture of the ditosylate phenanthroline derivative **4** (100 mg, 118 μmol) and catechol derivative **33** (44.4 mg, 118 μmol) in DMF (20 mL) was degassed, transferred to an addition funnel, and added dropwise to a degassed suspension of Cs_2CO_3 (231 mg, 708 μmol) in DMF (30 mL) over a period of 2 h. The mixture was then heated to 90°C and stirred under argon for 16 h. After evaporation of the solvent, the remaining solid was dissolved in dichloromethane (50 mL), washed with water (3 × 50 mL) and dried over Na_2SO_4. The organic layer was evaporated, and the crude product was purified by alumina column chromatography in dichloromethane/methanol (100:0.4) to yield macrocycle **34** as a pale yellow solid (62 mg, 60%). **^{1}H NMR** (500 MHz, $CDCl_3$): δ = 8.41 (d, 2H, ^3J = 8.5 Hz, H_{op2}), 8.34 (d, 2H, ^3J = 8.5 Hz, H_{op1}), 8.24 (d, 1H, ^3J = 8.5 Hz, H_7), 8.21 (d, 1H, ^3J = 8.5 Hz, H_4), 8.04 (d, 1H, ^3J = 8.5 Hz, H_8), 8.00 (d, 1H, ^3J = 8.5 Hz, H_3), 7.72 (s, 2H, $H_{5,6}$), 7.48 (d, 2H, ^3J = 8.5 Hz, H_{ob1}), 7.42 (s, 1H, H_{c1}), 7.21 (d, 2H, ^3J = 8.5 Hz, H_{mp2}), 7.10 (d, 2H, ^3J = 8.5 Hz, H_{mp1}), 6.86 (d, 4H, ^3J = 8.5 Hz, H_{ob2} + H_{mb1}), 6.78 (s, 1H, H_{c2}), 6.75 (d, 2H, ^3J = 8.5 Hz, H_{mb2}), 5.22 (s, 2H, CH_2), 4.37 (t, 2H, ^3J = 5.5 Hz, $H_{\alpha1}$), 4.35 (t, 2H, ^3J = 5.5 Hz, $H_{\alpha2}$), 4.32 (t, 2H, ^3J = 5.5 Hz, $H_{\delta1}$), 4.18 (t, 2H, ^3J = 5.5 Hz, $H_{\delta2}$), 4.00 (t, 2H, ^3J = 5.5 Hz, $H_{\gamma1}$), 3.92 (t, 2H, ^3J = 5.5 Hz, $H_{\beta1}$), 3.86 (t, 2H, ^3J = 5.5 Hz, $H_{\gamma2}$), 3.81 (t, 2H, ^3J = 5.5 Hz, $H_{\beta2}$), 3.80 (s, 3H, Me_1), 3.72 ppm (s, 3H, Me_2). **^{13}C NMR** (125 MHz, $CDCl_3$): δ = 160.77, 160.07, 159.15, 156.46, 156.37, 153.07, 146.92, 146.69, 146.12, 146.06, 137.34, 136.80, 136.71, 133.10, 132.72, 130.58, 130.34, 129.27, 129.13, 128.48, 127.52, 127.49, 127.32, 125.71, 125.63, 122.45, 119.31, 119.24, 116.08, 115.72, 114.49, 114.22, 105.19, 98.33, 70.25, 69.96, 69.93, 69.62, 69.49, 69.15, 68.03, 67.89, 55.49, 55.41, 48.08 ppm. **ES-MS**: calcd for $C_{54}H_{49}N_4O_8^+$ (**34** + H^+) m/z = 881.36; found 881.33.

4,5-Dibromocatechol 35 [288]

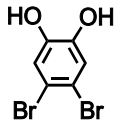

A solution of Br_2 (4.7 mL, 91 mmol) in $CHCl_3$ (6 mL) was added dropwise over 1 h to a suspension of catechol (5.00 g, 45.4 mmol) in $CHCl_3$ (50 mL) at 0 °C. The reaction mixture was then allowed to warm up to room temperature and was stirred for 20 h. The precipitate was isolated by filtration to give dibromocatechol **35** (6.47 g, 53%) as an off-white solid.

^{1}H NMR (500 MHz, $CDCl_3$): δ = 7.38 (s, 2H, H_{Ar}), 5.46 ppm (br s, 2H, OH).

Dibromo macrocycle 36

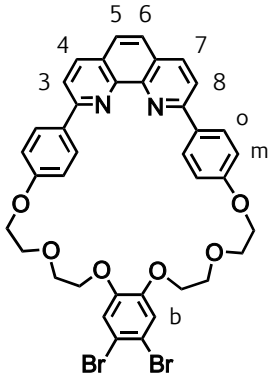

A mixture of the ditosylate phenanthroline derivative **4** (750 mg, 0.883 mmol) and 4,5-dibromocatechol **35** (237 mg, 0.883 mmol) in DMF (75 mL) was degassed, transferred to an addition funnel, and added dropwise to a degassed suspension of Cs_2CO_3 (1.73 g, 5.30 mmol) in DMF (110 mL) over a period of 4 h. The mixture was then heated to 90°C and stirred under argon for 16 h. After evaporation of the solvent, the remaining solid was dissolved in dichloromethane (150 mL), washed with water (3 × 150 mL) and dried over Na_2SO_4. The organic layer was evaporated, and the crude product was purified by silica gel chromatography in dichloromethane/methanol (100:1) to yield the macrocycle **36** as a pale yellow solid (247 mg, 36%).

^{1}H NMR (400 MHz, $CDCl_3$): δ = 8.40 (d, ^3J = 8.8 Hz, 4H, H_o), 8.27 (d, ^3J = 8.4 Hz, 2H, $H_{3,8}$), 8.06 (d, ^3J = 8.4 Hz, 2H, $H_{4,7}$), 7.75 (s, 2H, $H_{5,6}$), 7.20 (s, 2H, H_b), 7.17 (d, ^3J = 8.8 Hz, 4H, H_m), 4.39 (t, ^3J = 5.6 Hz, 4H, CH_2), 4.20 (t, ^3J = 5.6 Hz, 4H, CH_2), 3.94 (t, ^3J = 5.6 Hz, 4H, CH_2), 3.89 ppm (t, ^3J = 5.6 Hz, 4H, CH_2).

Bis-imine macrocycle 37

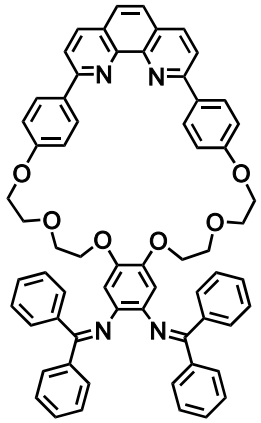

A toluene solution (10 mL) of tris(dibenzylideneacetone)dipalladium(0) (4.7 mg, 5.2 μmol) and *rac*-BINAP (6.4 mg, 10 μmol) was degassed with argon, and stirred at 110 °C for 30 min under argon. After cooling to room temperature, benzophenone imine (23 μL, 0.14 mmol), dibromo macrocycle **36** (40 mg, 52 μmol), and sodium *tert*-butoxide (13 mg, 0.13 mmol) were added to the solution, and the reaction mixture was stirred at 110 °C under argon for 48 h. The mixture was cooled to room temperature, diluted with CH_2Cl_2 (10 mL), filtered through a pad of Celite, and evaporated to dryness. The residue was subjected to column chromatography on silica gel with CH_2Cl_2/methanol (100:3) as eluent. The desired bis-imine macrocycle **37** could not be completely purified but was detected by mass spectrometry.

ES-MS: calcd for $C_{64}H_{53}N_4O_6^+$ (**37** + H^+) m/z = 973.39; found 973.40.

Free-base porphyrin tetra-macrocycle 38

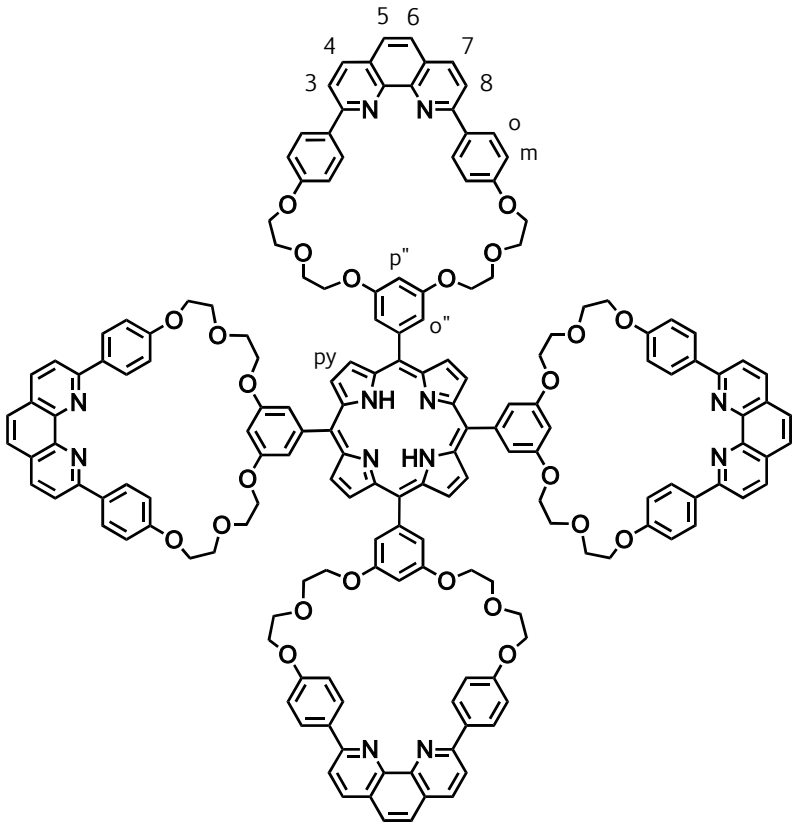

Macrocycle **5** (0.40 g, 0.62 mmol) was dissolved in a 7:3 mixture of propionic acid and nitrobenzene (3 mL) in a 10 mL reaction vessel. Pyrrole (43 μL, 0.62 mmol) was added by syringe. The reaction vessel was sealed and subjected to microwave irradiation (maximum power 300 W) for 10 minutes at a controlled temperature of 140 °C. The resulting black solution was diluted with chloroform (100 mL), washed with water (3 × 100 mL) and dried with Na_2SO_4. After evaporation of the solvent, the crude product was purified by silica gel chromatography (gradient of chloroform/methanol from 100:0 to 98:2) and size-exclusion chromatography (Biobeads S-X1 in ethanol-free chloroform) to give porphyrin **38** as a purple solid (0.11 g, 25%). **^{1}H NMR** (300 MHz, $CDCl_3$): δ = 8.81 (s, 8H, H_{py}), 8.46 (d, ^3J = 8.7 Hz, 16H, H_o), 8.24 (d, ^3J = 8.4 Hz, 8H, $H_{3,8}$), 8.06 (d, ^3J = 8.4 Hz, 8H, $H_{4,7}$), 7.72 (s, 8H, $H_{5,6}$), 7.33 (d, ^4J = 2.4 Hz, 8H, $H_{o"}$), 7.22 (d, ^3J = 8.7 Hz, 16H, H_m), 7.02 (t, ^4J = 2.1 Hz, 4H, $H_{p"}$), 4.36 (t, ^3J = 5.1 Hz, 16H, CH_2), 4.27-4.24 (m, 16H, CH_2), 3.97-3.93 (m, 32H, CH_2), -2.98 (br s, 2H, NH) ppm. **^{13}C NMR** (75.48 MHz, $CDCl_3$): δ = 160.05, 157.93, 156.17, 145.94, 143.87, 136.69, 132.63, 129.04, 127.96, 127.40, 125.54, 119.75, 119.09, 115.51, 114.09, 102.48, 70.05, 69.56, 67.63. **ES-MS**: calcd for $C_{172}H_{143}N_{12}O_{24}^+$ [**38** + H^+] *m/z* = 2,760.03; found 2,760.10. **UV-visible absorption** (CH_2Cl_2): λ_{max} (log ε) = 284 (5.36), 323 (5.10), 421 (5.65), 515 (4.30), 550 (3.78), 588 (3.76), 645 (3.51) nm.

Zinc porphyrin tetra-macrocycle 39

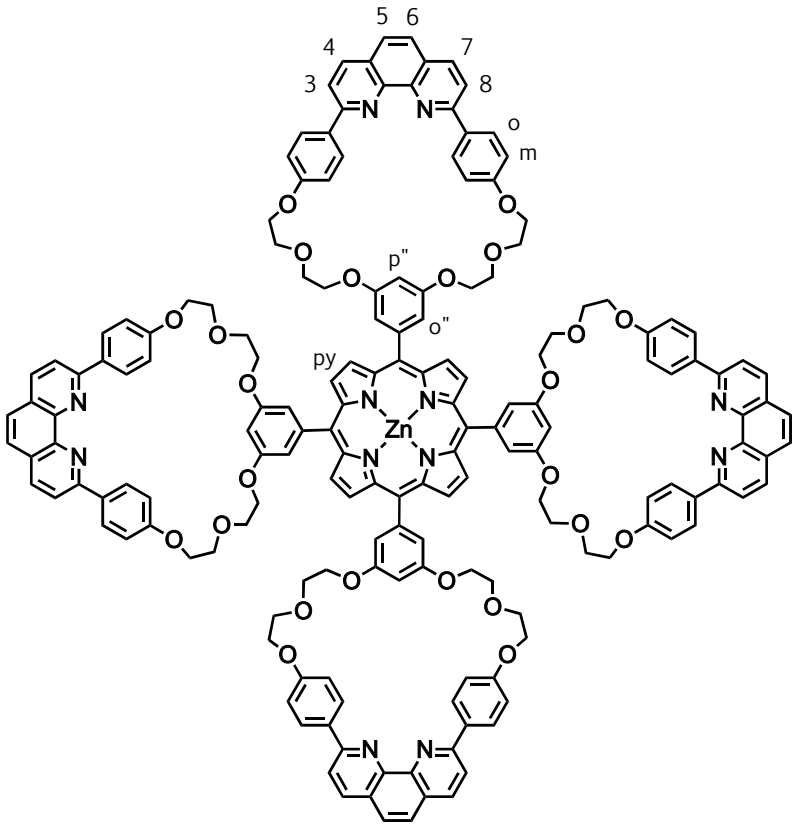

Free-base porphyrin **38** (44 mg, 16 μmol) was dissolved in $CHCl_3$ (25 mL), and a saturated solution of $Zn(OAc)_2 \cdot 2H_2O$ in methanol (5 mL) was added. The solution was heated to reflux and stirred for 5 h under argon. The solvents were evaporated and the solid was taken up with chloroform (25 mL) and washed with water (2 × 25 mL). An aqueous solution of Na_4EDTA (0.1 M, 25 mL) was added to the organic layer and the biphasic mixture was vigorously stirred for further 24 hours at room temperature. The organic layer was separated, washed twice with water, dried with Na_2SO_4 and evaporated under reduced pressure to give Zn-porphyrin **39** as a purple solid in quantitative yield (45 mg).

^{1}H NMR (300 MHz, $CDCl_3$): δ = 8.92 (s, 8H, H_{py}), 8.39 (d, ^3J = 8.7 Hz, 16H, H_o), 8.14 (d, ^3J = 8.4 Hz, 8H, $H_{3,8}$), 7.96 (d, ^3J = 8.4 Hz, 8H, $H_{4,7}$), 7.62 (s, 8H, $H_{5,6}$), 7.30 (d, ^4J = 2.4 Hz, 8H, $H_{o''}$), 7.11 (d, ^3J = 8.7 Hz, 16H, H_m), 6.92 (t, ^4J = 2.1 Hz, 4H, $H_{p''}$), 4.18 (t, ^3J = 5.1 Hz, 16H, CH_2), 4.12-4.10 (m, 16H, CH_2), 3.73-3.76 (m, 32H, CH_2), ppm. **^{13}C NMR** (125 MHz, $CDCl_3$): δ = 160.15, 158.01, 156.32, 146.05, 143.99, 136.85, 132.73, 129.17, 127.54, 125.69, 119.84, 119.27, 115.62, 114.16, 102.57, 70.18, 69.68, 67.78. **ES-MS**: calcd for $C_{172}H_{141}N_{12}O_{24}Zn^+$ (**39** + H^+) m/z = 2,824.95; found 2,824.95. **UV-visible absorption** (CH_2Cl_2): λ_{max} (log ε) = 284 (5.39), 322 (5.13), 424 (5.75), 550 (4.35), 590 (3.52) nm.

[3]Rotaxane 40^{4+}

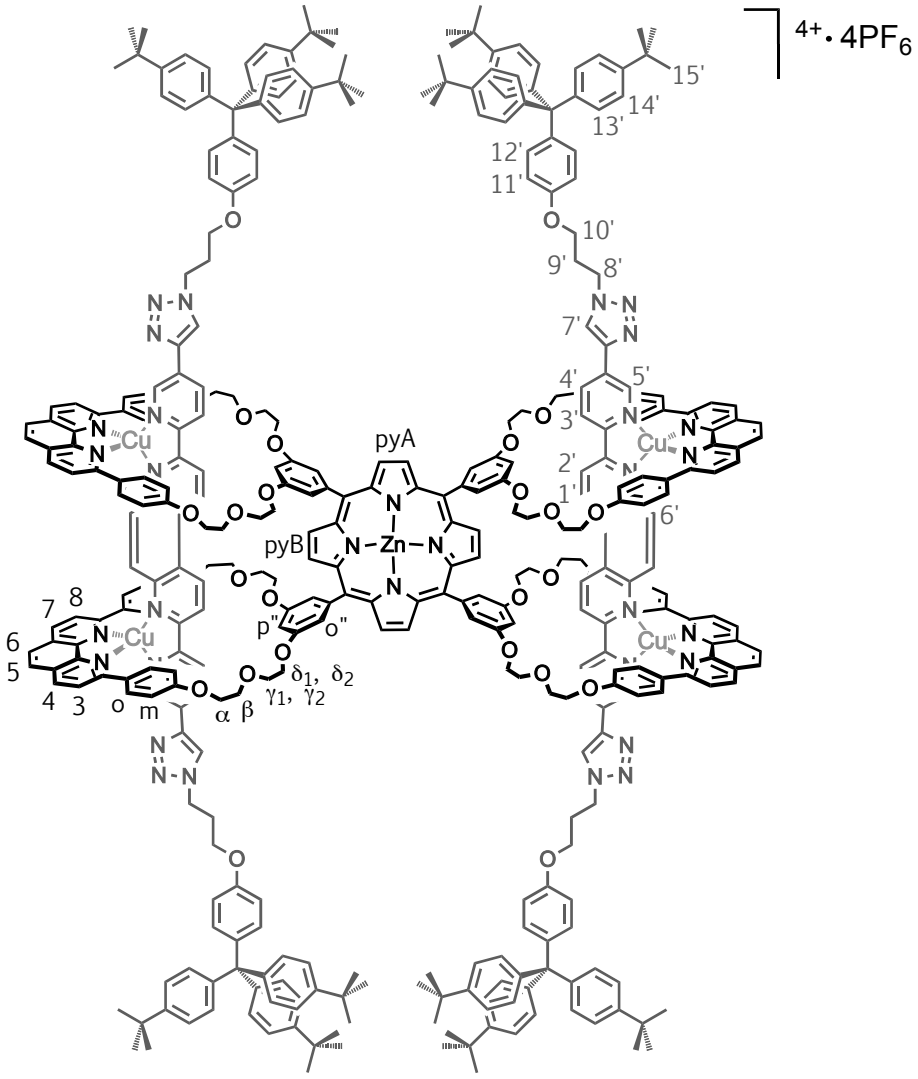

A degassed solution of $[Cu(CH_3CN)_4](PF_6)$ (16 mg, 43 μmol) in CH_3CN (5 mL) was added by cannula to a degassed solution of Zn-porphyrin **39** (30 mg, 11 μmol) in $CHCl_3$ (5 mL). The mixture was stirred under argon for 30 min. This solution was then added to a degassed suspension of acetylenic thread **16** (8.1 mg, 21 μmol) in $CHCl_3$ (5 mL). The mixture was stirred for 24 h under argon. Azide stopper **18** (37 mg, 64 μmol), $[Cu(CH_3CN)_4](PF_6)$ (7.9 mg, 21 μmol), Na_2CO_3 (0.9 mg, 8.5 μmol) and sodium ascorbate (1.7 mg, 8.5 μmol) were then added to the solution. The mixture was stirred under argon during 6 days. The solvents were then evaporated and the resulting deep red solid was purified by silica chromatography. Two consecutive columns using a gradient of eluent from CH_2Cl_2/MeOH 100:0 to 92:8 gave 32 mg of rotaxane $\mathbf{40^{4+}\cdot 4PF_6}$ (44%) as a dark red solid.

^{1}H NMR (300 MHz, CD_2Cl_2): δ = 9.38 (d, ^3J = 9.0 Hz, 4H, $H_{1'}$), 9.20 (s, 4H, H_{pyA}), 9.12 (s, 4H, H_{pyB}), 8.91 (d, ^4J = 1.5 Hz, 4H, $H_{5'}$), 8.79 (dd, ^3J = 8.4 Hz, ^4J = 1.8 Hz, 4H, $H_{4'}$), 8.69 (d, ^3J = 8.4 Hz, 8H, $H_{4,7}$), 8.62 (d, ^3J = 8.7 Hz, 4H, $H_{2'}$), 8.60 (d, ^3J = 8.4 Hz, 4H, $H_{3'}$), 8.37 (s, 4H, $H_{7'}$), 8.22 (s, 8H, $H_{5,6}$), 8.00 (d, ^3J = 8.4 Hz, 8H, $H_{3,8}$), 7.69 (d, ^4J = 2.1 Hz, 8H, $H_{o''}$), 7.27 (d,

^3J = 8.4 Hz, 16H, H_o), 7.24 (d, ^3J = 8.7 Hz, 24H, $H_{14'}$), 7.20 (d, ^3J = 9.0 Hz, 8H, $H_{12'}$), 7.18 (t, ^4J = 2.1 Hz, 4H, $H_{p''}$), 7.16 (d, ^3J = 8.7 Hz, 24 H, $H_{13'}$), 7.11 (s, 4H, $H_{6'}$), 6.85 (d, ^3J = 8.7 Hz, 8H, $H_{11'}$), 6.21 (d, ^3J = 9.0 Hz, 16H, H_m), 4.74 (t, ^3J = 6.3 Hz, 8H, $H_{8'}$), 4.58 (m, 8H, $H_{\delta 1}$), 4.32 (m, 8H, $H_{\delta 2}$), 4.15 (m, 8H, $H_{\gamma 1}$), 4.09 (t, ^3J = 6.0 Hz, 8H, $H_{10'}$), 3.90 (m, 8H, $H_{\gamma 2}$), 3.87 - 3.79 (m, 32H, H_α, H_β), 2.53 (q, ^3J = 5.7 Hz, 8H, $H_{9'}$), 1.27 (s, 108H, $H_{15'}$) ppm. **^{13}C NMR** (150 MHz, CD_2Cl_2): δ = 159.99, 158.66, 158.32, 156.85, 153.05, 150.55, 150.38, 150.04, 148.84, 146.22, 145.00, 144.83, 144.14, 143.49, 140.69, 138.26, 134.95, 132.63, 132.51, 132.43, 131.68, 131.37, 130.79, 130.73, 129.53, 128.50, 126.97, 125.92, 125.04, 124.72, 124.63, 124.22, 123.02, 121.43, 120.81, 114.43, 113.83, 113.63, 103.38, 70.32, 69.66, 68.68, 68.33, 64.66, 63.53, 48.10, 34.59, 31.48, 29.78 ppm. **HRES-MS**: calcd for $[C_{384}H_{364}Cu_4N_{32}O_{28}Zn]^{4+}/4$ (**40^{4+}**/4) *m/z* = 1548.615; found 1548.606. **UV-visible absorption** (CH_2Cl_2): λ_{max} (log ε) = 279 (5.19), 345 (5.24), 427 (5.62), 554 (4.37), 595 (3.93) nm.

List of Molecules

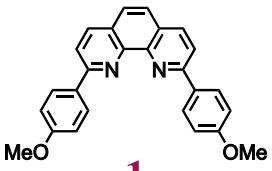

1

(dap)

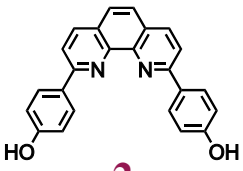

2

(dpp)

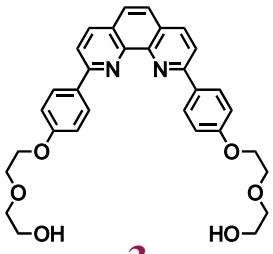

3

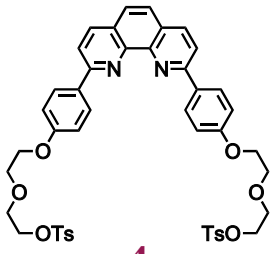

4

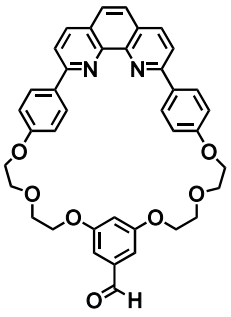

5

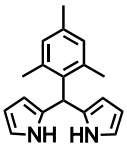

6

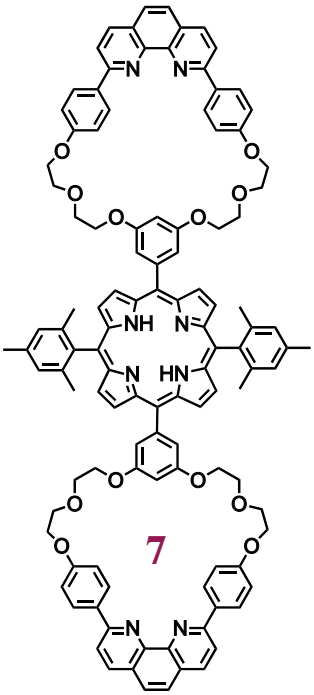

7

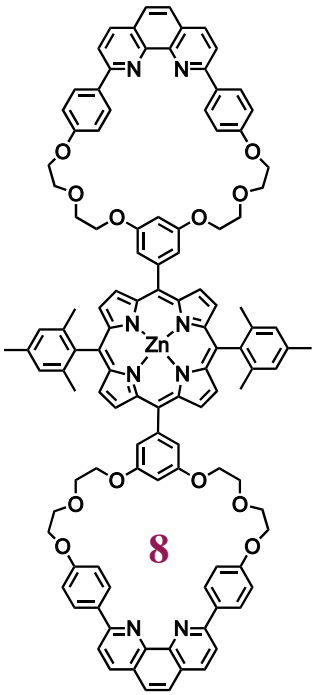

8

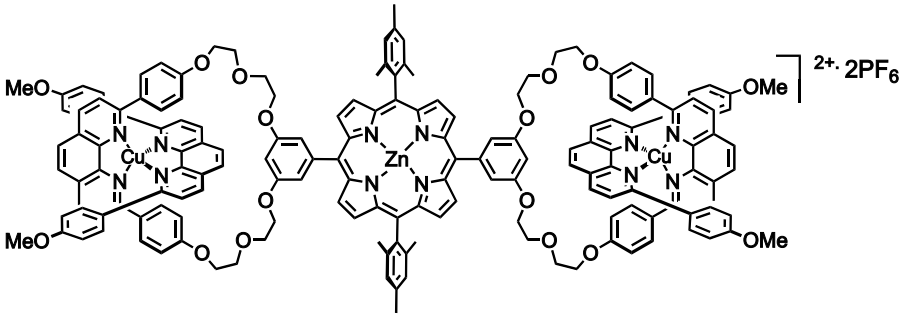

9^{2+}

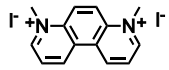

10

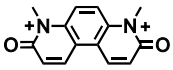

11

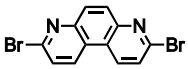

12

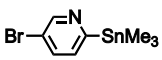

13

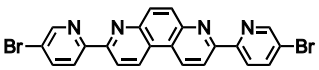

14

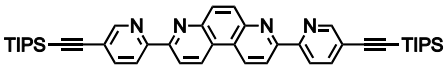

15

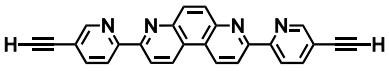

16

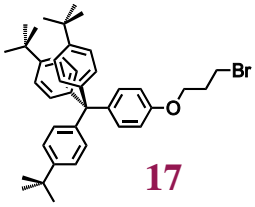

17

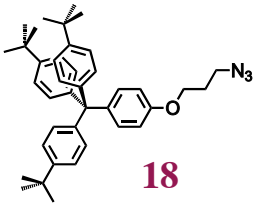

18

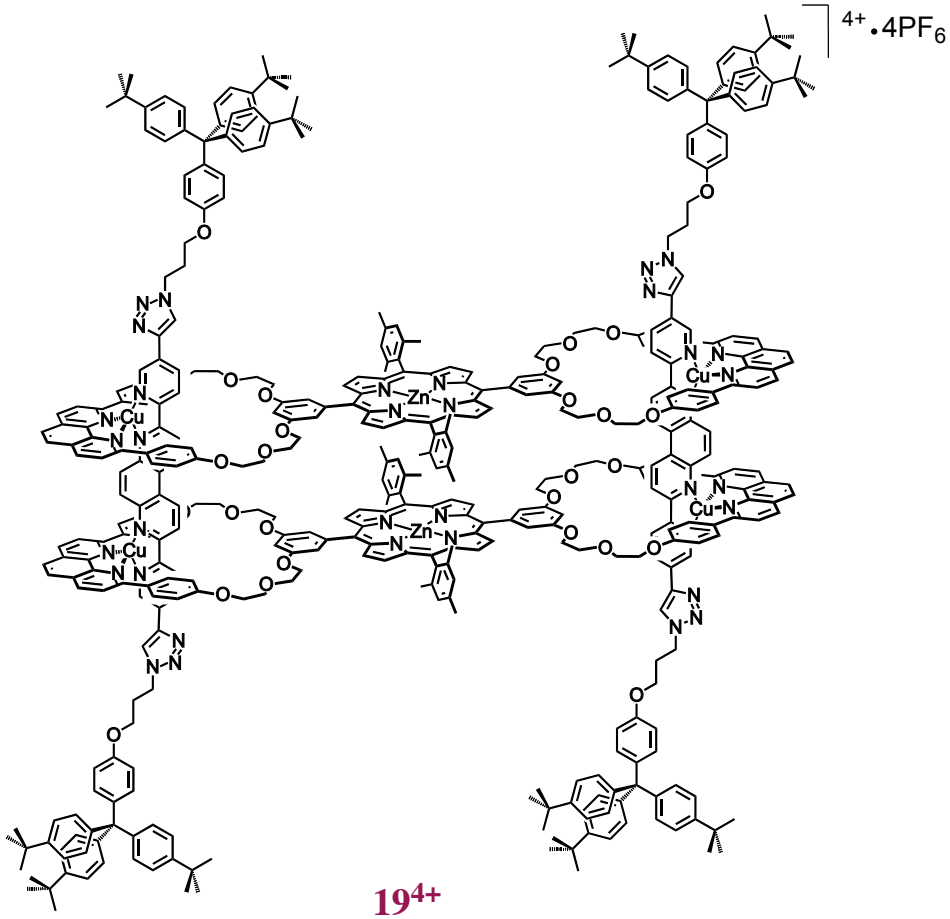

19^{4+}

G1

(DABCO)

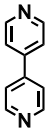

G2

(4,4'-bipyridine)

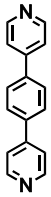

G3

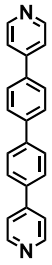

G4

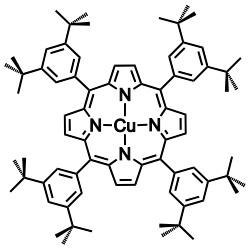

20

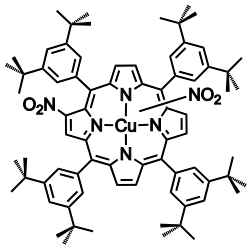

21

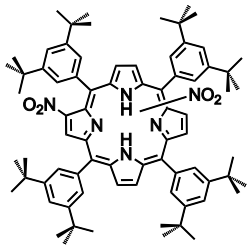

22

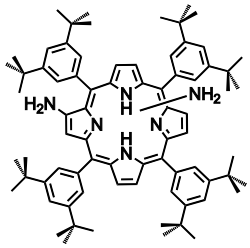

23

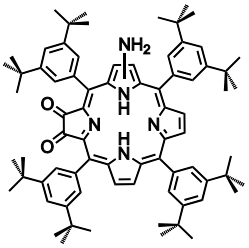

24

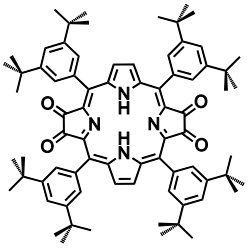

25

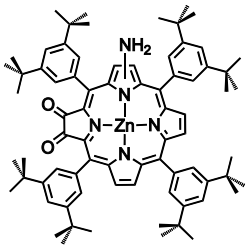

26

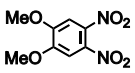

27

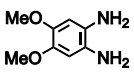

28

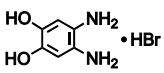

29

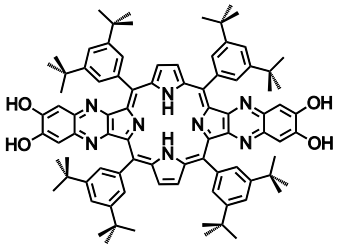

30

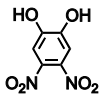

31

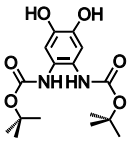

32

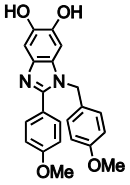

33

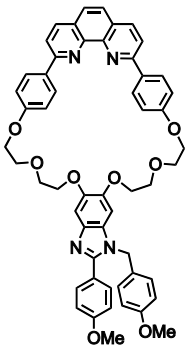

34

35

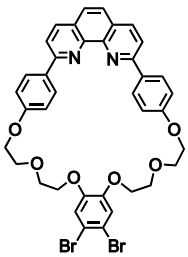

36

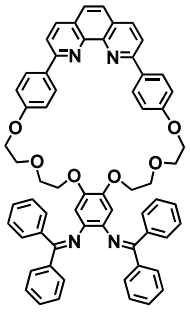

37

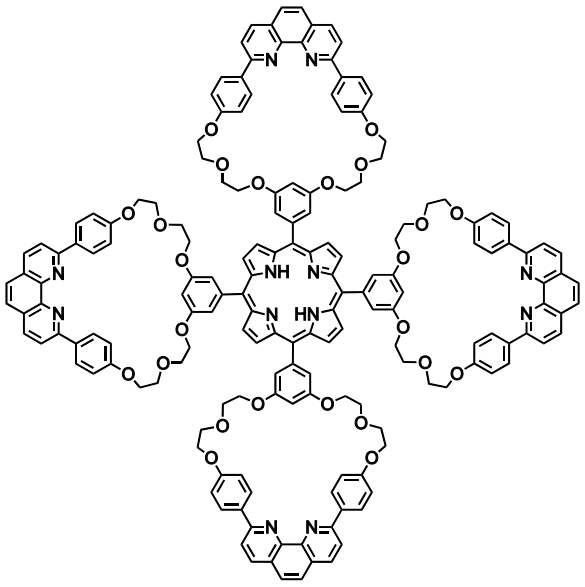

38

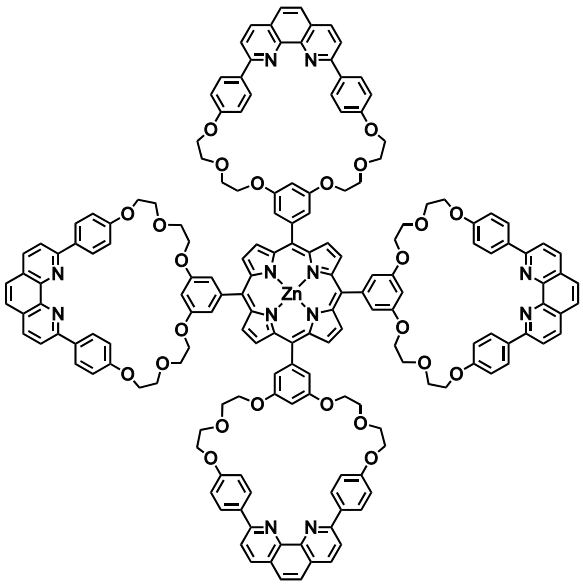

39

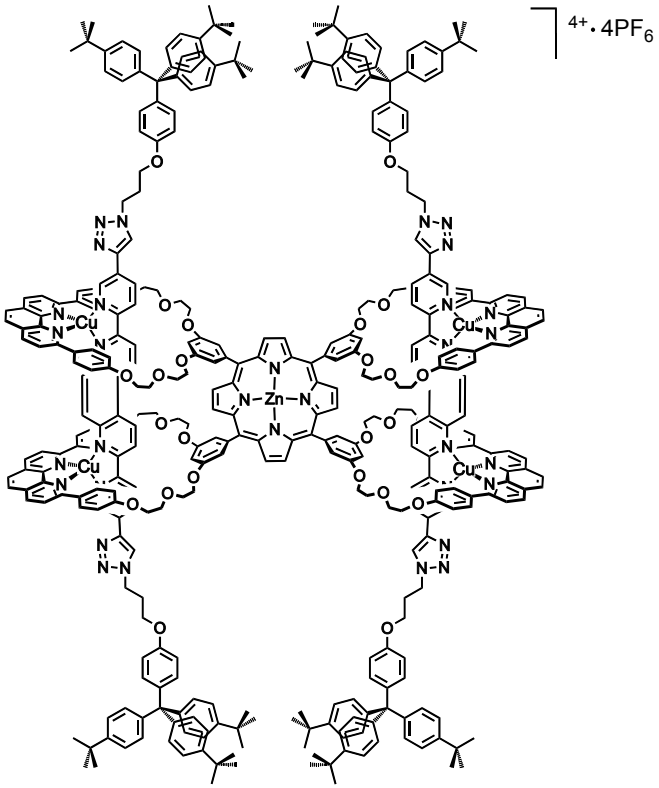

40^{4+}

References

(1) H. L. Frisch and E. Wasserman: Chemical Topology. *J. Am. Chem. Soc.* **1961**, *83*, 3789-3795.

(2) G. Schill and C. Zürcher: Mechanisch verknüpfte Moleküle Catenane und Rotaxane. *Naturwissenschaften* **1971**, *58*, 40-45.

(3) J. P. Sauvage: Interlacing Molecular Threads on Transition-Metals - Catenands, Catenates, and Knots. *Acc. Chem. Res.* **1990**, *23*, 319-327.

(4) D. B. Amabilino and J. F. Stoddart: Interlocked and intertwined structures and superstructures. *Chem. Rev.* **1995**, *95*, 2725-2828.

(5) F. Vögtle, T. Dünnwald and T. Schmidt: Catenanes and rotaxanes of the amide type. *Acc. Chem. Res.* **1996**, *29*, 451-460.

(6) J. S. Siegel: Chemical Topology and Interlocking Molecules. *Science* **2004**, *304*, 1256-1258.

(7) D. B. Amabilino and L. Perez-Garcia: Topology in molecules inspired, seen and represented. *Chem. Soc. Rev.* **2009**, *38*, 1562-1571.

(8) J. F. Stoddart: The chemistry of the mechanical bond. *Chem. Soc. Rev.* **2009**, *38*, 1802-1820.

(9) J. E. Beves, B. A. Blight, C. J. Campbell, D. A. Leigh and R. T. McBurney: Strategies and Tactics for the Metal-Directed Synthesis of Rotaxanes, Knots, Catenanes, and Higher Order Links. *Angew. Chem. Int. Ed.* **2011**, *50*, 9260-9327.

(10) R. S. Forgan, J. P. Sauvage and J. F. Stoddart: Chemical Topology: Complex Molecular Knots, Links, and Entanglements. *Chem. Rev.* **2011**, *111*, 5434-5464.

(11) L. F. Liu, R. E. Depew and J. C. Wang: Knotted single-stranded DNA rings: A novel topological isomer of circular single-stranded DNA formed by treatment with Escherichia coli ω protein. *J. Mol. Biol.* **1976**, *106*, 439-452.

(12) L. F. Liu, C.-C. Liu and B. M. Alberts: Type II DNA topoisomerases: Enzymes that can unknot a topologically knotted DNA molecule via a reversible double-strand break. *Cell* **1980**, *19*, 697-707.

(13) F. B. Dean, A. Stasiak, T. Koller and N. R. Cozzarelli: Duplex DNA knots produced by Escherichia coli topoisomerase I. Structure and requirements for formation. *J. Biol. Chem.* **1985**, *260*, 4975-4983.

(14) C. O. Dietrich-Buchecker and J. P. Sauvage: A Synthetic Molecular Trefoil Knot. *Angew. Chem. Int. Ed* **1989**, *28*, 189-192.

(15) C. Dietrich-Buchecker and G. Rapenne: Efficient synthesis of a molecular knot by copper(I)-induced formation of the precursor followed by ruthenium(II)-catalysed ring closing metathesis. *Chem. Commun.* **1997**, 2053-2054.

(16) C. O. Dietrich-Buchecker, J. Guilhem, C. Pascard and J.-P. Sauvage: Structure of a Synthetic Trefoil Knot Coordinated to Two Copper(I) Centers. *Angew. Chem. Int. Ed.* **1990**, *29*, 1154-1156.

(17) C. Dietrich-Buchecker, B. X. Colasson and J.-P. Sauvage: Molecular Knots. Templates in Chemistry II. Schalley, C. A., Vögtle, F., Dötz, K. H., Eds.; Springer Berlin / Heidelberg, 2005; Vol. 249; pp 211-225.

(18) O. Safarowsky, M. Nieger, R. Frohlich and F. Vogtle: A molecular knot with twelve amide groups - One-step synthesis, crystal structure, chirality. *Angew. Chem. Int. Ed.* **2000**, *39*, 1616-1618.

(19) H. Adams, E. Ashworth, G. A. Breault, J. Guo, C. A. Hunter and P. C. Mayers: Knot tied around an octahedral metal centre. *Nature* **2001**, *411*, 763-763.

(20) J. Guo, P. C. Mayers, G. A. Breault and C. A. Hunter: Synthesis of a molecular trefoil knot by folding and closing on an octahedral coordination template. *Nat. Chem.* **2010**, *2*, 218-222.

(21) C. R. Woods, M. Benaglia, S. Toyota, K. Hardcastle and J. S. Siegel: Trinuclear Copper(I)-bipyridine Triskelion: Template/Bascule Control of Coordination Complex Stereochemistry in a Trefoil Knot Precursor. *Angew. Chem. Int. Ed.* **2001**, *40*, 749-751.

(22) K. I. Arias, E. Zysman-Colman, J. C. Loren, A. Linden and J. S. Siegel: Synthesis of a D_3-symmetric "trefoil" knotted cyclophane. *Chem. Commun.* **2011**, *47*, 9588-9590.

(23) E. Wasserman: The Preparation Of Interlocking Rings: A Catenane. *J. Am. Chem. Soc.* **1960**, *82*, 4433-4434.

(24) G. Schill and A. Lüttringhaus: The Preparation of Catena Compounds by Directed Synthesis. *Angew. Chem. Int. Ed.* **1964**, *3*, 546-547.

(25) C. O. Dietrich-Buchecker, J. P. Sauvage and J. P. Kintzinger: Une nouvelle famille de molecules : les metallo-catenanes. *Tetrahedron Lett.* **1983**, *24*, 5095-5098.

(26) P. R. Ashton, T. T. Goodnow, A. E. Kaifer, M. V. Reddington, A. M. Z. Slawin, N. Spencer, J. F. Stoddart, C. Vicent and D. J. Williams: A [2]Catenane Made to Order. *Angew. Chem. Int. Ed.* **1989**, *28*, 1396-1399.

(27) C. A. Hunter: Synthesis and Structure Elucidation of a New [2]-Catenane. *J. Am. Chem. Soc.* **1992**, *114*, 5303-5311.

(28) F. Vögtle, S. Meier and R. Hoss: One-Step Synthesis of a Fourfold Functionalized Catenane. *Angew. Chem. Int. Ed.* **1992**, *31*, 1619-1622.

(29) M. Fujita, F. Ibukuro, H. Hagihara and K. Ogura: Quantitative self-assembly of a [2]catenane from two preformed molecular rings. *Nature* **1994**, *367*, 720-723.

(30) C. Dietrich-Buchecker, B. Frommberger, I. Lüer, J. P. Sauvage and F. Vögtle: Multiring Catenanes with a Macrobicyclic Core. *Angew. Chem. Int. Ed.* **1993**, *32*, 1434-1437.

(31) D. B. Amabilino, P. R. Ashton, A. S. Reder, N. Spencer and J. F. Stoddart: The Two-Step Self-Assembly of [4]- and [5]Catenanes. *Angew. Chem. Int. Ed.* **1994**, *33*, 433-437.

(32) A. Hori, K. Yamashita, T. Kusukawa, A. Akasaka, K. Biradha and M. Fujita: A circular tris[2]catenane from molecular 'figure-of-eight'. *Chem. Commun.* **2004**, 1798-1799.

(33) D. B. Amabilino, P. R. Ashton, A. S. Reder, N. Spencer and J. F. Stoddart: Olympiadane. *Angew. Chem. Int. Ed.* **1994**, *33*, 1286-1290.

(34) I. T. Harrison and S. Harrison: Synthesis of a stable complex of a macrocycle and a threaded chain. *J. Am. Chem. Soc.* **1967**, *89*, 5723-5724.

(35) G. Schill and H. Zollenkopf: Rotaxan-Verbindungen, I. *Justus Liebigs Ann. Chem.* **1969**, *721*, 53-74.

(36) C. Dietrich-Buchecker and J. P. Sauvage: Lithium templated synthesis of catenanes: efficient synthesis of doubly interlocked [2]-catenanes. *Chem. Commun.* **1999**, 615-616.

(37) K. S. Chichak, S. J. Cantrill, A. R. Pease, S. H. Chiu, G. W. V. Cave, J. L. Atwood and J. F. Stoddart: Molecular Borromean rings. *Science* **2004**, *304*, 1308-1312.

(38) D. B. Amabilino, P. R. Ashton, J. A. Bravo, F. M. Raymo, J. F. Stoddart, A. J. P. White and D. J. Williams: Molecular meccano, 52 - Template-directed synthesis of a rotacatenane. *Eur. J. Org. Chem.* **1999**, 1295-1302.

(39) G. Barin, A. Coskun, D. C. Friedman, M. A. Olson, M. T. Colvin, R. Carmielli, S. K. Dey, O. A. Bozdemir, M. R. Wasielewski and J. F. Stoddart: A Multistate Switchable [3]Rotacatenane. *Chem. Eur. J.* **2011**, *17*, 213-222.

(40) J. C. Chambron, V. Heitz and J. P. Sauvage: A Rotaxane with Two Rigidly Held Porphyrins as Stoppers. *J. Chem. Soc., Chem. Commun.* **1992**, 1131-1133.

(41) C. Seel, A. H. Parham, O. Safarowsky, G. M. Hubner and F. Vogtle: How selective threading of amides through macrocylic lactam wheels leads to rotaxane synthesis. *J. Org. Chem.* **1999**, *64*, 7236-7242.

(42) P. L. Anelli, P. R. Ashton, R. Ballardini, V. Balzani, M. Delgado, M. T. Gandolfi, T. T. Goodnow, A. E. Kaifer, D. Philp, M. Pietraszkiewicz, L. Prodi, M. V. Reddington, A. M. Z. Slawin, N. Spencer, J. F. Stoddart, C. Vicent and D. J. Williams: Molecular Meccano .1. [2]Rotaxanes and a [2]Catenane Made to Order. *J. Am. Chem. Soc.* **1992**, *114*, 193-218.

(43) F. Diederich, C. Dietrich-Buchecker, J. F. Nierengarten and J. P. Sauvage: A Copper(I)-Complexed Rotaxane with Two Fullerene Stoppers. *J. Chem. Soc., Chem. Commun.* **1995**, 781-782.

(44) K. Li, D. I. Schuster, D. M. Guldi, M. A. Herranz and L. Echegoyen: Convergent synthesis and photophysics of [60]fullerene/porphyrin-based rotaxanes. *J. Am. Chem. Soc.* **2004**, *126*, 3388-3389.

(45) S. Durot, P. Mobian, J. P. Collin and J. P. Sauvage: Synthesis of new copper(I)-complexed rotaxanes via click chemistry. *Tetrahedron* **2008**, *64*, 8496-8503.

(46) H. Ogino: Relatively High-Yield Syntheses of Rotaxanes - Syntheses and Properties of Compounds Consisting of Cyclodextrins Threaded by α , ω -Diaminoalkanes Coordinated to Cobalt(III) Complexes. *J. Am. Chem. Soc.* **1981**, *103*, 1303-1304.

(47) C. C. Hsu, N. C. Chen, C. C. Lai, Y. H. Liu, S. M. Peng and S. H. Chiu: Solvent-free synthesis of the smallest rotaxane prepared to date. *Angew. Chem. Int. Ed.* **2008**, *47*, 7475-7478.

(48) V. Aucagne, K. D. Hanni, D. A. Leigh, P. J. Lusby and D. B. Walker: Catalytic "click" rotaxanes: A substoichiometric metal-template pathway to mechanically interlocked architectures. *J. Am. Chem. Soc.* **2006**, *128*, 2186-2187.

(49) S. Saito, E. Takahashi and K. Nakazono: Synthesis of [2]rotaxanes by the catalytic reactions of a macrocyclic copper complex. *Org. Lett.* **2006**, *8*, 5133-5136.

(50) D. Ackermann, T. L. Schmidt, J. S. Hannam, C. S. Purohit, A. Heckel and M. Famulok: A double-stranded DNA rotaxane. *Nat. Nanotechnol.* **2010**, *5*, 436-442.

(51) R. G. E. Coumans, J. A. A. W. Elemans, P. Thordarson, R. J. M. Nolte and A. E. Rowan: Synthesis of porphyrin-containing [3]rotaxanes by olefin metathesis. *Angew. Chem. Int. Ed.* **2003**, *42*, 650-654.

(52) J. S. Marois, K. Cantin, A. Desmarais and J. F. Morin: [3]rotaxane-porphyrin conjugate as a novel supramolecular host for fullerenes. *Org. Lett.* **2008**, *10*, 33-36.

(53) J. P. Collin, J. P. Sauvage, Y. Trolez and K. Rissanen: [3]Rotaxanes and [3]pseudorotaxanes with a rigid two-bidentate chelate axle threaded through two coordinating rings. *New J. Chem.* **2009**, *33*, 2148-2154.

(54) A. Joosten, Y. Trolez, J.-P. Collin, V. Heitz and J.-P. Sauvage: Copper(I)-Assembled [3]Rotaxane Whose Two Rings Act as Flapping Wings. *J. Am. Chem. Soc.* **2012**, *134*, 1802-1809.

(55) A. I. Prikhod'ko, F. Durola and J. P. Sauvage: Iron(II)-templated synthesis of [3]rotaxanes by passing two threads through the same ring. *J. Am. Chem. Soc.* **2008**, *130*, 448-449.

(56) A. I. Prikhod'ko and J. P. Sauvage: Passing Two Strings through the Same Ring Using an Octahedral Metal Center as Template: A New Synthesis of [3]Rotaxanes. *J. Am. Chem. Soc.* **2009**, *131*, 6794-6807.

(57) H. M. Cheng, D. A. Leigh, F. Maffei, P. R. McGonigal, A. M. Z. Slawin and J. Wu: En Route to a Molecular Sheaf: Active Metal Template Synthesis of a [3]Rotaxane with Two Axles Threaded through One Ring. *J. Am. Chem. Soc.* **2011**, *133*, 12298-12303.

(58) J. B. Wittenberg, M. G. Costales, P. Y. Zavalij and L. Isaacs: A clipped [3]rotaxane derived from bis-nor-seco-cucurbit[10]uril. *Chem. Commun.* **2011**, *47*, 9420-9422.

(59) S. M. Goldup, D. A. Leigh, P. R. McGonigal, V. E. Ronaldson and A. M. Z. Slawin: Two Axles Threaded Using a Single Template Site: Active Metal Template Macrobicyclic [3]Rotaxanes. *J. Am. Chem. Soc.* **2010**, *132*, 315-320.

(60) F. H. Huang and H. W. Gibson: Polypseudorotaxanes and polyrotaxanes. *Prog. Polym. Sci.* **2005**, *30*, 982-1018.

(61) H. W. Gibson, M. C. Bheda and P. T. Engen: Rotaxanes, Catenanes, Polyrotaxanes, Polycatenanes and Related Materials. *Prog. Polym. Sci.* **1994**, *19*, 843-945.

(62) A. M. L. Fuller, D. A. Leigh and P. J. Lusby: One template, multiple rings: Controlled iterative addition of macrocycles onto a single binding site rotaxane thread. *Angew. Chem. Int. Ed.* **2007**, *46*, 5015-5019.

(63) J. Yin, S. Dasgupta and J. S. Wu: Synthesis of [n]Rotaxanes by Template-Directed Clipping: The Role of the Dialkylammonium Recognition Sites. *Org. Lett.* **2010**, *12*, 1712-1715.

(64) J. Wu, K. C. F. Leung and J. F. Stoddart: Efficient production of [n]rotaxanes by using template-directed clipping reactions. *Proc. Natl. Acad. Sci.* **2007**, *104*, 17266-17271.

(65) Z. J. Zhang, H. Y. Zhang, H. Wang and Y. Liu: A Twin-Axial Hetero[7]rotaxane. *Angew. Chem. Int. Ed.* **2011**, *50*, 10834-10838.

(66) J. C. Chambron and J. P. Sauvage: Functional rotaxanes: From controlled molecular motions to electron transfer between chemically nonconnected chromophores. *Chem. Eur. J.* **1998**, *4*, 1362-1366.

(67) X. Ma and H. Tian: Bright functional rotaxanes. *Chem. Soc. Rev.* **2010**, *39*, 70-80.

(68) D. I. Schuster, K. Li and D. M. Guldi: Porphyrin-fullerene photosynthetic model systems with rotaxane and catenane architectures. *C. R. Chim.* **2006**, *9*, 892-908.

(69) J. Y. Wang, J. M. Han, J. Yan, Y. G. Ma and J. Pei: A Mechanically Interlocked [3]Rotaxane as a Light-Harvesting Antenna: Synthesis, Characterization, and Intramolecular Energy Transfer. *Chem. Eur. J.* **2009**, *15*, 3585-3594.

(70) M. E. Gallina, B. Baytekin, C. Schalley and P. Ceroni: Light-Harvesting in Multichromophoric Rotaxanes. *Chem. Eur. J.* **2012**, *18*, 1528-1535.

(71) P. Thordarson, E. J. A. Bijsterveld, A. E. Rowan and R. J. M. Nolte: Epoxidation of polybutadiene by a topologically linked catalyst. *Nature* **2003**, *424*, 915-918.

(72) N. H. Evans, C. J. Serpell and P. D. Beer: A redox-active [3]rotaxane capable of binding and electrochemically sensing chloride and sulfate anions. *Chem. Commun.* **2011**, *47*, 8775-8777.

(73) A. Brown and P. D. Beer: Porphyrin-functionalised rotaxanes for anion recognition. *Dalton Trans.* **2012**, *41*, 118-129.

(74) X. Y. Wang, X. F. Bao, M. McFarland-Mancini, I. Isaacsohn, A. F. Drew and D. B. Smithrud: Investigation of the intracellular delivery of fluoresceinated peptides by a host-[2]rotaxane. *J. Am. Chem. Soc.* **2007**, *129*, 7284-7293.

(75) J. M. Baumes, J. J. Gassensmith, J. Giblin, J. J. Lee, A. G. White, W. J. Culligan, W. M. Leevy, M. Kuno and B. D. Smith: Storable, thermally activated, near-infrared chemiluminescent dyes and dye-stained microparticles for optical imaging. *Nat. Chem.* **2010**, *2*, 1025-1030.

(76) V. Balzani, A. Credi, F. M. Raymo and J. F. Stoddart: Artificial molecular machines. *Angew. Chem. Int. Ed.* **2000**, *39*, 3349-3391.

(77) K. Kinbara and T. Aida: Toward intelligent molecular machines: Directed motions of biological and artificial molecules and assemblies. *Chem. Rev.* **2005**, *105*, 1377-1400.

(78) W. R. Browne and B. L. Feringa: Making molecular machines work. *Nat. Nanotechnol.* **2006**, *1*, 25-35.

(79) E. R. Kay, D. A. Leigh and F. Zerbetto: Synthetic molecular motors and mechanical machines. *Angew. Chem. Int. Ed.* **2007**, *46*, 72-191.

(80) P. D. Boyer: Molecular motors - What makes ATP synthase spin? *Nature* **1999**, *402*, 247-249.

(81) M. Yoshida, E. Muneyuki and T. Hisabori: ATP synthase - A marvellous rotary engine of the cell. *Nat. Rev. Mol. Cell. Biol.* **2001**, *2*, 669-677.

(82) Z. H. Xu, A. L. Horwich and P. B. Sigler: The crystal structure of the asymmetric GroEL-GroES-$(ADP)_7$ chaperonin complex. *Nature* **1997**, *388*, 741-750.

(83) B. Bukau and A. L. Horwich: The Hsp70 and Hsp60 chaperone machines. *Cell* **1998**, *92*, 351-366.

(84) H. Yébenes, P. Mesa, I. G. Muñoz, G. Montoya and J. M. Valpuesta: Chaperonins: two rings for folding. *Trends Biochem. Sci* **2011**, *36*, 424-432.

(85) M. G. L. van den Heuvel and C. Dekker: Motor proteins at work for nanotechnology. *Science* **2007**, *317*, 333-336.

(86) M. Morimoto and M. Irie: A Diarylethene Cocrystal that Converts Light into Mechanical Work. *J. Am. Chem. Soc.* **2010**, *132*, 14172-14178.

(87) N. Koumura, R. W. J. Zijlstra, R. A. van Delden, N. Harada and B. L. Feringa: Light-driven monodirectional molecular rotor. *Nature* **1999**, *401*, 152-155.

(88) R. A. van Delden, M. K. J. ter Wiel, M. M. Pollard, J. Vicario, N. Koumura and B. L. Feringa: Unidirectional molecular motor on a gold surface. *Nature* **2005**, *437*, 1337-1340.

(89) A. R. Karim, A. Linden, K. K. Baldridge and J. S. Siegel: Symmetry and polar-pi effects on the dynamics of enshrouded aryl-alkyne molecular rotors. *Chem. Sci.* **2010**, *1*, 102-110.

(90) N. Ruangsupapichat, M. M. Pollard, S. R. Harutyunyan and B. L. Feringa: Reversing the direction in a light-driven rotary molecular motor. *Nat. Chem.* **2011**, *3*, 53-60.

(91) C. Lemouchi, C. S. Vogelsberg, L. Zorina, S. Simonov, P. Batail, S. Brown and M. A. Garcia-Garibay: Ultra-fast Rotors for Molecular Machines and Functional Materials via Halogen Bonding: Crystals of 1,4-Bis(iodoethynyl)bicyclo[2.2.2]octane with Distinct Gigahertz Rotation at Two Sites. *J. Am. Chem. Soc.* **2011**, *133*, 6371-6379.

(92) C. Joachim, H. Tang, F. Moresco, G. Rapenne and G. Meyer: The design of a nanoscale molecular barrow. *Nanotechnology* **2002**, *13*, 330-335.

(93) T. Muraoka, K. Kinbara, Y. Kobayashi and T. Aida: Light-driven open-close motion of chiral molecular scissors. *J. Am. Chem. Soc.* **2003**, *125*, 5612-5613.

(94) Y. Shirai, A. J. Osgood, Y. M. Zhao, K. F. Kelly and J. M. Tour: Directional control in thermally driven single-molecule nanocars. *Nano Lett*. **2005**, *5*, 2330-2334.

(95) T. Kudernac, N. Ruangsupapichat, M. Parschau, B. Macia, N. Katsonis, S. R. Harutyunyan, K. H. Ernst and B. L. Feringa: Electrically driven directional motion of a four-wheeled molecule on a metal surface. *Nature* **2011**, *479*, 208-211.

(96) D. K. Frantz, A. Linden, K. K. Baldridge and J. S. Siegel: Molecular Spur Gears Comprising Triptycene Rotators and Bibenzimidazole-Based Stators. *J. Am. Chem. Soc*. **2012**, *134*, 1528-1535.

(97) J. P. Sauvage: Transition metal-containing rotaxanes and catenanes in motion: Toward molecular machines and motors. *Acc. Chem. Res*. **1998**, *31*, 611-619.

(98) A. H. Flood, R. J. A. Ramirez, W. Q. Deng, R. P. Muller, W. A. Goddard and J. F. Stoddart: Meccano on the nanoscale - A blueprint for making some of the world's tiniest machines. *Aust. J. Chem*. **2004**, *57*, 301-322.

(99) E. Coronado, P. Gavina and S. Tatay: Catenanes and threaded systems: from solution to surfaces. *Chem. Soc. Rev*. **2009**, *38*, 1674-1689.

(100) J. P. Sauvage, J. P. Collin, S. Durot, J. Frey, V. Heitz, A. Sour and C. Tock: From chemical topology to molecular machines. *C. R. Chim*. **2010**, *13*, 315-328.

(101) A. Livoreil, C. O. Dietrich-Buchecker and J. P. Sauvage: Electrochemically Triggered Swinging of a [2]-Catenate. *J. Am. Chem. Soc*. **1994**, *116*, 9399-9400.

(102) D. J. Cardenas, A. Livoreil and J. P. Sauvage: Redox control of the ring-gliding motion in a Cu-complexed catenane: A process involving three distinct geometries. *J. Am. Chem. Soc*. **1996**, *118*, 11980-11981.

(103) D. B. Amabilino, C. O. Dietrich-Buchecker, A. Livoreil, L. Perez-Garcia, J. P. Sauvage and J. F. Stoddart: A switchable hybrid [2]-catenane based on transition metal complexation and pi-electron donor-acceptor interactions. *J. Am. Chem. Soc*. **1996**, *118*, 3905-3913.

(104) M. Asakawa, P. R. Ashton, V. Balzani, A. Credi, C. Hamers, G. Mattersteig, M. Montalti, A. N. Shipway, N. Spencer, J. F. Stoddart, M. S. Tolley, M. Venturi, A. J. P. White and D. J. Williams: A chemically and electrochemically switchable [2]catenane incorporating a tetrathiafulvalene unit. *Angew. Chem. Int. Ed*. **1998**, *37*, 333-337.

(105) P. Mobian, J. M. Kern and J. P. Sauvage: Light-driven machine prototypes based on dissociative excited states: Photoinduced decoordination and thermal recoordination of a ring in a ruthenium(II)-containing [2]catenane. *Angew. Chem. Int. Ed*. **2004**, *43*, 2392-2395.

(106) D. A. Leigh, P. J. Lusby, A. M. Z. Slawin and D. B. Walker: Half-rotation in a [2] catenane via interconvertible Pd(II) coordination modes. *Chem. Commun*. **2005**, 4919-4921.

(107) A. V. Leontiev, C. J. Serpell, N. G. White and P. D. Beer: Cation-induced molecular motion of spring-like [2]catenanes. *Chem. Sci*. **2011**, *2*, 922-927.

(108) D. A. Leigh, J. K. Y. Wong, F. Dehez and F. Zerbetto: Unidirectional rotation in a mechanically interlocked molecular rotor. *Nature* **2003**, *424*, 174-179.

(109) S. Durot, F. Reviriego and J. P. Sauvage: Copper-complexed catenanes and rotaxanes in motion: 15 years of molecular machines. *Dalton Trans*. **2010**, *39*, 10557-10570.

(110) W. Yang, Y. Li, H. Liu, L. Chi and Y. Li: Design and Assembly of Rotaxane-Based Molecular Switches and Machines. *Small* **2012**, *8*, 504-516.

(111) L. Raehm, J. M. Kern and J. P. Sauvage: A transition metal containing rotaxane in motion: Electrochemically induced pirouetting of the ring on the threaded dumbbell. *Chem. Eur. J.* **1999**, *5*, 3310-3317.

(112) V. Bermudez, N. Capron, T. Gase, F. G. Gatti, F. Kajzar, D. A. Leigh, F. Zerbetto and S. W. Zhang: Influencing intramolecular motion with an alternating electric field. *Nature* **2000**, *406*, 608-611.

(113) I. Poleschak, J. M. Kern and J. P. Sauvage: A copper-complexed rotaxane in motion: pirouetting of the ring on the millisecond timescale. *Chem. Commun*. **2004**, 474-476.

(114) L. M. Hancock and P. D. Beer: Sodium and barium cation-templated synthesis and cation-induced molecular pirouetting of a pyridine N-oxide containing [2]rotaxane. *Chem. Commun*. **2011**, *47*, 6012-6014.

(115) J. P. Collin, C. Dietrich-Buchecker, P. Gavina, M. C. Jimenez-Molero and J. P. Sauvage: Shuttles and muscles: Linear molecular machines based on transition metals. *Acc. Chem. Res*. **2001**, *34*, 477-487.

(116) S. Silvi, M. Venturi and A. Credi: Artificial molecular shuttles: from concepts to devices. *J. Mater. Chem*. **2009**, *19*, 2279-2294.

(117) J. Berna, D. A. Leigh, M. Lubomska, S. M. Mendoza, E. M. Perez, P. Rudolf, G. Teobaldi and F. Zerbetto: Macroscopic transport by synthetic molecular machines. *Nature Materials* **2005**, *4*, 704-710.

(118) J. P. Collin, F. Durola, J. Lux and J. P. Sauvage: A copper-based shuttling [2]rotaxane with two bidentate chelates in the axis: steric control of the motion. *New J. Chem*. **2010**, *34*, 34-43.

(119) J. D. Badjic, V. Balzani, A. Credi, S. Silvi and J. F. Stoddart: A molecular elevator. *Science* **2004**, *303*, 1845-1849.

(120) J. Deisenhofer and H. Michel: The Photosynthetic Reaction Center from the Purple Bacterium Rhodopseudomonas-Viridis. *Science* **1989**, *245*, 1463-1473.

(121) N. Nelson and C. F. Yocum: Structure and function of photosystems I and II. *Annu. Rev. Plant. Biol*. **2006**, *57*, 521-565.

(122) G. D. Scholes, G. R. Fleming, A. Olaya-Castro and R. van Grondelle: Lessons from nature about solar light harvesting. *Nat. Chem*. **2011**, *3*, 763-774.

(123) H. Imahori and S. Fukuzumi: Porphyrin- and fullerene-based molecular photovoltaic devices. *Adv. Funct. Mater*. **2004**, *14*, 525-536.

(124) M. J. Crossley, P. J. Sintic, J. A. Hutchison and K. P. Ghiggino: Chemical models for aspects of the photosynthetic reaction centre: synthesis and photophysical properties of tris- and tetrakis-porphyrins that resemble the arrangement of chromophores in the natural system. *Org. Biomol. Chem.* **2005**, *3*, 852-865.

(125) A. Satake and Y. Kobuke: Artificial photosynthetic systems: assemblies of slipped cofacial porphyrins and phthalocyanines showing strong electronic coupling. *Org. Biomol. Chem.* **2007**, *5*, 1679-1691.

(126) N. Aratani, D. Kim and A. Osuka: Discrete Cyclic Porphyrin Arrays as Artificial Light-Harvesting Antenna. *Acc. Chem. Res.* **2009**, *42*, 1922-1934.

(127) D. Gust, T. A. Moore and A. L. Moore: Solar Fuels via Artificial Photosynthesis. *Acc. Chem. Res.* **2009**, *42*, 1890-1898.

(128) S. H. Lee, A. G. Larsen, K. Ohkubo, Z. L. Cai, J. R. Reimers, S. Fukuzumi and M. J. Crossley: Long-lived long-distance photochemically induced spin-polarized charge separation in beta,beta '-pyrrolic fused ferrocene-porphyrin-fullerene systems. *Chem. Sci.* **2012**, *3*, 257-269.

(129) E. D. Sternberg, D. Dolphin and C. Bruckner: Porphyrin-based photosensitizers for use in photodynamic therapy. *Tetrahedron* **1998**, *54*, 4151-4202.

(130) M. Ethirajan, Y. H. Chen, P. Joshi and R. K. Pandey: The role of porphyrin chemistry in tumor imaging and photodynamic therapy. *Chem. Soc. Rev.* **2011**, *40*, 340-362.

(131) K. M. Kadish, K. M. Smith and R. Guilard: *The Porphyrin Handbook: Inorganic, organometallic and coordination chemistry*; Academic Press, 1999; Vol. 3.

(132) T. Hasobe, Y. Kashiwagi, M. A. Absalom, J. Sly, K. Hosomizu, M. J. Crossley, H. Imahori, P. V. Kamat and S. Fukuzumi: Supramolecular photovoltaic cells using porphyrin dendrimers and fullerenes. *Adv. Mater.* **2004**, *16*, 975-979.

(133) C. M. Drain, A. Varotto and I. Radivojevic: Self-Organized Porphyrinic Materials. *Chem. Rev.* **2009**, *109*, 1630-1658.

(134) M. Jurow, A. E. Schuckman, J. D. Batteas and C. M. Drain: Porphyrins as molecular electronic components of functional devices. *Coord. Chem. Rev.* **2010**, *254*, 2297-2310.

(135) C. Martelli, J. Canning, T. Khoury, N. Skivesen, M. Kristensen, G. Huyang, P. Jensen, C. Neto, T. J. Sum, M. B. Hovgaard, B. C. Gibson and M. J. Crossley: Self-assembled porphyrin microrods and observation of structure-induced iridescence. *J. Mater. Chem.* **2010**, *20*, 2310-2316.

(136) J. S. Lindsey and D. F. Bocian: Molecules for Charge-Based Information Storage. *Acc. Chem. Res.* **2011**, *44*, 638-650.

(137) E. Rose, B. Andrioletti, S. Zrig and M. Quelquejeu-Ehteve: Enantioselective epoxidation of olefins with chiral metalloporphyrin catalysts. *Chem. Soc. Rev.* **2005**, *34*, 573-583.

(138) C. M. Che and J. S. Huang: Metalloporphyrin-based oxidation systems: from biomimetic reactions to application in organic synthesis. *Chem. Commun.* **2009**, 3996-4015.

(139) A. Satake and Y. Kobuke: Dynamic supramolecular porphyrin systems. *Tetrahedron* **2005**, *61*, 13-41.

(140) I. Beletskaya, V. S. Tyurin, A. Y. Tsivadze, R. Guilard and C. Stern: Supramolecular Chemistry of Metalloporphyrins. *Chem. Rev.* **2009**, *109*, 1659-1713.

(141) M. Beyler, V. Heitz and J. P. Sauvage: Quantitative formation of a tetraporphyrin [2] catenane via copper and zinc coordination. *Chem. Commun.* **2008**, 5396-5398.

(142) M. Beyler, V. Heitz and J. P. Sauvage: Coordination Chemistry-Assembled Porphyrinic Catenanes. *J. Am. Chem. Soc.* **2010**, *132*, 4409-4417.

(143) M. C. O'Sullivan, J. K. Sprafke, D. V. Kondratuk, C. Rinfray, T. D. W. Claridge, A. Saywell, M. O. Blunt, J. N. O'Shea, P. H. Beton, M. Malfois and H. L. Anderson: Vernier templating and synthesis of a 12-porphyrin nano-ring. *Nature* **2011**, *469*, 72-75.

(144) H. L. Anderson: Conjugated Porphyrin Ladders. *Inorg. Chem.* **1994**, *33*, 972-981.

(145) P. N. Taylor and H. L. Anderson: Cooperative self-assembly of double-strand conjugated porphyrin ladders. *J. Am. Chem. Soc.* **1999**, *121*, 11538-11545.

(146) C. A. Hunter and S. Tomas: Accurate length control of supramolecular oligomerization: Vernier assemblies. *J. Am. Chem. Soc.* **2006**, *128*, 8975-8979.

(147) T. R. Kelly, R. L. Xie, C. K. Weinreb and T. Bregant: A molecular vernier. *Tetrahedron Lett.* **1998**, *39*, 3675-3678.

(148) M. J. Crossley and P. Thordarson: Assignment of stereochemistry of facially protected bis-porphyrins by use of a "molecular ruler". *Angew. Chem. Int. Ed.* **2002**, *41*, 1709-1712.

(149) P. Thordarson, A. Marquis and M. J. Crossley: The synthesis and studies towards the self-replication of bis(capped porphyrins). *Org. Biomol. Chem.* **2003**, *1*, 1216-1225.

(150) J. A. Hutchison, P. J. Sintic, P. R. Brotherhood, C. Scholes, I. M. Blake, K. P. Ghiggino and M. J. Crossley: Control of Photoinduced Charge Transfer Lifetimes in Porphyrin Arrays by Ligand Addition. *Journal of Physical Chemistry C* **2009**, *113*, 11796-11804.

(151) D. J. Cram and J. M. Cram: Host-Guest Chemistry. *Science* **1974**, *183*, 803-809.

(152) P. Leighton, J. A. Cowan, R. J. Abraham and J. K. M. Sanders: Geometry of Porphyrin Porphyrin Interactions. *J. Org. Chem.* **1988**, *53*, 733-740.

(153) C. A. Hunter, M. N. Meah and J. K. M. Sanders: Dabco Metalloporphyrin Binding - Ternary Complexes, Host Guest Chemistry, and the Measurement of Pi-Pi-Interactions. *J. Am. Chem. Soc.* **1990**, *112*, 5773-5780.

(154) A. L. Kieran, S. I. Pascu, T. Jarrosson and J. K. M. Sanders: Inclusion of C_{60} into an adjustable porphyrin dimer generated by dynamic disulfide chemistry. *Chem. Commun.* **2005**, 1276-1278.

(155) H. L. Anderson, C. A. Hunter, M. N. Meah and J. K. M. Sanders: Thermodynamics of Induced-Fit Binding inside Polymacrocyclic Porphyrin Hosts. *J. Am. Chem. Soc.* **1990**, *112*, 5780-5789.

(156) M. J. Crossley, T. W. Hambley, L. G. Mackay, A. C. Try and R. Walton: Porphyrin Analogs of Trogers Base - Large Chiral Cavities with a Bimetallic Binding-Site. *J. Chem. Soc., Chem. Commun.* **1995**, 1077-1079.

(157) P. R. Brotherhood, R. A. S. Wu, P. Turner and M. J. Crossley: Cavity effect amplification in the recognition of dicarboxylic acids by initial ditopic H-bond formation followed by kinetic trapping. *Chem. Commun.* **2007**, 225-227.

(158) P. R. Brotherhood, I. J. Luck, I. M. Blake, P. Jensen, P. Turner and M. J. Crossley: Regioselective Reactivity of an Asymmetric Tetravalent Di[dihydroxotin(IV)] Bis-Porphyrin Host Driven by Hydrogen-Bond Templation. *Chem. Eur. J.* **2008**, *14*, 10967-10977.

(159) J. N. H. Reek, A. P. H. J. Schenning, A. W. Bosman, E. W. Meijer and M. J. Crossley: Templated assembly of a molecular capsule. *Chem. Commun.* **1998**, 11-12.

(160) G. Proni, G. Pescitelli, X. F. Huang, K. Nakanishi and N. Berova: Magnesium tetraarylporphyrin tweezer: A CD-sensitive host for absolute configurational assignments of alpha-chiral carboxylic acids. *J. Am. Chem. Soc.* **2003**, *125*, 12914-12927.

(161) K. Tashiro and T. Aida: Metalloporphyrin hosts for supramolecular chemistry of fullerenes. *Chem. Soc. Rev.* **2007**, *36*, 189-197.

(162) W. J. Meng, B. Breiner, K. Rissanen, J. D. Thoburn, J. K. Clegg and J. R. Nitschke: A Self-Assembled M_8L_6 Cubic Cage that Selectively Encapsulates Large Aromatic Guests. *Angew. Chem. Int. Ed.* **2011**, *50*, 3479-3483.

(163) T. Haino, A. Watanabe, T. Hirao and T. Ikeda: Supramolecular Polymerization Triggered by Molecular Recognition between Bisporphyrin and Trinitrofluorenone. *Angew. Chem. Int. Ed.* **2012**, *51*, 1473-1476.

(164) S. Yagi, M. Ezoe, I. Yonekura, T. Takagishi and H. Nakazumi: Diarylurea-linked zinc porphyrin dimer as a dual-mode artificial receptor: Supramolecular control of complexation-facilitated photoinduced electron transfer. *J. Am. Chem. Soc.* **2003**, *125*, 4068-4069.

(165) M. Yoshizawa, J. K. Klosterman and M. Fujita: Functional Molecular Flasks: New Properties and Reactions within Discrete, Self-Assembled Hosts. *Angew. Chem. Int. Ed.* **2009**, *48*, 3418-3438.

(166) R. J. Hooley and J. Rebek: Chemistry and Catalysis in Functional Cavitands. *Chemistry & Biology* **2009**, *16*, 255-264.

(167) D. Ajami and J. Rebek: Compressed alkanes in reversible encapsulation complexes. *Nat. Chem.* **2009**, *1*, 87-90.

(168) A. Asadi, D. Ajami and J. Rebek: Bent Alkanes in a New Thiourea-Containing Capsule. *J. Am. Chem. Soc.* **2011**, *133*, 10682-10684.

(169) N. Fujita, K. Biradha, M. Fujita, S. Sakamoto and K. Yamaguchi: A Porphyrin Prism: Structural Switching Triggered by Guest Inclusion. *Angew. Chem. Int. Ed.* **2001**, *40*, 1718-1721.

(170) S. Tashiro, M. Kobayashi and M. Fujita: Folding of an Ala-Ala-Ala Tripeptide into a β-Turn via Hydrophobic Encapsulation. *J. Am. Chem. Soc.* **2006**, *128*, 9280-9281.

(171) Y. Hatakeyama, T. Sawada, M. Kawano and M. Fujita: Conformational Preferences of Short Peptide Fragments. *Angew. Chem. Int. Ed.* **2009**, *48*, 8695-8698.

(172) F. Y. Ji, L. L. Zhu, X. Ma, Q. C. Wang and H. Tian: A new thermo- and photo-driven [2]rotaxane. *Tetrahedron Lett.* **2009**, *50*, 597-600.

(173) S. Saha, A. H. Flood, J. F. Stoddart, S. Impellizzeri, S. Silvi, M. Venturi and A. Credi: A redox-driven multicomponent molecular shuttle. *J. Am. Chem. Soc.* **2007**, *129*, 12159-12171.

(174) T. Muraoka, K. Kinbara and T. Aida: Mechanical twisting of a guest by a photoresponsive host. *Nature* **2006**, *440*, 512-515.

(175) T. Muraoka, K. Kinbara and T. Aida: A self-locking molecule operative with a photoresponsive key. *J. Am. Chem. Soc.* **2006**, *128*, 11600-11605.

(176) A. Guenet, E. Graf, N. Kyritsakas, L. Allouche and M. W. Hosseini: A molecular gate based on a porphyrin and a silver lock. *Chem. Commun.* **2007**, 2935-2937.

(177) A. Guenet, E. Graf, N. Kyritsakas and M. W. Hosseini: Design and Synthesis of Sn-Porphyrin Based Molecular Gates. *Inorg. Chem.* **2010**, *49*, 1872-1883.

(178) T. Lang, E. Graf, N. Kyritsakas and M. W. Hosseini: Open and closed states of a porphyrin based molecular turnstile. *Dalton Trans.* **2011**, *40*, 3517-3523.

(179) T. Lang, A. Guenet, E. Graf, N. Kyritsakas and M. W. Hosseini: Porphyrin based molecular turnstiles. *Chem. Commun.* **2010**, *46*, 3508-3510.

(180) A. Guenet, E. Graf, N. Kyritsakas and M. W. Hosseini: Porphyrin-Based Switchable Molecular Turnstiles. *Chem. Eur. J.* **2011**, *17*, 6443-6452.

(181) K. Chichak, M. C. Walsh and N. R. Branda: Axially coordinated porphyrins as new rotaxane stoppers. *Chem. Commun.* **2000**, 847-848.

(182) M. J. Gunter, N. Bampos, K. D. Johnstone and J. K. M. Sanders: Thermodynamically self-assembling porphyrin-stoppered rotaxanes. *New J. Chem.* **2001**, *25*, 166-173.

(183) P. R. Ashton, M. R. Johnston, J. F. Stoddart, M. S. Tolley and J. W. Wheeler: The Template-Directed Synthesis of Porphyrin-Stoppered [2]Rotaxanes. *J. Chem. Soc., Chem. Commun.* **1992**, 1128-1131.

(184) J. C. Chambron, V. Heitz and J. P. Sauvage: Transition-Metal Templated Formation of [2]-Rotaxanes and [3]-Rotaxanes with Porphyrins as Stoppers. *J. Am. Chem. Soc.* **1993**, *115*, 12378-12384.

(185) N. Solladié, J. C. Chambron, C. O. Dietrich-Buchecker and J. P. Sauvage: Multicomponent molecular systems incorporating porphyrins and copper(I) complexes: Simultaneous synthesis of [3]- and [5]rotaxanes. *Angew. Chem. Int. Ed* **1996**, *35*, 906-909.

(186) C. A. Hunter, C. M. R. Low, M. J. Packer, S. E. Spey, J. G. Vinter, M. O. Vysotsky and C. Zonta: Noncovalent assembly of [2]rotaxane architectures. *Angew. Chem. Int. Ed.* **2001**, *40*, 2678-2682.

(187) M. J. Gunter, S. M. Farquhar and K. M. Mullen: Amide-appended porphyrins as scaffolds for catenanes, rotaxanes and anion receptors. *New J. Chem.* **2004**, *28*, 1443-1449.

(188) A. E. Rowan, P. P. M. Aarts and K. W. M. Koutstaal: Novel porphyrin-viologen rotaxanes. *Chem. Commun.* **1998**, 611-612.

(189) H. Sasabe, N. Kihara, Y. Furusho, K. Mizuno, A. Ogawa and T. Takata: End-capping of a pseudorotaxane via Diels-Alder reaction for the construction of C_{60}-terminated [2]rotaxanes. *Org. Lett.* **2004**, *6*, 3957-3960.

(190) M. Linke, J. C. Chambron, V. Heitz, J. P. Sauvage and V. Semetey: Complete rearrangement of a multi-porphyrinic rotaxane by metallation-demetallation of the central coordination site. *Chem. Commun.* **1998**, 2469-2470.

(191) D. Tuncel, N. Cindir and U. Koldemir: [5]rotaxane and [5]pseudorotaxane based on cucurbit[6]uril and anchored to a meso-tetraphenyl porphyrin. *J. Inclusion Phenom. Macrocyclic Chem.* **2006**, *55*, 373-380.

(192) M. C. Feiters, M. C. T. Fyfe, M. V. Martínez-Díaz, S. Menzer, R. J. M. Nolte, J. F. Stoddart, P. J. M. van Kan and D. J. Williams: A supramolecular analog of the photosynthetic special pair. *J. Am. Chem. Soc.* **1997**, *119*, 8119-8120.

(193) Y. Yamada, M. Okamoto, K. Furukawa, T. Kato and K. Tanaka: Switchable Intermolecular Communication in a Four-Fold Rotaxane. *Angew. Chem. Int. Ed.* **2012**, *51*, 709-713.

(194) J. Frey, C. Tock, J. P. Collin, V. Heitz and J. P. Sauvage: A [3]rotaxane with two porphyrinic plates acting as an adaptable receptor. *J. Am. Chem. Soc.* **2008**, *130*, 4592-4593.

(195) J. P. Collin, J. Frey, V. Heitz, J. P. Sauvage, C. Tock and L. Allouche: Adjustable Receptor Based on a [3]Rotaxane Whose Two Threaded Rings Are Rigidly Attached to Two Porphyrinic Plates: Synthesis and Complexation Studies. *J. Am. Chem. Soc.* **2009**, *131*, 5609-5620.

(196) J. P. Collin, F. Durola, J. Frey, V. Heitz, F. Reviriego, J. P. Sauvage, Y. Trolez and K. Rissanen: Templated Synthesis of Cyclic [4]Rotaxanes Consisting of Two Stiff Rods Threaded through Two Bis-macrocycles with a Large and Rigid Central Plate as Spacer. *J. Am. Chem. Soc.* **2010**, *132*, 6840-6850.

(197) J. P. Collin, F. Durola, V. Heitz, F. Reviriego, J. P. Sauvage and Y. Trolez: A Cyclic [4]rotaxane that Behaves as a Switchable Molecular Receptor: Formation of a Rigid Scaffold from a Collapsed Structure by Complexation with Copper(I) Ions. *Angew. Chem. Int. Ed.* **2010**, *49*, 10172-10175.

(198) C. O. Dietrich-Buchecker and J. P. Sauvage: Synthesis of Macrocyclic Polyether Compounds Derived from 1,10-Phenanthroline 2,9-Diphenyl. *Tetrahedron Lett.* **1983**, *24*, 5091-5094.

(199) C. Dietrich-Buchecker and J. P. Sauvage: Templated Synthesis of Interlocked Macrocyclic Ligands, the Catenands - Preparation and Characterization of the Prototypical Bis-30 Membered Ring-System. *Tetrahedron* **1990**, *46*, 503-512.

(200) D. B. Amabilino and J. P. Sauvage: Copper(I)-templated synthesis of [2]catenates bearing pendant porphyrins. *New J. Chem.* **1998**, *22*, 395-409.

(201) M. Cesario, C. O. Dietrich-Buchecker, J. Guilhem, C. Pascard and J. P. Sauvage: Molecular-Structure of a Catenand and Its Copper(I) Catenate - Complete Rearrangement of the Interlocked Macrocyclic Ligands by Complexation. *J. Chem. Soc., Chem. Commun.* **1985**, 244-247.

(202) G. P. Arsenault, E. Bullock and S. F. MacDonald: Pyrromethanes and Porphyrins Therefrom1. *J. Am. Chem. Soc.* **1960**, *82*, 4384-4389.

(203) C. H. Lee and J. S. Lindsey: One-Flask Synthesis of Mesosubstituted Dipyrromethanes and Their Application in the Synthesis of Trans-Substituted Porphyrin Building-Blocks. *Tetrahedron* **1994**, *50*, 11427-11440.

(204) B. J. Littler, Y. Ciringh and J. S. Lindsey: Investigation of conditions giving minimal scrambling in the synthesis of trans-porphyrins from dipyrromethanes and aldehydes. *J. Org. Chem.* **1999**, *64*, 2864-2872.

(205) G. R. Geier, B. J. Littler and J. S. Lindsey: Investigation of porphyrin-forming reactions. Part 3. The origin of scrambling in dipyrromethane plus aldehyde condensations yielding *trans*-A_2B_2-tetraarylporphyrins. *J. Chem. Soc., Perkin Trans. 2* **2001**, 701-711.

(206) G. R. Geier and J. S. Lindsey: Effects of aldehyde or dipyrromethane substituents on the reaction course leading to meso-substituted porphyrins. *Tetrahedron* **2004**, *60*, 11435-11444.

(207) B. J. Littler, M. A. Miller, C. H. Hung, R. W. Wagner, D. F. O'Shea, P. D. Boyle and J. S. Lindsey: Refined synthesis of 5-substituted dipyrromethanes. *J. Org. Chem.* **1999**, *64*, 1391-1396.

(208) C. O. Dietrich-Buchecker and J. P. Sauvage: Interlocking of Molecular Threads - from the Statistical Approach to the Templated Synthesis of Catenands. *Chem. Rev.* **1987**, *87*, 795-810.

(209) C. O. Dietrich-Buchecker, P. A. Marnot, J. P. Sauvage, J. R. Kirchhoff and D. R. Mcmillin: Bis(2,9-Diphenyl-1,10-Phenanthroline)Copper(I) - a Copper Complex with a Long-Lived Charge-Transfer Excited-State. *J. Chem. Soc., Chem. Commun.* **1983**, 513-515.

(210) J. Frey, W. Dobbs, V. Heitz and J. P. Sauvage: A 1,10-phenanthroline-containing ring connected to a porphyrin by a rigid aromatic spacer and its copper-complexed pseudorotaxane. *Eur. J. Inorg. Chem.* **2007**, 2416-2419.

(211) H. C. Kolb, M. G. Finn and K. B. Sharpless: Click chemistry: Diverse chemical function from a few good reactions. *Angew. Chem. Int. Ed.* **2001**, *40*, 2004-2021.

(212) J. F. Lutz: 1,3-dipolar cycloadditions of azides and alkynes: A universal ligation tool in polymer and materials science. *Angew. Chem. Int. Ed.* **2007**, *46*, 1018-1025.

(213) A. C. Fahrenbach and J. F. Stoddart: Reactions under the Click Chemistry Philosophy Employed in Supramolecular and Mechanostereochemical Systems. *Chem. Asian J.* **2011**, *6*, 2660-2669.

(214) R. Huisgen, G. Szeimies and L. Möbius: 1.3-Dipolare Cycloadditionen, XXXII. Kinetik der Additionen organischer Azide an CC-Mehrfachbindungen. *Chem. Ber.* **1967**, *100*, 2494-2507.

(215) V. V. Rostovtsev, L. G. Green, V. V. Fokin and K. B. Sharpless: A stepwise Huisgen cycloaddition process: Copper(I)-catalyzed regioselective "ligation" of azides and terminal alkynes. *Angew. Chem. Int. Ed.* **2002**, *41*, 2596-2599.

(216) J. E. Moses and A. D. Moorhouse: The growing applications of click chemistry. *Chem. Soc. Rev.* **2007**, *36*, 1249-1262.

(217) J. P. Collin, F. Durola, J. Frey, V. Heitz, J. P. Sauvage, C. Tock and Y. Trolez: Quantitative formation of [4]pseudorotaxanes from two rods and two bis-macrocycles incorporating porphyrinic plates between the rings. *Chem. Commun.* **2009**, 1706-1708.

(218) J. P. Collin, S. Durot, J. P. Sauvage and Y. Trolez: Synthesis of [2]-, [3]-, and [4]rotaxanes whose axis contains two bidentate and two tridentate chelates. *New J. Chem.* **2011**, *35*, 2009-2012.

(219) J. P. Collin, S. Durot, M. Keller, J. P. Sauvage, Y. Trolez, M. Cetina and K. Rissanen: Synthesis of [5]Rotaxanes Containing Bi- and Tridentate Coordination Sites in the Axis. *Chem. Eur. J.* **2011**, *17*, 947-957.

(220) P. N. W. Baxter, R. G. Khoury, J. M. Lehn, G. Baum and D. Fenske: Adaptive self-assembly: Environment-induced formation and reversible switching of polynuclear metallocyclophanes. *Chem. Eur. J.* **2000**, *6*, 4140-4148.

(221) J. P. Collin, J. Frey, V. Heitz, E. Sakellariou, J. P. Sauvage and C. Tock: Copper(I)-induced threading of two bis-macrocycles on two rods: a cyclic [4]rotaxane. *New J. Chem.* **2006**, *30*, 1386-1389.

(222) B. X. Colasson, C. Dietrich-Buchecker and J. P. Sauvage: Improved synthesis of 5,5 "-dibromo-2,2 ': 6 ',2 "-terpyridine. *Synlett* **2002**, 271-272.

(223) J. C. Chambron, J. P. Sauvage, K. Mislow, A. De Cian and J. Fischer: A [2]catenane and a [2]rotaxane as prototypes of topological and euclidean molecular "Rubber gloves". *Chem. Eur. J.* **2001**, *7*, 4085-4096.

(224) H. W. Gibson, S. H. Lee, P. T. Engen, P. Lecavalier, J. Sze, Y. X. Shen and M. Bheda: New Triarylmethyl Derivatives - Block Groups - for Rotaxanes and Polyrotaxanes. *J. Org. Chem.* **1993**, *58*, 3748-3756.

(225) C. Wu, P. R. Lecavalier, Y. X. Shen and H. W. Gibson: Synthesis of a Rotaxane Via the Template Method. *Chem. Mater.* **1991**, *3*, 569-572.

(226) D. J. Cardenas, P. Gavina and J. P. Sauvage: Construction of interlocking and threaded rings using two different transition metals as templating and connecting centers: Catenanes and rotaxanes incorporating Ru(terpy)$_2$-units in their framework. *J. Am. Chem. Soc.* **1997**, *119*, 2656-2664.

(227) P. Mobian, J. P. Collin and J. P. Sauvage: Efficient synthesis of a labile copper(I)-rotaxane complex using click chemistry. *Tetrahedron Lett*. **2006**, *47*, 4907-4909.

(228) W. R. Dichtel, O. S. Miljanic, J. M. Spruell, J. R. Heath and J. F. Stoddart: Efficient templated synthesis of donor - Acceptor rotaxanes using click chemistry. *J. Am. Chem. Soc*. **2006**, *128*, 10388-10390.

(229) A. B. Braunschweig, W. R. Dichtel, O. S. Miljanic, M. A. Olson, J. M. Spruell, S. I. Khan, J. R. Heath and J. F. Stoddart: Modular synthesis and dynamics of a variety of donor-acceptor interlocked compounds prepared by click chemistry. *Chem. Asian J*. **2007**, *2*, 634-647.

(230) J. J. Gassensmith, L. Barr, J. M. Baumes, A. Paek, A. Nguyen and B. D. Smith: Synthesis and photophysical investigation of squaraine rotaxanes by "clicked capping". *Org. Lett*. **2008**, *10*, 3343-3346.

(231) P. R. Ashton, M. Grognuz, A. M. Z. Slawin, J. Fraser Stoddart and D. J. Williams: The template-directed synthesis of a [2]rotaxane. *Tetrahedron Lett*. **1991**, *32*, 6235-6238.

(232) N. H. Evans, C. J. Serpell and P. D. Beer: A meta-xylenediamide macrocycle containing rotaxane anion host system constructed by a new synthetic clipping methodology. *New J. Chem*. **2011**, *35*, 2047-2053.

(233) I. T. Harrison: The effect of ring size on threading reactions of macrocycles. *J. Chem. Soc., Chem. Commun*. **1972**.

(234) P. R. Ashton, M. Belohradsky, D. Philp and J. F. Stoddart: Slippage - an Alternative Method for Assembling [2]Rotaxanes. *J. Chem. Soc., Chem. Commun*. **1993**, 1269-1274.

(235) I. Yoon, M. Narita, T. Shimizu and M. Asakawa: Threading-followed-by-shrinking protocol for the synthesis of a [2]rotaxane incorporating a Pd(II) - Salophen moiety. *J. Am. Chem. Soc*. **2004**, *126*, 16740-16741.

(236) S. Y. Hsueh, J. L. Ko, C. C. Lai, Y. H. Liu, S. M. Peng and S. H. Chiu: A Metal-Free "Threading-Followed-by-Shrinking" Protocol for Rotaxane Synthesis. *Angew. Chem. Int. Ed*. **2011**, *50*, 6643-6646.

(237) C. W. Chiu, C. C. Lai and S. H. Chiu: "Threading-followed-by-swelling": A new protocol for rotaxane synthesis. *J. Am. Chem. Soc*. **2007**, *129*, 3500-3501.

(238) J. L. Ko, S. H. Ueng, C. W. Chiu, C. C. Lai, Y. H. Liu, S. M. Peng and S. H. Chin: Using a Threading-Followed-by-Swelling Approach to Synthesize [2]Rotaxanes. *Chem. Eur. J*. **2010**, *16*, 6950-6960.

(239) Y. Tokunaga, K. Akasaka, N. Hashimoto, S. Yamanaka, K. Hisada, Y. Shimomura and S. Kakuchi: Using Photoresponsive End-Closing and End-Opening Reactions for the Synthesis and Disassembly of [2]Rotaxanes: Implications for Dynamic Covalent Chemistry. *J. Org. Chem*. **2009**, *74*, 2374-2379.

(240) K. D. Zhang, X. Zhao, G. T. Wang, Y. Liu, Y. Zhang, H. J. Lu, X. K. Jiang and Z. T. Li: Foldamer-Tuned Switching Kinetics and Metastability of [2]Rotaxanes. *Angew. Chem. Int. Ed*. **2011**, *50*, 9866-9870.

(241) K. D. Hanni and D. A. Leigh: The application of CuAAC 'click' chemistry to catenane and rotaxane synthesis. *Chem. Soc. Rev.* **2010**, *39*, 1240-1251.

(242) D. E. Koshland: Application of a Theory of Enzyme Specificity to Protein Synthesis. *Proc. Natl. Acad. Sci.* **1958**, *44*, 98-104.

(243) W. N. Lipscomb: Structure and Catalysis of Enzymes. *Annu. Rev. Biochem* **1983**, *52*, 17-34.

(244) H. Daniel: The role of induced fit and conformational changes of enzymes in specificity and catalysis. *Bioorg. Chem.* **1988**, *16*, 62-96.

(245) G. E. Schulz: Induced-fit movements in adenylate kinases. *Faraday Discuss.* **1992**, *93*, 85-93.

(246) R. M. Daniel, R. V. Dunn, J. L. Finney and J. C. Smith: The role of dynamics in enzyme activity. *Annu. Rev. Biophys. Biomol. Struct.* **2003**, *32*, 69-92.

(247) P. Csermely, R. Palotai and R. Nussinov: Induced fit, conformational selection and independent dynamic segments: an extended view of binding events. *Trends Biochem. Sci* **2010**, *35*, 539-546.

(248) M. C. Jimenez, C. Dietrich-Buchecker, J. P. Sauvage and A. De Cian: A hermaphrodite molecule: Quantitative copper(I)-directed formation of a doubly threaded assembly from a ring attached to a string. *Angew. Chem. Int. Ed.* **2000**, *39*, 1295-1298.

(249) E. O. Stejskal and J. E. Tanner: Spin Diffusion Measurements: Spin Echoes in the Presence of a Time-Dependent Field Gradient. *J. Chem. Phys.* **1965**, *42*, 288-292.

(250) C. S. Johnson, Jr.: Diffusion ordered nuclear magnetic resonance spectroscopy: principles and applications. *Prog. Nucl. Magn. Reson. Spectrosc.* **1999**, *34*, 203-256.

(251) Y. Cohen, L. Avram and L. Frish: Diffusion NMR Spectroscopy in Supramolecular and Combinatorial Chemistry: An Old Parameter—New Insights. *Angew. Chem. Int. Ed.* **2005**, *44*, 520-554.

(252) M. R. Kasha, H. R.; Ashraf El-Bayoumi, M.: The exciton model in molecular spectroscopy. *Pure Appl. Chem.* **1965**, *11*, 371-392.

(253) A. Osuka and K. Maruyama: Synthesis of Naphthalene-Bridged Porphyrin Dimers and Their Orientation-Dependent Exciton Coupling. *J. Am. Chem. Soc.* **1988**, *110*, 4454-4456.

(254) C. A. Hunter, J. K. M. Sanders and A. J. Stone: Exciton Coupling in Porphyrin Dimers. *Chem. Phys.* **1989**, *133*, 395-404.

(255) V. S. Y. Lin, S. G. Dimagno and M. J. Therien: Highly Conjugated, Acetylenyl Bridged Porphyrins - New Models for Light-Harvesting Antenna Systems. *Science* **1994**, *264*, 1105-1111.

(256) P. D. Harvey, C. Stern, C. P. Gros and R. Guilard: The photophysics and photochemistry of cofacial free base and metallated bisporphyrins held together by covalent architectures. *Coord. Chem. Rev.* **2007**, *251*, 401-428.

(257) K. Biradha and M. Fujita: Selective formation of rectangular grid coordination polymers with grid dimensions 10 x 15, 10 x 20 and 15 x 20 angstrom. *Chem. Commun.* **2001**, 15-16.

(258) A. L. Kieran, A. D. Bond, A. M. Belenguer and J. K. M. Sanders: Dynamic combinatorial libraries of metalloporphyrins: templated amplification of disulfide-linked oligomers. *Chem. Commun.* **2003**, 2674-2675.

(259) E. Alessio: *Non-covalent multi-porphyrin assemblies: synthesis and properties*; Springer, 2006.

(260) A. Camara-Campos, C. A. Hunter and S. Tomas: Cooperativity in the self-assembly of porphyrin ladders. *Proc. Natl. Acad. Sci.* **2006**, *103*, 3034-3038.

(261) Y. F. Han, Y. J. Lin, W. G. Jia and G. X. Jin: Synthesis, characterization, and electrochemical properties of molecular rectangles of half-sandwich iridium complexes containing bridging chloranilate Ligands. *Organometallics* **2008**, *27*, 4088-4097.

(262) A. Tsuge, T. Kunimune, Y. Ikeda, T. Moriguchi and K. Araki: Binding Properties of Calixarene-based Cofacial Bisporphyrins. *Chem. Lett.* **2010**, *39*, 1155-1157.

(263) M. J. Crossley and L. G. King: Novel Heterocyclic-Systems from Selective Oxidation at the Beta-Pyrrolic Position of Porphyrins. *J. Chem. Soc., Chem. Commun.* **1984**, 920-922.

(264) M. J. Crossley and P. L. Burn: Rigid, Laterally-Bridged Bis-Porphyrin Systems. *J. Chem. Soc., Chem. Commun.* **1987**, 39-40.

(265) M. J. Crossley, L. J. Govenlock and J. K. Prashar: Synthesis of Porphyrin-2,3,12,13-Tetraones and Porphyrin-2,3,7,8-Tetraones - Building-Blocks for the Synthesis of Extended Porphyrin Arrays. *J. Chem. Soc., Chem. Commun.* **1995**, 2379-2380.

(266) M. J. Crossley and P. L. Burn: An Approach to Porphyrin-Based Molecular Wires - Synthesis of a Bis(Porphyrin)Tetraone and Its Conversion to a Linearly Conjugated Tetrakisporphyrin System. *J. Chem. Soc., Chem. Commun.* **1991**, 1569-1571.

(267) M. J. Crossley, A. C. Try and R. Walton: Synthesis of accurate distance models of the primary donor primary acceptor pair of bacterial photosynthetic reaction centres. *Tetrahedron Lett.* **1996**, *37*, 6807-6810.

(268) M. J. Crossley and L. A. Johnston: Laterally-extended porphyrin systems incorporating a switchable unit. *Chem. Commun.* **2002**, 1122-1123.

(269) T. Khoury and M. J. Crossley: Expansion of the porphyrin pi-system: stepwise annelation of porphyrin beta,beta '-pyrrolic faces leading to trisquinoxalinoporphyrin. *New J. Chem.* **2009**, *33*, 1076-1086.

(270) T. Khoury and M. J. Crossley: A strategy for the stepwise ring annulation of all four pyrrolic rings of a porphyrin. *Chem. Commun.* **2007**, 4851-4853.

(271) L. J. Govenlock. PhD Thesis, The University of Sydney, **1996**.

(272) L. L. Cheng, C. Aw, S. S. Ong and Y. X. Lu: Facile cleavage of ethers in ionic liquid. *Bull. Chem. Soc. Jpn.* **2007**, *80*, 2008-2010.

(273) M. Node, K. Nishide, K. Fuji and E. Fujita: Hard Acid and Soft Nucleophile System. 2. Demethylation of Methyl Ethers of Alcohol and Phenol with an Aluminum Halide-Thiol System. *J. Org. Chem.* **1980**, *45*, 4275-4277.

(274) M. Albrecht, P. Stortz, J. Runsink and P. Weis: Preparation of tripeptide-bridged dicatechol Ligands and their macrocyclic molybdenum(VI) complexes: Fixation of the RGD sequence and the WKY sequence of urotensin II in a cyclic conformation. *Chem. Eur. J.* **2004**, *10*, 3657-3666.

(275) D. T. Rosa, R. A. Reynolds, S. M. Malinak and D. Coucouvanis: 4,5-diaminocatechol: A useful building block in synthesis of multimetallic complexes. *Inorganic Synthesis* **2002**, *33*, 112-119.

(276) J. Hu, D. Zhang, S. Jin, S. Z. D. Cheng and F. W. Harris: Synthesis and properties of planar liquid-crystalline bisphenazines. *Chem. Mater.* **2004**, *16*, 4912-4915.

(277) P. G. M. Wuts and T. W. Greene: *Greene's protective groups in organic synthesis*; Wiley-Interscience, 2007.

(278) T. Vilaivan: A rate enhancement of tert-butoxycarbonylation of aromatic amines with Boc_2O in alcoholic solvents. *Tetrahedron Lett.* **2006**, *47*, 6739-6742.

(279) A. P. Bindra and J. A. Elix: 15*H*-Dibenzo[*c.e*]benzimidazo[1.2-*a*]azepine. *Tetrahedron* **1969**, *25*, 3789-3794.

(280) P. Salehi, M. Dabiri, M. A. Zolfigol, S. Otokesh and M. Baghbanzadeh: Selective synthesis of 2-aryl-1-arylmethyl-1*H*-1,3-benzimidazoles in water at ambient temperature. *Tetrahedron Lett.* **2006**, *47*, 2557-2560.

(281) I. Sheikhshoaie, F. Belaj and W. M. F. Fabian: 1-(4-dimethylaminobenzyl)-2-(4-dimethylaminophenyl)-benzimidazole: Synthesis, X-ray crystallography and density functional theory calculations. *J. Mol. Struct.* **2006**, *794*, 244-250.

(282) S. Perumal, S. Mariappan and S. Selvaraj: A microwave assisted synthesis of 2-aryl-1-arylmethyl-1*H*-1,3-benzimidazoles in the presence of K-10. *Arkivoc* **2004**, 46-51.

(283) F. Z. C. Fellah, J. P. Costes, C. Duhayon, J. C. Daran and J. P. Tuchagues: Mononuclear Cu and dinuclear Cu-Ln complexes of benzimidazole based ligands including N and O donors: Syntheses, characterization, X-ray molecular structures and magnetic properties. *Polyhedron* **2010**, *29*, 2111-2119.

(284) F. Paul, J. Patt and J. F. Hartwig: Palladium-Catalyzed Formation of Carbon-Nitrogen Bonds - Reaction Intermediates and Catalyst Improvements in the Hetero Cross-Coupling of Aryl Halides and Tin Amides. *J. Am. Chem. Soc.* **1994**, *116*, 5969-5970.

(285) A. S. Guram and S. L. Buchwald: Palladium-Catalyzed Aromatic Aminations with in-Situ Generated Aminostannanes. *J. Am. Chem. Soc.* **1994**, *116*, 7901-7902.

(286) J. Louie and J. F. Hartwig: Palladium-Catalyzed Synthesis of Arylamines from Aryl Halides - Mechanistic Studies Lead to Coupling in the Absence of Tin Reagents. *Tetrahedron Lett.* **1995**, *36*, 3609-3612.

(287) A. S. Guram, R. A. Rennels and S. L. Buchwald: A Simple Catalytic Method for the Conversion of Aryl Bromides to Arylamines. *Angew. Chem. Int. Ed.* **1995**, *34*, 1348-1350.

(288) M. J. Fleming, H. A. McManus, A. Rudolph, W. H. Chan, J. Ruiz, C. Dockendorff and M. Lautens: Concise enantioselective total syntheses of (+)-homochelidonine, (+)-chelamidine, (+)-chelidonine, (+)-chelamine and (+)-norchelidonine by a Pd(II)-catalyzed ring-opening strategy. *Chem. Eur. J.* **2008**, *14*, 2112-2124.

(289) J. P. Wolfe, J. Ahman, J. P. Sadighi, R. A. Singer and S. L. Buchwald: An ammonia equivalent for the palladium-catalyzed amination of aryl halides and triflates. *Tetrahedron Lett.* **1997**, *38*, 6367-6370.

(290) L. Chen, J. Kim, T. Ishizuka, Y. Honsho, A. Saeki, S. Seki, H. Ihee and D. L. Jiang: Noncovalently Netted, Photoconductive Sheets with Extremely High Carrier Mobility and Conduction Anisotropy from Triphenylene-Fused Metal Trigon Conjugates. *J. Am. Chem. Soc.* **2009**, *131*, 7287-7292.

(291) J. S. Lindsey: Synthetic Routes to meso-Patterned Porphyrins. *Acc. Chem. Res.* **2010**, *43*, 300-311.

(292) A. D. Adler, F. R. Longo, J. D. Finarelli, J. Goldmacher, J. Assour and L. Korsakoff: A simplified synthesis for meso-tetraphenylporphine. *J. Org. Chem.* **1967**, *32*, 476-476.

(293) P. Rothemund and A. R. Menotti: Porphyrin Studies. IV.1 The Synthesis of $\alpha, \beta, \gamma, \delta$-Tetraphenylporphine. *J. Am. Chem. Soc.* **1941**, *63*, 267-270.

(294) J. S. Lindsey, H. C. Hsu and I. C. Schreiman: Synthesis of Tetraphenylporphyrins under Very Mild Conditions. *Tetrahedron Lett.* **1986**, *27*, 4969-4970.

(295) J. S. Lindsey, I. C. Schreiman, H. C. Hsu, P. C. Kearney and A. M. Marguerettaz: Rothemund and Adler-Longo Reactions Revisited - Synthesis of Tetraphenylporphyrins under Equilibrium Conditions. *J. Org. Chem.* **1987**, *52*, 827-836.

(296) M. J. Crossley, P. Thordarson, J. P. Bannerman and P. J. Maynard: A convenient procedure for moderate-scale Rothemund synthesis of lipophilic porphyrins: an alternative to the Adler-Longo and Lindsey methodologies. *J. Porphyrins Phthalocyanines* **1998**, *2*, 511-516.

(297) H. Sharghi and A. H. Nejad: Novel synthesis of meso-tetraarylporphyrins using CF_3SO_2Cl under aerobic oxidation. *Tetrahedron* **2004**, *60*, 1863-1868.

(298) R. Lucas, J. Vergnaud, K. Teste, R. Zerrouki, V. Sol and P. Krausz: A facile and rapid iodine-catalyzed meso-tetraphenylporphyrin synthesis using microwave activation. *Tetrahedron Lett.* **2008**, *49*, 5537-5539.

(299) A. Kumar, S. Maji, P. Dubey, G. J. Abhilash, S. Pandey and S. Sarkar: One-pot general synthesis of metalloporphyrins. *Tetrahedron Lett.* **2007**, *48*, 7287-7290.

(300) B. F. O. Nascimento, M. Pineiro, A. M. D. R. Gonsalves, M. R. Silva, A. M. Beja and J. A. Paixao: Microwave-assisted synthesis of porphyrins and metalloporphyrins: a rapid and efficient synthetic method. *J. Porphyrins Phthalocyanines* **2007**, *11*, 77-84.

(301) J. P. Collin, V. Heitz and J. P. Sauvage: A Porphyrin Rigidly Linked to One or Two Terpyridine Chelates Used as Assembling Subunits. *Tetrahedron Lett.* **1991**, *32*, 5977-5980.

(302) K. Araki, P. Losco, F. M. Engelmann, H. Winnischofer and H. E. Toma: Modulation of vectorial energy transfer in the tetrakis[tris(bipyridine)ruthenium(II)]porphyrinate zinc complex. *J. Photochem. Photobiol., A* **2001**, *142*, 25-30.

(303) C. M. Elliott, J. R. Dunkle and S. C. Paulson: Electrochemical olefin epoxidation employing an iron(IV)porphyrin/trisbipyridineruthenium(III) polymer catalyst. *Langmuir* **2005**, *21*, 8605-8608.

(304) T. J. Cho, C. D. Shreiner, S. H. Hwang, C. N. Moorefield, B. Courneya, L. A. Godinez, J. Manriquez, K. U. Jeong, S. Z. D. Cheng and G. R. Newkome: 5,10,15,20-Tetrakis[4'-(terpyridinyl)phenyl] porphyrin and its Ru^{II} complexes: Synthesis, photovoltaic properties, and self-assembled morphology. *Chem. Commun.* **2007**, 4456-4458.

(305) G. J. Kubas: Tetrakis(Acetonitrile)Copper(1+) Hexafluorophosphate(1-). *Inorg. Synth.* **1990**, *28*, 68-70.

(306) H. Gampp, M. Maeder, C. J. Meyer and A. D. Zuberbuhler: Calculation of Equilibrium-Constants from Multiwavelength Spectroscopic Data II. Specfit: Two User-Friendly Programs in Basic and Standard Fortran 77. *Talanta* **1985**, *32*, 257-264.

Cécile ROCHE

Porphyrin-based [3]- and [4]Rotaxanes

Towards an Adaptable Molecular Receptor

Résumé

La synthèse et l'étude de rotaxanes et de porphyrines sont deux domaines particulièrement actifs de la recherche en chimie. Cependant, les composés combinant les propriétés intéressantes de ces deux types de structures sont plus rares. De nouveaux multi-rotaxanes à base de porphyrines, dont la préparation représente un défi synthétique, sont décrits dans cette thèse.

Des porphyrines liées à deux ou quatre anneaux coordinants ont été synthétisées. Des rails moléculaires à deux chélates ont été enfilés dans les anneaux grâce à l'effet template du cuivre(I); l'introduction de bouchons a mené à la formation de rotaxanes. Dans le cas du bis-macrocycle porphyrinique, un [4]rotaxane a été obtenu. Des études de complexation hôte/invité avec des ligands azotés rigides ont montré que ce rotaxane est un récepteur moléculaire qui peut s'adapter à la taille du substrat invité en se "gonflant" ou en se "dégonflant". Dans le cas du tétra-macrocycle porphyrinique, la formation d'un [3]rotaxane d'architecture originale a été observée.

La synthèse d'un nouveau bis-macrocycle plus rigide est en cours. Ce composé sera utilisé pour la construction d'un [4]rotaxane, qui pourrait montrer un caractère de presse moléculaire capable de modifier la conformation d'un substrat invité en le comprimant.

Mots-clés: rotaxane, porphyrine, macrocycle, phénanthroline, bipyridine, cuivre(I), zinc(II), synthèse organique, chimie de coordination, effet template, système hôte/invité, récepteur moléculaire.

Résumé en anglais

Rotaxanes and porphyrins are two particularly active fields of research in chemistry. However, molecules that *combine* the interesting properties of these types of structures are not so common. In this thesis we describe new porphyrin-based multi-rotaxanes, whose syntheses constitute interesting challenges.

Porphyrins linked to two or four coordinating macrocycles were synthesised. The "gathering-and-threading" effect of copper(I) was used to thread molecular rods through the rings; the subsequent introduction of stoppers led to the formation of rotaxanes. In the case of the porphyrinic bis-macrocycle a [4]rotaxane was obtained. Host/guest complexation studies with rigid nitrogen ligands showed that the rotaxane behaves as a distensible molecular receptor that can adopt an "inflated" or "deflated" conformation and adjust its shape to the size of the guest. In the case of the porphyrinic tetra-macrocycle the formation of a [3]rotaxane of novel architecture was observed.

The synthesis of a new, more rigid bis-macrocycle is in progress. This compound will be used for the construction of a [4]rotaxane that could act as a molecular press able to change the conformation of a guest substrate by compression.

Keywords: rotaxane, porphyrin, macrocycle, phenanthroline, bipyridine, copper(I), zinc(II), organic synthesis, coordination chemistry, template effect, host-guest chemistry, molecular receptor.